IDENTIFYING OF KEY PROTEOGLYCANS IN DIFFERENT ANATOMICAL REGIONS OF THE CANINE CRANIAL CRUCIATE LIGAMENT FROM DOG BREEDS AT AN ALTERED RISK TO LIGAMENT DISEASE AND RUPTURE

Thesis submitted in accordance with the requirements of the University of Liverpool for the degree of Doctor in Philosophy

By

Sumaya Allaith

March 2016

Abstract

Cranial cruciate ligament disease and rupture (CCLD/ R) is a common orthopaedic condition in dogs. CCLD/ R can be due to trauma (least common) or to non-contact injury (most common). Once the cranial cruciate ligament (CCL) is damaged complications such as stifle osteoarthritis can occur. Different dog breeds are at an altered risk to CCLD/ R. Previous biochemical and ultrastructural studies have found that glycosaminoglycans (GAGs) were altered in high risk dog breeds when compared to CCLs from a dog breed at low risk of ligament rupture. We hypothesise that proteoglycans and GAGs may vary between different anatomical regions of the CCL, and between differentially predisposed dog breeds to CCLD/ R. Proteoglycans were determined by semi-quantitative Western blotting, quantitative RT-PCR (qRT-PCR), quantitative biochemistry, semi-objective histology scoring, and immunohistochemistry. Water and GAG content in the CCLs was also measured. Further qRT-PCR analysis was conducted to determine the expression of ECM proteases (ADAMTS -4 & -5) in the canine CCL. We showed with Western blot analysis that certain proteoglycans and GAGs were significantly different between anatomical regions of Staffordshire bull terrier CCLs. Data analysis between differentially predisposed dog breeds showed that the Staffordshire bull terrier CCLs (a moderate-high risk dog breed to CCLD/ R) had a significant increase in water content compared to greyhound CCLs (a low risk dog breed to CCLD/ R). Further, gene expression and Western blot analysis of fibromodulin, gene expression of aggrecan, and Western blot analysis of chondroitin-6 sulphate stubs were significantly increased in Staffordshire bull terrier CCLs compared to greyhounds. Decorin and ADAMTS-4 gene expression were significantly increased in greyhounds compared to Staffordshire bull terrier CCLs. Histology analysis showed that fibrocartilaginous regions were present in the CCL and were mainly observed in predisposed dog breeds to CCLD/ R. Furthermore, immunohistochemistry analysis showed that each proteoglycan had a different distribution throughout the CCL, which indicates that proteoglycans provide essential functionality to the CCL. The increase of certain proteoglycans and GAGs in CCLs of Staffordshire bull terriers might indicate increased fibrocartilage regions as a result of compressive loads. These changes in ECM content in the Staffordshire bull terrier indicate higher loading pressure on the CCL and could compromise the tissue, leading to increased incidence of disease and rupture. The increase of decorin in greyhounds could be essential for maintaining collagen fibril strength, whilst the increase of ADAMTS-4 could indicate a higher rate of turnover to regulate normal CCL homeostasis.

TABLE OF CONTENTS

INDEX OF FIGURES

INDEX OF TABLES

LIST OF ABBREVIATIONS

ACL	Anterior cruciate ligament
ADAMTS	A Disintegrin-like and Metalloproteinase with Thrombospondin Motifs
ANOVA	Analysis of variance
B2M	Beta-2 microglobulin
BMP-1	Bone morphogenetic protein 1
BSA	Bovine serum albumin
CaCL	Caudal cruciate ligament
CCL	Cranial cruciate ligament
CL	Cruciate ligament complex
cDNA	Complementary Deoxyribonucleic acid
ChABC	Chondroitinase ABC
CLB	Craniolateral band
CMB	Craniomedial band
DMMB	Dimethyl-methylene blue
DAB 3,3'	Diaminobenzidine
DNA	Deoxyribonucleic acid
DNase	Deoxyribonuclease
D.P.X.	Di-n-butyl phthalate in xylene
ECM	Extracellular matrix
EDTA	Ethylenediaminetetraacetic acid
EGF	Epidermal growth factor
ELISA	Enzyme-linked Immunosorbent Assay
ER	Endoplasmic reticulum

GAPDH	Gylceraldehyde 3-Phosphate Dehydrogenase
G	Globular
GAGs	Glycosaminoglycans
Gal	Galactose
GalN	Galactosamine
GlcN	Glucosamine
GlcUA	Glucoronic acid
H & E	Hematoxylin and Eosin
HCl	Hydrochloride
IdUA	Iduronic acid
Ig	Immunoglobulin
kDa	Kilo Dalton
LLRs	Leuicne rich repeats
M	Molar
MCL	Medial collateral ligament
mg	Miligram
ml	Mililitre
mM	Millimolar
MMP	Matrix Metalloproteinase
mTLD	Mammalian tolloid
N/ A	Not available
Nm	Nanomolar
OD	Optical density
PBS	Phosphate buffer saline

PNPP	P-nitrophenyl alkaline phosphatase substrate
PDGF	Platelet derived growth factor
RNA	Ribonucleic Acid
RT-qPCR	Reverse transcription quantitative real-time-PCR
SDS-PAGE	Sodium dodecyl sulphate polyacrylamide gel electrophoresis
SLRPs	Small leucine rich proteoglycans
sGAG	Sulphated glycosaminoglycans
SEM	Standard error of the mean
TEM	Transmission electron microscopy
TIMP	Tissue inhibitor of metalloproteinase
TBS	Tris-buffered saline
TLL-1	Tolloid like 1
TPA	Tibial plateau angel
Tris	Trizma
µl	Microlitre
UA	Uronic acid

DEDICATION

May god bless my family for their love, care and discipline, to which made it possible for me to undertake this study.

ACKNOWLEDGEMENTS

I wish to express my heartfelt appreciation and thanks to my primary supervisor, Dr. Eithne Comerford, who not only gave me the opportunity to undertake this work, but also with enthusiasm gave her advice, care, support, and faithful contribution to my study. I would also like to thank Prof. Peter Clegg, Dr. Simon Tew, and Dr. Elizabeth laird, for their time and guidance through processes of this research project. Many thanks to Dr. Peter Millner and Dr. Rachel Oldershaw for being my advisors. I also acknowledge Prof. Bruce Caterson and Dr. Clare Hughes for providing sufficient materials to undertake my project. Thanks to my colleagues in the department of musculoskeletal biology I; Yalda, Donae, Kate, Ben, Fai, Alan, Mandy, Rhiannon, Loiuse, Eleri, Othman, Jade, James, Karen, Katie and Megan, for their continuous advice and help with laboratory techniques. I would also like to thank my house mates; Bethan and Hannah, for their care, entertainment, and company.

Finally, I wish to express my deep appreciation to my family for their funding and support throughout all the years of my studies.

AUTHOR'S DECLARATION

I declare that the work in this dissertation was carried out in accordance with the regulations of the University of Liverpool. The work is original except where indicated by references in the text.

Any views expressed in this thesis are those of the author and in no way represent those of the University of Liverpool.

This thesis has not been presented to any other university for examination in the United Kingdom or overseas.

Chapter 1: Introduction.

1.1 **Ligament overview**

Ligaments are a unique type of connective tissue which function to stabilise the joint and have interesting biomechanical properties (Frank 2004). Ligaments have been shown to differ from one another in regard to their biochemical composition and structural morphology, depending on their location within the skeletal joint (Amiel, Frank et al. 1984; Rumian, Wallace et al. 2007).

1.1.1 **Gross appearance**

Ligaments can be classified into two subgroups that classify ligaments; skeletal ligaments which cross joints, and non-skeletal ligaments, which adhere to soft tissue such as abdominal suspensory ligaments (Frank, Amiel et al. 1985). A normal healthy skeletal ligament consists of a white, homogenous, dense connective tissue (Frank, Amiel et al. 1985).

1.1.2 **Hierarchical microstructure**

The hierarchical microstructure of ligaments is similar to what has been reported in tendon, consisting of collagen fibre bundles, fibres, subfibrils, microfibrils, and tropocollagen (Kastelic, Galeski et al. 1978) (Figure 1-1). In ligament, collagen fibre bundles are divided by cells (Amiel, Frank et al. 1984; Clark and Sidles 1990) and bundles are grouped into interdigitating structures named fascicles (Clark and Sidles 1990). Fascicles are separated by a septae (Clark and Sidles 1990), and are enveloped in a thin connective sheath named endoligament (Chowdhury, Matyas et al. 1991). The endoligament is connected to the epiligament, which is a vascular tissue (Chowdhury, Matyas et al. 1991). Collagen fibre bundles harbour a crimping pattern which is crucial for ligament elongation and recoiling without continuous damage (Frank, Amiel et al. 1985).

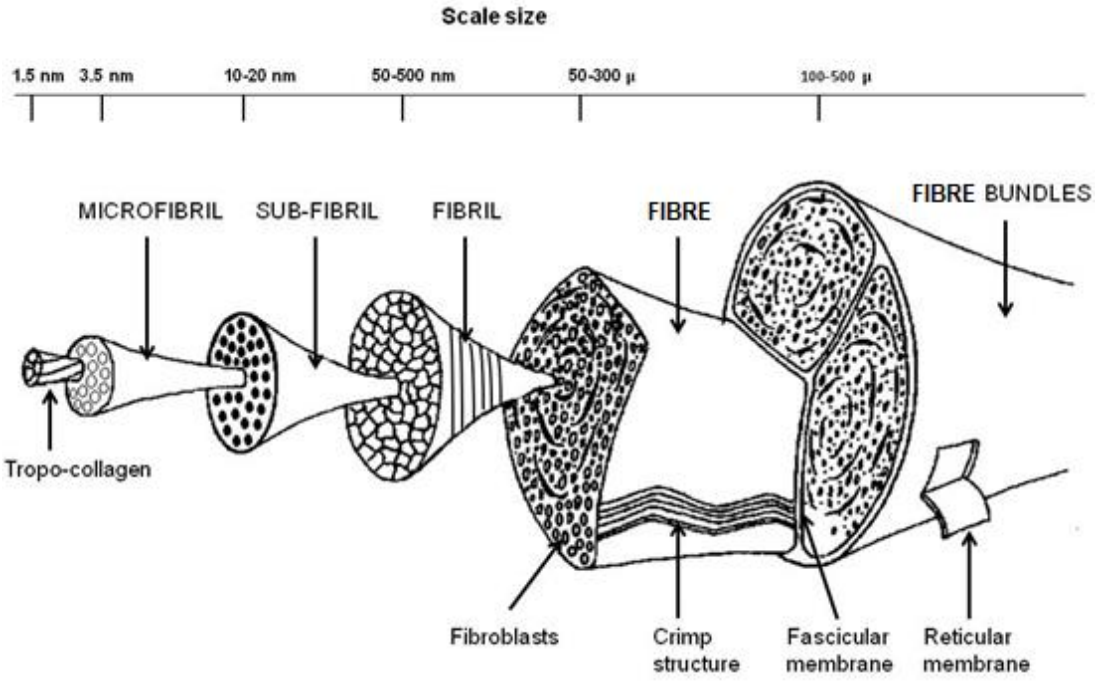

Figure 1-1: The hierarchical structure of tendons and ligaments.

(Adapted from Kastelic, Galeski et al. 1978).

1.1.3 **Cells**

Cells in the ligament substance are primarily fibroblasts which can range in shape from spindle-shaped to rounded (Arnoczky 1983; Zhu, Zhang et al. 2012; Kharaz 2015). These fibroblastic cells are named ligamentoblasts in immature tissue (Heffron and Campbell 1978). As the tissue matures, they appear spindled shaped and are then termed ligamentocytes (Heffron and Campbell 1978). In ligament, cells are known to harbour gap junctions, which allow direct cell to cell communication (Lo, Ou et al. 2002; Chi, Rattner et al. 2005). Gap junctions are found at the end of the cytoplasmic processes which form a 3-dimensional network within the tissue (McNeilly 1997; Lo, Marchuk et al. 2001). Long cytoplasmic processes that extend to adjacent cells have been observed in the healthy medial collateral ligament and cruciate ligaments (Lo, Ou et al. 2002; Smith, Vaughan-Thomas et al. 2012).

1.1.4 **Function**

Ligaments transfer load from bone to bone (Benjamin, Evans et al. 1986). They passively stabilise joints and so aid in regulating joint motion (Frank 2004). Ligaments are also viscoelastic in nature and this is essential for normal joint homeostasis, as they display a viscoelastic behaviour when they creep (stretching of the ligament with continuous load) and relax (the force necessary to maintain a

fixed position as it decreases overtime) (Frank 2004). Furthermore, they play a role in proprioception (Frank 2004; Birch, Thorpe et al. 2013), which is predominantly provided by the joint, muscle and cutaneous receptors (Frank 2004).

Ligaments and tendons attach to bone in two different ways; either by a fibrocartilaginous attachment or a fibrous attachment (Benjamin and Ralphs 1998). The different mechanical environment of ligaments however, leads to the variation of their attachment sites (Benjamin, Qin et al. 1995). A fibrocartilaginous attachment has a role in dispersing stresses by supplying a gradual transition in mechanical properties between tendon/ ligament and bone (Benjamin, Evans et al. 1986; Woo, Maynard et al. 1988). The cruciate ligaments are a good example of a fibrocartilage attachment, as the cruciate ligaments attach to bone by four gradual stages; ligament, fibrocartilage, mineralised fibrocartilage, and finally bone (Benjamin, Qin et al. 1995). Fibrocartilage in tendon has a similar phenotype to cartilage, and can be distinguished from the non-fibrocartilage sites in tendon by four main characteristics; loss of the parallel arrangement of collagen fibre bundles; the presence of type I and type II collagen in similar ratios; the accumulation of the large aggregating proteoglycan aggrecan and; the presence of fibrocartilage cells (rounded nucleus with halo formation) (Vogel 2004), and these changes may also relate to fibrocartilaginous sites in ligament.

1.2 Cruciate ligaments

1.2.1 Introduction

The canine stifle joint is extremely complex and relies on ligamentous support to maintain its strength (Tirgari and Vaughan 1975). Within the stifle joint, there are four major ligaments that provide passive support to the canine stifle joint namely the cranial cruciate, caudal cruciate, medial collateral, and lateral collateral ligaments (Carpenter and Cooper 2000). The cruciate ligament (CL) complex in the dog is composed of two ligaments; cranial (CCL) and caudal (CaCL) (anterior (ACL) and posterior (PCL) for human and other species) (Arnoczky and Marshall 1977) (Figure 1-2). These two ligaments wrap around each other and lie underneath the femoral intercondylar notch (Arnoczky and Marshall 1977). The CL complex is vital in providing internal rotation and cranial-caudal support of the stifle (knee) joint (Arnoczky and Marshall 1977; Stouffer, Butler et al. 1983).

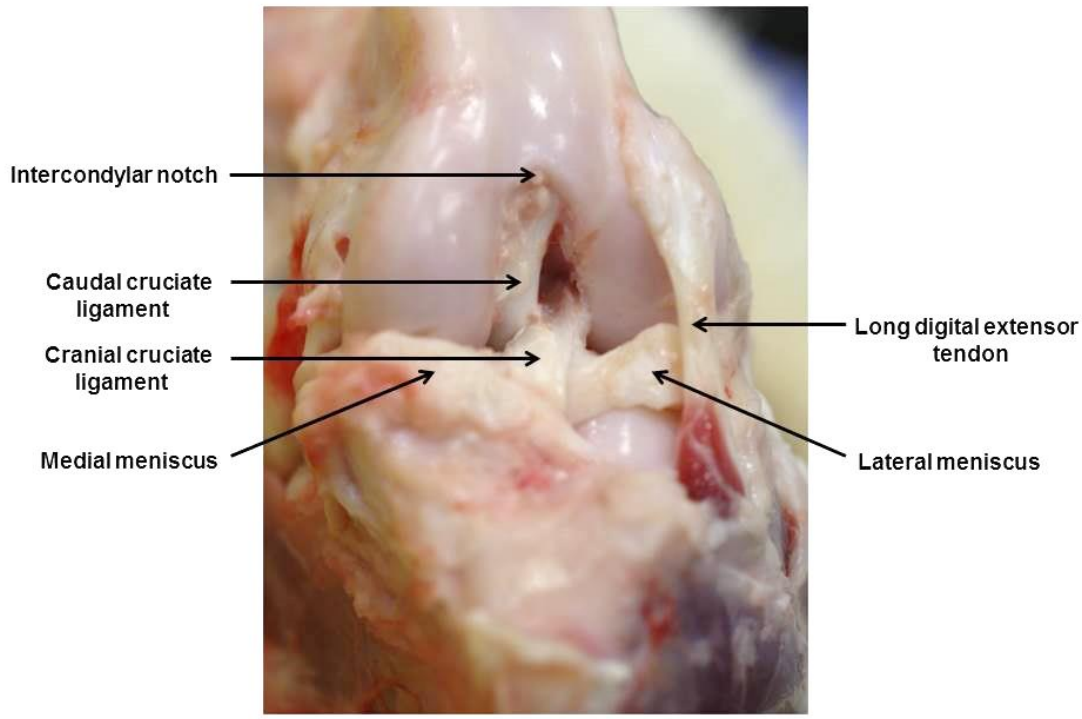

Figure 1-2: Canine stifle joint anatomy.

The patellar tendon has been removed to observe the cruciate ligaments.

1.2.2 **Anatomy**

The CCL origin site starts from the medial side of the lateral femoral condyle and wraps around the CaCL (Arnoczky and Marshall 1977). The CCL runs cranially, medially, and distally to insert into the intercondylar areas of the tibia (Arnoczky and Marshall 1977). The canine CCL is distinguished by having a proximal to distal outward spiral appearance of approximately 90° (Arnoczky and Marshall 1977). This spiral configuration gives the CCL the appearance of two bands which alter in function with flexion and extension of the stifle joint; the craniomedial (CMB) and caudolateral (CLB) band (anteriomedial AMB and posteriolateral PMB in man and other species) (Arnoczky and Marshall 1977) (Figure 1-3). The CMB is spiral in shape and is in tension during extension and flexion, whereas the CLB is shorter and straighter and is under greatest tension during extension but becomes relaxed during flexion (Heffron and Campbell 1978; Arnoczky, Rubin et al. 1979). When comparing the two bands, the CMB is longer than the CLB (Heffron and Campbell 1978; Arnoczky, Rubin et al. 1979). The CLs are known to be intra-articular, but they remain extra-synovial as the synovium surrounds the CLs (Arnoczky, Rubin et al. 1979). The anatomical location of the CaCL is different from the CCL as it originates from the medial aspect of the tibial popliteal notch and inserts into the lateral aspect of the medial femoral condyle (Arnoczky and Marshall 1977). The CaCL is comprised of two bands; the large cranial band and the smaller caudal band (Arnoczky and Marshall 1977). When the stifle joint is extended, the small caudal band is taut in flexion and loose in extension and the bigger cranial band is loose in flexion and taut in extension (Arnoczky and Marshall 1977).

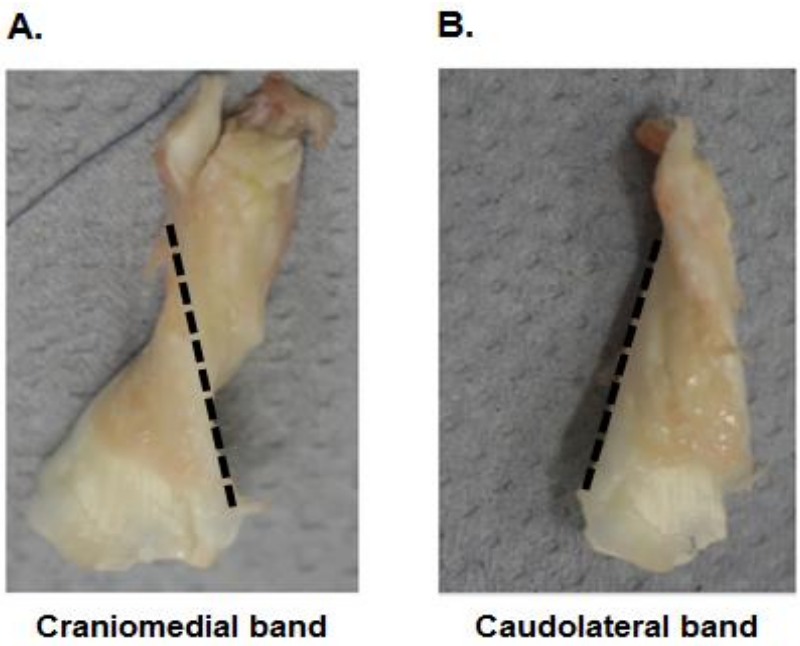

Figure 1-3: Canine cranial cruciate ligament (CCL).

A) CCL craniomedial band (black dashed line). B) CCL caudolateral band (black dashed line).

1.2.3 **Blood supply**

The middle genicular artery is the main blood supply for the canine stifle joint (Tirgari 1978; Arnoczky, Rubin et al. 1979). The blood supply of the cruciate ligaments comes primarily from the synovial vessels and infrapatellar fat pad (Tirgari 1978, Arnoczky, Rubin et al. 1979). The CaCL synovial vessels are known to be more richly supplied compared to the CCL (Arnoczky, Rubin et al. 1979). The synovial vessels then transition into a finely meshwork network of periligamentous vessels which cover the CLs entirely (Arnoczky, Rubin et al. 1979; Kobayashi, Baba et al. 2006). Endoligamentous vessels are known to enrich the collagen fibrils of the cruciate ligaments (Arnoczky, Rubin et al. 1979). Epiligamentous vessels anastomose with the endoligamentous vessels by infiltrating transversely into the CLs (Arnoczky, Rubin et al. 1979; Kobayashi, Baba et al. 2006). The blood supply of the CL complex is minor due to its location in the transarticular area of the stifle joint (Clark and Sidles 1990; De Rooster, De Bruin et al. 2006), and both CCL and CaCLs are reported to have less blood supply in the core region (Tirgari 1978; Vasseur, Pool et al. 1985; Narama, Masuoka-Nishiyama et al. 1996).

1.2.4 **Nerve supply**

The three major articular nerves that innervate the canine stifle joint are the saphenous nerve, tibial nerve, and the common peroneal nerve (O'Connor and Woodbury 1982). The largest nerve supply of the stifle joint is the medial articular nerve that originates from the major saphenous nerve (O'Connor and Woodbury 1982). The nerve fibres of the CCL arise from the tibial nerve branches, as they enter the caudal joint capsule and pass along the ligament, and are surrounded by the synovial and periligamentous tissue (Arnoczky 1983). Mechanoreceptors play a role in proprioception of the knee joint (Johansson, Sjolander et al. 1991; Dhillon, Bali et al. 2012). It has been reported that the highest number of mechanoreceptors were found at the proximal one third of the CCL, whilst the lowest number of were found at the distal third of the CCL (Arcand, Rhalmi et al. 2000). Depletion of mechanoreceptors has been linked with ageing in rabbit anterior cruciate ligament (Aydog, Korkusuz et al. 2006).

1.2.5 **Functional anatomy**

The cruciate ligaments are very important for the maintenance of craniocaudal, mediolateral, and rotatory stability of the stifle joint (Arnoczky and Marshall 1977). They prevent cranial translation of the tibial on the femur and resist tibial rotation to a lesser degree (Arnoczky and Marshall 1977). During stifle flexion, the CMB is elongated and the CLB is shortened (Arnoczky and Marshall 1977; Heffron and Campbell 1978). The importance of the CaCL in knee stability is less clear, its primary function is to limit caudal translation of the tibia on the femur (Arnoczky and Marshall 1977).

1.3 **Ligament extracellular matrix components**

The biochemical composition of ligament has been well described (Frank 2004; Rumian, Wallace et al. 2007). Two-thirds of the wet weight of ligaments is composed of water with collagen being the principle solid component of the remainder, comprising 70-80 % of the ligament dry weight (Frank 2004). Collagen type I is the predominant collagen in ligament (Frank 2004; De Rooster, De Bruin et al. 2006), accounting for nearly of 90% of the total collagen with the remainder commonly made up of types III, VI, V, XI and XIV (Frank 2004).

1.3.1 **Collagen**

1.3.1.1 **Collagen biosynthesis**

Fibril forming collagens are secreted as procollagens (Myllyharju and Kivirikko 2004). Procollagen is composed of a C-terminal propeptide and an N-terminal propeptide (Myllyharju and Kivirikko 2004). Several enzymes associated with procollagen processing are involved in regulating the initial formation of collagen into fibrils. The C-propeptides are processed by tolloid family members including bone morphogenetic protein 1 (BMP-1), mammalian tolloid (mTLD), tolloid like 1 (TLL-1) or furin (Scott, Blitz et al. 1999; Unsold, Pappano et al. 2002; Gopalakrishnan, Wang et al. 2004). N-propeptides processing is carried out by the disintegrin and metalloproteinase with thrombospondin like motifs proteases family (ADAMTS) namely ADAMTS-2, ADAMTS-3, and ADAMTS-14 (Colige, Li et al. 1997; Fernandes, Hirohata et al. 2001; Colige, Vandenberghe et al. 2002). After propeptides are processed, collagen molecules can spontaneously assemble into fibrils with a distinctive D-periodic surface structure (Canty and Kadler 2005).

1.3.1.2 **Collagen types**

The common collagen types in ligaments are similar to what has been reported for tendon (Birch, Bailey et al. 1999; Riley 2004; Riley 2005). The fibril forming collagen type I is the main collagen in tendon (Birch, Bailey et al. 1999; Kadler, Baldock et al. 2007), The second most common is collagen type III, which is another fibril forming collagen and is known to regulate collagen type I fibrillogenesis (Riley 2005: Kadler, Baldock et al. 2007). Type II and XI are also fibril forming collagens, however, collagen type II is restricted to the fibrocartilaginous sites of tendon (Riley 2005). Type V collagen provides a template for fibril formation as it is commonly located in the core of type I fibrils (Riley 2004). Other types of collagen include those forming beaded filaments (type VI), and the fibril associated collagens with interrupted triple helices (type XIV) (Riley 2005).

1.3.2 **Elastin**

Elastic fibres are widely distributed in connective tissues such as skin, lungs and ligaments (Kielty, Sherratt et al. 2002). Their structural role is to provide tissues with elastic recoil and flexibility (Kielty, Sherratt et al. 2002). Elastin content varies between different ligament tissues and species (Uitto 1979; Nakagawa, Mikawa et al. 1994; Smith, Clegg et al. 2014; Kharaz 2015). In canine CCL, elastin has been shown to comprise approximately 10 % of its dry weight in greyhounds (Smith,

Clegg et al. 2014), and 4.6 % of its dry weight in Staffordshire bull terriers (Kharaz 2015).

1.3.3 **Glycoproteins**

Glycoproteins are defined as a core protein covalently linked to a carbohydrate, and contain a monosaccharide or a polysaccharide (Sharon 1986). Proteoglycans are a subtype of glycoproteins where the core protein is attached to one or more polysaccharide chains consisting of amino sugars and termed glycosaminoglycans (Sharon 1986).

1.3.4 **Glycosaminoglycans**

Glycosaminoglycans (GAGs) are covalently attached to a proteoglycan core protein with the exception of hyaluronic acid (Hardingham 1981; Ajit Varki 2009). They consist of a long branched polysaccharide chain, and one or more of the repeating units containing either an acidic, carboxylate or sulphate group (Hardingham and Fosang 1992; Ajit Varki 2009). GAGs comprise a hexosamine (i.e, glucosamine (GlcN) or galactosamine (GalN)), an uronic acid (glucoronic acid (GlcUA) and or iduronic acid (IdUA)) or galactose (Gal) (Hardingham and Fosang 1992). The hexosamine composition of the repeating disaccharide is mostly N-acetylated and both sugar components of the disaccharide can be sulphated as well (Ajit Varki 2009). These sugar and disaccharide units are linked by different glyosidic linkages (a1-4, b1-3, or b1-4) (Hardingham and Fosang 1992; Ajit Varki 2009). Within the sugar hydroxyl groups, the carboxyl groups of the two hexuronic acid isomers GlcUA and IdUA and the existence of sulphation on both or either of the disaccharide sugars produces a very strong negative charge on GAG chains (Hardingham and Bayliss 1990). This negative charge creates a high affinity for water and ment that GAGs bind to many cationic molecules present in cells and tissue matrices (Hardingham and Bayliss 1990).

There are seven different types of GAGs in mammalian tissue, namely; hyaluronic acid or hyaluronan, chondroitin sulphate-4, chondroitin sulphate-6, dermatan sulphate, keratan sulphate, and heparin/heparan sulphate (Hardingham 1981). Unlike other types of GAGs, hyaluronic acid is not further processed by sulphation or by epimerisation of glucuronic acid to iduronic acid (Ajit Varki 2009). The structures of GAGs are illustrated in Figure (1-4). GAGs have been shown to regulate collagen fibrillogenesis (Redaelli, Vesentini et al. 2003; Douglas, Heinemann et al. 2006; Ruehland, Schonherr et al. 2007).

Hyaluronic acid

Hyaluronic acid is composed of repeating sugar units of glucuronic and N-acetyl glucosamine that are unsulphated, giving it a much less complex structure than the other sulphated GAGs (Hardingham and Fosang 1992; Ajit Varki 2009). Hyaluronan exhibits a high degree of viscosity and viscoelastic properties (Ajit Varki 2009). It is important for lubricating the vitreous humour of the eye and joints (Ajit Varki 2009). In the synovial fluid of articular joints, hyaluronan functions to transmit load during joint movement thus protecting the cartilage surface (Ajit Varki 2009).

Keratan sulphate

Keratan sulphate is composed of disaccharide repeats of N-acetyl glucosamine and galactose (Hardingham and Fosang 1992; Funderburgh 2000). The unique feature of keratan sulphate is that it does not contain an uronic acid (Funderburgh 2000). Within the mammalian tissue, there are three types of keratan sulphates namely keratan sulphate I (corneal keratan sulphate) (Antonsson, Heinegard et al. 1991; Hardingham and Fosang 1992), keratan sulphate II (skeletal keratan sulphate) (Hardingham and Fosang 1992; Fukuda, Tsuboi et al. 1999), and keratan sulphate III (found in the brain tissue) (Chai, Yuen et al. 1999).

Chondroitin sulphate

Chondroitin sulphate is abundant in bone and articular cartilage (Sato, Rahemtulla et al. 1985; Bayliss, Osborne et al. 1999). It is composed of disaccharide repeats of glucuronic acid and N-acetyl galacotosamine (Hardingham and Fosang 1992; Ajit Varki 2009).

Dermatan sulphate

Dermatan sulphate is an alternative form of chondroitin sulphate in which some of its glucuronic acid residues have undergone C-5 epimerisation into iduronic acid (Hardingham and Fosang 1992). It is composed of disaccharide repeats of iduronic acid and N-acetyl galacotosamine (Hardingham and Fosang 1992; Trowbridge and Gallo 2002). Dermatan sulphate is found in tendon, cartilage, skin, sclera and other connective tissues (Rosenberg, Choi et al. 1986). 2-sulphated residues are more commonly found with dermatan sulphate rather than chondroitin sulphate (Hardingham and Fosang 1992).

Heparin and Heparan sulphate

Heparin and heparan sulphate are compound structures that consist of a repeating disaccharide unit of N-acetylated glucosamine or N-sulphated glucosamine, iduronic acid, and glucuronic acid (Hardingham and Fosang 1992). Some of the glucuronic acid residues may be epimerised to iduronic acid (Carlsson, Presto et al. 2008). Heparin and heparan sulphate differ in many aspects (Ajit Varki 2009). Heparin is synthesised in connective tissue mast cells, whilst heparan sulphate is found on cell surfaces and matrix proteoglycans (Hardingham and Fosang 1992; Ajit Varki 2009). Furthermore, the anticoagulant activity of heparan sulphate is much less than that of heparin (Ajit Varki 2009). In terms of biosynthesis, heparin undergoes more extensive sulphation and uronic acid epimerisation than that of heparan sulphate (Hardingham and Fosang 1992; Ajit Varki 2009).

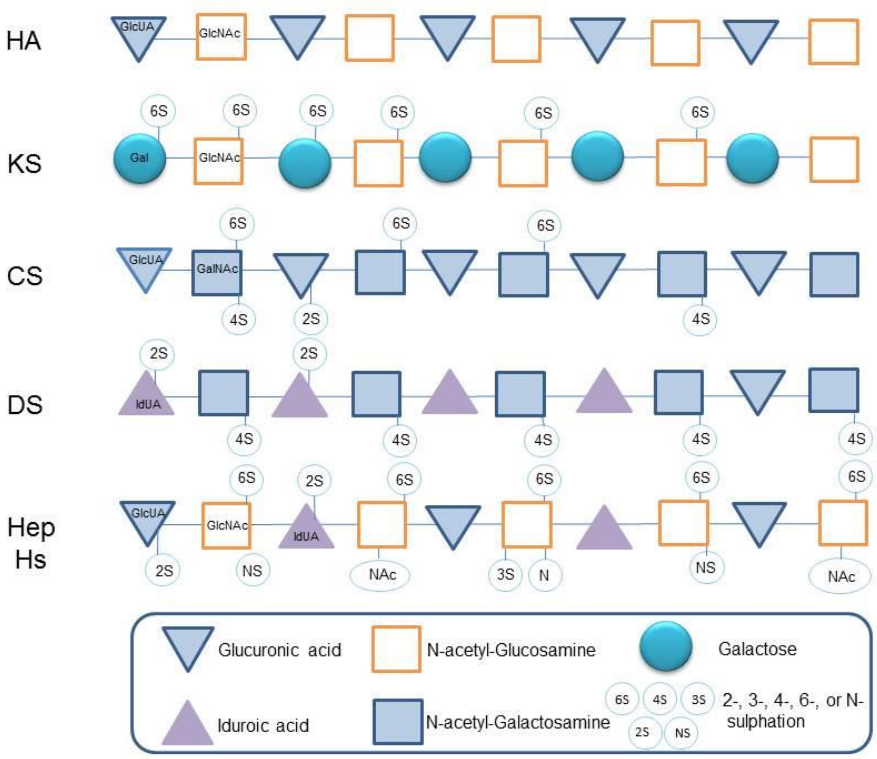

Figure 1-4: The structural variations of glycosaminoglycans (GAGs).

The disaccharide repeating units of hyaluronan (HA), keratan sulphate (KS), chondroitin sulphate (CS), dermatan sulphate (DS), and heparin (Hep)/ heparan sulphate (HS) contains of a hexosamine [either glucosamine (GlcN) or galactosamine (GalN) in squares], and a uronic acid [either glucuronic (GlcUA) or iduronic acid (IdUA) in triangles] or galactose (Gal) in circles. The hexosamine, uronic acid and galactose sugars in every disaccharide unit can be substituted as well with sulphate groups on the sugar hydroxyls at the 2-(2S), 3-(3S), 4-(4S) and 6-(6S) sites. The hexosamine is regularly N-acetlyated (NAc), but in Hep⁄HS, it can also be non-sulphated (NS) or present as a free amine (N). HA is the only GAG that is not sulphated and is not covalently attached to a proteoglycan core protein (Adapted from Hardingham and Fosang 1992).

1.3.4.1 **Glycosaminoglycan biosynthesis**

Heparan sulphate & chondroitin sulphate/ dermatan sulphate

The synthesis of chondroitin, dermatan, and heparan sulphate is initiated by the development of a neutral trisaccharide of galactose-galactose-xylose at the reducing terminal of the GAG chain (Hardingham 1981). The GAGs are linked by serine or threonine residue that is attached to xylose via an O-linked oligosaccharide (Hardingham 1981). The synthesis begins by transferring xylose to a serine residue, and is catalysed by the enzyme xylosyltranferases (Gotting, Kuhn et al. 2000). Furthermore, two galactose residues are inserted by the activation of galactosyltranferase I (Almeida, Levery et al. 1999; Okajima, Yoshida et al. 1999) and galactosyltransferase II (Bai, Zhou et al. 2001). The linkage region is complete by the addition of one glucuronic acid that is catalysed by the enzyme glucuronosyltransferase I (Kitagawa, Tone et al. 1998). A diagram illustrating the trisaccharide linkage region process is shown in Figure 1-5. The enzymes responsible for the sulphation of chondroitin sulphate N-acetyl galactosamine are 4-O-sulfotransferases and 6-O-sulfotransferases, whereas N-deacetylase and N-sulfotransferases are responsible for the generation of N-sulphated glucosamine units present on N-acetyl galactosamine of heparan sulphate (Ajit Varki 2009).

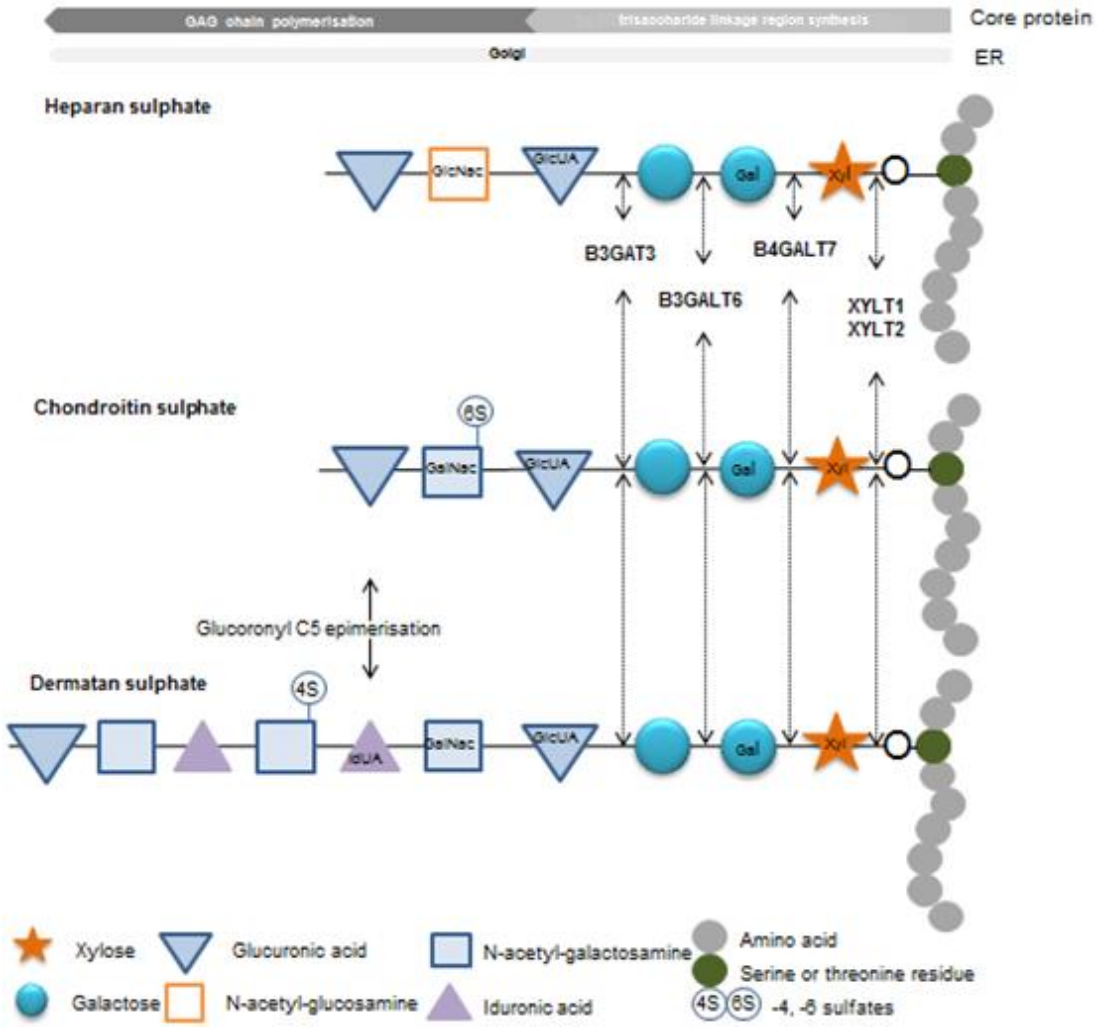

Figure 1-5: Diagrammatic illustration of the biosynthesis process of the heparin sulphate, chondroitin sulphate, and the dermatan sulphate GAG.

The biosynthesis of heparan sulphate, chondroitin sulphate, and dermatan sulphate are initiated by the formation of a linkage region trisaccharide. The GAGs are linked by serine residue that is attached to xylose via an O-linked oligosaccharide. The further addition of two galatose (Gal) and one glucuronic acid (GlcUA) completes the linkage region process. Afterwards, the GAG chains are polymerised to form heparan sulphate, chondroitin sulphate, and dermatan sulphate. The addition of the first hexosamine determines the GAG to be chondroitin sulphate (N-acetyl galactosamine (GalNac)) or heparin sulphate (N-acetyl glucosamine (GlcNac)). Epimerisation of some of the chondroitin sulphate glucuronic acid hexosamines into iduronic acid (IdUA) forms the GAG dermatan sulphate. The following enzymes are essential for the formation of the GAG linkage region; XYLT= xylosyltransferases; B4GALT7= galactosyltransferase I; B3GALT6= galatosyltransferase II; B3GAT3= glucuronosyltransferase I (Adapted from Malfait, Kariminejad et al. 2013).

Keratan sulphate

Keratan sulphate does not contain a neutral trisaccharide (Hardingham 1981). The linkage region of keratan sulphate varies according to the keratan sulphate type (Hardingham 1981). Keratan sulphate I is linked via an N-glycosylamine binding from N-acetyl galactosamine to asparagine (Antonsson, Heinegard et al. 1991; Hardingham and Fosang 1992: Ajit Varki 2009). N-linked oligosaccharides have been found on keratan sulphate proteoglycans such as fibromodulin (Plaas, Neame et al. 1990), lumican, and keratocan (Dunlevy, Neame et al. 1998). In addition, different lengths of keratan sulphate chains have been found on the N-linked oligosaccharide of fibromodulin (Plaas, Neame et al. 1990). Keratan sulphate II is linked by an O-glycosidic bond between N-acetylgalactosamine to serine or threonine (Hardingham and Fosang 1992; Fukuda, Tsuboi et al. 1999; Ajit Varki 2009). Keratan sulphate III is linked via 2-O-mannose, and is attached to the protein core via a serine residue (Chai, Yuen et al. 1999). A diagram illustrating the linkage region process of the three different keratan sulphate types is shown in Figure 1-6.

The two enzymes known to catalyse the sulphation reaction for keratan sulphate hexosamines are N-acetyl glucosamine 6-O sulfotransferases and galactose 6-O sulfotransferases (Ajit Varki 2009). N-acetyl glucosamine 6-O sulphation only occurs at the non-reducing terminal of N-acetyl galactosamine residue, whereas galactose 6-O sulphation occurs at both of the non-reducing terminal and internal galactose residue (Ajit Varki 2009).

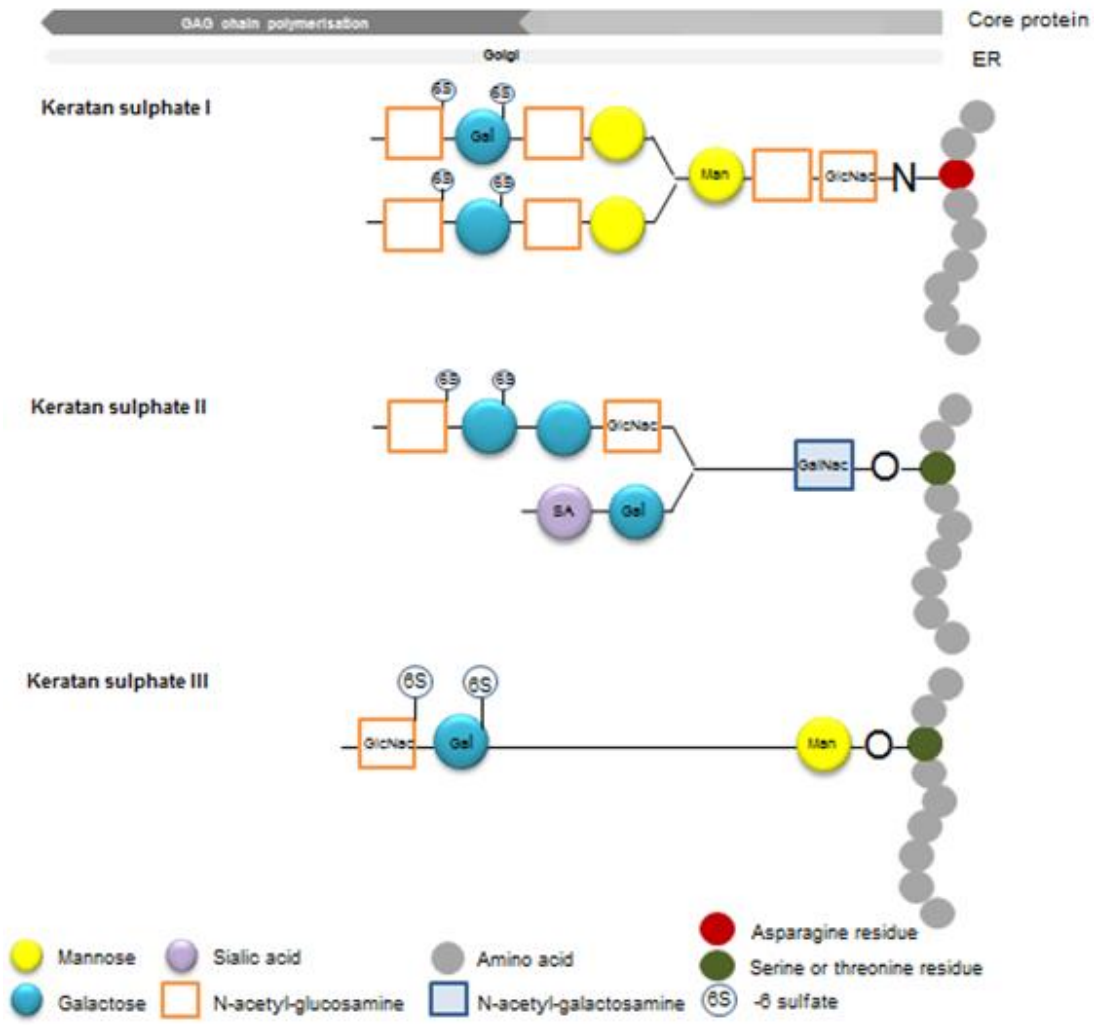

Figure 1-6: Diagrammatic illustration of the biosynthesis process of the keratan sulphate GAG.

The oligosaccharides linking the core protein to keratan sulphate determine the three types of keratan sulphate. Keratan sulphate I is attached to asparagine residue via N-linked oligosaccharides, whereas keratan sulphate II is O-linked to N-acetyl galactosamine to serine or threonine residue via a mucin like core-2 structure. Keratan sulphate III is linked to the protein core by mannose O-linked to serine (Modified from Hardingham and Fosang 1992; Funderburgh 2000).

Hyaluronic acid

Hyaluronic acid biosynthesis occurs at the inner surface of the plasma membrane in eukaryotes, and hyaluronic acid synthases is the main enzyme in catalysing hyaluronic acid (Ajit Varki 2009). Unlike other GAGs, hyaluronic acid biosynthesis does not occur on core proteins of proteoglycans (Ajit Varki 2009).

1.3.5 **Proteoglycans**

Proteoglycans are widely distributed in mammalian tissues and are a large family of macromolecules. However, there are four major classes of proteoglycans; the intracellular, cell-surface, pericellular and ECM proteoglycans (Iozzo and Schaefer 2015; Schaefer and Schaefer 2010). Once proteoglycans are synthesised and secreted into the extracellular matrix (ECM), they are important in contributing to the tensile strength of skin and tendon, transparency of the cornea, viscoelasticity of blood vessels, compressive properties of cartilage, and mineralisation of bone matrices (Iozzo 1999; Iozzo and Schaefer 2015). Proteoglycans are also involved in regulating growth factors and cytokines (Iozzo 1999; Iozzo and Schaefer 2015). These molecules are extremely hydrophilic, and are important for hydrating the ECM.

1.3.5.1 **Proteogycan biosynthesis in skeletal tissues**

The original proteoglycan core protein is synthesised within the rough endoplasmic reticulum where N-linked mannose oligosaccharides are attached (Hassell, Kimura et al. 1986). Most of the posttranslational modification occurs in the Golgi complex which involves one or more of the followings (Figure 1-7) (Hassell, Kimura et al. 1986).

1. Insertion of the glycosaminoglycan chain onto a suitable serine or threonine residue.

2. Insertion of O-linked oligosaccharide onto suitable serine or threonine residues.

3. Alteration of high mannose N-linked oligosaccharides into compound forms.

4. Potential processing of the protein by elimination of portions of the polypeptide.

Once a proteoglycan is formed within the Golgi complex, it is processed depending on the function and the cell type. For example, proteoglycans may be packaged within storage granules as it is the case for heparan sulphate proteoglycans in mast

cells or they may be transported via secretary vesicles to the extracellular space to perform structural roles within connective tissues (Hassell, Kimura et al. 1986).

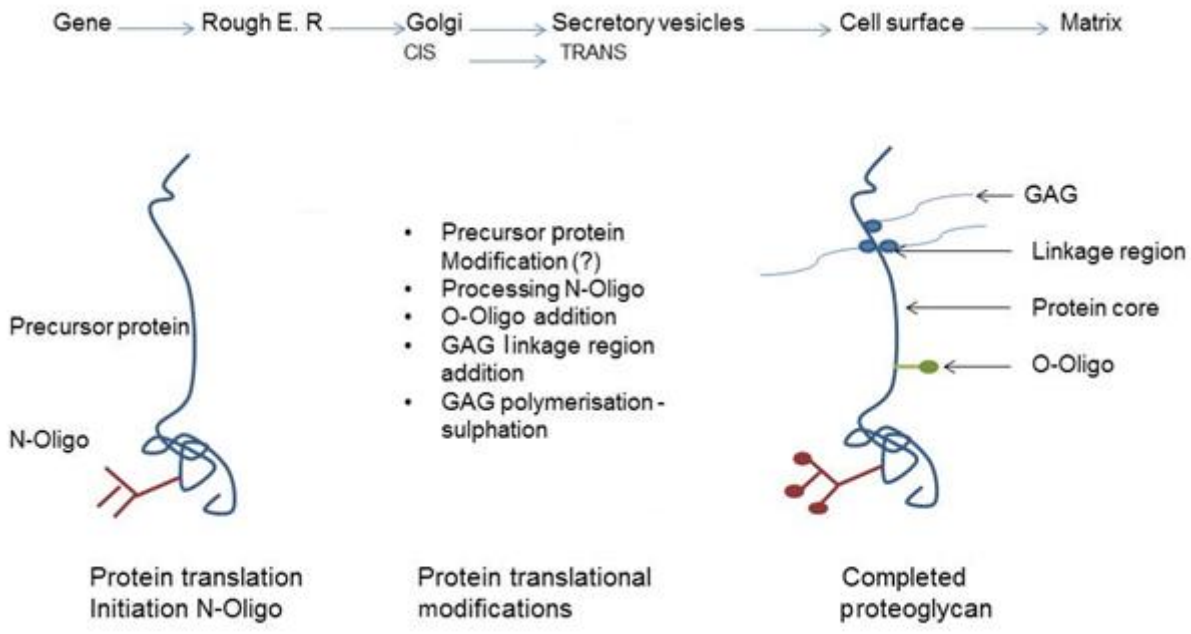

Figure 1-7: Proteoglycan biosynthesis in the skeletal tissue.

(Adapted from Hassell, Kimura et al. 1986).

1.3.5.2 **Hyalectans: proteoglycans interacting with hyaluronan and lectins**

This family is composed of four different types of proteoglycans; versican, aggrecan, neurocan, and brevican (Iozzo and Murdoch 1996; Iozzo 1998; Iozzo and Schaefer 2015). Hyalectans share common features in which they bind to hyaluronan via their globular 1 (G1) domains at their N-terminal regions. They also carry a C-type lectin domain, and an elongated central region that contains the majority of the GAG chains (Iozzo and Murdoch 1996; Iozzo 1998; Iozzo and schaefer 2015). A detailed structure representing the hyalectans can be shown in Figure 1-8.

1.3.5.2.1 **General structural features of hyalectans**

<u>Versican</u>

Versican is the largest proteoglycan member of the hyalectan family (Krusius, Gehlsen et al. 1987) and is also the major hyalectan in bovine collateral ligament (Ilic, Carter et al. 2005). Versican globular domain 1 (G1) consist of an N–terminal G1 domian that binds to hyaluronan, and a C-terminal G3 domain that contains a C-type lectin region near to the complementary regulatory like domain and the epidermal growth factor regions (Naso, Zimmermann et al. 1994). In the middle part

of versican, two large exons are present which code for the glycosaminoglycan chondroitin sulphate, and are called α GAG and β GAG (Dours-Zimmermann and Zimmermann 1994). Versican has four mRNA transcript variants (v) that arise as a result of alternative splicing which are v0, v1, v2, and v3 (Dours-Zimmermann and ZimmermannS 1994; Ito, Shinomura et al. 1995; Iozzo 1998; Schmalfeldt, Dours-Zimmermann et al. 1998). The largest versican variant is variant 0, and variant 0 and 1 are believed to be the major variants in dense connective tissue (Schmalfeldt, Dours-Zimmermann et al. 1998). A diagram illustrating versican structure is shown in Figure 1-8.

Aggrecan

Aggrecan is the main proteoglycan of cartilage (Iozzo 1998), and is the second largest proteoglycan in ligament (Ilic, Carter et al. 2005). Its core protein molecular weight is about 250 000 to 350 000 (Hardingham 1981). Aggrecan interacts with hyaluronan and link protein to form aggregates (Hardingham and Muir 1974; Hardingham, Bayliss et al 1990), and link protein functions to stabilise aggregate formation (Hardingham and Bayliss 1990) (Figure 1-3). These aggregates are non-covalently bound to hyaluronic acid and link protein (Hardingham and Bayliss 1990). Aggrecan is mostly attached to chondroitin sulphate chains, and the remainder are keratan sulphate chains and O- and N- linked oligosaccharides (Hardingham and Fosang 1992). Aggrecan contains three domains (G1, G2, and G3) (Doege, Garrison et al. 1994). The region between the G1 domain and the G2 domain is called the interglobular domain (Doege, Garrison et al. 1994). The G3 domain is located at the carboxylic terminus of the core protein, and is known to be essential for normal post-translational processing of the aggrecan core protein molecule (Zheng, Luo et al. 1998).

Neurocan

Neurocan is a chondroitin sulphate proteoglycan found in early postnatal brain, and plays a role in inhibiting neurite outgrowth *in vitro* (Liu, Cafferty et al. 2006; Tang, Yang et al. 2009). Neurocan's amino and carboxyl – terminal globular domains are homologous with those in aggrecan and versican, sharing 60% similarity (Margolis and Margolis 1994). The interglobular domain is unique however, containing up to 7 GAG attachment sites and shows no homology to other hyalectans (Margolis and Margolis 1994). Neurocan is catabolised during tissue maturation, which results in

loss of its amino terminal globular domain due to proteinase cleavage (Rauch, Karthikeyan et al. 1992).

Brevican

Brevican is the most recently discovered hyalectan of the central nervous system, and is also a chondroitin sulphate proteoglycan, and it contains the shortest GAG-binding domain amongst the hyalectan family (Yamada, Watanabe et al. 1994). Similarly to neurocan, brevican is present *in vivo* either as a full-length proteoglycan or as a processed form (Yamanda, Wantanabe et al. 1994).

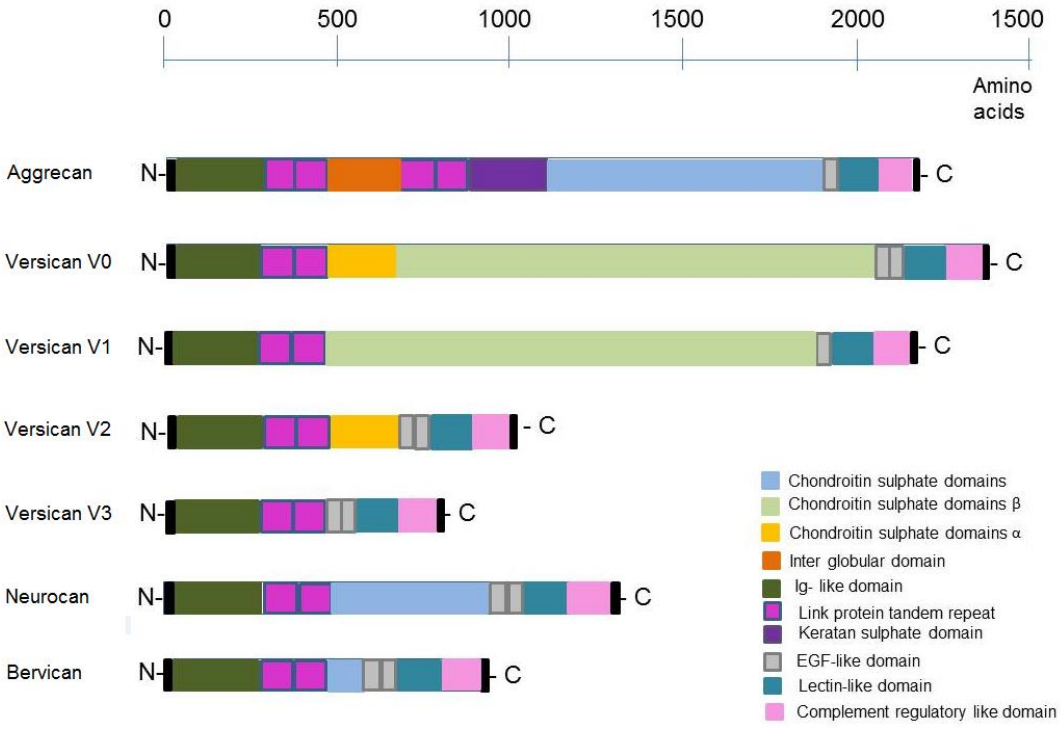

Figure 1-8: A schematic representation of the hyalectan family.

Hyalectans commonly carry hyaluronan and lectin-binding modules and consist of aggrecan, versican splice variants, neurocan and bervican (Modified from Iozzo and Schaefer 2015).

1.3.5.2.2 **Expression and functional control of hyalectans**

Versican

The different transcripts of versican vary within their expression in tissues. For example, versican V0 and V1 are present in fibroblasts, chondrocytes, hepatocytes, myocytes (Dours-Zimmermann and Zimmermann 1994), and tenocytes (Samiric, Ilic et al. 2004), whereas keratinocytes only express versican V1 (Dours-Zimmermann and Zimmermann 1994). In ligament, the three expressed versican variant transcripts are; V0, V1, and V2 (Ilic, Carter et al. 2005).

It has been shown that versican is expressed in tensional and compressional regions of tendon (Vogel and Heinegård 1985; Waggett, Ralphs et al. 1998) Furthermore, versican organises the tendon cells in linear arrays between collagen fascicles present in the pericellular matrix (Ritty, Roth et al. 2003). It interacts with proteins associated with elastin and elastic fibers (Isogai, Aspberg et al. 2002), and interacts with a number of growth factors, such as trasforming growth factor beta TGF-β and platelet derived growth factor (PDGF) (Schonherr, Jarvelainen et al. 1991).

Aggrecan

Aggrecan is predominantly expressed in cartilage (Hardingham 1981), tendon (Rees, Flannery et al. 2000), and ligament (Clements, Carter et al. 2008).

In cartilage, the multiple chondroitin sulphates adhered to aggrecan core protein create a negatively-charged molecule which acts to hydrate the cartilage tissue and regulate its normal homeostasis (Hardingham and Bayliss 1990). When anionic proteoglycans are present in high concentrations, the tissue starts to create a large osmotic swelling pressure drawing water into the tissue which allows the tissue to expand and swell, and this is essential for cartilage to withstand high compressive forces (Hardingham and Bayliss 1990; Kiani, Chen et al. 2002). Aggrecan has also been shown to withstand compressive forces in tendon (Vogel and Heinegård 1985; Waggett, Ralphs et al. 1998). Figure (1-9) shows an example of the components of an aggregating cartilage proteoglycan, aggrecan.

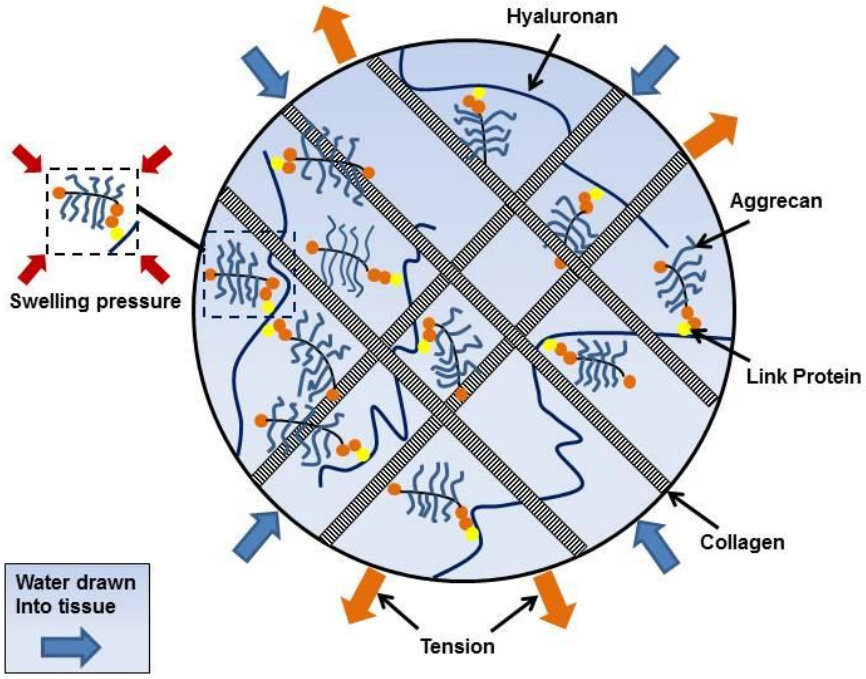

Figure 1-9: Aggrecan in articular cartilage.

The main components of articular cartilage are aggrecan and collagen. The tensile strength of collagen fibres, osmotic swelling pressure, and high quantities of negatively charged aggrecan gives cartilage the ability to withstand compressive forces. Aggrecan forms aggregates with hyaluronic acid and link protein forming a stable meshwork within the matrix (Modified from Kiani, Chen et al. 2002).

Neurocan and brevican

Nuerocan and brevican are expressed in the brain tissue (Oohira, Matsui et al. 1994; Yamada, Watanabe et al. 1994). Neurocan interacts with the ECM protein tenascin-R (Grumet, Milev et al. 1994). It also binds and regulates neural cells (Grumet, Flaccus et al. 1993). Similar to neurocan, brevican has been shown to bind to tenascin–R mediated by a protein-protein interaction (Aspberg, Miura et al. 1997).

1.3.5.3 Small leucine rich-proteoglycan (SLRPs)

The SLRP family has been classified into five groups (Iozzo 1999; Schaefer and Iozzo 2008). These groupings are determined by the number and size of exons, the presence of the N-terminal cysteine rich clusters, and chromosomal orientation (Iozzo 1999). The five groups can be divided into two categories; the canonical (class I-III) and non-canonical (class IV and V) SLRPs (Figure 1-10). Class I-III SLRPs have been found to be present in ligament, tendon, cartilage, eye, and kidney (Waggett, Ralphs et al. 1998; Schaefer and Iozzo 2008; Schaefer 2011; Yang, Culshaw et al. 2011).

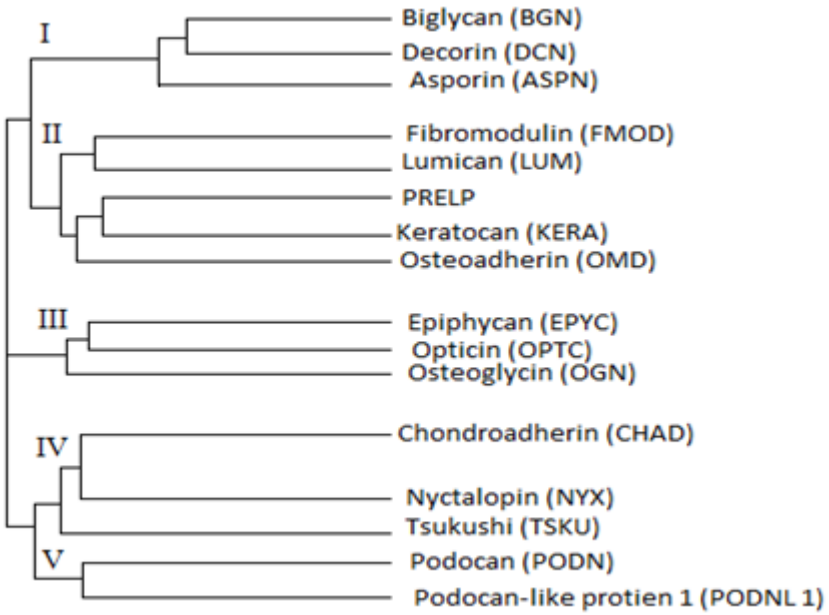

Figure 1-10: A comprehensive category of the small leucine rich proteoglycans (SLRPs) based on their sequence homology.

(Adapted from Schaefer and Iozzo 2008). PRELP= prolargin.

The leucine rich repeat (LRR) structure in SLRPs is flanked by an N- and C-terminal domain at either end of the repeats (Iozzo 1999). SLRPs contain four structural domains (Iozzo 1998). Domain I contains the single peptide and a propeptide (Iozzo 1998). The propeptide is only present in class I SLRPs (Fisher, Termine et al. 1989). Domain II consists of the glycosaminoglycan attachment site and four equally spaced cysteine residues (Iozzo 1998). Domain III contains the LRRs which function to interact with various proteins, and domain IV contains two cysteine residues (Iozzo 1998). A detailed diagram of the four domains of decorin is shown in Figure 1-11.

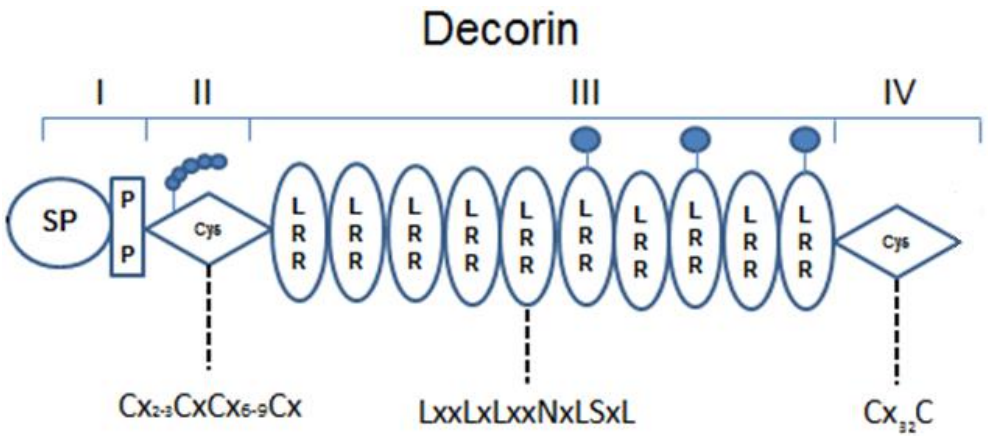

Figure 1-11: Decorin classical four domain structure.

The glycosaminglycans and N-linked oligosaccharide are shown as circles. The consensus sequences of the cysteine residues as well for the leucine rich repeat are indicated (Adapted from Iozzo 1998). SP= single peptide, PP= propeptide, Cys= cysteine region, LRR= leucine rich repeat.

LRRs have been reported to be folded containing both concave and convex surfaces. In addition, the LRRs of SLRPs have been provided with a “horseshoe” shaped structure (Scott 1996; Weber, Harrison et al. 1996). However, X-ray data indicate that decorin 12 LRRs have a “banana-shaped” structure (Scott, McEwan et al. 2004), and it has been described that decorin LRRs are short which might be responsible for the banana shaped structure (McEwan, Scott et al. 2006). This suggests that SLPRs other than decorin might also have a bannana shaped structure.

Decorin LRR 11 extends laterally where its C-terminal conserved cysteine residue forms a disulphide bond with another cysteine residue in the last LRR 12 therefore creating an “ear repeat”. This “ear repeat” feature has been similarly shown for other SLRPs (class I-III) where their C-terminal conserved cysteine residue spans from the beginning to the last LRR (Scott, McEwan et al. 2004). It has been proposed that decorin dimerises through the concave surfaces of its LRR domains, and this could indicate that other SLRPs dimerise as well (Scott, McEwan et al. 2004). The dimerisation of decorin could be essential for its role in collagen fibrillogenesis (Weber, Harrison et al. 1996).

1.3.5.3.1 **Structural differences between class I-III SLRPs**

Class I

This class contains decorin, biglycan, and asporin (Iozzo 1999; Schaefer and Iozzo 2008). Their unique feature is that they contain a typical cysteine cluster that forms two disulphide bonds (Iozzo 1999; Schaefer and Iozzo 2008). Decorin consists of one GAG attachment site which is either linked to a chondroitin or dermatan sulphate chain (Hardingham and Fosang 1992; Schaefer and Iozzo 2008). Decorin molecular weight has been found to be approximately 40 kDa in cartilage, tendon and ligament (Rees, Flannery et al. 2000; Melrose, Fuller et al. 2008; Yang, Culshaw et al. 2011).

Biglycan carries two chondroitin or dermatan sulphate chains (Hardingham and Fosang 1992; Schaefer and Iozzo 2008). The molecular weight of biglycan has been found to be similar to decorin (approximately 40 kDa) in cartilage, tendon and ligament (Rees, Flannery et al. 2000; Melrose, Fuller et al. 2008; Yang, Culshaw et al. 2011). Asporin is known to be an exception for this class, as it does not carry glycosaminoglycan side chains (Schaefer and Iozzo 2008). A diagram of class I and II SLRPs is shown in Figure 1-12.

Class II

This class includes fibromodulin, lumican, keratocan, osteoadherin, and prolargin (PRELP) (Schaefer and Iozzo 2008; Iozzo and Schaefer 2015). They are linked to keratan sulphate or polylactosamine, a non-sulphated form of keratan sulphate (Schaefer and Iozzo 2008). All class II SLRPs contain a tyrosine rich domian with the exception of PRELP. The molecular weights for fibromodulin and lumican are around 50 kDa in cartilage and ligament (Melrose, Fuller et al. 2008; Yang, Culshaw et al. 2011), whilst the molecular weight of keratocan has been found to be 30 kDa

in cartilage and tendon after enzymatic removal of its keratan sulphate chains (Melrose, Fuller et al. 2008; Rees, Wagget et al. 2009). A diagram of class I and II SLRPs is shown in Figure 1-12.

Class III

This class consists of epiphycan, opticin, and osteoadherin (Schaefer and Iozzo 2008; Iozzo and Schaefer 2015). They contain a low number of leucine rich repeats (seven leucine rich repeats) and have a genomic organisation of seven exons (Schaefer and Iozzo 2008).

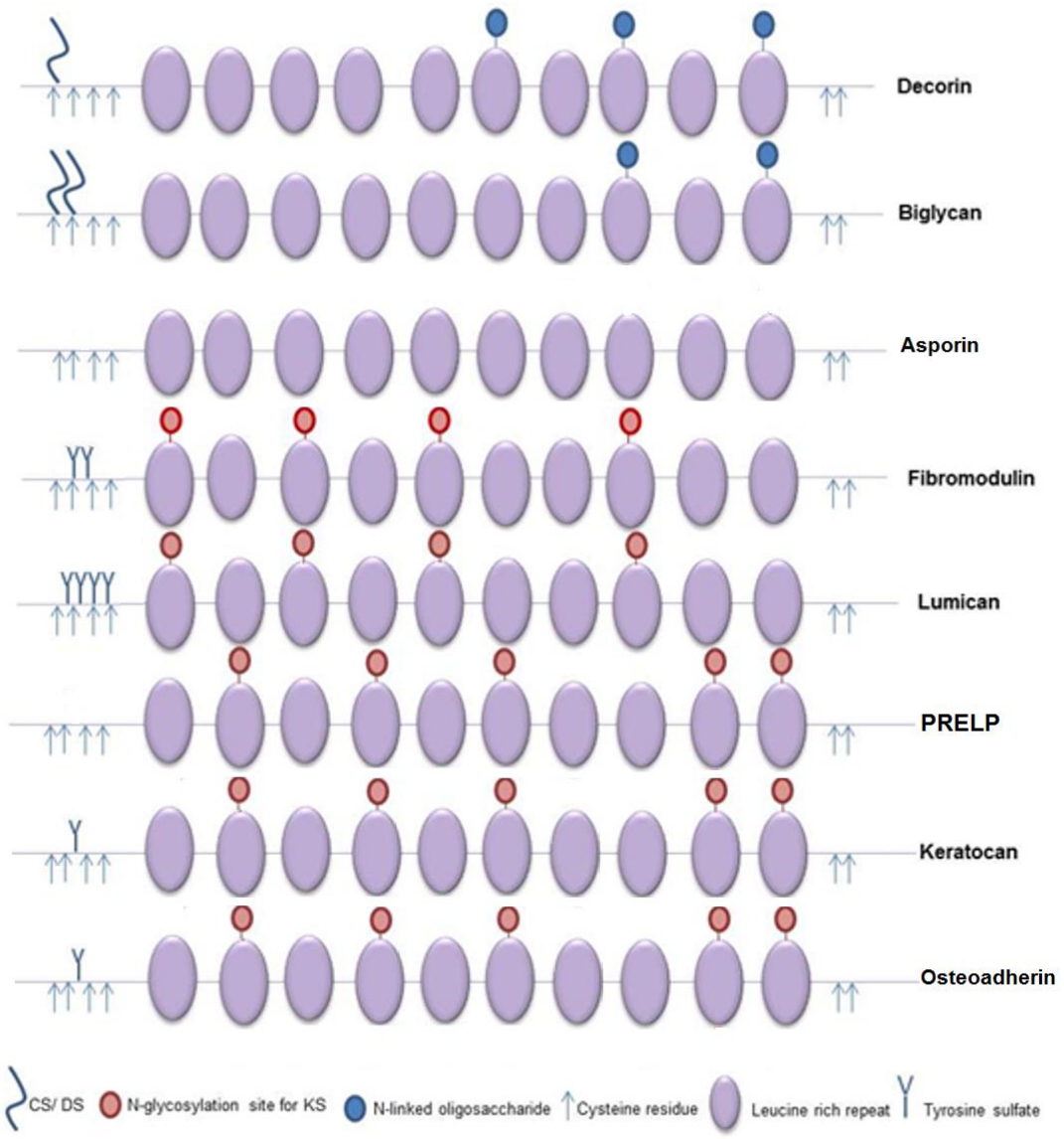

Figure 1-12: Domain structure of class I and II SLRPs.

(Modified from Iozzo and Murdoch 1996).

1.3.5.3.2 **Role of SLRPs in collagen fibrillogenesis**

The GAG chain of decorin and its important role in collagen fibrillogenesis has been well studied (Redaelli, Vesentini et al. 2003; Ruehland, Schonherr et al. 2007). A three dimentional cell culture model was used to study the effect of the glycosylated (with GAG chain) and non-glycosylated (without GAG chains) decorin on collagen fibrillogenesis, and it was found that non-glycosylated decorin had produced irregular diameters collagen fibril sizes compared to the glycosylated decorin, which had a uniform size of collagen fibrils (Ruehland, Schonherr et al. 2007). Computational studies have shown that chondroitin-6-sulphate regulates collagen fibril length, and is predicted to facilitate lateral force transfer between nearby fibrils, thereby providing collagen fibrils with mechanical strength (Redaelli, Vesentini et al. 2003).

The protein cores of decorin, lumican, and fibromodulin are also known to bind to collagen at specific sites and regulate collagen fibrillogenesis (Vogel, Paulsson et al. 1984; Scott and Haigh 1988; Pringle and Dodd 1990; Scott 1996; Miyagawa, Kobayashi et al. 2001; Orgel, Eid et al. 2009). Vesentini and others have shown with molecular modelling that decorin core protein had a stronger molecular binding force to collagen type I fibrils than its GAG chains (Vesentini, Redaelli et al. 2005). Morphometric analysis and polypeptide sequencing showed that decorin can bind to two neighbouring collagen molecules, thus aiding in stabilising and aligning collagen fibrils (Scott 1996). In addition, biochemical analysis, immunohistochemistry, and transmission electron microscopy (TEM) showed that decorin inhibits lateral fusion during collagen fibril growth and tendon maturation *in situ* (Birk, Nurminskaya et al. 1995). Other studies have also suggested a role for decorin in inhibiting lateral fusion of collagen fibrils (Danielson, Baribault et al. 1997; Doughlas, Heinemann et al. 2006). TEM revealed that chondroitin/ dermatan sulphate proteoglycans in rat tail tendon have a role in bridging between collagen fibrils, and may therefore contribute to tendon strength (Cribb and Scott 1995). Weber and others showed that decorin is able to accommodate a single collagen triple helix (Weber, Harrison et al. 1996).

TEM of the rabbit and bovine corneal collagen fibres showed that the keratan sulphate proteoglycans and chondroitin/ dermatan sulphate proteoglycans are located at different collagen fibril bands, where the chondroitin/ dermatan sulphate proteoglycans were located at the d and e band of collagen fibrils, and the keratan sulphate proteoglycans were located at the a and c bands (Scott and Haigh 1988). Using similar methods, Miyagawa and others also confirmed that keratan sulphate

proteoglycans are located at the a and c band of the D periodic collagen fibrils of the human cornea (Miyagawa, Kobayashi et al. 2001). In addition, Immunoelectromicroscopy analysis showed that decorin was located near the d and e bands of the D periodic collagen fibrils of adult bovine tail tendon (Pringle and Dodd 1990). Hedbom and others also confirmed with collagen binding assays that decorin and fibromodulin bind to separate sites on both collagens I and II (Hedbom and Heinegard 1993).

SLRPs have been shown to bind to collagen fibrils via their leucine rich repeats. For example, decorin binds to collagen by its leucine rich repeats 4-6 (Svensson, Heinegard et al. 1995), and asporin via its leucine rich repeats 10-12 (Kalamajski, Aspberg et al. 2009). Fibromodulin and lumican have been shown to bind to the same region on collagen type I (Svensson, Narlid et al. 2000), and both proteoglycans compete for collagen binding between with their leucine rich repeats 5-7 (Kalamajski and Oldberg 2009). Fibromodulin contains another binding site for collagen at its leucine rich repeat 11, between the Glu-353 and Lys-355 region (Kalamajski and Oldberg 2007). The two different attachment sites present on fibromodulin suggest that it has a higher affinity for collagen binding (Kalamajski and Oldberg 2009).

Douglas and others investigated the influence of decorin and biglycan on collagen I, II, and III binding during fibrillogenesis *in vitro* (Douglas, Heinemann et al. 2006). Interestingly, biglycan had a higher affinity to all three types of collagen compared to decorin. Furthermore, biglycan had a higher affinity for collagen type II binding compared to type I and III (Douglas, Heinemann et al. 2006). In the same study, turbidity measurements were performed to determine the effect of SLRPs on collagen binding and the rate of fibrillogenesis, and was found that biglycan did not have any effect on collagen fibril diameter or the rate of fibrillogenesis, however, decorin reduced the fibril diameter for all three collagens suggesting its essential role in inhibiting lateral collagen fibril growth (Douglas, Heinemann et al. 2006). Taken together, these studies indicate that the biglycan core protein may not have a role in collagen fibrillogenesis. However, its high quantity of GAG chains compared to decorin may result in higher affinity for all three collagen types (Douglas, Heinemann et al. 2006).

Solid phase assays have shown decorin core protein binding to the beaded filament forming collagen type VI which may suggest that decorin has a role in regulating collagen VI activity (Bidanset, Guidry et al. 1992). In addition, TEM suggests that

decorin and biglycan bind near to the N-terminal region of type VI collagen triple helix (Wiberg, Hedbom et al. 2001). Fibril associated collagens with interrupted triple helices are also shown to interact with SLRPs such as collagen type XIV (binds to decorin) (Font, Aubert-Foucher et al. 1993; Ehnis, Dieterich et al. 1997), and type XII (binds to decorin and fibromodulin) (Font, Eichenberger et al. 1996). Furthermore, ECM molecules such as tropoelastin, microfibril-associated glycoprotein-1 complex (Reinboth, Hanssen et al. 2002) and aggrecan (Wiberg, Klatt et al. 2003; Dunlevy and Rada 2004) have been shown to interact with SLRPS.

1.3.5.3.3 **The effect of SLRPs on the extracellular matrix**

Knockout mouse studies suggest that altered expression of SLRPs disrupts matrix integrity, and knockout mice been assessed using ultrastructural observations, Western blot analysis, gene expression analysis, biochemical analysis, and fibril diameter analysis (Danielson, Baribault et al. 1997; Svensson, Aszódi et al. 1999; Chakravarti, Petroll et al. 2000; Ezura, Chakravarti et al. 2000; Corsi, Xu et al. 2002; Chakravarti, Paul et al. 2003; Liu, Birk et al. 2003; Zhang, Chen et al. 2009).

Decorin has been shown to have a role in regulating collagen fibrilllogenesis in tendon, as the tensile strength of tendon was shown to be reduced in the decorin null mice (Danielson, Baribault et al. 1997). In addition, ultrastructural analysis with tendon cross sections showed that collagen fibres had an irregular outline and varied in size, whilst wild type mice had a regular collagen fibre outline that was uniform in size (Danielson, Baribault et al. 1997).

Fibromodulin knockout mice had revealed thinner and weaker collagen fibrils in tendon. In addition, irregular outlines of collagen fibrils were observed in TEM cross-sections (Svensson, Aszódi et al. 1999). This indicates that fibromodulin has a similar role to decorin in that it inhibits lateral fusion of collagen fibrils. Furthermore, fibromodulin knockout mice resulted in increased expression of lumican, which suggests that these two proteoglycans compensate for one another (Svensson, Aszódi et al. 1999). A further study has analysed the differential expression of fibromodulin and lumican during tendon growth and maturation of postnatal mice at day 4, day 10, 1 month, and 3 months, and it was found that lumican functions during early stages in fibrillogenesis, while fibromodulin functions throughout this period with a more prominent role in regulation of the later stages of collagen fibril assembly, furthermore, lumican knockout mice in early stages had collagen fibril alterations (Ezura, Chakravarti et al. 2000). However, in mature tendons, lumican

deficient mice exhibit similar features to wild type mice, whilst fibromodulin knockout mice had deceased collagen fibril size and integrity (Ezura, Chakravarti et al. 2000). The compensatory role of fibromodulin and lumican in developing tendon has also been similarly shown for decorin and biglycan, as biglycan expression decreases during tendon maturation and decorin expression increases (Zhang, Ezura et al. 2006). In addition, biglycan expression has been shown to increase when the decorin gene is knocked down in tendon (Zhang, Ezura et al. 2006) and in corneal tissue (Zhang, Chen et al. 2009).

Corsi and others studied the different roles of decorin and biglycan in mouse skin, tendon and bone (Corsi, Xu et al. 2002). The findings revealed that decorin knockout mice specifically exhibited skin laxity and fragility, whilst biglycan knockout mice had abnormal bone mass and reduced skeletal growth (Corsi, Xu et al. 2002). Reduced growth rates and a decrease in bone mass of biglycan knockout mice has also been confirmed previously by Xu and others (Xu, Bianco et al 1998). Decreased rates of bone formation and mineral apposition are also found in keratocan knockout mice (Igwe, Gao et al. 2011). The effect of biglycan and fibromodulin single and double knockouts on the knee joint has also been investigated, where the quadriceps tendons, menisci, cruciate ligaments, and patellar ligaments showed signs of ectopic ossification. In addition, the cruciate ligament was found to be ruptured (Kilts, Ameye et al. 2009). These finding suggest that fibromodulin and biglycan are essential in regulating tendon and ligament normal homeostasis.

In cornea, decorin and biglycan knockout mice exhibit an increase in collagen fibril diameter, and the collagen fibrils are irregular in both anterior and posterior stroma (Zhang, Chen et al. 2009). However, collagen fibril abnormalities in lumican knock out mice are only observed in the posterior stroma, indicating that lumican could only regulate collagen fibrils of the posterior stroma (Chakravarti, Petroll et al. 2000).

Fibromodulin knockout mice showed a decrease in collagen fibril diameter of the sclera, suggesting its important role the maturation and assembly of the scleral collagen fibrils (Chakravarti, Paul et al. 2003). Keratocan knockout mice displayed abnormal diameter of corneal collagen fibres, thinner corneal stroma, and abnormal packing of the stromal collagen (Liu, Birk et al. 2003). These results suggest that SLRPs play a significant role in corneal fibrillogenesis and developement.

Several mutations in the SLRP genes have been associated with eye alterations in humans. For instance, the three frameshift mutations in the C-terminal region of decorin structure have been linked with congenital stromal corneal dystrophy in humans which leads to corneal opacity (Bredrup, Knappskog et al. 2005). In addition, corneal plana (a congenital malformation of the cornea) has been linked to missense or frameshifts mutations in the keratocan gene (Lehmann, El-ashry et al. 2001). High myopia (increased ocular axial length, thin sclera, and retinal detachment) has been linked to single nucleotide polymorphisms (SNPs) and intron variations in fibromodulin, prolargin and opticin genes (Majava, Bishop et al. 2007). In addition, mice deficient in dermatan sulphate epimerase-1 have a disorganised collagen structure in skin (Maccarana, Kalamajski et al. 2009).

SLRPs knockout mice are also known to exhibit signs similar to human disorders (Ameye, Aria et al. 2002; Corsi, Xu et al. 2002; Jepsen, Wu et al. 2002). Double knockouts of the decorin and biglycan gene results in sever skin fragility and marked osteopenia, thus mimicking clinical signs of Ehlers-Danlos syndrome (Corsi, Xu et al. 2002). Double knockouts of lumican and fibromodlin carry a syndrome of joint laxity, tendinopathy (Jepsen, Wu et al. 2002), and high myopia (Chakravarti, Paul et al. 2003). Furthermore, biglycan or fibromodulin deficient mice exhibit abnormal collagen fibrils in tendon which leads to gait impairment, ectopic ossification, and osteoarthritis (Ameye, Aria et al. 2002).

1.3.5.3.4 **The role of SLRPS in tendon/ ligament biomechanics**

Several studies have suggested that chondroitin and dermatan sulphate GAGs play a biomechanical role in tendon (Millesi, Reihsner et al. 1995; Legerlotz, Riley et al. 2013; Rigozzi, Muller et al. 2013) and ligament (Henninger, Underwood et al. 2010).

Millesi and others showed that the digestion of GAGs reduced the viscoelasticity of the palmaris longus muscle tendon of human (Millesi, Reihsner et al. 1995). GAG removal has also an impact on the permeability of the tissue and the dynamic compressive modulus of the porcine medial collateral ligament (Henninger, Underwood et al. 2010). In addition, reduction of GAGs caused alterations in stress relaxation of the bovine extensor tendon fascicles (Legerlotz, Riley et al. 2013). Achilles tendons from mice showed higher levels of collagen fibril strains compared to non-enzymatic digested tendons, and suggested that the GAG content in native tendon is related to lower collagen strains (increased collagen fibril stretching and a decrease in collagen fibril sliding) (Rigozzi, Muller et al. 2013). However, other

studies have showed that GAG removal had no effect on the elastic modulus or viscoelastic response during compressive or tensile loading in mice tail tendon fascicles (Fessel and Snedeker 2009), or the viscoelastic and quasi-static elastic material properties of human medial collateral ligament (Lujan, Underwood et al. 2007; Lujan, Underwood et al. 2009).

The biomechanical properties of tendon have been tested in decorin and biglycan knockout mice models (Robinson, Huang et al. 2005; Dourte, Pathmanathan et al. 2013). Robinson and others have analysed three different types of tendon (tail tendon, flexor digitorium tendon, and patellar tendon) from decorin and biglycan knockout mice. Interestingly, the loss of decorin in patellar tendon created an increase in stress relaxation and modulus but had no effect when it was double knocked out with biglycan, whilst biglycan knockout mice caused the flexor digitorium tendon to decrease in its maximum stress and modulus (Robinson, Huang et al. 2005). The mechanical properties of tendon in decorin and biglycan knockouts have also been studied by Dourte and others, where tendons showed a significant increase in the viscoelastic and tensile dynamic modulus in biglycan null and heterozygous mice compared to wild type. In addition, decorin null mice exhibited a decrease in collagen content (Dourte, Pathmanathan et al. 2013). Furthermore, decorin heterozygous mice showed a significant decrease in viscoelastic and tensile dynamic modulus (Dourte, Pathmanathan et al. 2013). This indicates that decorin and biglycan may have different effect on the mechanical properties of tendon and ligament.

Other reports showed that GAGs and certain proteoglycans contribute to the biomechanical properties of tendons at different anatomical regions (Buckley, Huffman et al. 2013). Biglycan knockout mice showed a decrease in mechanical properties and tensile dynamic modulus in the mice flexor carpi ulnaris tendons, especially at the middle anatomical region compared to the insertion region (Buckley, Huffman et al. 2013). Further to this, sGAGs depletion resulted in a significant decrease in tensile dynamic modulus in mouse Achilles tendon that was specific to the bony attachment region (Rigozzi, Muller et al. 2009). These studies suggest that the mechanical enviroment of the tendon or ligament may result in certain proteoglycans and GAGs to residing in different anatomical regions in order to contribute to the biomechanical properties of the tendon or ligament at that location.

1.3.5.4 **The role of proteoglycans in different anatomical regions in ligament/ tendon**

GAGs were found to be more abundant in the fibrocartilaginous region of the porcine deep and superficial digital flexor tendon (where tendon wraps around bone) (Feitosa, Reis et al. 2006). This may suggest that GAGs levels are elevated in fibrocartilage sites as a result of tendon/ ligament compression. Certain proteoglycans have also been shown to increase in the compressive sites (Vogel and Koob 1989; Evanko and Vogel 1993; Feitosa, Reis et al. 2006; Rees, Wagget et al.2009) and tension sites (Evanko and Vogel 1993; Vogel, Sandy et al. 1994; Vogel and Petres 2005) of the tendon.

In compressive sites of tendons, aggrecan gene expression was elevated at the tendon to bone attachment region of the rabbit Achilles tendon (Huisman, Andersson et al. 2014). In addition, biglycan was found to increase with aggrecan under cyclic compressive loading in a tendon *in vitro* model (Evanko and Vogel 1993). Vogel and others have also found that certain proteoglycans (aggrecan, versican, biglycan and type II collagen) were increased in the compressive sites of bovine tendon (Vogel and Koob 1989). Keratocan has also been reported to increase in the compressed region of bovine tendon compared to its tensional region (Rees, Wagget et al. 2009). Versican was also found to be a major component in the tensile region of tendon (Vogel, Sandy et al. 1994; Vogel and Petres 2005). Decorin, on the other hand, is especially located at the tensional sites of tendon (Evanko and Vogel 1993; Vogel and Petres 2005; Matuszewski, Chen et al. 2012). These results indicate that certain proteoglycans and GAGs might play a significant role in specific anatomical regions of tendon and ligament.

1.3.5.5 **The role of proteoglycans in ligament/ tendon pathology**

GAGs have been shown to play a role in tendon/ ligament pathology (Riley, Harral et al. 1994a; Comerford, Innes et al. 2004; Halper, Kim et al. 2006; Fu, Chan et al. 2007; Samiric, Parkinson et al. 2009). Dermatan sulphate was found to increase in human pathological patellar tendons (Fu, Chan et al. 2007). Furthermore, chondroitin sulphate, dermatan sulphate, and hyaluronic acid have been shown to be significantly increased in human supraspinatus tendinitis (Riley, Harral et al. 1994a). In ligament, an increase in GAGs have been found in equine suspensory desmitis (Halper, Kim et al. 2006), and in human patellar tendinopathy (Samiric, Parkinson et al. 2009).

Proteoglycans have also been found to increase in pathological tendons and ligaments (Lo, Marchuk et al. 1998; Corps, Robinson et al. 2006; Clements, Carter et al. 2008; Samiric, Parkinson et al. 2009).

Gene expression of aggrecan, versican, fibromodulin, biglycan was found to increase in human patellar tendinopathy. However, the gene expression of decorin showed no increase in these diseased tendons (Samiric, Parkinson et al. 2009). In addition, another study indicated a significant increase in gene expression levels for aggrecan and biglycan in the fibrocartilage site (where tendon attaches to bone) of human Achilles tendinopathy, however, versican and decorin showed no increase (Corps, Robinson et al. 2006). In human ruptured ACL, biglycan mRNA expression levels were found to be significantly increased compared to intact ACLs (Lo, Marchuk et al. 1998), whereas in the dog, lumican and aggrecan mRNAs were found to be significantly increased in ruptured CCLs of the Labrador retriever in comparison to intact CCLs (Clements, Carter et al. 2008). These results demonstrate that the increase of proteoglycans in pathological tendon and ligament is variable and could be dependent on the tissue type and anatomical region.

1.3.5.6 **Role of extracellular matrix proteases in proteoglycan degradation**

1.3.5.6.1 **Disintegrin and metalloproteinase domain with a thrombospondin motif**

The ADAMTS are muti-domain metalloproteases that are released into the extracellular space as furin-actived proteases (Kashiwagi, Enghild et al. 2004). The domain structure of ADAMTSs comprises a single peptide, prodomain, metalloproteinase domain, disintegrin-like domain, a cysteine rich domain, spacer region, and thrombospondin motif and sub-motifs (Jones and Riley 2005; Apte 2009) (Figure 1-13). It has been shown that removal of the prodomain for ADAMTS-4 (Longpre, McCulloch et al. 2009) and ADAMTS-5 (Tortorella, Arner et al. 2005) is essential for cleaving aggrecan. ADAMTS aggrecanase family members (which cleaves aggrecan and other proteoglycans) are ADAMTS-1, ADAMTS-4, ADAMTS-5, ADAMTS-8, ADAMTS-9, ADAMTS-15, and ADAMTS-20 (Porter, Clark et al. 2005; Kelwick, Desanlis et al. 2015).

ADAMTS degradation of the large aggregating proteoglycans

ADAMTS-1, -4, -5, -8, -9, -15 are known to cleave aggrecan (Porter, Clark et al. 2005). ADAMTS-5 null mice in tendon have increased levels of aggrecan deposition in the pericellular and interfibrillar matrix of tendon, with an increase in collagen fibril diameter (Wang, Bell et al. 2012). In addition, the biomechanical properties of tendon are also altered with a higher tensile modulus and weakened enthesis. This data suggest that ADAMTS-5 is important in regulating the tendon collagen architecture and aggrecan turnover (Wang, Bell et al. 2012). It has also been reported that versican is a substrate for ADAMTS-1, -4, -5, -9, -15, and -20 (Sandy, Westling et al 2001; Kelwick, Desanlis et al. 2015).

ADAMTS degradation in small leucine rich proteoglycans

Biglycan, decorin, and fibromodulin have both been shown to be substrates for ADAMTS-4 (Porter, Clark et al. 2005; Melching, Fisher et al. 2006), whilst biglycan is known to be a substrate for ADAMTS-4 and -5 (Kashiwagi, Enghild et al. 2004).

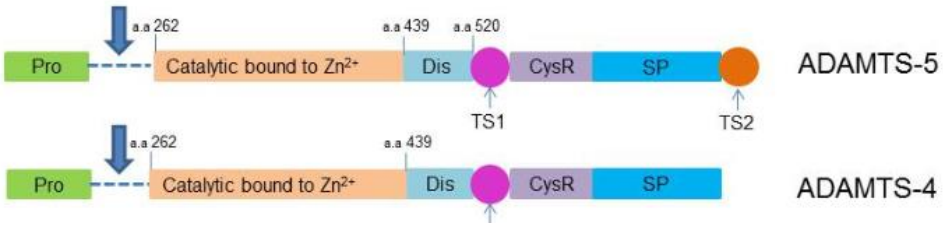

Figure 1-13: Schematic representation of the domain structure of ADAMTS4 and ADAMTS5.

(Adapted from Jones and Riley 2005; Apte 2009)

1.3.5.6.2 **Matrix metalloproteinases**

It has been reported that decorin is cleaved by gelatinase A (MMP-2), stromelysin (MMP-3), and matrylisin 1 (MMP-7) (Imai, Hiramatsu et al. 1997). In addition, decorin, biglycan, lumican, and fibromodulin have been shown to be cleaved by collagenase 3 (MMP-13) in cartilage (Monfort, Tardif et al. 2006). MMP-7 has been also indicated to be more efficient in cleaving versican more than other MMPs (Halpert, Sires et al. 1996). Despite the degradation of SLRPs by MMPs, SLRPs can also protect the degradation of collagen by MMPs *in vitro* (Sztrolovics, White et

al. 1999; Geng, McQuillan et al. 2006; Pietraszek, Chatron-Colliet e al. 2014), as decorin, lumican and fibromodulin can protect the surface of collagen fibrils from cleavage by collagenase-1 (MMP-1) and MMP-13 (Geng, McQuillan et al. 2006). Lumican has also shown to protect collagen from cleavage by the membrane type MMP (MMP-14) (Pietraszek, Chatron-Colliet e al. 2014).

1.4 Aetiopathogenesis of cranial cruciate ligament disease and rupture (CCLD/ R)

Cranial cruciate ligament disease and rupture (CCLD/ R) is one of the most common orthopaedic conditions to affect dogs leading to stifle joint osteoarthritis (Bennett, Tennant et al. 1988). CCLD/ R is defined as a spontaneous degeneration of the CCL (Vasseur, Pool et al. 1985; Narama, Masuoka-Nishiyama et al. 1996) eventually leading to rupture secondary to minor trauma. Certain dog breeds are at differing risk of ligament rupture (Duval, Budsberg et al. 1999; Whitehair, Vasseur et al. 1993).

In humans, this condition is known as non-contact ACL injury and has been commonly shown to affect woman athletes (Renstrom, Ljungqvist et al. 2008). However, the majority of human injuries are via contact injury (Goldberg, Burstein et al. 1982; Klein, Player et al. 1982).

1.4.1 Epidemiology

1.4.1.1 Bodyweight, age and breed

CCLD/ R is known to affect larger dog breeds at a younger age (Duval, Budsberg et al. 1999), and it has been reported that dogs over four years of age were significantly more prone to develop CCLD/ R (Witsberger, Villamil et al. 2008). Another study examined a population of 328 dogs and found that the average age of CCL rupture in large breeds (>15 kg) was 5.5 years, whereas the smaller breeds (<15 kg) had a mean age of 7.4 years (Harasen 2008). The prevalence of CCL rupture in certain dog breeds has also been well documented (Whitehair, Vasseur et al. 1993; Duval, Budsberg et al. 1999). Labrador Retrievers, Rottweilers, and Newfoundland's are the breeds most commonly affected with CCLD/ R (Witsberger, Villamil et al. 2008). However, other dog breeds are also considered to be high at risk of CCLD/ R (Wustefeld-Janssens, Pettitt et al. 2015). CCLD/ R has also known to be increased in obese dogs (Barnes 1977; Vasseur, Pool et al. 1985; Bennett, Tennant et al. 1988; Whitehair, Vasseur et al. 1993).

1.4.1.2 **Gender and neuter status**

Neutered females are reported to have a higher risk of CCLD/ R (Doverspike, Vasseur et al. 1993; Whitehair, Vasseur et al. 1993; Slauterbeck, Pankratz et al. 2004; Harasen 2008). Obesity may be one of the factors leading to CCLD/ R, as neutered females tend to be overweight (Edney and Smith 1986). In humans, increased oestrogen levels in the pre-ovulatory phase of the menstrual cycle in female athletes has been linked to non-contact ACL injury (Renstrom, Ljungqvist et al. 2008).

1.4.1.3 **Genetics**

Genetics has been studied in breeds predisposed to CCLD/ R (Nielen, Knol et al. 2003; Wilke, Conzemius et al. 2006; Baird, Carter et al. 2014a; Baird, Carter et al. 2014b). Dogs predisposed to CCLD/ R were found to have a heridability estimate of 0.27 in Newfoundlands (Wilke, Conzemius et al. 2006), and 0.28 in Boxers (Nielen, Knol et al. 2003). Genotypic mapping has been perform in Newfoundlands and has found that chromosome 3, 5, 13 were associated with CCLD/ R (Baird, Carter et al. 2014a). In addition, certain genes (collagen type V alpha 1 and 2, collagen type I alpha 1, collagen type XI alpha 1, collagen type III alpha 1, fibrillin 1, lysyle oxidase, latent transforming growth factor beta binding protein-2) were found to be significantly associated with CCLD/ R in four highly predisposed dog breeds (Baird, Carter et al. 2014b).

1.4.1.4 **Exercise**

A study found that sGAGs were increased around the lateral condyles and patellar surface of the femur in young beagles that had undergone exercise, and suggested that the increase of sGAG content could be due to alterations of the biological properties of cartilage at regions bearing high loads (Kiviranta, Tammi et al. 1988). In addition, Newton and others performed an exercise regime persistently on two groups of dogs (Newton, Mow et al. 1997). The first groups had a restricted activity, whereas the other group had an unlimited activity to the treadmill (Newton, Mow et al. 1997). Results indicated that there were no cartilage erosions, osteophytes, ligament or meniscal injuries present in the stifle joints of dogs that have undergone exercise (Newton, Mow et al. 1997). In addition increased ACL stiffness and strength has been shown in rats that had undergone an endurance-type exercise (Cabaud, Chatty et al. 1980). Overall, these studies demonstrate that exercise has beneficial effects on ACL/ CCL and should be recommended on a regular basis.

1.4.2 **Compromise of blood supply**

The lack of blood supply and its contribution to CCLD/ R remains unclear (Vasseur, Pool et al. 1985). The middle anatomical region of the CCL has been shown to have a reduced vascular supply in comparison to other parts of the CCL and could therefore be more susceptible to rupture (Paatasma 1952; Arnoczky, Rubin et al. 1979). It has been reported in the CCL that free passage of macromolecules occurs from the synovial fluid into the blood (Kobayashi, Baba et al. 2006). Therefore, changes in osmotic pressure could be another factor that can alter the blood supply in the CCL.

1.4.3 **Cruciate ligament cells**

Variation in cell morphology has been identified in two dog breeds with a different predisposition to CCLD/ R (Smith, Vaughan-Thomas et al. 2012). The greyhound CCL cells (low risk to CCLD/ R) commonly had longer cytoplasmic processes ranging from 100-200 μm and were accompanied with narrowed and very long nuclei, whereas the Labrador retrievers CCL cells (high in risk to CCLD/ R) contained shorter, thicker, and frequently extended cytoplasmic processes (Smith, Vaughan-Thomas et al. 2012). The longer cell processes found in the low risk greyhound may strengthen the cell-to-cell communication, thereby decreasing the risk to CCLD/ R. The smaller cell processes in the high risk Labrador retriever might indicate poor communication between cells and might therefore predispose this high risk dog breed to CCLD/ R (Smith, Vaughan-Thomas et al. 2012).

Fibrocartilage-like cells (rounded cells with a surrounding halo) have been identified in intact CCL tissues of the Labrador retriever and greyhound. It was proposed that fibrocartilage in the Labrador retriever could be a degenerative sign progressing to CCLD/ R, whereas this fibrocartilage change in the greyhound could be an adaptation to tensile or compressive loading thus protecting its CCL from disease and rupture (Comerford, Tarlton et al. 2006b).

Fibrocartilaginous change has also been found to occur in CCLs of young laboratory beagles and was considered to be an early degenerative change due to the lack of exercise (Narama, Masuoka-Nishiyama et al. 1996). In addition, it has been reported that in dogs over 5 years of age with an increase in bodyweight (15> kg) had a reduction in CCL mechanical properties as well as histological signs of fibrocartilage, therefore, age and bodyweight may also be important (Vasseur, Pool

et al. 1985). In ruptured CCLs decreased cellularity accompanied by the occurrence of fibrocartilage-like cells with a disorganised collagen fibril architecture has been also described in the middle anatomical where damage occurred (Hayashi, Frank et al. 2003). Loss of cells as a result of apoptosis or necrosis has also been studied in ruptured and partially ruptured canine CCLs (Hayashi, Frank et al. 2003; Gyger, Botteron et al. 2007; Krayer, Rytz et al. 2008). Reduced cell density has been found to occur as a consequence of ageing in normal (Murray and Spector 1999), and degenerative human ACLs (Hasegawa, Otsuki et al. 2012; Hasegawa, Nakahara et al. 2013), and has been accompanied with fibrocartilage looking cells and a disruptive collagenous matrix (Hasegawa, Otsuki et al. 2012).

1.4.4 **Extracellular matrix**

It has been reported that proteoglycans (aggrecan, decorin, lumican), collagens (collagen I alpha 2, collagen III alpha I), and proteases (such as cathepsins B and D and MMPs -2 and -9) were significantly increased in ruptured CCLs of the Labrador retriever (high risk to CCLD/ R) compared to its non-ruptured CCLs (Clements, Carter et al. 2008). These findings may suggest that these ECM molecules are associated with pathology. Furthermore, a significant increase of sGAGs, water content, MMP-2, and MMP-9 were found in ruptured compared to intact Labrador retriever CCLs (Comerford, Innes et al. 2004). The significant elevation of these ECM molecules in ruptured ligaments suggests that they could be involved in the pathology of CCLD/ R. In addition, reduced gene expression of decorin, biglycan and lumican were observed in pregnant rabbit ACLs, and it has been suggested that the ACL during pregnancy could exhibit signs of knee joint laxity, thus contributing to CCL rupture (Hart, Sciore et al. 1998).

1.4.5 **Bilateral and unilateral CCL rupture**

The prevalence of bilateral CCL rupture is between 59% to 61% (Cabrera, Owen et al. 2008; Buote, Fusco et al. 2009), and 22% to 54% of patients with unilateral CCL rupture consequently rupture their contralateral CCL (Doverspike, Vasseur et al. 1993; Moore and Read 1995; De Bruin, De Rooster et al. 2007; Cabrera, Owen et al. 2008; Buote, Fusco et al. 2009; Grierson, Asher et al. 2011; Muir, Schwartz et al. 2011). In addition, survival analysis performed on a large group of dogs showed that patients with unilateral CCL rupture consequently rupture their contralateral joint within a median of 947 days (Muir, Schwartz et al. 2011). Subsequent contralateral CCL rupture has also been significantly associated with the severity of radiographic

stifle effusion and osteophytosis in the contralateral stifle joint (Chuang, Ramaker et al. 2014). Radiographic effacement of the infrapatellar fat pad has been known to appear with CCL rupture and inflammation of the stifle joint, and has been termed the infrapatellar fat pad sign (Widmer, Buckwalter et al. 1994). The fat pad sign is a predominant risk factor associated with subsequent CCL rupture of the contralateral stifle joint (Fuller, Hayashi et al. 2014).

1.4.6 **Stifle joint factors**

1.4.6.1 **Mechanics**

The structural (load of failure and deformation) and material (tangent modulus and ultimate stress) properties of the canine CCL have been studied (Butler and Stouffer 1983; Wingfield, Amis et al. 2000a). CCLs from the greyhound (low risk to CCLD/ R) were shown to have significantly greater material and structural properties when compared to CCLs of the Rottweiler (high risk to CCLD/ R) (Wingfield, Amis et al. 2000a). Craniocaudal laxity of the canine stifle joint has also been studied in dog breeds at a high and low risk of CCLD/ R (Wingfield, Amis et al. 2000b; Comerford, Tarlton et al. 2005). Wingfield and others showed that the high risk Rottweiler had a greater stifle joint laxity compared to the low risk greyhound (Wingfield, Amis et al. 2000b) and this was further confirmed by Comerford and others where they compared the stifle joint laxity and CCL properties of the Labrador retriever (high risk to CCLD/ R) to greyhounds (low risk to CCLD/ R). These authors found that Labradors had a significantly greater anterior-posterior stifle joint laxity and weaker CCL material properties (ultimate tensile stress) compared to the greyhounds (Comerford, Tarlton et al. 2005).

1.4.6.2 **Proprioception**

Lack of proprioception and its role in contributing to CCLD/ R in the dog is not well understood (O'Connor and Woodbury 1982). Stifle joint and CCL innervation is compulsory for optimal postoperative rehabilitation and joint damage prevention (Salo 1999).

The impact of denervation on the injured rabbit medial collateral ligaments has been previously studied (Ivie, Bray et al. 2002; Beye, Hart et al. 2006). The first study found that innervated injured medial collateral ligaments had a higher density of blood vessels and a higher blood flow rate compared to injured ligaments that were denervated (Ivie, Bray et al. 2002). In addition, biomechanical testing showed that

injured innervated medial collateral ligaments had a significantly higher force for ultimate failure and a significantly lower static and total creep compared to injured denervated medial collateral ligaments (Ivie, Bray et al. 2002). A further study has examined the gene expression of several ECM proteins in innervated and denervated injured medial collateral ligaments of the rabbit, and found that several genes of interest were significantly upregulated in injured deneravted ligaments at two weeks post injury (collagen I, collagen III, TGF-β, MMP-13, TIMP-3, and angiogenesis inhibitor thrombospondin-1 (TSP-1)) compared to innervated injured medial collateral ligaments (Beye, Hart et al. 2006). These studies further suggest that innervation is necessary for healing and normal ligament function.

1.4.6.3 **Conformational variation**

Deformity of the proximal tibial has been associated with CCLD/ R in dogs (Read and Robins 1982; Selmi and Padilha Filho 2001; Macias, McKee et al. 2002). CCLD/ R and excessive tibial plateu angle of the stifle joint has been found to occur as consequence of early neutering in large dog breeds (Duerr, Duncan et al. 2007).

A narrowed intercondylar notch (ICN) has been linked to human ACL injuries (Laprade and Burnett 1994; Shelbourne, Davis et al. 1998). In the dog, narrowing of the intercondylar notch has been associated with CCLD/ R and osteoarthritis (Aiken, Kass et al. 1995; Wada, Tatsuo et al. 1999). In addition, ACL function is impeded when it passes through a narrowed intercondylar notch causing damage and knee joint laxity (Muneta, Takakuda et al. 1997).

The intercondylar notch index and femoral condyle height and width have been shown to be significantly lower in Labrador retriever and Golden retriever (high risk breeds to CCLD/ R) compared to greyhounds (low risk breed to CCLD/ R) (Comerford, Tarlton et al. 2006a). In addition, immature collagen cross-links, matrix metalloproteinase-2 and sulphated glycosaminoglycans (sGAGs) are significantly increased in the CCL impingement region of high risk dog breeds compared to low risk dog breeds. These findings may indicate that CCL structure is altered in the high risk Labrador retriever with a narrowed ICN therefore predisposing it to CCLD/ R (Comerford, Tarlton et al. 2006a).

The tibial plateau angle (TPA) was compared in intact and ruptured CCLs from the Labrador retriever (high risk to CCLD/ R), however, the study found no correlation between the magnitude TPA and CCLD/ R (Reif, Probst et al. 2003). TPA and CCL stress can also be altered with muscular force, body size, obesity, rapid weight gain,

relative inactivity, and exercise in dogs (Colborne, Innes et al. 2005). In human ACLs, it has been shown that narrowing of the intercondylar notch and increased TPA may be associated with ACL injuries in both males and females. Furthermore, reduced intercondylar notch index has found to be linked with knee joint osteoarthritis (Quasnichka, Anderson-MacKenzie et al. 2005; Stein, Li et al. 2010).

The effect of ruptured CCLs on hind limb conformation has been studied in the high risk Labrador retriever CCLs (Ragetly, Griffon et al. 2008; Mostafa, Griffon et al. 2009; Ragetly, Griffon et al. 2010). Ragetly and others studied the body segment parameters (mass, mass moment of inertia, centre of mass) for the foot, crus and thigh in Labrador retriever patients with and without CCLD/ R, and found that the thigh and crus weighed less in limbs with CCLD/ R compared to their non-ruptured contralateral limbs, whereas only the thigh weighed less in limbs with CCLD/ R compared to dogs without CCLD/ R. In addition, the thigh moment of inertia was less in limbs with ruptured CCLs compared to their non-ruptured contralateral limbs, and the crural centre of mass was positioned more distally in dogs without CCLD/ R compared with dogs with CCLD/ R (Ragetly, Griffon et al. 2008). The same authors investigated hind limb mechanics and kinematics, and found that dogs exhibited hindlimb lameness with a tendency to apply force across the contralateral limb (Ragetly, Griffon et al. 2010). In addition, Mostafa and others have found that the cranial angulation of the proximal portion of the tibia and excessive TPA were highly associated in Labrador retriever patients with CCLD/ R (Mostafa, Griffon et al. 2009). Overall, these studies indicate that such anatomical variations in high risk dog breeds could contribute to CCLD/ R.

1.4.7 **Healing potential**

Poor healing of the ACL is one of the main reasons why ruptured ACLs fail to undergo primary repair (Arnoczky, Rubin et al. 1979; Frank, Amiel et al. 1985). The mechanisms of poor ACL healing include intrinsic defects of cellular migration and proliferation (Nagineni, Amiel et al. 1992; Geiger, Green et al. 1994; Spindler, Andrish et al. 1996). An *in vitro* injured model of both ACL and medial collateral ligament found that matrix metalloproteinase-2 gene expression was significantly increased in the rat ACL when compared to its medial collateral ligament (Tang, Yang et al. 2009) suggesting that an increase in MMP-2 might contribute to poor ACL healing.

Loss of the provisional scaffold (fibrin-platelet plug) has been shown to occur in the CCL when compared to the medial collateral ligament, suggesting that the loss of provisional scaffolds could be one of the mechanisms which impairs CCL healing (Murray, Spindler et al. 2007). A lack of provisional scaffold production accompanied with low levels of ECM proteins and cytokines were found to occur within the wounded CCL (Spindler, Devin et al. 2006). In human ACLs urokinase plasminogen activator can prevent arthrofibrosis (Rosc, Powierza et al. 2002). However, elevated levels of urokinase plasminogen activator may impair the ACL normal production of provisional scaffolds leading to further ACL trauma and rupture (Rosc, Powierza et al. 2002).

Inorganic free radical nitric oxide has been associated with CCLD/ R in the dog (Spreng, Sigrist et al. 2000; Jauernig, Schweighauser et al. 2001). There are two type of nitric oxide synthase; constitutive and inducible (Nathan 1992). Inducible nitric oxide synthase levels are increased in ruptured and intact CCLs compared to other ligaments of the stifle joint (Spreng, Sigrist et al. 2000; Jauernig, Schweighauser et al. 2001), and have also been shown to increase in CCL explants *in vitro* when exposed to an inducible nitric oxide synthase cocktail (tumor necrosis factor, interlukin-1, and lipopolysaccharide), whilst levels did not increase with other ligament explants (medial collateral or ligament of the femoral head) (Louis, Remer et al. 2006). Proteoglycan and collagen production might also be hindered by the increase of inducible nitric oxide levels in the ACL (Cao, Stefanovic-Racic et al. 2000). Overall, these studies suggest that CCL/ ACL produces high levels of inducible nitric oxide synthase that may affect the normal metabolism of proteoglycan and collagen, and therefore may compromise the ligament to rupture.

1.5 **HYPOTHESIS**

This thesis examines the hypothesis that GAGs/ proteoglycans may have a role in different anatomical regions of the canine CCL that may experience different tensional and compressional loads. We further hypothesise that GAG/ proteoglycan content may differ between dog breeds with a differing predisposition to CCLD/ R.

1.6 **AIMS AND OBJECTIVES**

The project aims to identify GAGs/ proteoglycans in different anatomical regions in the canine CCL, and identify the alterations with disease and breed variation with different risks of CCLD/ R. The aims will be addressed with two key objectives;

1. To determine whether there are regional differences in canine CCL GAG/ proteoglycan composition by performing quantitative real time RT-PCR analysis, semi-quantitative western blotting, quantitative biochemistry, semi-objective histology scoring, and immunohistochemistry staining.

2. To determine whether there are differences in GAGs/ proteoglycans in the CCL in dogs with a low predisposition compared to dogs with a high predisposition to CCLD/ R by performing quantitative real time RT-PCR analysis, semi-quantitative western blotting, quantitative biochemistry, semi-objective histology scoring, and immunohistochemistry staining.

Chapter 2: Materials and methods.

2.1 Tissue collection

2.1.1 Cruciate ligaments obtained from Staffordshire bull terrier dogs

Cranial cruciate ligaments (CCLs) were harvested from Staffordshire bull terrier dogs. For experimental procedures, ligaments were either divided into three regions (origin, middle, and insertion) or processed without cutting (Figure 2-1). Cruciate ligaments (CL) were obtained from stifle joints with no macroscopic evidence of joint pathology. The dogs were euthanised for purposes not related to this study and were clinical waste material donated to the University of Liverpool. Ethical approval for use of this material in this project was granted by the Veterinary Research Ethics Committee, School of Veterinary Science (RETH0000553 and VREC65).

2.1.2 Cruciate ligaments obtained from greyhounds and Labrador Retrievers

CCLs obtained from greyhound and Labrador retriever dogs (Figure 2-2) were archived samples sourced from Prof. Eithne Comerford. Ligaments samples were previously obtained from the craniomedial and caudolateral band of each of these two dog breeds. Additional archived samples of greyhounds were divided into two sections (femoral end (origin), tibial end (insertion)). A summary of the cruciate ligament samples collected from different dog breeds are documented beside their usage in each experimental procedure are shown in Tables 1-1, and 2-1.

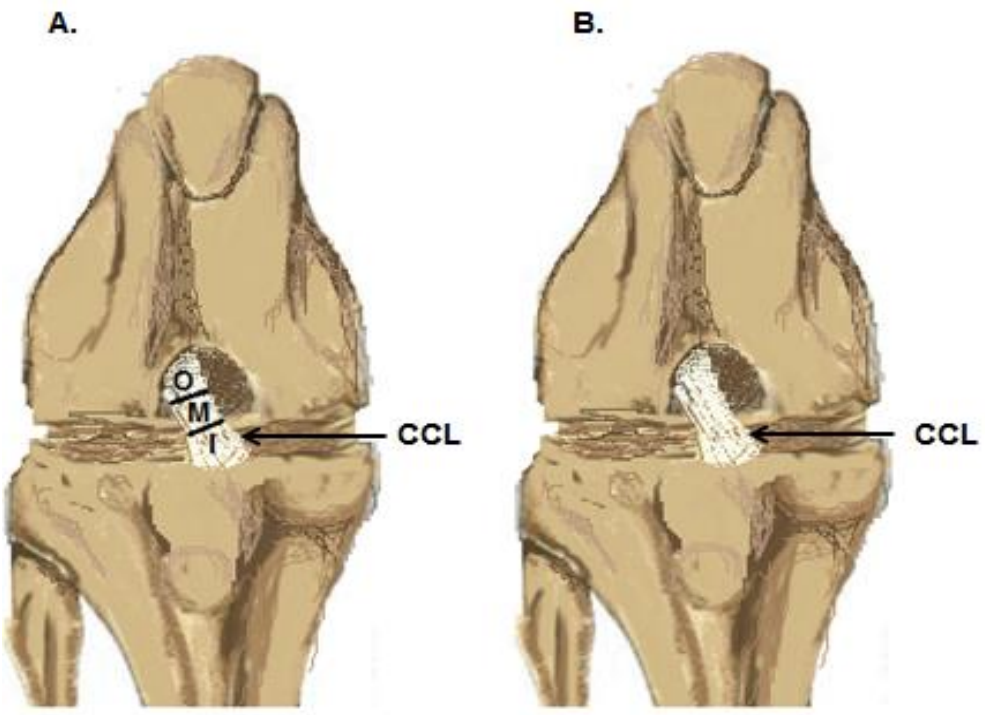

Figure 2-1: Sample collection obtained from the Staffordshire bull terrier.

The Figure shows a cranial view of the canine stifle joint after removal of the collateral ligaments. The Figure illustrates CCL preparation from Staffordshire bull terriers. Ligaments were either separated into origin, middle, and insertion (A) or were harvested as an entire ligament without cutting (B) (produced by paint software). (O= origin; M= middle; I= insertion; CCL= cranial cruciate ligament).

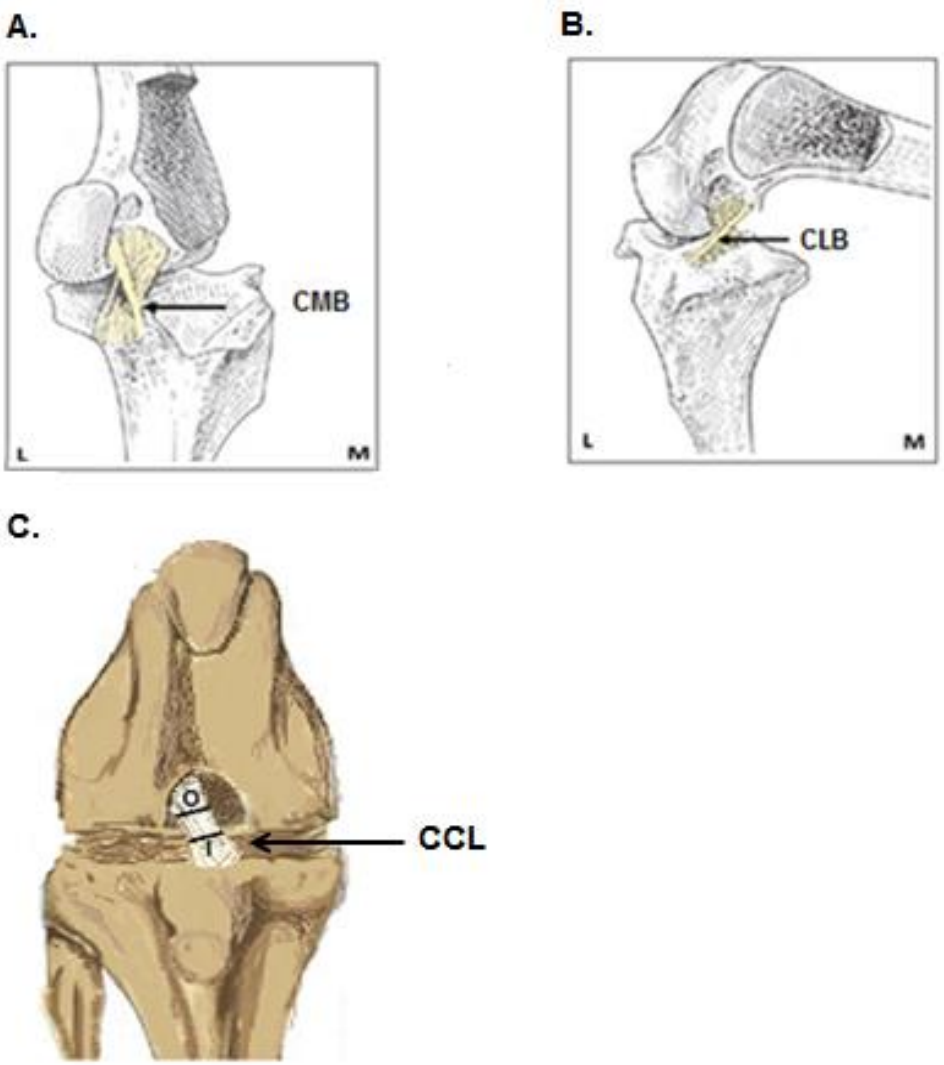

Figure 2-2: Sample collection obtained from the Labrador retriever and greyhound.

The Figure shows a craniomedial (A, B) and a cranial view (C) of the canine stifle joint after removal of the collateral ligaments. The graph demonstrates archived CCL samples from greyhounds and Labrador retriever. Ligaments were preserved as craniomedial (A) and caudolateral bands (B) (Adapted from Arnoczky and Marshall 1977). Other CCLs from greyhounds were collected from the origin and insertion anatomical regions (C) (produced by paint software). (O= origin; I= insertion; CMB= craniomedial band; CLB= caudolateral band; CCL= cranial cruciate ligament; L= lateral view; M= medial view).

Sample No.	Ligament	Breed	Procedure
1	CCL	SBT	**SDS-PAGE and Western blot**
2	CCL	SBT	
3	CCL	SBT	
4	CCL	SBT	
5	CCL	SBT	
6	CCL	SBT	
7	CCL	SBT	
8	CCL	SBT	
9	CCL	SBT	
10	CCL	SBT	
11	CCL	SBT	
12	CCL	SBT	
13	CCL	SBT	**Real time RT-qPCR**
14	CCL	SBT	
15	CCL	SBT	
16	CCL	SBT	
17	CCL	SBT	
28	CCL	SBT	
19	CCL	SBT	**Biochemistry**
20	CCL	SBT	
21	CCL	SBT	
22	CCL	SBT	
23	CCL	SBT	
24	CCL	SBT	**Histology**
25	CCL	SBT	
26	CCL	SBT	
27	CCL	SBT	
28	CCL	SBT	
29	CCL	SBT	
30	CCL	SBT	**Immunohistochemistry**
31	CCL	SBT	
32	CCL	SBT	
33	CCL	SBT	
34	CCL	SBT	
35	CCL	SBT	

Table 2-1: Details of CCLs obtained from SBT along with their related experimental procedures.

(SBT= Staffordshire bull terrier; CCL= cranial cruciate ligament).

Sample No.	Ligament	Breed	Procedure
36	CCL	GH	**SDS-PAGE and Western blot**
37	CCL	GH	
38	CCL	GH	
39	CCL	GH	
40	CCL	GH	
41	CCL	GH	
42	CCL	GH	
43	CCL	GH	
44	CCL	GH	
45	CCL	GH	
46	CCL	GH	**RT-qPCR**
47	CCL	GH	
48	CCL	GH	
49	CCL	GH	
50	CCL	GH	
51	CCL	GH	**Biochemistry**
52	CCL	GH	
53	CCL	GH	
54	CCL	GH	
55	CCL	GH	
68	CCL	GH	**Histology & Immunohistochemistry**
69	CCL	GH	
70	CCL	GH	
71	CCL	GH	
72	CCL	GH	
73	CCL	GH	
74	CCL	GH	
75	CCL	GH	
76	CCL	LR	**Histology**
77	CCL	LR	
78	CCL	LR	
79	CCL	LR	
80	CCL	LR	
81	CCL	LR	
82	CCL	LR	

Table 2-2: Detail of CCLs obtained from GH and LR along with their related experimental procedures.

(GH= greyhound; LR= Labrador retriever; CCL= cranial cruciate ligament).

2.2 Reagents

All reagents were purchased from Sigma, UK unless stated. For more details, see Appendix I.

2.3 Biochemical assays to measure glycosaminoglycans

CCLs from Staffordshire bull terriers (n=5) samples were cut into three sections (origin, middle, and insertion), snap frozen in liquid nitrogen and then stored at -20°C until use. Other archived CCLs from greyhounds (n=5) that were cut into femoral end (origin) and tibial end (insertion) were also used.

2.3.1 Water content

Samples were allowed to thaw at room temperature and the CCL wet weight was measured. In order to obtain the CCL dry weight, the samples were freeze dried overnight and then the CCL weight was measured the next day. The water content % was calculated using the following equation;

Water content % = ([wet weight – dry weight] / wet weight) x 100

2.3.2 Sulphated glycosaminoglycan (sGAG) assay

CCL samples were digested for 24 hours with 10 unit/ ml papain in 100 mM sodium acetate, 2.4 mM EDTA and 5 mM cysteine HCl at 60ºC. sGAG content in the samples was determined using the 1, 9-dimethlylmethylene blue (DMMB) dye binding assay (Farndale, Buttle et al. 1986). 40 µl duplicates of papain-digested ligament samples were immediately analysed at 570 nm following the addition of 250 µl of DMMB dye. Shark chondroitin sulphate was used as a standard over a concentration range of 0-70 µg/ ml (Figure 2-3) and sGAG concentrations were calculated by comparison with the standard curve. In order to determine the proportion of chondroitin sulphate (CS) and dermatan sulphate (DS) in each sample, samples were digested at 37ºC for 24 hours with 0.05 U/ ml of chondroitinase ABC (ChABC) prior to the DMMB assay (Riley, Harrall et al. 1994a).

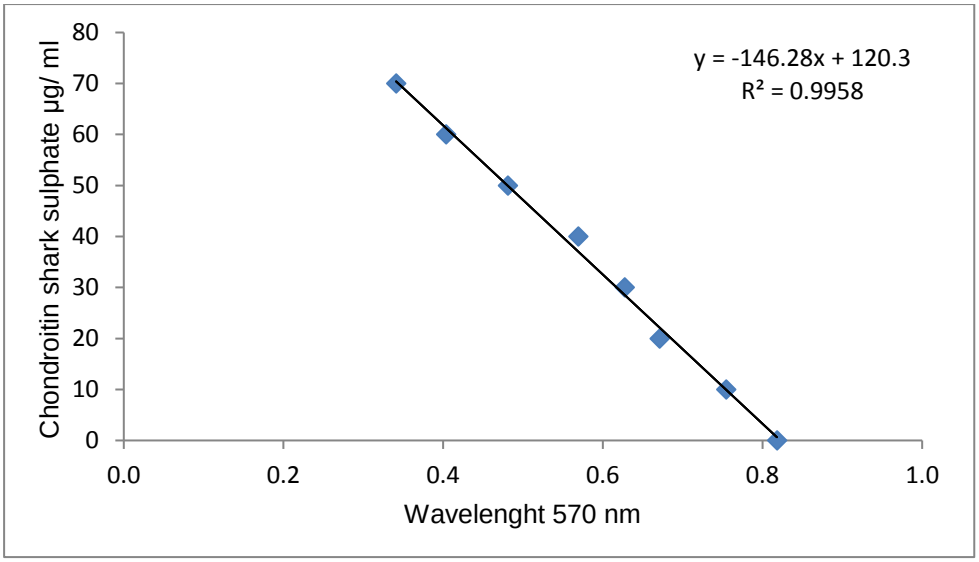

Figure 2-3: An example of a standard curve for the quantification of sulphated glycocaminoglycans (sGAGs).

Chondroitin shark sulphate was used as a standard ranging from 0-70 µg/ ml.

2.3.3 **Uronic acid assay**

Uronic acid (UA) levels were quantified using the methodology described by Bitter and others (Bitter and Muir 1962). UA assay solution was prepared by liquefying 0.05 M Sodium tetraborate in 50 ml concentrated sulphuric acid (Fisher Scientific, UK), followed by dissolving 1.7 mM carbazole in the solution to form the UA assay formula. 150 µl of the solution was placed in 96 microtiter well plates and stored at -80^{o}C for 24 hours. Next, 30 µl standards or papain digested samples CCLs were cooled with ice and added to the UA assay formula, mixed and then heated at 80^{o}C for one hour. Glucuronic acid lactone was used as a standard at concentrations from 0-70 µg/ ml (Figure 2-4) and UA concentrations of papain digests were obtained by comparison with the standard curve. Standards and samples were then measured at a wavelength of 530 nm. The UA concentration was presented as µg per mg dry weight of tissue. The concentration of hyaluronic acid (HA) in the tissue was indirectly estimated using the following equation;

$$[HA] = \frac{[UA] - ([Total\ sGAG] \times 0.36)}{0.45}$$

This calculation assumed that UA comprised 36 % of the dry weight of GAGs and 45 % of the dry weight of HA (Riley, Harrall et al. 1994).

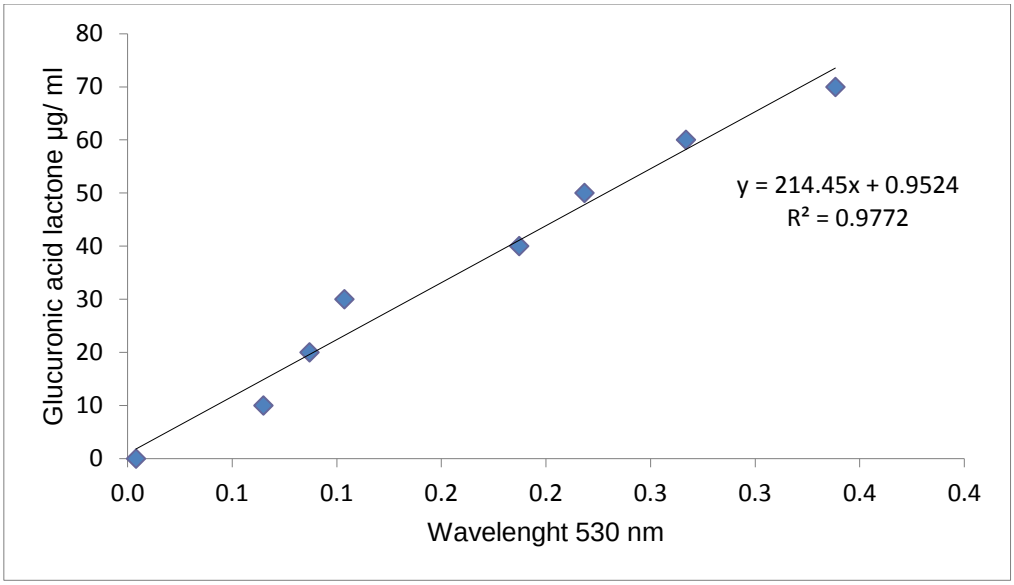

Figure 2-4: An example of a standard curve for uronic acid quantification.

Glucuronic acid lactone was used as a standard at concentrations ranging from 0-70 µg/ml.

2.3.4 Competitive enzyme linked immunosorbent assay for keratan sulphate

Keratan sulphate levels were measured using the methodology obtained from Caterson and others (Caterson, Cristner et al. 1983). Bovine articular cartilage aggrecan and keratan sulphate monoclonal antibody 5D4 were materials kindly provided by Prof. Bruce Caterson. In brief, ELISA plates were coated with the antigen solution, which consisted of 131.6 µg of GAG/ ml of bovine articular cartilage aggrecan, by passive adsorption overnight at 4ºC. The plates were washed with PBS-sodium azide, and blocking solution (1 % BSA/ PBS-sodium azide) then added for one hour at 37ºC. A 1:16000 dilution of the 5D4 monoclonal primary antibody in 1 % BSA/ PBS-sodium azide was then added to both standards and ligament samples in 1.5 ml centrifuge tubes and incubated for 1 hour at 37°C. Standards were prepared by diluting bovine articular cartilage aggrecan solution in PBS-sodium azide in order to produce concentrations ranging from 13.6-0 µg GAG/ ml in a 1:3 dilution series. The standard concentration of 0 µg GAG/ ml was the non-competing antigen for the assay. After discarding the blocking solution, the previously incubated standards and samples with the primary antibody were then added to the plate in duplicate and incubated again for 1 hour at 37°C. The main principle of this assay is that the greater the antigen concentration present in the sample, the fewer antibodies will be able to attach to it. Each well was then washed three times in PBS-sodium azide to remove any unbound antibody. The secondary antibody was alkaline phosphatase conjugated goat anti-mouse IgG was diluted

1:5000 in 1 % BSA/ PBS-sodium azide TSA and added to the plate to be incubated for an additional hour at 37°C. Each well was then washed three times in PBS-sodium azide. 1mg/ ml of P-nitrophenyl alkaline phosphatase (PNPP) substrate (Fisher scientific, UK) were then dissolved in 1x diethanolamine buffer and incubated for 30-60 min at 37°C until sufficient colour developed. The more chromogenic signal detected on samples/ standards indicated less antibody binding to the antigen. The ELISA plate was measured at 405 nm when the non-competing antigen reached an optical density (OD) of 1. Standard dilutions were calculated against ligament sample concentrations (µg GAGs/ ml) after obtaining the reciprocal of each absorbance measurement (Figure 2-5). At the beginning of the assay, initial experiments were carried out to assess both optimal primary antibody concentration (1:16000) and antigen coating (1:250) of the non-competing antigen as this was essential for ideal assay reproducibility and sensitivity.

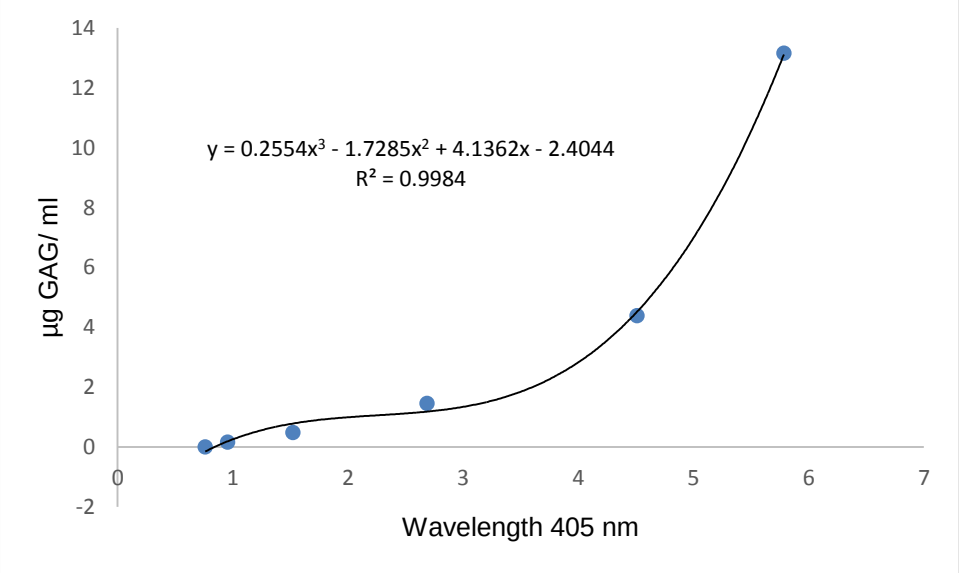

Figure 2-5: An example of a standard curve for keratan sulphate quantification.

The standard was obtained from bovine articular cartilage aggrecan at concentrations ranging from 13.6 µg to 0 µg GAGs.

2.4 **Western blot analysis to detect proteoglycans and GAGs**

CCL samples from Staffordshire bull terriers (n=12) were either divided into three regions (origin, middle and insertion; n=5) or harvested intact (n=7). All samples were snap frozen in liquid nitrogen and then stored at -80°C until required. Archived intact CCLs from greyhounds (n=10) were also used for this study.

2.4.1 **Protein extraction**

Samples were immersed in liquid nitrogen and pulverised whilst frozen with a dismembrator (B. Brown Biotech Micro Dismembrator, U.S.A). Proteins were extracted twice in 15 volumes (w/ v) of 4M guanidinium HCl (Sigma, UK) containing complete protease cocktail inhibitor tablets (Roche, UK) using end-over-end mixing for 24 hours at 4^{o}C. After extraction, the soluble fraction (containing proteins) was removed following centrifugation at 13000 x g for 15 min at 4^{o}C. Ligament extracts were dialysed in a 20,000 kD cut-off membrane (Spectrapor, Breda, NL) for 24 h at 4^{o}C against sodium acetate buffer containing 100 mM 6-aminohexanoic acid, 5 mM benzamidine and 10 mM *N*-ethylmaleimide as proteinase inhibitors, all from Sigma, UK. The dimethymethylene blue (DMMB) dye binding assay based on Farndale and others was used to determine the sulphated glycosaminoglycan content when required (Farndale, Buttle et al. 1986). Samples were then digested for 24 hours at 37^{o}C with the glycosaminoglycan-digesting enzymes as followed; Chondroitinase ABC (Yamagata, Saito et al. 1968) (0.00001IU/ 10 µg) (Sigma, UK); Keratanase I (Fukuda 2001) (0.1IU/ 10 µg) (AMS); and or Keratanase II (Yamagishi, Suzuki et al. 2003) (0.01IU/ 10 µg) (AMS). Enzyme units were adapted from Rees and others (Rees, Flannery et al. 2000). Samples were finally dialysed in ultrapure water, freeze dried and reconstituted in 1x SDS sample buffer containing 0.0625 M Tris-HCL (pH 6.8) with 2 % SDS (w/v), 10 % (v/v) Glycerol, and 0.005 % (w/v) Bromophenol Blue.

2.4.2 Sodium dodecyl sulphate Polyacrylamide Gel Electrophoresis (SDS-PAGE)

Samples were heated either under reduced or non-reduced conditions and loaded onto a 4-12 % Nupage Bis-Tris gel (Invitrogen). Samples were loaded as mg per equal wet weight of tissue (Melrose, Fuller et al. 2008; Plaas, Sandy et al. 2011). Loading with equal wet weight is more effective than other conventional methods (e.g. loading with equal protein, and equal GAG) as it is the most appropriate way of normalising the highly hydrated, heterogeneous tissue components. Samples were prepared and denatured by heating at 90^{o}C for 10 minutes. Where required, samples were reduced by adding 5 % of 2-mercaptoethanol to 1x SDS sample buffer. Samples and pre-stained molecular weight markers (Fisher scientific, UK) were loaded and run on NuPAGE 4-12 % bis-tris Gels (Life Technologies, UK) at 200V for 35 minutes, and then transferred to nitrocellulose membranes (Whatman, UK) in an X-Cell blot module (Life technologies, UK) at 35V for 90 minutes. Membranes were then blocked in phosphate-buffered saline (PBS) containing 5 % skimmed milk powder (blocking buffer) for one hour at room temperature with gentle agitation. The milk is used to block the membrane with non-specific protein, reducing the likelihood of the primary or secondary antibodies from non-specifically binding to the membrane. The membranes were then incubated in blocking buffer containing primary antibody and 0.05% Tween-20 (Sigma, UK) overnight at 4^{o}C with agitation. Primary antibodies and the concentrations in which they were used are presented (Table 2-3). The primary antibody was removed and the membranes washed for five minutes three times with PBS + 0.05 % Tween (PBS-T) before adding the appropriate secondary antibody (Table 2-4). Secondary antibodies were diluted in blocking buffer + 0.05 % Tween and incubated with the membrane at room temperature for one hour with gentle agitation. The membrane was again washed three times in PBS-T. Antibody localisation was visualised using an enhanced chemiluminescent detection kit (ECL Plus Western Blotting Detection Reagents Perkin Elmer, U.S.A). Enhanced luminol and oxidizing reagent were mixed in equal ratios before adding them to the membrane. The membrane was shaken vigorously for one minute then wrapped in clear plastic with luminescence being visualised using a UVP ChemiDoc-it Imaging System (UVP, UK). Images were acquired using VisionWorksLS image acquisition and analysis software (UVP, U.S.A). A summary of the Western blotting procedure is shown in Figure 2-6.

Table 2-3: Primary antibodies used in Western blotting.

Antibody Isotype	Proteoglycan/ GAG	Dilution	Label	Antibody recognition site
Mouse monoclonal IgG	Decorin	1:200	*DECN 70.6	Specific for the core protein of decorin
Mouse monoclonal IgG	Biglycan	1:200	**PR8A4	C-terminal amino acid sequence of human biglycan
Mouse monoclonal IgM	Lumican	1:100	*LUM1	Unknown
Mouse monoclonal IgG	Keratocan	1:200	*KER1	Specific for the core protein of keratocan
Rabbit polyclonal IgG	Fibromodulin	1:500	**PR184	C-terminal amino acid sequence of human fibromodulin
Mouse monoclonal IgG	Versican	1:200	12C5	G1 domain of versican
Mouse monoclonal IgG	Aggrecan	1:500	*7D1	G1 and chondroitin sulphate attachment domains
Mouse monoclonal IgG	Chondroitin-0-sulphate stub	1:200	*1B5	Chondroitinase ABC-generated-0 sulphated CS stub
Mouse monoclonal IgG	Chondroitin-4-sulphate stub	1:200	*2B6	Chondroitinase ABC-generated-4 sulphated CS stub
Mouse monoclonal IgG	Chondroitin-6-sulphate stub	1:200	*3B3	Chondroitinase ABC-generated-6 sulphated CS stub
Mouse monoclonal IgG	Keratan sulphate stub	1:200	*BKS1	Keratanase generated keratan sulphate stub

*Kindly donated by Prof. Bruce Caterson and Dr. Clare Hughes

**Kindly donated by Prof. Peter Roughly

Table 2-4: Secondary antibodies used in Western blotting.

Secondary antibody	Dilution	Concentration
Peroxidase conjugated Rabbit anti-mouse IgG	1:1000	5 µg/ ml
Peroxidase conjugated goat anti-mouse IgM	1:1000	5 µg/ ml
Peroxidase conjugated rabbit-anti goat IgG	1:2000	5 µg/ ml

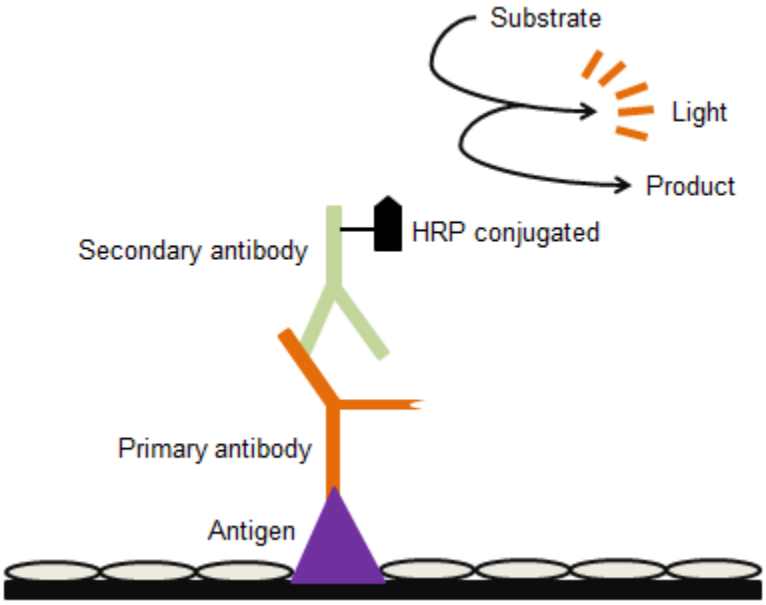

Figure 2-6: Representative image of the Western blot methodology.

The primary antibody is attached to the antigen on the nitrocellulose membrane. The membrane is then washed to remove unbound antibodies. The secondary antibody conjugated with the enzyme horseradish peroxidase attaches to the primary antibody and is followed by another washing step. A chemiluminescent substrate is then added in order to react with horseradish peroxidase conjugate and produce a light signal. The signal is then detected by capturing the blot with VisionWorksLS image acquisition and analysis software package system.

2.4.3 **Detecting the linear response of the Western blot signal**

Lumican antibody was used to validate the linearity of the Western blot signal by undertaking a series of 1:2 serial dilutions with a 4 molar guanidine extract sample of CCL (Figure 2-7). The intensity of Western blot signal is also demonstrated in Figure 2-8.

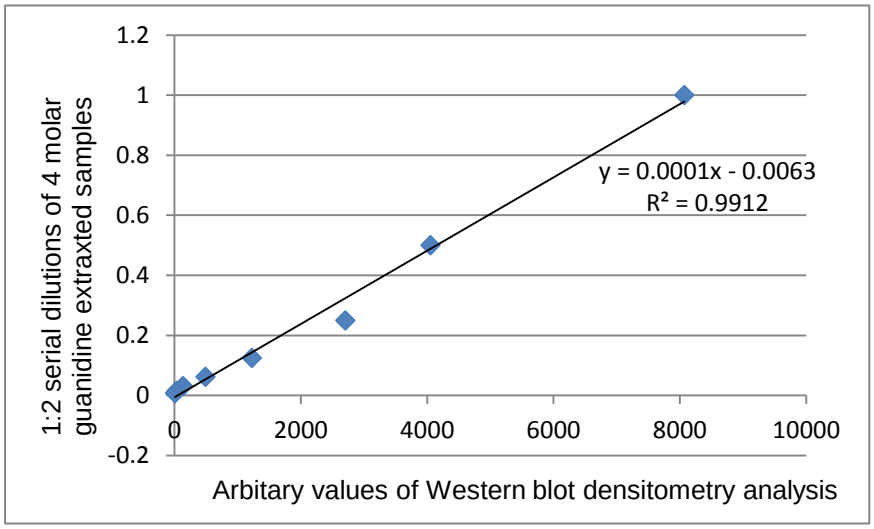

Figure 2-7: An example of a standard curve of the CCL proteins extracted with 4 molar guanidine HCL.

The graph shows a linear response of the Western blot signal.

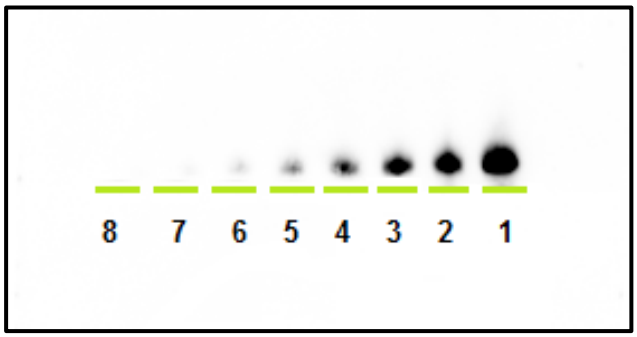

Figure 2-8: Gradual intensity changes of the Western blot signal.

A serial dilution of 1:2 was performed that ranged from a sequence from 1 to 8. The intensity is altered with decreasing protein load. The CCL protein sample transferred into the blot membrane has been probed with lumican antibody. The numbers on the Figure represents the $\log_2$ of the dilution.

2.4.4 **Western blot quantification**

1- Data were analysed using VisionWorksLS (UVP, USA) image acquisition and analysis software package.

2- The area density was measured for each band to detect differences in GAGs and proteoglycans between CCL anatomical regions of Staffordshire bull terrier and in between dog breeds with a differing predisposition to CCL rupture (Staffordshire bull terrier vs. greyhound).

3- Two 10 well NuPAGE 4-12 % Bis-Tris Gels (Life Technologies, UK) were used to detect differences for GAGs and proteoglycans between CCL anatomical regions of Staffordshire bull terrier. The values were normalised between the two gels by loading one of the same samples into each gel (Figure 2-9).

4- One 12 well NuPAGE 4-12 % Bis-Tris Gel (Life Technologies, UK) was used to detect differences for GAGs and proteoglycans between Staffordhsire bull terrier and greyhound. Mean density value was measured without using a sample standard as all samples were loaded into the same gel (Figure 2-10).

Figure 2-9: Area density measurement for lumican core protein in different anatomical regions of the CCL from Staffordshire bull terrier.

The anatomical regions of the CCL were obtained from the Staffordshire bull terrier (n=5). In order to calculate the results, values were standardised by loading one of the same samples to each gel (O= origin; M= middle; I= insertion).

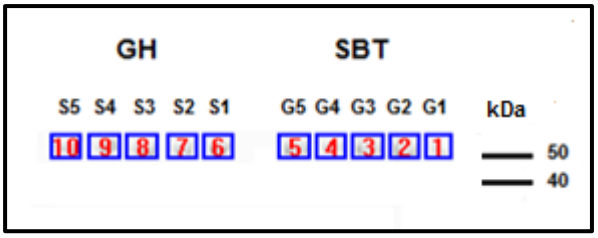

Figure 2-10: Area density measurement for lumican core protein fromStaffordshire bull terrier and greyhound CCLs.

CCLs were obtained from Staffordshire bull terrier and greyhound (n=5). The mean density was calculated without normalising with a standard as all samples were loaded into the same gel (G= greyhound; S= Staffordshire bull terrier).

2.5 Histology and immunohistochemistry

CCLs (n=12) harvested from Staffordshire bull terriers were fixed in 4% paraformaldyhyde overnight at 4°C then processed and embedded in paraffin wax. Other archived tissue blocks from greyhound (n=8) and Labrador retriever (n=7) CCLs were also used for this study. 4 µm sections of these tissues were cut and mounted onto “POLY FROST”, poly lysine coated slides (Solmedia, UK). Images were captured (x10 and x40 magnifications) using a Nikon Eclipse 80i microscope (Nikon, Japan).

2.5.1 Histology

2.5.1.1 Haematoxylin and Eosin stain

Slides were stained with Haematoxylin and Eosin (H&E) to assess cell morphology and tissue architecture, and to investigate whether there were any signs of degeneration of the tissue. Slides were also stained with Toluidine blue or Alcian blue to allow distribution of sGAGs in the tissue to be identified. The ligaments stained included CCL sections from Labrador retrievers (n=8) and greyhounds (n=13).

2.5.1.2 Toluidine blue stain

The Toluidine blue staining protocol was adapted from Schmitz and others (Schmitz, Laverty et al. 2010). Sections were rehydrated (Table 2-5) then stained from 5-10 minutes with 0.04 % Toluidine blue in 0.2 M acetate buffer solution; pH 3.75-4.25. Slides were then rinsed with tap water before being dehydrated (table 2-5) and mounted under coverslips with Di-n-butyl phthalate in xylene (D.P.X).

2.5.1.3 **Alcian blue stain**

This method was based on one previously described by Vogel and others (Vogel and Petres et al. 2005). Tissue sections were rehydrated (Table 2-5) and immersed for 3 minutes in 3% acetic acid; pH 2.5, followed by staining with Alcian blue solution for 1 hour at 25 ^{o}C. Slides were then counterstained with Eosin Y, rinsed under tap water, dehydrated (Table 2-5) and mounted under coverslips with D.P.X.

Table 2-5: Rehydration and dehydration steps used prior to staining of tissue sections in both histology and immunohistochemistry techniques.

Rehydration (time)	Dehydration (time)
Xylene x2 10 minutes	Distilled water x2 5 minutes
100 % Alcohol x2 10 minutes	95 % Alcohol x2 10 minutes
95 % Alcohol x2 10 minutes	100 % Alcohol x2 10 minutes
Distilled water x2 5 minutes	Xylene x2 10 minutes

Table 2-6: Tris buffered saline solution used in immunohistochemistry.

10x TBS	0.06 M Trizma, 1:3 dilution of 1 M HCL, pH 7.6
1X TBS TWEEN	1:10 dilution of 10x TBS, 0.0072 M NaCl, 0.05 % TWEEN,

2.5.1.4 **Histology scoring**

Histology scoring was performed with 2 different scoring schemes. All CCL tissue sections were assessed twice, at least one week apart, by two independent observers that were blinded to dog breed and tissue location. Calculated scores from each observer were averaged as the final result. The agreement between inter and intra-observer scores was assessed using Kendall's coefficient of concordance. The H&E scoring sheet included 12 categories (Table 2-7), whilst for Toluidine blue and Alcian blue, the scoring criteria involved 7 categories (Table 2-8). A score from 0-3 was assigned for each category as follows; 0= 0% absence of factor, 1= 0-25% factor present up to one quarter of tissue, 2= 25-50% factor present up to half of tissue, 3= >50% factor present above 50 % of tissue. Each factor had a range of percentages of the amount of tissue section affected; 0 %, 0-25 %, 25-50 %, and >50 % depending on extent of presence or absence of each component.

H&E scoring:

Collagen architecture	>50	25-50	0-25	0
Normal collagen architecture	☐	☐	☐	☐
Reduced collagen architecture	☐	☐	☐	☐
Abnormal collagen architecture	☐	☐	☐	☐

Cellular distribution and shape

Cell shape	>50	25-50	0-25	0
Spindle	☐	☐	☐	☐
Mixed (spindle and rounded cells)	☐	☐	☐	☐
Rounded	☐	☐	☐	☐

Cell distribution	>50	25-50	0-25	0
Normal distribution of cells	☐	☐	☐	☐
Formation of cell chains	☐	☐	☐	☐

Vascularity of the ligament substance	>50	25-50	0-25	0
Low vascularisation	☐	☐	☐	☐
Moderate to high vascularisation	☐	☐	☐	☐

Inflammation	>50	25-50	0-25	0
No evidence of inflammatory cells	☐	☐	☐	☐
Increased numbers of inflammatory cells	☐	☐	☐	☐

Table 2-7: Haematoxylin and Eosin scoring sheet. The scoring system gives a range from 0-3. 3= 50 % present, 2= 25-50 % present, 1= 25 % present, 0= absent.

(Adapted from Kharaz 2015).

Toluidine blue and Alcian blue scoring:

sGAG distribution and location

Overall	>50	25-50	0-25	0
Marked staining	☐	☐	☐	☐
Faint staining	☐	☐	☐	☐

Location	>50	25-50	0-25	0
Interfascicular	☐	☐	☐	☐
Interbundle	☐	☐	☐	☐
Ligament substance	☐	☐	☐	☐

Location of stain with cells	>50	25-50	0-25	0
Around the cells	☐	☐	☐	☐
Within the cells	☐	☐	☐	☐

Table 2-8: Toluidine blue and Alcian blue scoring system sheet. The scoring system gives a range from 0-3. 3= 50 % present, 2= 25-50 % present, 1= 25 % present, 0= absent.

(Adapted from Kharaz 2015).

2.5.2 **Immunohistochemistry**

Slides were rehydrated as described previously (Table 2-5) and endogenous peroxidase activity was blocked by incubating tissue sections with 3 % H_2O_2 for 10 minutes at room temperature. Prior to their localisation, tissue sections were washed in water, followed by pre-digestion with chondroitinase ABC solution for 30 minutes at room temperature (0.5 units/ ml of ChABC in 100 mM Tris HCL, pH 7.2-7.4). Non-specific binding was blocked using 20 % goat serum in 1x Tris buffered saline-TWEEN (TBS-T) (solution described in Table 2-2) for 10 minutes at room temperature. The serum was removed by washing sections in TBS-T (Table 2-8) and sections were then incubated overnight at 4^{o}C with primary antibody diluted 1:50 in TBS-T (Table 2-9). Following incubation, sections were washed in TBS-T and then incubated with secondary antibody (Table 2-10). All secondary antibodies were diluted in 20 % swine or goat serum in TBS-T for 30 minutes at room temperature. Finally, after further washes in TBS-T, a pair of diaminobenzidine tablets was dissolved in 5 ml ultrapure water solution for one minute. The solution was then added to the section until a brown colour developed, sections were rinsed in distilled water. Sections were counterstained with Haematoxylin, dehydrated (Table 2-5) and cover slipped with D.P.X mounting solution. A schematic of the principles of immunohistochemistry is illustrated in Figure 2-11.

Table 2-9: Primary antibodies used for immunohistochemistry.

Antibody isotype	Proteoglycan/ GAG	Label	Antibody recognition site
Mouse monoclonal IgG	Decorin	*DECN 70.6	Specific for core protein of decorin
Mouse monoclonal IgG	Biglycan	**PR8A4	C-terminal amino acid sequence of human biglycan
Mouse monoclonal IgM	Lumican	*LUM1	Unknown
Mouse monoclonal IgG	Keratocan	*KER-1	Specific for the core protein of keratocan
Rabbit polyclonal IgG	Fibromodulin	**PR184	C-terminal amino acid sequence of human fibromodulin
Mouse monoclonal IgG	Versican	12C5	G1 domain of versican
Mouse monoclonal IgG	Aggrecan	*7D1	G1 and chondroitin sulphate attachment domains

** Kindly donated by Prof. Peter Roughly

*Kindly donated by Prof. Bruce Caterson and Dr. Clare Hughes

Table 2-10: Secondary antibodies used for immunohistochemistry.

Secondary antibody	Dilution	Concentration
Peroxidase conjugated Rabbit anti-mouse IgG	1:50	5 µg/ ml
Peroxidase conjugated goat anti-mouse IgM	1:50	5 µg/ ml
Peroxidase conjugated rabbit-anti goat IgG	1:50	5 µg/ ml

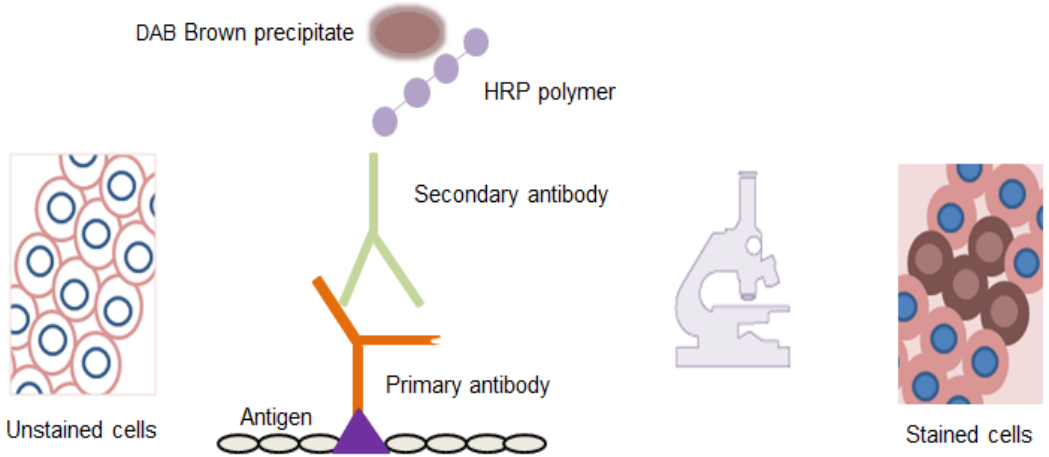

Figure 2-11: Representative image of the immunohistochemistry methodology.

The primary antibody binds to the antigen on the tissue section, and slides are then rinsed to remove unattached antibodies. The secondary antibody that carries the enzyme horse radish peroxidase (HRP) binds to the primary antibody. The slides are washed again before adding the substrate of 3, 3′-Diaminobenzidine tablets (DAB) substrate. Once DAB is added, it reacts with HRP enzyme and transforms the DAB substrate into a brownish precipitate in the tissue at the reaction site that can be visualised by microscopy.

2.6 Reverse transcription quantitative real time polymerase chain reaction (RT-qPCR)

CCL samples obtained from Staffordshire bull terrier dogs (n=6) were cut into three sections (origin, middle, and insertion). Archived CCLs from greyhound (n=5) were obtained from either the caudolateral or caudomedial band. All samples were immersed in RNA later overnight at 4°C then stored at -20°C until required.

2.6.1 Ribonucleic acid (RNA) isolation

Frozen samples were pulverised with a dismembrenator (B. Brown Biotech Micro Dismembrator, U.S.A). A low temperature was achieved by cooling the instrument components and tissue using liquid nitrogen. RNA was extracted from the samples by incubating them in 1 ml of TRIzol reagent for one hour at room temperature. 0.1 ml of 1-bromo-2 chloropropane was then added to each sample with gentle shaking for 15 seconds. Samples were rested for 3 minutes at room temperature and were placed in centrifuge at 12,000 x g for 20 minutes at 4°C. The clear, aqueous top phase that formed after centrifugation was removed and then added to a clean RNAse-free 1.5 ml centrifuge tube. To precipitate ribonucleic acid (RNA), 250 µl of isopropanol was added to the aqueous phase and incubated at room temperature for 10 minutes. 2 µl of GlycoBlue (Ambion, UK) was also added to the samples to be used as a co-precipitant for RNA. Samples were then centrifuged at 12,000 x g for 20 minutes at 4°C, and the supernatant removed leaving a visible RNA pellet. The pellet was washed with 1 ml of 75 % ethanol and centrifuged at 12,000 x g for 5 minutes at 4°C. Finally, RNA was air-dried, reconstituted in Tris-EDTA (TE) buffer (Ambion, UK) and concentrations determined by measuring the absorbance between 260 and 280 nm using a NanoDrop spectrophotometer (ND-1000, Thermo scientific, U.S.A). RNA quality was confirmed using an optical density 260:280 ratio between 1.8-2.1. All products were from Sigma, UK unless noted.

2.6.2 **Deoxyribonuclease treatment**

Deoxyribonuclease (DNase) treatment was performed to prevent contaminating genomic DNA interfering with downstream qPCR assays. In order to degrade single- and double-stranded DNA, samples were incubated with an endonuclease (DNase I). DNase buffer (10X diluted to 1X) and 4U DNase I enzyme (both from Ambion, UK) were combined with 10ug total RNA in a 50 µl final volume and incubated at 37°C for 30 minutes. RNA samples were brought up to 100 µl by adding RNAse-free water, and then an equal volume of phenol: chloroform was added to stop the DNase I activity (Ambion, UK). Samples were then centrifuged at 12,000 x g for 5 minutes at 4°C. The upper aqueous phase was removed and added to a clean 1.5 ml centrifuge tube. 10 µl of ammonium acetate (Ambion, UK) and 300 µl of 100 % ethanol were then added to precipitate the RNA (Ambion, UK), followed by 2 µl of GlycoBlue as a co-precipitant. Samples were mixed and then incubated on ice for 30 minutes. Next, the samples were centrifuged at 12,000 x g for 20 minutes at 4°C, the supernatant removed and the RNA pellet rinsed with 1 ml of 75 % ethanol. Following a final centrifugation step at 12,000 x g for 5 minutes at 4°C, the RNA pellet was air-dried, reconstituted in Tris EDTA Buffer (Ambion, UK) and the concentration determined using a NanoDrop spectrophotometer (ND-1000, Thermo scientific, U.S.A).

2.6.3 **Reverse transcription of DNase treated RNA**

1 µg of total RNA was reverse transcribed to cDNA. For the annealing step, random primers (2µg/ µl) were added to 1 µg of total RNA, the solution heated for 5 minutes at 70°C and then directly transferred onto ice for one minute. For the extension step, Molony murine leukemia virus reverse transcriptase (M-MLV-RT) (200u/ µl), 5x M-MLV-RT buffer, 0.6 µl (40u/ µl) RNasin® Plus RNase Inhibitor, and 100 Mm dNTP mix were all combined into a total volume of 11.6 µl (all from Promega, UK) and added to the RNA samples. cDNA was synthesised by incubating the reactions at 37°C for 60 minutes. The mixture was then heated to 90°C for 5 minutes to deactivate the reverse transcriptase enzyme, and then stored at -20°C until required.

2.6.4 **Amplification of RT-qPCR**

Reverse transcription quantitative real-time-PCR (RT-qPCR) was performed to quantify the expression of the genes. cDNA samples were diluted to a final concentration of 10ng/ µl with RNase-free water. RT-qPCR was performed in a 25 µl volume containing; 50 ng cDNA, 6 pmol/ µl forward and reverse primers designed for the particular gene of interest (Eurogentic, UK), and GoTaq(R) qPCR Master Mix (Promega, UK) diluted to 1x. Samples were run in duplicate with non-template control on an Applied Biosystems 7300 Real-Time PCR using the given amplification conditions as represented in table 2-11.

Table 2-11: Amplification process for Applied Biosystems 7300 Real-Time PCR.

Phase	Period	Temperature	Number of cycles
AmpErase Uracil N-Glycosylase (**UNG**)	2 minutes	50°C	x1
AmpliTaq Gold® DNA Polymerase Activation	10 minutes	95°C	x1
Denaturation	15 seconds	95°C	x40
Annealing	60 seconds	60°C	
Extension	60 seconds	60°C	

The SYBR Green RT-qPCR procedure is shown in Figure 2-12. SYBR Green is a dye that interacts with double-stranded DNA to generate a fluorescent signal, and RT-qPCR measures the amount of the amplified product while the reaction occurs. The increase of florescent dye is directly related to the amplified product. The threshold cycle (C_T) is the quantitative endpoint for RT-qPCR, as the amount of starting material to be amplified is inversely related to the numerical value of the C_T. For example, the greater the original amount of target sequence, the lower the C_T value will be. Primer efficiencies were validated performing a sequence (1 to 8) of 1:2 serial dilutions, and were compared with those targeting two reference gene (GAPDH and B2M). All primers were found to lie within 10 % of GAPDH and B2M percentage (see appendix II). Primers (Table 2-12) were then chosen to be normalised against GAPDH, and the fold change in gene expression level calculated using the ΔC_T method (Schmittgen and Zarkrajsek 2000). For melt curve analysis, see appendix III.

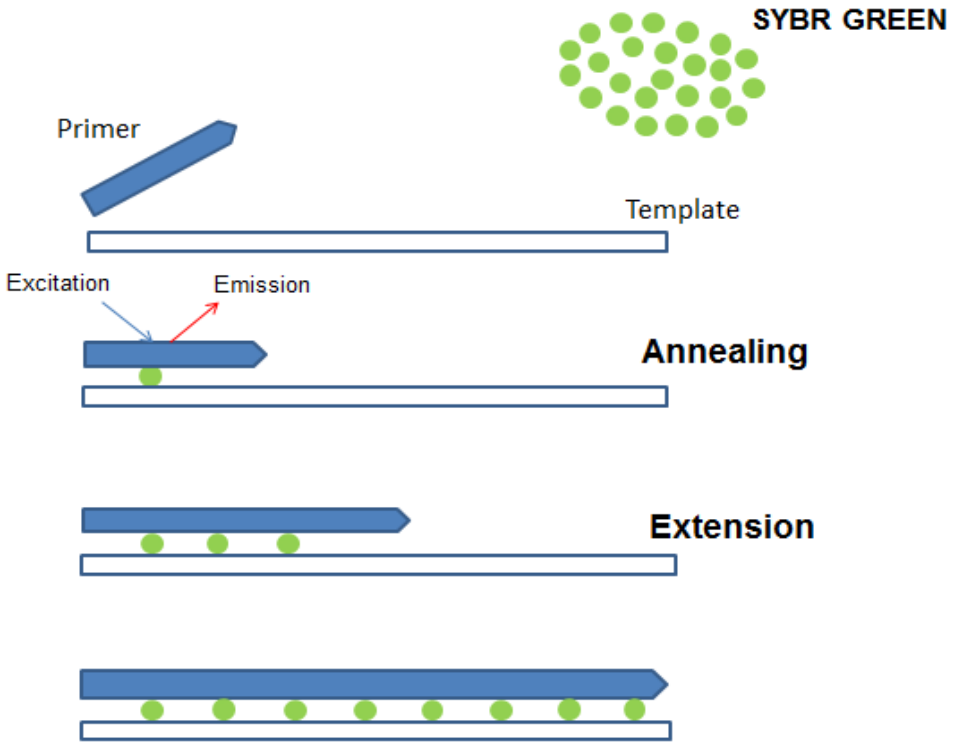

Figure 2-12: Amplification process for Real-time RT-PCR.

The Figure demonstrates RT-PCR with SYBR GREEN to detect gene expression levels. During the annealing step, SYBR GREEN interacts with double-stranded DNA. This interaction causes SYBR GREEN to fluoresce. As the fluorescent dye accumulates, the PCR cycle continues and the amplified product is measured at the end point of each cycle (Adapted from Williamson 2012).

Table 2-12: Reference and target gene sequences for primers used in real time RT-qPCR.

Gene	Sequence	Reference
GAPDH	Forward 5' CTGGGGCTCACTTGAAAGG 3' / Reverse 5' CAAACATGGGGGCATCAG 3'	(Clements, Carter et al. 2006)
Aggrecan	Forward 5' GGGACCTGTGTGAGATCGAC 3' / Reverse 5' GTAACAGTGGCCCTGGAACT 3'	(Clements, Carter et al. 2006)
Versican	Forward 5' GGGACCTGTGTGAGATCGAC 3' / Reverse 5' GTAACAGTGGCCCTGGAACT 3'	(Clements, Carter et al. 2006)
Decorin	Forward 5' CGCTGTCAGTGCCATCTC 3' / Reverse 5' GGGGGAAGATCTTTTGGTACTT 3'	(Clements, Carter et al. 2006)
Biglycan	Forward 5' CAGAACAACGACATCTCAGAGC 3' / Reverse 5' TCACCAGGACGAGAGCGTA 3'	(Clements, Carter et al. 2006)
Lumican	Forward 5' ACCTGGAAATTCTTTTAATGTATCATC 3' / Reverse 5' CGGTATGTTTTTAAGCTTATTGTAGGA 3'	(Clements, Carter et al. 2006)
Fibromodulin	Forward 5' CCTCCAAGGCAATAGGATCA 3' / Reverse 5' GAAGTTCATGACGTCCACCAC 3'	(Yang, Culshaw et al. 2012)
ADAMTS-4	Forward 5' GACCAGTGCAAACTCACCTG 3' / Reverse 5' CAGGGAGTCCCATCTACCAC 3'	(Clements, Carter et al. 2008)
ADAMTS-5	Forward 5' TGGGTTCCCAAATATGCAG 3' / Reverse 5' CTGTCCCATCCGTCACCT 3'	(Clements, Carter et al. 2006)

Chapter 3: Characterising regional and breed differences in the proteoglycan and glycosaminoglycan content of the canine cranial cruciate ligament.

3.1 Introduction

Proteoglycans consist of a core protein attached to one or more glycosaminoglycan (GAG) chains and perform both structural and regulatory functions (Iozzo 1998; Iozzo and Schaefer 2015). The small leucine rich proteoglycan (SLRPs), such as decorin, biglycan and fibromodulin bind to collagen fibrils and organise collagen fibrillogenesis (Scott and Haigh 1988; Iozzo 1999; Douglas, Heinemann et al. 2006). Aggrecan and versican are known as the large aggregating proteoglycans (Iozzo and Murdoch 1996). Aggrecan allows tendon the capacity to withstand compressive forces associated with loading (Vogel and Koob 1989; Evanko and Vogel 1993; Huisman, Andersson et al. 2014). Versican, on the other hand, regulates cell migration, adhesion, and contributes to the extracellular matrix (ECM) structural properties (Dours-Zimmermann and ZimmermannS 1994; Isogai, Aspberg et al. 2002).

A disintegrin-like and metalloproteinase with thrombospondin motifs -4 and -5 (ADAMTS-4 and -5) are ECM proteases that are known to cleave proteoglycans, such as aggrecan, versican, decorin, biglycan, and fibromodulin (Sandy, Westling et al 2001; Kashiwagi, Enghild et al. 2004; Porter, Clark et al. 2005; Melching, Fisher et al. 2006). Several studies have detected the presence of decorin, biglycan, and fibromodulin catabolic products in tendon explant cultures without a catabolic stimulus (Rees, Flannery et al. 2000; Rees, Dent et al. 2009), which suggests that ADAMTS -4 and -5 may be required for normal functioning of SLRPs in tendon.

Proteoglycan and GAG deposition have been shown to vary accordingly to the anatomical regions of tendon (Vogel, Ordog et al. 1993; Feitosa, Reis et al. 2006; Matuszewski, Chen et al. 2012; Buckley, Huffman et al. 2013). Despite this, it is still unknown whether proteoglycans and GAGs exhibit regional variations in the canine cranial cruciate ligament (CCL). For more details, see Chapter 1 - Section 1.3.5.3.4 & 1.3.5.4.

Previous studies using Western blot analysis have identified SLRPs, large aggregating proteoglycans, and GAGs in different anatomical regions of tendon tissues (Robbins, Evanko et al. 1997; Waggett, Ralphs et al. 1998; Rees, Flannery et al. 2000; Samiric, Ilic et al. 2004; Ilic, Carter et al. 2005; Rees, Wagget et al. 2009). Decorin, biglycan, and chondroitin -6, -4, and -0 sulphate stubs have been investigated in bovine young and mature tendon in regions subjected to tension and compression (Rees, Flannery et al. 2000). Aggrecan and aggrecanase fragments of

the aggrecan core protein were also found in tendon (Rees, Flannery et al. 2000). In addition, aggrecan, biglycan, and keratocan were previously found to be expressed in tendon especially within sites subjected to compression (Robbins, Evanko et al. 1997; Rees, Wagget et al. 2009). However, none of these studies have performed densitometry analysis on the molecular weight bands of proteoglycans and GAGs to fully quantify the differences between compressional and tensional regions of tendon. Overall, these studies may suggest that proteoglycans and GAGs may vary in different anatomical regions (tension vs. compression) of tendon and ligament in order to adjust for their mechanical and biological needs.

Certain GAGs and proteoglycans have been shown to increase in tendon/ ligament pathology (Riley, Harral et al. 1994a; Lo, Marchuk et al. 1998; Corps, Robinson et al. 2006; Halper, Kim et al. 2006; Fu, Chan et al. 2007; Samiric, Parkinson et al. 2009) (See Chapter 1 - Section 1.3.5.5 for details). Aggrecan, versican, fibromodulin, biglycan gene expression were increased in human patellar tendinopathy, however, decorin gene expression levels did not (Samiric, Parkinson et al. 2009). Another study have reported increased aggrecan and biglycan gene expression levels in the compressed region (where tendon attaches to bone) of human Achilles tendinopathy, however, versican and decorin gene expression levels were not increased (Corps, Robinson et al. 2006). These findings suggest that increased levels of certain proteoglycans and GAGs may lead to tendon and ligament pathology.

Increased proteoglycan levels have been shown to be linked to CCLD/ R in the dog, where lumican and aggrecan gene expression levels were found to be significantly increased in ruptured CCLs of the Labrador retrievers (high risk breeds to CCLD/ R) in comparison to their intact CCLs (Clements, Carter et al. 2008).

In the dog, narrowing of the intercondylar notch has been associated with CCLD/ R and osteoarthritis (Aiken, Kass et al. 1995; Wada, Tatsuo et al. 1999). In addition, ACL normal function has been shown to be impeded when it passes through a narrowed intercondylar notch, and therefore damage occurs to the ACL (Muneta, Takakuda et al. 1997). The intercondylar notch index and femoral condyle height and width have been shown to be significantly lower in the Labrador retriever and golden retriever (high risk to CCLD/ R) compared to the greyhound (low risk to CCLD/ R) (Comerford and Tarlton et al. 2006a).

A previous study has shown a significant increase in sulphated glycosaminoglycans (sGAGs) content in the high risk Labrador retriever CCLs compared to those of the low risk greyhound at the region where the CCL is compressed by the intercondylar notch (Comerford, Tarlton et al. 2006a). The increased compression in the high risk Labrador retriever CCL could result in the deposition of proteoglycans and GAGs associated with compressive sites of tendon and ligament.

We hypothesise that the content and metabolism of proteoglycans and GAGs vary in different anatomical regions of the Staffordshire bull terrier CCL and in different dog breeds (Staffordshire bull terrier vs. greyhound) with an altered predisposition to CCLD/ R.

The Staffordshire bull terrier is a breed with moderate-high risk for CCLD/ R, therefore, it was selected as a good model to determine the proteoglycan/ GAG content and gene expression within anatomical regions of the CCL. In order to compare proteoglycan/ GAG content and gene expression between two differentially predisposed dog breeds to CCLD/ R, we have chosen Staffordshire bull terrier CCLs (moderate-high risk to CCLD/ R) and compared it to greyhounds (low risk to CCLD/ R).

Therefore, the aim of this work was to use Western blot analysis to identify and measure whether there are regional differences in proteoglycans and GAGs in the CCL. Furthermore, the aim was to identify and measure whether there are differences in proteoglycans and GAGs between dog breeds with a differing predisposition to CCLD/ R. We further aimed to use real time RT-PCR to characterise proteoglycans and ECM proteases (ADAMTS 4 & 5) between two dog breeds with a different predisposition to CCLD/ R.

3.2 Materials and methods

3.2.1 Canine sample collection

CCLs were harvested from Staffordshire bull terriers (n=17) with no macroscopic evidence of stifle joint pathology or any other musculoskeletal disease. Archived samples from ex racing greyhounds (n=15) were used for this study. These samples were obtained with ethical permission and full owner consent where appropriate. Inclusion/ exclusion criteria for samples and ethical permission are described in Chapter 2 - Table 2-1 and 2-2.

CCL samples for Western blot analysis were dissected from Staffordshire bull terriers (n=5) and separated into origin, middle and insertion parts in order to detect specific proteoglycans and GAGs in different anatomical regions of the CCL. In addition, other CCLs from Staffordshire bull terriers (n=5) and greyhounds (n=5) were obtained without dividing them into separate ligament regions, and this was performed in order to detect specific proteoglycans and GAGs in two dog breeds with a different predisposition to CCLD/ R. Samples were snap frozen in liquid nitrogen and stored in -80^{o}C until required.

For real time RT-PCR analysis, CCLs from Staffordshire bull terriers (n=5) and greyhounds (n=5) were similarly collected as described above. Samples were immersed in RNA later overnight at 4^{o}C in liquid nitrogen and stored in -80^{o}C until required.

3.2.2 Western blot analysis

CCL samples were extracted with 4M guanidine hydrochloride and digested with enzymes specific for eliminating GAG chains. Enzymes used were chondroitinase ABC (to eliminate dermatan and chondroitin sulphate chains), keratanase I (to eliminate keratan sulphate I chains), and keratanase II (to eliminate keratan sulphate II chains). These enzymes are necessary in order to detect the proteoglycan core protein and GAG stubs (See Appendix I for product manufacturers). Samples were heated either under reducing or non-reducing conditions and loaded onto a 4-12 % Nupage Bis-Tris gel (Invitrogen). Details for Western blot analysis procedure are described in Chapter 2 - Section 2.4. The monoclonal/ polyclonal antibodies specific for the proteoglycans and GAG stubs are listed in details in Chapter 2 - Table 2-3.

3.2.3 **Real time RT-qPCR**

Ribonucleic acid (RNA) was extracted from CCL samples with 1 ml of TRIzol reagent. Complementary deoxyribonucleic acid (cDNA) was reverse transcribed with 1 µg of total RNA in order to be amplified. Primers were normalised against GAPDH, and the fold change in gene expression level was calculated using the Δ CT method (Schmittgen and Zarkrajsek 2000). The primers specific for proteoglycans and ADAMTS's are shown in Chapter 2 - Table 2-12.

3.3 **Statistical analysis**

Statistical analysis was performed on gene expression data and Western blot densitometry results. Data were primarily tested for normality using Kolmogorov-Smirnov test. Statistical analysis involved comparing three groups (origin, middle, and insertion parts of Staffordshire bull terrier CCL) or two groups (Staffordshire bull terrier vs. greyhound). If data had a normal distribution, the three groups were tested by performing a one-way ANOVA followed by a Bonferroni post-hoc test for multiple comparisons, whereas the two groups were tested by selecting a student t-test. When data did not have a normal distribution, the three groups were tested by performing a Kruskal-Wallis test followed by a Dunn's test for multiple comparisons, while the two groups were tested by selecting a Mann Whitney U test. Results are presented as mean values ± standard error of the mean (SEM). Exact p-values are presented and a significance level of $p < 0.05$ was used. Graphpad Prism (Version 6, GraphPad Software, La Jolla California, USA) software was used for statistical analysis of all data.

3.4 **Results**

3.4.1 **Canine CCL data summary**

The history of canine cadavers was recorded which consisted of the dog breed, age, bodyweight and gender where applicable.

Table 3-1: Summary of the age, bodyweight and gender of canine cadaveric CCL samples selected for Western blot and RT-PCR analysis.

(SBT= Staffordshire bull terrier; GH= greyhound; N/ A= not available).

Procedure	Breed	Ligaments	Age	Weight (Mean ± SEM)	Male	Female
Western blot	SBT	n= 12	2-5 years	20.3 ± 2.8 kg	12	0
	GH	n= 10	3-5 years	N/ A	N/ A	N/ A
RT-PCR	SBT	n= 5	2-5 years	19 ± 1.7 kg	5	1
	GH	n= 5	3-5 years	25 ± 1.2 kg	N/ A	N/ A

3.4.2 **Western blot analysis**

3.4.2.1 **Negative controls**

Negative controls for Western blot analysis were performed by omitting the addition of the primary antibody. No or non-specific bands were detected in the absence of primary antibodies. Negative control Figures are provided in appendix IV.

3.4.2.2 **Comparison between different anatomical regions of Staffordshire bull terrier**

3.4.2.2.1 **Large aggregating proteoglycans**

Analysis using the anti-aggrecan antibody did not consistently detect aggrecan in any regions of the CCL. Despite the high concentrations of the antibody that were able to produce a non-specific inverted signal (white bands on blots in Figure 3-1 A), no positive signal was observed at the expected high molecular weights. The only positive signal was observed was in Figure 3-1 A, where an approximately 55 kDa protein was identified, which might represent a degradation product contained within the tissue. Analysis with anti-versican antibody revealed that versican is present in the anatomical regions of the Staffordshire bull terrier CCL at molecular weights ranging from 40 to 260 kDa and above (Figure 3-1 B). To compare relative amounts of these proteoglycans between different anatomical regions of the CCL, densitometry was carried out. The extent of each lane included is indicated by the green bar in Figure 3-1 B. Versican was found to be significantly lower in origin ($p=0.003$) and insertion ($p=0.003$) anatomical regions compared to the middle ($p=0.16$) region (Figure 3-5).

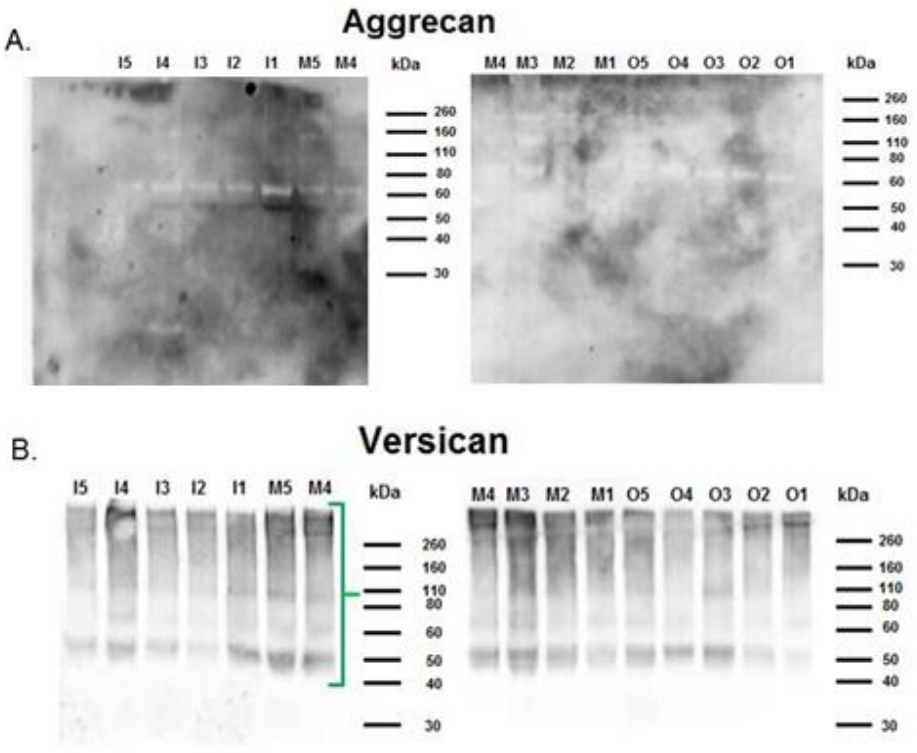

Figure 3-1: Western blot analysis of aggrecan and versican in different anatomical regions of the Staffordshire bull terrier CCL.

The Figure shows A) Aggrecan mAb 7D1 and B) Versican mAb 12C5. Lanes are labelled with sample identifiers as follows; O= origin; M= middle; and I= insertion whilst the number refers to the donor animals, n= 5. The core protein fragments of versican (40-260 kDa) are marked in green.

3.4.2.2.2 **Chondroitin/ dermatan sulphate proteoglycans**

Analysis using the anti-decorin antibody revealed that decorin is present in different anatomical regions of the Staffordshire bull terrier at molecular weights ranging from 40-50 kDa which corresponds with the expected size of the decorin core protein (Figure 3-2, A). Other molecular weight bands of interest for decorin were at 80 kDa (blue arrow). Western blotting using anti-biglycan antibody revealed that biglycan is present in different anatomical regions of the Staffordshire bull terrier CCL at molecular weights ranging from 40-50 kDa which corresponds to the expected size of the biglycan core protein (Figure 3-2 B). To compare relative amounts of these proteoglycans between different anatomical regions of the CCL, densitometry was carried out. The extent of each lane included is indicated by the green bar in Figure 3-2 A, B. Densitometric analysis showed that there was no statistically significant differences in the levels of decorin and biglycan core proteins between the anatomical regions examined.

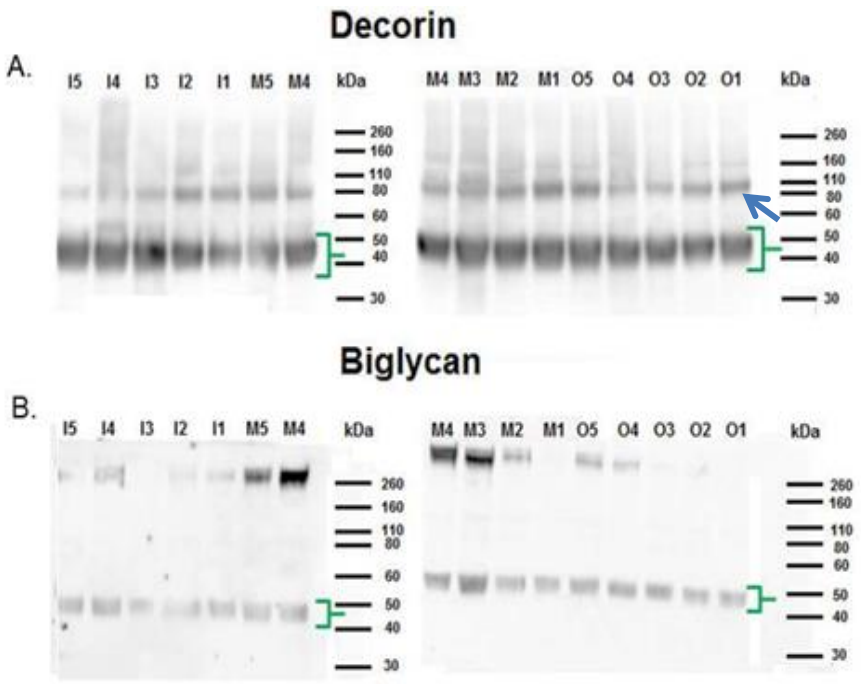

Figure 3-2: Western blot analysis of decorin and biglycan in different anatomical regions of the Staffordshire bull terrier CCL.

The Figure shows A) Decorin mAb 70.6 and B) Biglycan mAb PR8A4. Lanes are labelled with sample identifiers as follows; O= origin; M= middle; and I= insertion whilst the number refers to the donor animals, n= 5. The core protein of decorin (40-50 kDa) and biglycan (40-50 kDa) proteoglycans are marked in green. Other bands of interest are the 80 kDa band (blue arrow) in decorin.

3.4.2.2.3 **Keratan sulphate proteoglycans**

Analysis using anti-fibromodulin and anti-lumican antibody revealed that fibromodulin and lumican were present in different anatomical regions of the Staffordshire bull terrier at a molecular weight of 50 kDa corresponding to their expected size (Figure 3-3 A, B). Further analysis using an anti-keratocan antibody revealed that keratocan was present between different anatomical regions of the Staffordshire bull terrier CCL at a molecular weight of 30 kDa corresponding to its expected size (Figure 3-3 C). To compare relative amounts of these proteoglycans between different anatomical regions of the CCL, densitometry was carried out. The extent of each lane included is indicated by the green bar in Figure 3-3 A, B, C. Densitometric analysis showed that keratocan protein levels were significantly lower in the origin anatomical region compared to the middle region ($p=0.046$) of the Staffordshire bull terrier CCL (Figure 3-5).

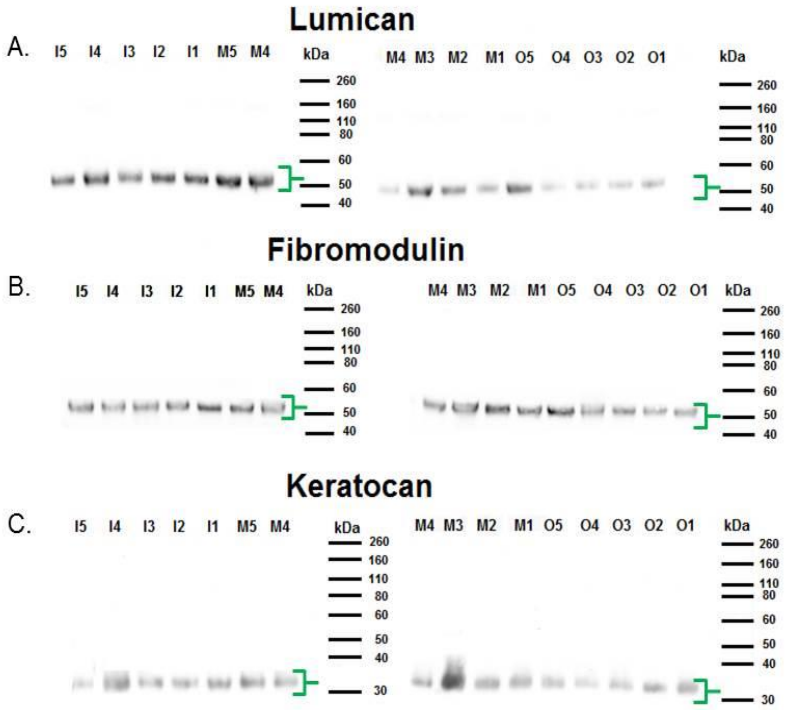

Figure 3-3: Western blot analysis of lumican, fibromodulin, and keratocan in different anatomical regions of the Staffordshire bull terrier CCL.

The Figure shows A) Lumican mAb LUM-1, B) Fibromodulin mAb PR184, and C) Keratocan mAb KER-1. Lanes are labelled with sample identifiers as follows; O= origin; M= middle; and I= insertion whilst the number refers to the donor animal, n= 5. The core proteins of lumican (50 kDa), fibromodulin (50 kDa), and keratocan (30kDa) are marked in green.

3.4.2.2.4 **Glycosaminoglycans**

Analysis using the anti-chondroitin-6 sulphate stub antibody detected chondroitin-6 sulphate stub in different anatomical regions of the Staffordshire bull terrier CCL at a range of molecular weights from 80-260 kDa (Figure 3-4 A). Analysis using an anti-chondroitin-4 sulphate stub antibody detected stubs in different anatomical regions of the Staffordshire bull terrier across a wide spectrum of sizes ranging from 80-260 kDa, which were termed high molecular weight bands (Figure 3-4 green, lane B). The chondroitin-4 sulphate stub antibody also detected a more discretely sized set of stubs of around 40-50 kDa that were termed low molecular weight bands (Figure 3-4, purple, lane B). Analysis using anti-chondroitin-0-sulphate stub antibody revealed that chondroitin-0 sulphate stubs between the different anatomical regions of the Staffordshire bull terrier ranged from 260 kDa and above (Figure 3-4 C). Analysis using anti-keratan sulphate stub antibody revealed that keratan sulphate stubs ranged between 80-260 kDa by Western blotting (Figure 3-4 D). To compare relative amounts of these proteoglycans between different anatomical regions of the CCL, densitometry was carried out. The extent of each lane included is indicated by the green or purple bar in Figure 3-4 A, B, C, D. There were no statistically significant differences between anatomical regions examined in regards to chondroitin -0 sulphate stub, chondroitin -6 sulphate stub, chondroitin -4 sulphate low molecular weight stub, and keratan sulphate stubs between anatomical regions examined. However, chondroitin -4 sulphate high molecular weight stubs were found to be significantly higher in middle ($p=0.01$) and insertion ($p=0.003$) anatomical regions in relation to the origin (Figure 3-5).

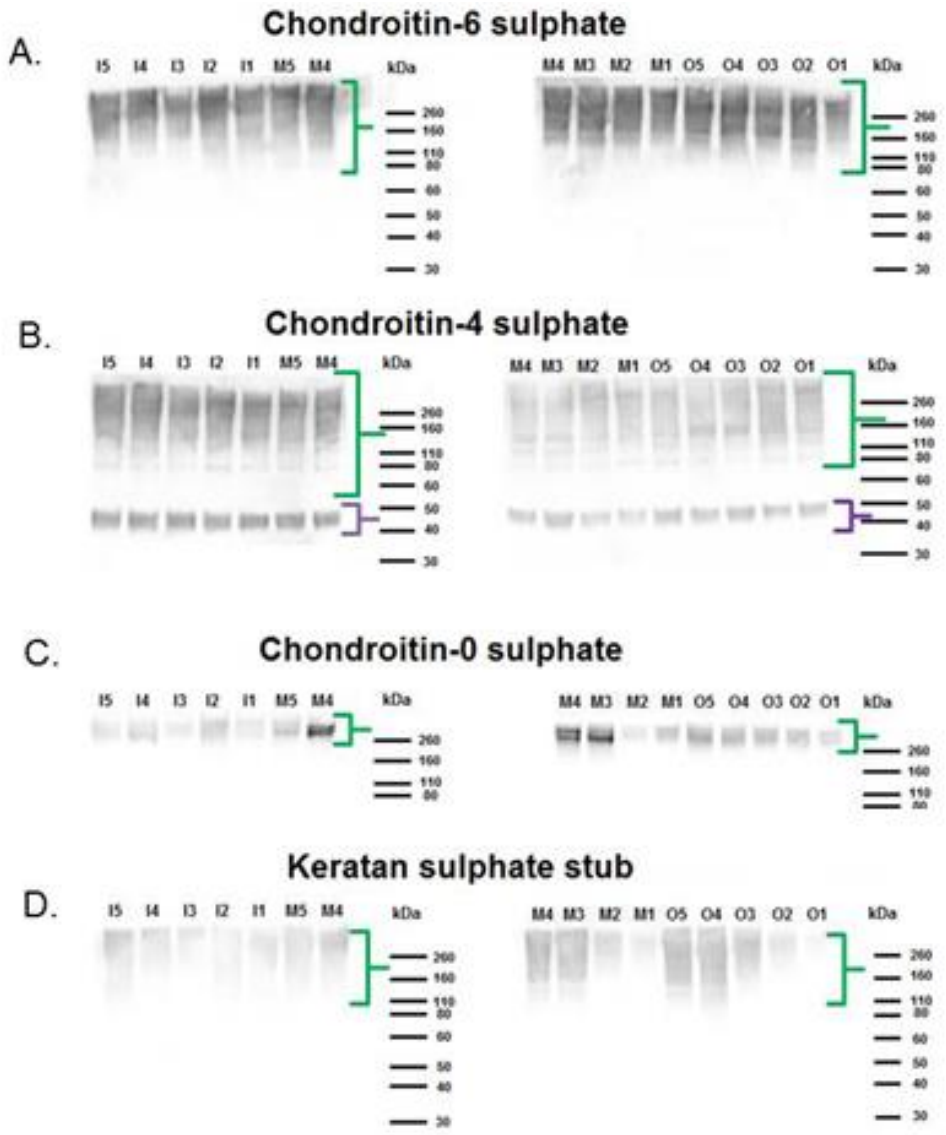

Figure 3-4: Western blot analysis of chondroitin and keratan sulphate stubs in different anatomical regions of Staffordshire bull terrier CCL.

The Figure shows A) chondroitin-6-sulphate stubs mAb 3B3, B) chondroitin-4-sulphate stubs mAb 2B6, C) chondroitin-0-sulphate stubs mAb 1B5, and D) keratan sulphate stubs mAb 5D4. Lanes are labelled with sample identifiers as follows; O= origin; M= middle; and I= insertion whilst the number refers to the donor animal, n= 5. The high molecular weights of chondroitin -6, -4, keratan sulphate stubs (80-260 kDa), and chondroitin-0 sulphate stubs (260 and above) are marked in green, and the low molecular weight stubs of chondroitin-4 sulphate stub (40-50 kDa) are highlighted in purple.

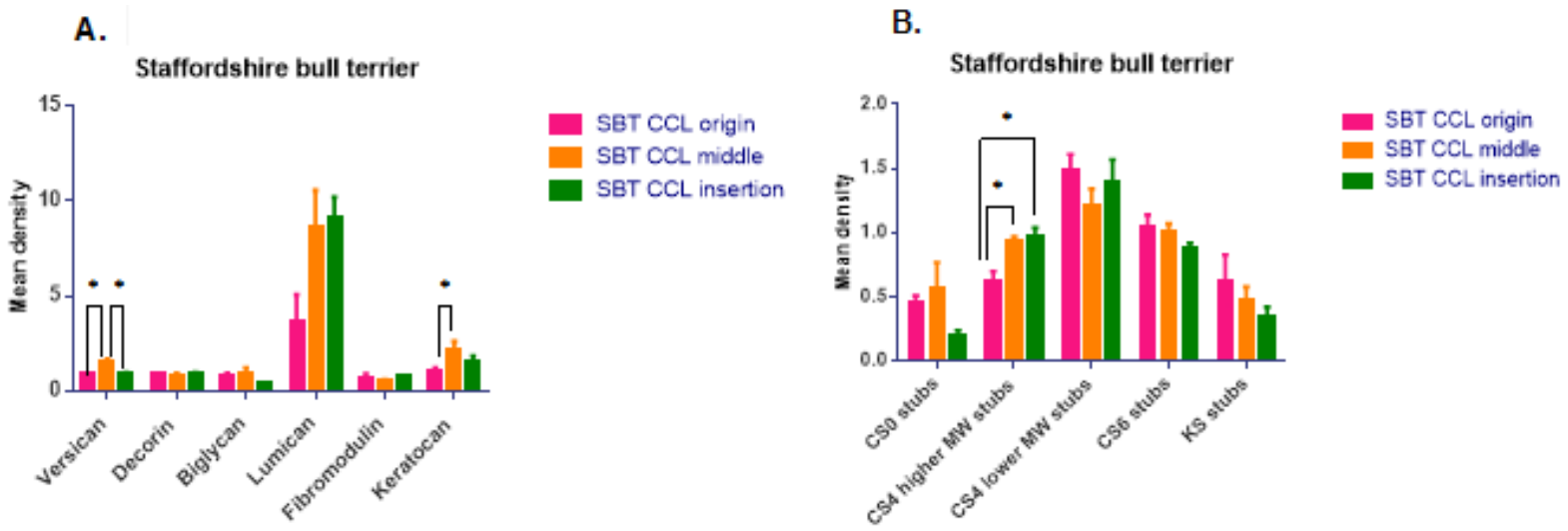

Figure 3-5: Densitometry analysis of proteoglycans and GAGs in different anatomical regions of Staffordshire bull terrier CCL.

A) Densitometry of proteoglycans between different anatomical regions of the Staffordshire bull terrier CCL, n= 5. Versican was signficantly higher in middle anatomical regions compared to origin (p=0.003) and insertion (p=0.003). Keratocan was found to be significantly higher in middle in relation to origin (p=0.046) anatomical region. B) Densitometry analysis of GAG stubs between between different anatomical regions of the Staffordshire bull terrier CCL, n= 5. Chondroitin-4-sulphate higher molecular weight stub was significantly higher in middle (p=0.01), and insertion (p=0.003) regions in relation to origin anatomical region. (CS0=chondroitin-0 sulphate stubs; CS4=chondroitin-4 sulphate stubs; CS6=chondroitin-6 sulphate stubs; KS= keratan sulphate stubs; MW= molecular weight; SBT= Staffordshire bull terrier). * indicates a significant difference at $p < 0.05$. Comparisons should be made between samples and not between antibodies as the efficiencies of the primary antibodies vary from one another.

Table 3-2: Densitometry results for Western blot analysis of proteoglycans and GAGs found in the different anatomical regions of the Staffordshire bull terrier CCL.

Values shown as mean ± SEM of Arbitary units, n= 5. * indicates a significant difference at $p < 0.05$.

Proteoglycan	Origin arbitrary units	Middle arbitrary units	Insertion arbitrary units
Aggrecan core protein fragment at 50 kDa	N/ A	N/ A	N/ A
Versican core protein fragment at 40-260 kDa*	0.9 ± 0.04	1.5 ± 0.2	0.9 ± 0.1
Decorin core protein at 40-50 kDa	0.9 ± 0.04	0.9 ± 0.1	0.9 ± 0.1
Biglycan core protein at 40-50 kDa	0.8 ± 0.1	0.9 ± 0.3	0.4 ± 0.1
Lumican core protein at 50 kDa	3.6 ± 1.4	8.6 ±2	9.2 ± 1.02
Fibromodulin core protein at 50 kDa	0.7 ± 0.2	0.6 ± 0.03	0.8 ± 0.1
Keratocan core protein at 30 kDa*	1.0 ± 0.2	2.2 ± 0.5	1.6 ± 0.3
Chondroitin-0-sulphate stub at 260 kDa and above	0.5 ± 0.1	0.6 ± 0.2	0.2 ± 0.04
Chondroitin-4-sulphate stub (high molecular weight 80-260 kDa)*	0.6 ± 0.1	0.9 ± 0.03	1.0 ± 0.1
Chondroitin-4-sulphate stub (low molecular weight 40-50 kDa)	1.5 ± 0.1	1.2 ± 0.1	1.4 ± 0.2
Chondroitin-6-sulphate stub at 80-260 kDa	1.0 ± 0.1	1.0 ± 0.1	0.9 ± 0.04
Keratan sulphate stub at 80-260 kDa	0.6 ± 0.2	0.5 ± 0.1	0.3 ± 0.1

3.4.2.3 Comparison between two dog breeds differentially predisposed to CCLD/ R.

3.4.2.3.1 **Large aggregating proteoglycans**

Analysis of anti-aggrecan antibody showed a band at 55 kDa that appeared to be different between the two dog breeds, and corresponded to one of its expected fragment sizes (Figure 3-6 A). Anti-versican antibody showed a similar molecular weight size between the two dog breeds (Figure 3-6 B) compared to what has been already observed between the anatomical regions of Staffordshire bull terrier CCLs (Figure 3-1 B). To compare relative amounts of these proteoglycans between the two dog breeds, densitometry was carried out. The extent of each lane included is indicated by the green bar in Figure 3-6 A, B. There were no statistically significant differences in versican or aggrecan core protein fragments between the two dog breeds.

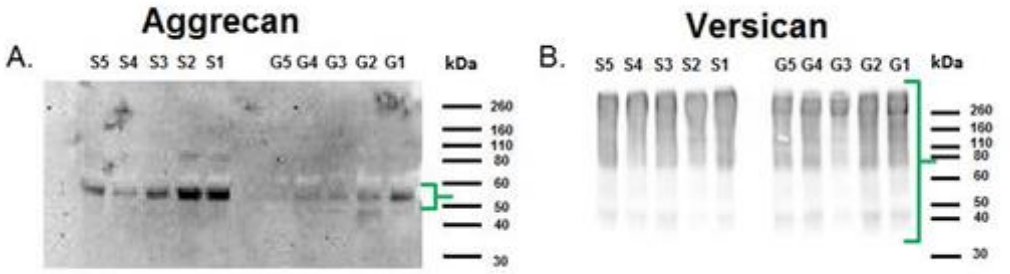

Figure 3-6: Western blot analysis of aggrecan and versican in two differentially predisposed dog breeds.

The Figure shows A) Aggrecan mAb 7D1 and B) Versican mAb 12C5. This Figure compares two dog breeds with a different predisposition to CCLD/ R. The number refers to the donor animal, n= 5. The core protein fragment(s) of aggrecan (50 kDa) and versican (40-260 kDa) are labelled in green. (S= Staffordshire bull terrier; G= greyhound).

3.4.2.3.2 **Chondroitin/ dermatan sulphate proteoglycans**

Analysis using anti-decorin antibody and anti-biglycan antibody showed a similar molecular weight between the two dog breeds (Figure 3-7 A, B) compared to what has been already observed between different anatomical regions of the Staffordshire bull terrier (Figure 3-2 A, B). However, we detected a prominent catabolic fragment below the decorin core protein at 30 kDa in greyhounds compared to Staffordshire bull terrier CCLs (Figure 3-7 A, black arrow). The decorin band at 80 kDa, which corresponded to its expected dimer size, was also quantified as it appeared to be significantly different between the two dog breeds. To compare relative amounts of these proteoglycans between the two dog breeds, densitometry was carried out. The extent of each lane included is indicated by the green bar in Figure 3-7 A, B. Statistical analysis showed that there were no statistically significant differences between the two dog breeds in terms of monomeric decorin core protein. However, decorin dimeric core protein was significantly higher in the greyhound compared to the Staffordshire bull terrier CCLs ($p=0.008$) (Figure 3-10). There were no statistically significant differences in the biglycan core protein between the two dog breeds. However, there was some variations observed in the biglycan band density in different greyhound samples (Figure, 3-7 B).

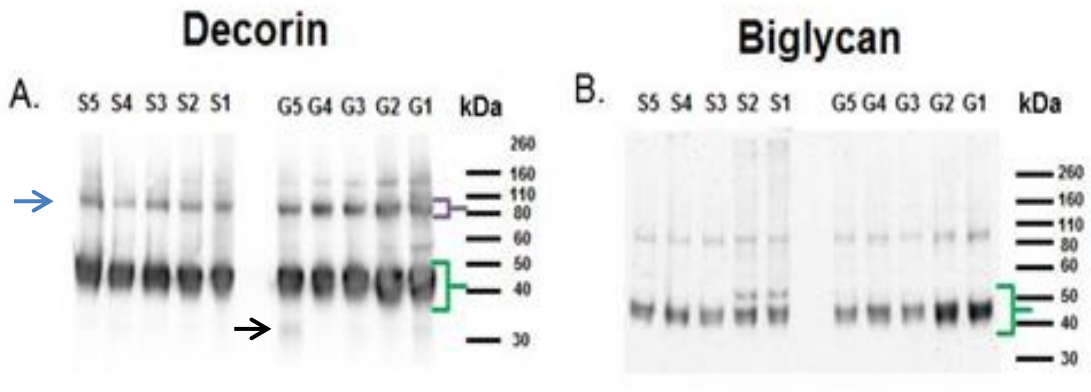

Figure 3-7: Western blot analysis of decorin and biglycan in two differentially predisposed dog breeds.

The Figure shows A) Decorin mAb 70.6 and B) Biglycan mAb PR 8A4. This Figure compares two dog breeds with a different predisposition to CCLD/ R. The number refers to the donor animal, n= 5. The core proteins of decorin (40-50 kDa) and biglycan (40-50 kDa) are highlighted in green. Other bands of interest are the 80 kDa band highlighted in purple (blue arrow) and the catabolic product (30 kDa) prominent in greyhound (black arrow). (S= Staffordshire bull terrier; G= greyhound).

3.4.2.3.3 **Keratan sulphate proteoglycans**

Analysis using anti-lumican antibody, anti-fibromodulin antibody and anti-keratocan antibodies showed that the size of each of these proteoglycans showed a similar molecular weight between the two dog breeds compared to what has been already observed between different anatomical regions of the Staffordshire bull terrier CCLs (Figure 3-3 A, B, and C). To compare relative amounts of these proteoglycans between the two dog breeds, densitometry was carried out. The extent of each lane included is indicated by the green bar in Figure 3-8 A, B, and C. There were no statistically significant differences for the content of and keratocan between dog breeds. However, fibromodulin was significantly higher in the Staffordshire bull terrier CCLs compared to those of the greyhounds (p=0.02) (Figure 3-10).

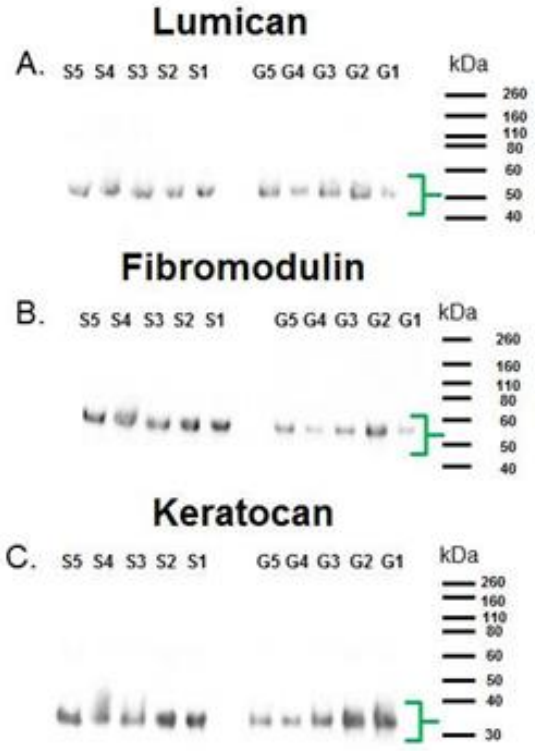

Figure 3-8: Western blot analysis of lumican, fibromodulin and keratocan between two differentially predisposed dog breeds.

The Figure shows A) Lumican mAb LUM1, B) Fibromodulin pAb PR184, and C) Keratocan mAb KER-1. This Figure compares two dog breeds with a different predisposition to CCLD/R. The number refers to the donor animal, n= 5. The core proteins of lumican (50 kDa), fibromodulin (50 kDa), and keratocan (30 kDa) are marked in green. (S= Staffordshire bull terrier; G= greyhound).

3.4.2.3.4 **Glycosaminoglycans**

Analysis using anti-chondroitin-0-sulphate stub antibody, anti-chondroitin-6-sulphate stub antibody, anti-chondroitin-4-sulphate stub antibody, and anti-keratan sulphate stub antibody showed a similar molecular weight between the two dog breeds compared to what has been already observed between different anatomical regions of the Staffordshire bull terrier CCLs (Figure 3-4). Levels of chondroitin-0-sulphate as well as keratan sulphate found on high molecular weight proteoglycans exhibited a considerable variability between the Staffordshire bull terrier donors (Figure 3-9 C, D). To compare relative amounts of these proteoglycans between the two dog breeds, densitometry was carried out. The extent of each lane included is indicated by the green or purple bar in Figure 3-9 A, B, C. There were no statistically significant differences between the dog breeds in regards to chondrotin-4-sulphate high molecular weight stub, chondrotin-4-sulphate low molecular weight stub, chondroitin-0-sulphate high molecular weight stub, and keratan sulphate high molecular weight stub. However, chondroitin-6-sulphate stub was significantly higher in the Staffordshire bull terrier in relation to the greyhound CCLs (p=0.0144) (Figure 3-10).

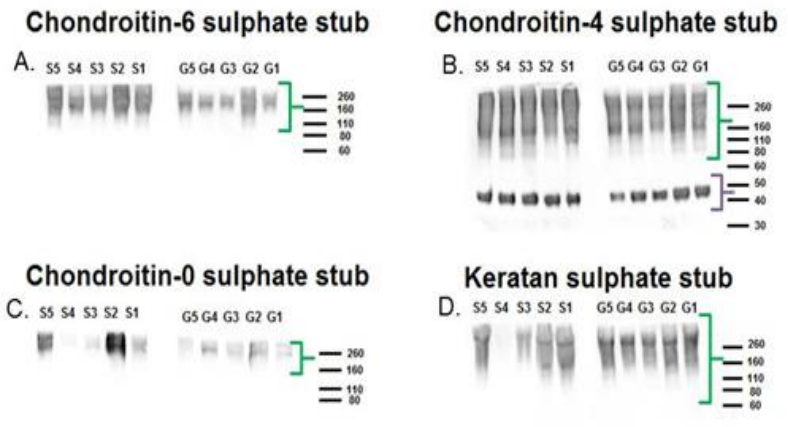

Figure 3-9: Western blot analysis of chondroitin sulphate and keratan sulphate stubs between two differentially predisposed dog breeds.

The Figure shows A) chondroitin-6 sulphate stub mAb 3B3, B) chondroitin-4 sulphate stub mAb 2B6, C) chondroitin-0 sulphate stubs mAb 1B5, and D) keratan sulphate stubs mAb 5D4. The Figure compares two dog breeds with a different predisposition to CCLD/ R. The number refers to the donor animal, n= 5. The high molecular weights of chondroitin -6, -4, -0, keratan sulphate stubs (80-260 kDa), and chondroitin sulphate stubs (260 kDa and above) are highlighted in green, and the low molecular weight of chondroitin -4 sulphate stubs (40 kDa) are highlighted in purple. (S= Staffordshire bull terrier; G= greyhound).

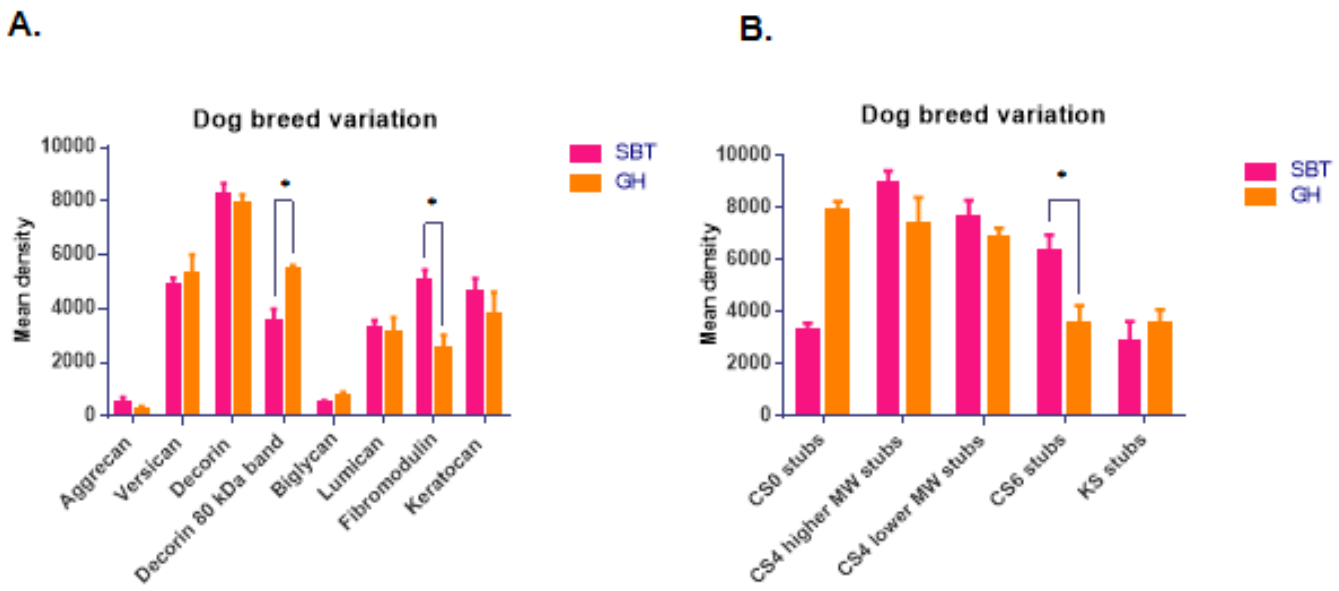

Figure 3-10: Densitometry analysis of proteoglycans and GAGs between two differentially predisposed dog breeds.

A) Densitometry analysis for proteoglycans between two differentially predisposed dog breeds to CCLD/ R, n= 5. Core proteins of all proteoglycans were measured unless stated. Decorin 80 kDa band was significantly higher in greyhound (p=0.008) compared to Staffordshire bull terrier CCL, whilst fibromodulin was significantly higher in Staffordshire bull terrier (p=0.02) compared to greyhound CCLs. B) Densitometry analysis for GAG stubs between two differentially predisposed dog breeds to CCLD/ R. Chondroitin-6-sulphate was found to be significantly higher in Staffordshire bull terrier (p=0.0144) compared to greyhound CCL. (CS0= chondroitin-0 sulphate stubs; CS4= chondroitin-4 sulphate stubs; CS6= chondroitin-6 sulphate stubs; KS= keratan sulphate stubs; MW= molecular weight; SBT= Staffordshire bull terrier; GH =greyhound). * indicates a significant difference at $p < 0.05$. Comparisons shouls be made between samples and not between antibodies as the efficiencies of the primary antibodies vary from one another.

Table 3-3: Densitometry results for Western blot analysis for proteoglycans and GAGs found in the CCL from differentially predisposed dog breeds to CCLD/ R.

Values shown as mean ± SEM of arbitrary units, n= 5 of each dog breed. * indicates a significant difference at $p < 0.05$ (SBT= Staffordshire bull terrier; GH= greyhound).

Proteoglycan	SBT arbitary units	GH arbitary units
Aggrecan core protein fragment at 50 kDa	530.7 ± 172.3	248.9 ± 112.9
Versican core protein fragments between 40-260 kDa	4873.6 ± 282.1	5335.8 ± 678.9
Decorin core protein at 40-50 kDa	8283.8 ± 379.9	7902.5± 342.2
Decorin band ~80 kDa*	3507.3± 482.9	5442.6 ± 175.3
Biglycan core protein at 40-50 kDa	532.9 ± 42.7	764.3 ± 134.3
Lumican core protein at 50 kDa	3314.1 ± 256.3	3145 ± 533.5
Fibromodulin core protein at 50 kDa*	5084.5 ± 356.9	2554 ± 745.2
Keratocan core protein at 30 kDa	4648.4 ± 481.3	3813.± 803.5
Chondroitin-0-sulphate stub at 260 kDa and above	4848 ± 2699	1749 ± 439.9
Chondroitin-4-sulphate stub (high molecular weight 80-260 kDa)	8945.6 ± 466.2	7408.6 ± 980.3
Chondroitin-4-sulphate stub (low molecular weight 40-50 kDa)	7669.5 ± 624.1	6835.5 ± 392.1
Chondroitin-6-sulphate stub 80-260 kDa*	6357.5 ± 605.5	3603.5 ± 645.1
Keratan sulphate stub between 80-260 kDa	2842.5 ± 803.3	3596.9 ± 509.2

3.4.3 Real time RT-qPCR

3.4.3.1 Large aggregating proteoglycans

The gene expression of aggrecan was found to be significantly greater in Staffordshire bull terrier CCLs compared to those of the greyhound (p=0.0003) (Figure 3-11). However, the gene expression of versican in CCLs was not found to be statistically different between the two dog breeds but the mean value was higher in the greyhound (Figure 3-11).

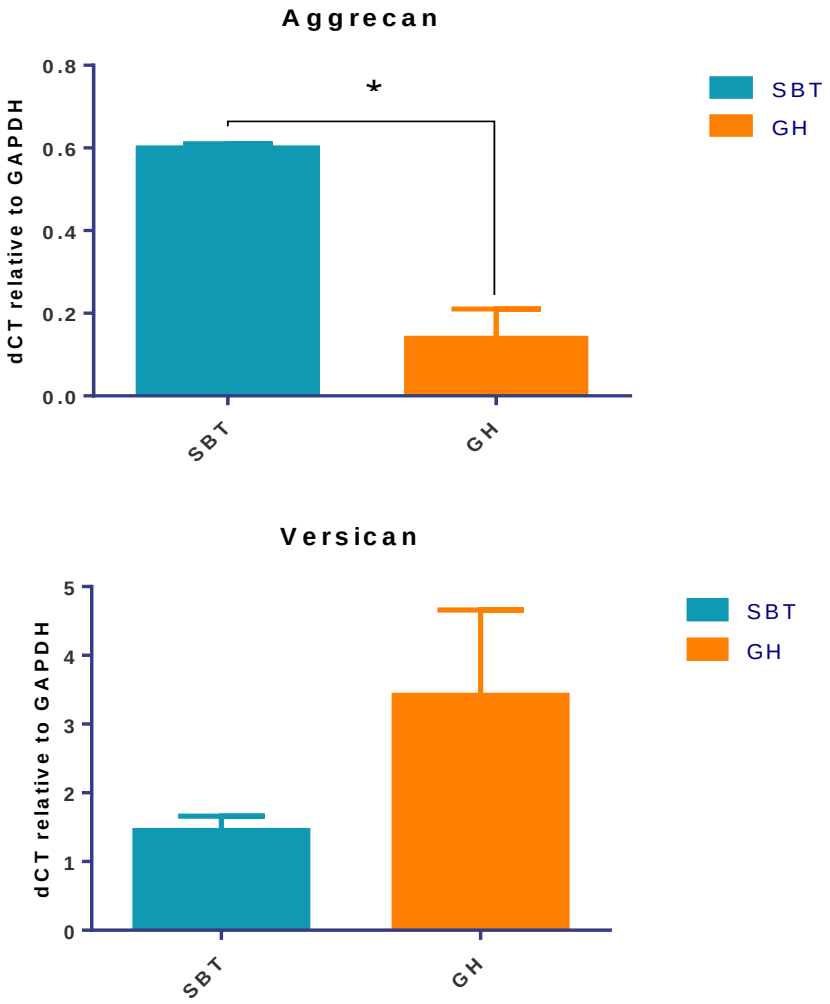

Figure 3-11: Summary of large aggregating proteoglycans gene expression data performed on the CCLs from two dog breeds with a different predisposition to CCLD/R.

Data presented as MEAN ± SEM, n= 5 biological replicate of each dog breed. (SBT= Staffordshire bull terrier; GH= greyhound). Aggrecan was significantly higher in the Staffordshire bull terrier CCLs compared to those of the greyhounds (p=0.0003). * indicates a significant difference at $p < 0.05$.

3.4.3.2 Chondroitin/ dermatan sulphate proteoglycans

The Staffordshire bull terrier CCLs had significantly reduced decorin gene expression in relation to greyhound CCLs (p=0.03) (Figure 3-12). Biglycan gene expression did not show any significance between the two dog breeds (Figure 3-12).

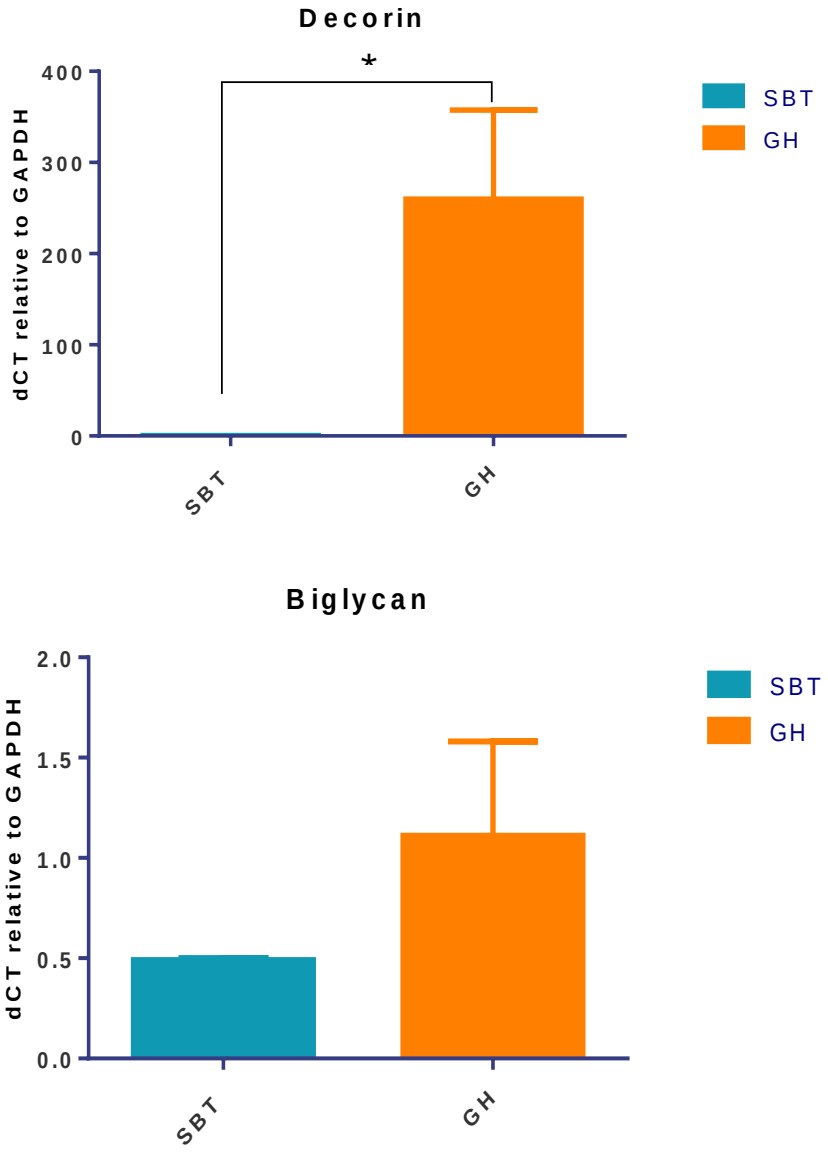

Figure 3-12: Summary of chondroitin/ dermatan sulphate proteoglycans gene expression data performed on the CCLs from dog breeds with a different predisposition to CCLD/ R.

Data presented as MEAN ± SEM, n= 5 biological replicate of each dog breed (SBT= Staffordshire bull terrier; GH= greyhound). Decorin was significantly reduced in the Staffordshire bull terrier CCLs compared to those of the greyhounds (p= 0.03). * indicates a significant difference at $p < 0.05$.

3.4.3.3 **Keratan sulphate proteoglycans**

Lumican gene expression showed no significant difference in the CCLs from two dog breeds but the mean value was higher in the greyhound (Figure 3-13). However, fibromodulin gene expression was found to be significantly higher in Staffordshire bull terrier CCLs in comparison to those of the greyhounds (p=0.03) (Figure 3-13).

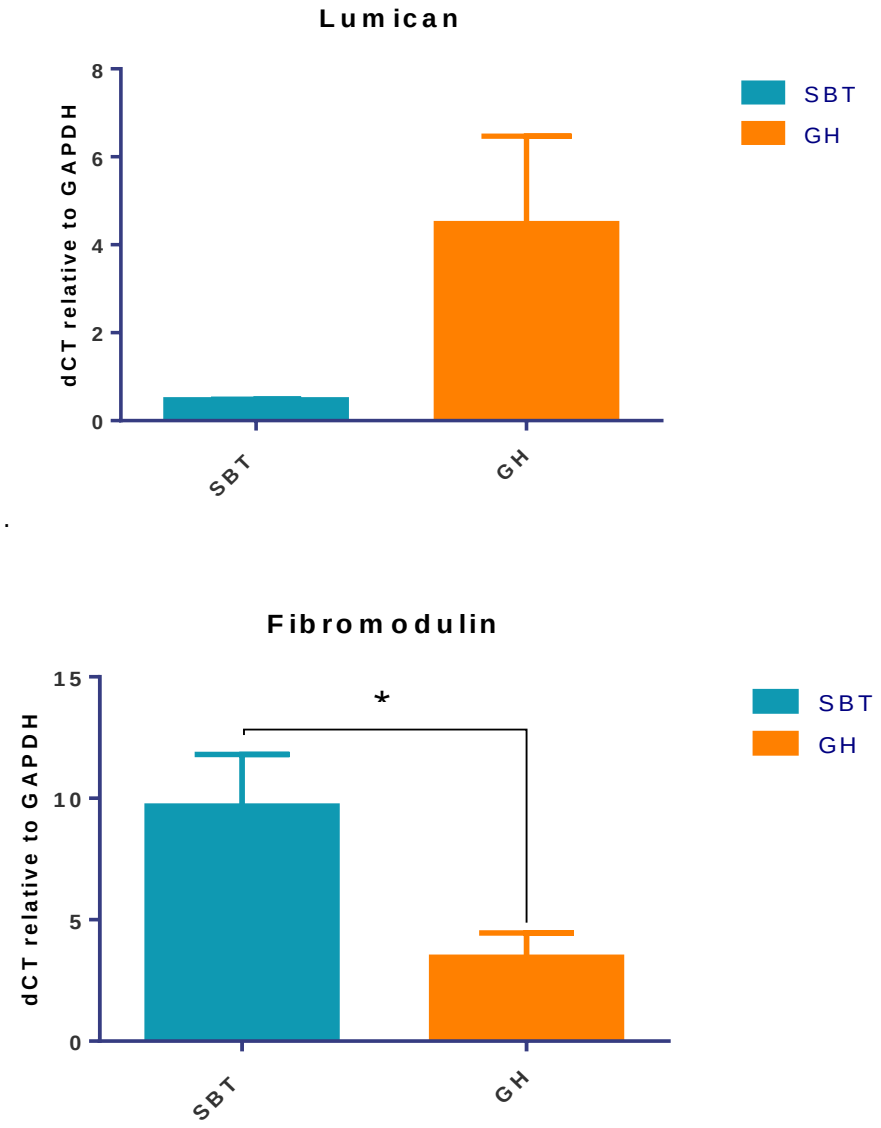

Figure 3-13: Summary of keratan sulphate proteoglycans gene expression data performed on the CCLs from dog breeds with a different predisposition to CCLD/ R.

Data presented as MEAN ± SEM, n= 5 biological replicate of each dog breed. (SBT= Staffordshire bull terrier, GH= greyhound). Fibromodulin was significantly higher in the Staffordshire bull terrier CCLs compared to those of greyhounds (p= 0.03). * indicates a significant difference at $p < 0.05$.

3.4.3.4 **Extracellular matrix proteases**

Staffordshire bull terrier CCLs had significantly reduced ADAMTS-4 gene expression in relation to greyhound (p=0.04) (Figure 3-14). However, the gene expression of ADAMTS-5 did not show any statistical significant differences in the CCLs from the two dog breeds (Figure 3-14).

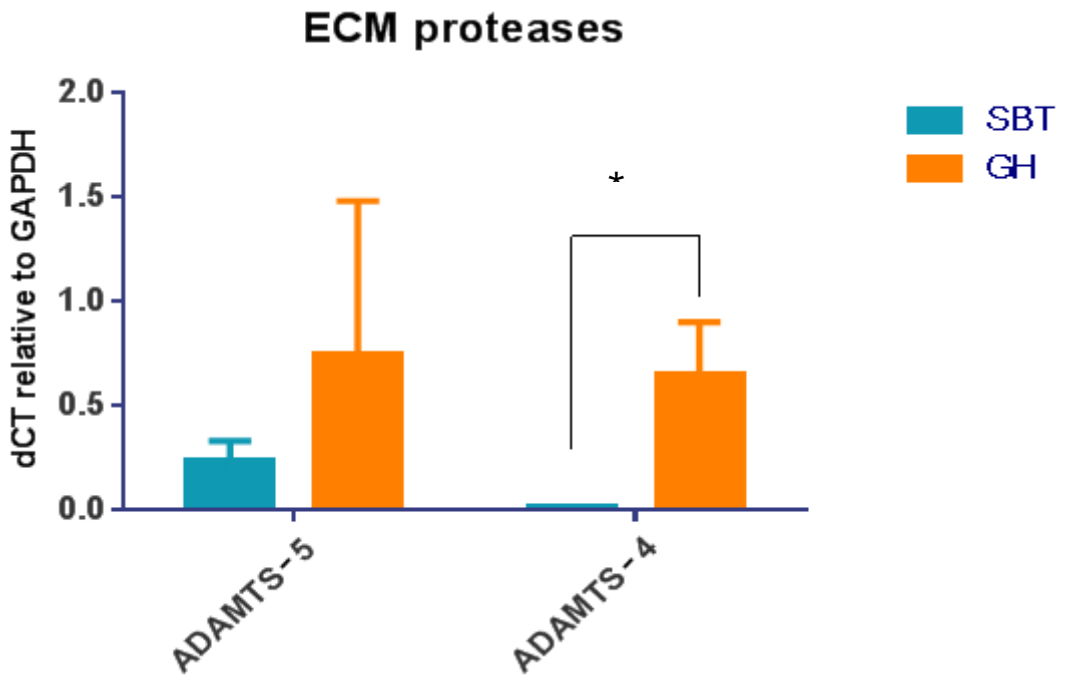

Figure 3-14: Summary of ADAMTS-4 and -5 gene expression data performed on the CCLs from dog breeds with a different predisposition to CCLD/ R.

Data presented as MEAN ± SEM, n= 5 biological replicate of each dog breed. (SBT= Staffordshire bull terrier, GH= greyhound, ECM= extracellular matrix). ADAMTS-4 was significantly reduced in the Staffordshire bull terrier CCLs in relation to greyhounds (p=0.04). * indicates a significant difference at $p < 0.05$.

Table 3-4: Gene expression levels of proteoglycans and ECM proteases in the CCLs from two dog breeds differentially predisposed to CCLD/ R.

2^-dCT values are displayed (mean ± SEM), n= 5 of each dog breed. * indicates a significant difference at $p < 0.05$ in proteoglycans or ECM proteases gene expression between the two groups.

Proteoglycan	Staffordshire bull terrier	Greyhound
Aggrecan*	0.60 ± 0.01	0.14 ± 0.07
Versican	1.45 ± 0.21	3.42 ± 1.24
Decorin*	0.41 ± 0.01	259.99± 97.64
Biglycan	0.49 ± 0.01	1.11 ± 0.47
Lumican	0.48 ± 0.01	4.48 ± 1.99
Fibromodulin*	9.68 ± 2.12	3.45 ± 1.01
ADAMTS5	0.24 ± 0.09	0.74 ± 0.74
ADAMTS4*	0.01 ± 0.00	0.65 ± 0.25

3.5 **Discussion**

In this study, Western blot analysis showed that specific proteoglycans and GAGs varied between anatomical regions of the Staffordshire bull terrier CCL, indicating that these particular proteoglycans and GAGs have different roles at specific anatomical sites. Proteoglycans, GAGs, and aggrecanases (ADAMTS-4 and -5) have been characterised by Western blot and RT-PCR analysis between CCLs of two dog breeds differentially predisposed to CCLD/ R, the greyhound (low risk) and the Staffordshire bull terrier (moderate-high risk). Our results showed that the presence of certain key proteoglycans, GAGs, and aggrecanases significantly differed in the CCLs from dogs at a varied risk to CCLD/ R. These differences may be important as proteoglycans and their catabolites may contribute to the aetiopathogenesis of this condition by having different roles in low and high risk dog breeds.

The results of our study showed that the molecular weights decorin, biglycan, fibromodulin, and lumican are similar to what has been previously reported in the canine CCL (Yang, Culshaw et al. 2012). Our findings are also consistent with previous reports of decorin, biglycan, lumican, fibromodulin, versican, and aggrecan molecular weights in ligament (Ilic, Carter et al. 2005), and keratocan, decorin, biglycan, aggrecan, versican, and GAGs stubs (3b3, 2b6, and 1b5) molecular weights in tendon (Rees, Flannery et al. 2000; Samiric, Ilic et al. 2004; Rees, Waggett et al. 2009). We were unable to measure aggrecan fragments with Western blot analysis between anatomical regions of the Staffordshire bull terrier CCL, as most of the bands were faded on the blot membrane when captured, and were therefore difficult to identify. The reason for this could be that the primary antibody did not detect aggrecan fragments at the level that was there. Another alternative antibody that may be used is aggrecan monoclonal anatibody 1C6, which recognises an epitope located at the G1 and G2 domains of aggrecan (Calabro, Hascall et al. 1992). In addition, the native keratan sulphate monoclonal antibody 5D4 could also detect high molecular weight bands on the aggrecan core protein (Caterson; Christner et al. 1983). Other studies have detected aggrecan fragments using an alternative anti-aggrecan monoclonal antibody mAb JD5 (Ilic, Carter et al. 2005). Using 4–15% gradient polyacrylamide/ Sodium Dodecyl Sulphate (SDS) slab gels, two discrete bands at 170 and 130 kDa were found in bovine collateral ligament (Ilic, Carter et al. 2005). Similar fragments have been also shown in tendon (Samiric, Ilic et al. 2004). The molecular weight of aggrecan fragments may vary due to tissue differences. In addition, antibodies specific for

aggrecan core protein may differ in that they may recognise aggrecan or aggrecan fragments at different locations of the aggrecan core protein (Samiric, Ilic et al. 2004; Ilic, Carter et al. 2005).

Western blotting analysis used to identify versican showed a range of bands from 180 kDa to 260 kDa and above (Figure 3-1 B). A study on bovine collateral ligament has shown a similar molecular weight range for versican, from 18 to 260 kDa and above (Ilic, Carter et al. 2005). The bands generated in versican may indicate fragments of its core protein (Figure 3-1 B). Such fragments could be generated by ECM proteases, such as ADAMTS's specific for cleaving versican (See Chapter 1 - Section 1.3.5.6.1) (Sandy, Westling et al. 2001; Kelwick, Desanlis et al. 2015). The core proteins of aggrecan and versican are likely to be too large to migrate into the SDS-PAGE gels, therefore we were only able to observe their fragments rather than the core protein. It would have been interesting to detect aggrecan and versican core proteins in the canine CCL by Western blotting. An alternative technique to quantify aggrecan and versican core protein is using composite agarose/ polyacrylamide gels, which allow native large proteoglycans to enter the gel (Varelas, Zenarosa et al.1991).

Densitometry analysis of Western blots of different anatomical regions of Staffordshire bull terrier CCLs showed that versican fragments were significantly lower in both origin and insertion regions, when compared to the middle region. The middle anatomical region of the CCL has been shown to be fibrocartilaginous as it twists around the caudal cruciate ligament (CaCL) (Paatsama 1952; Vasseur, Pool et al. 1985; Comerford, Tarlton et al. 2006). This fibrocartilaginous site is likely to be secondary to physical compression, and the significant increase of versican fragments in this middle region could be that its specific to this anatomical area, as it has been previously shown that versican content is increased in fibrocartilaginous regions of tendon (Vogel and Koob 1989).

Both decorin and biglycan monomeric core proteins were found to be around 40-50 kDa, similar to what has been shown previously in several tissues such as ligament, tendon and articular cartilage (Rees, Flannery et al. 2000; Samiric, Ilic et al. 2004; Ilic, Carter et al. 2005; Young, Smith et al. 2005; Melrose, Fuller et al. 2008).

An interesting band was found on the decorin Western blots at around 80 kDa, and we hypothesise that this band is likely to be a cross linked form of a decorin dimer (Milligan and Koshland 1988), as it is unlikely to be a complete dimer. Covalent

cross linking occurs when one polymer atoms attaches to another by sharing electron pais between atoms (Milligan and Koshland 1988; Talwar 2016). Covalent cross linking is essential for protein – protein interactions (Milligan and Koshland 1988). Dimers are a complex of macromolecules that are generated by bound proteins, and are essential for creating more that one binding site for proteins or for enzyme activation (Marianayagam, Sunde et al. 2004). A previous study has similarly reported a decorin band at 90 kDa that could represent decorin dimer (Rees, Flannery et al. 2000). Dimers are formed by electrostatic interactions, hydrogen bonds or Van der waals forces (Frieden 1975), and are usually denatured during the heating process prior loading samples into the gel (Grabski and Novagen 2010). It could be that these forces were very strong and were not overcome by heating. However, it seems more likely that covalent crosslinking of decorin occurred (Milligan and Koshland 1988), in which case no amount of boiling or reduction will separate them.

Fibromodulin, lumican, and keratocan appeared as single bands respectively at 50, 50, 30 kDa by Western blot analysis. Similar molecular weight bands for fibromodulin and lumican have been previously found in beagle CCLs (Yang, Culshaw et al. 2012). Amongst all SLRPs, Keratocan had the lowest molecular weight core protein at 30 kDa consistent to what has been previously observed in tendon (Rees, Waggett et al. 2009).

Densitometry analysis between different anatomical regions of Staffordshire bull terrier CCLs by Western blot showed that keratocan was significantly higher in the middle region compared to the origin region. The significant increase of keratocan content in the middle anatomical region of the canine CCL could be due to similar reasons as explained for versican, in that the fibrocartilage area is increased in the middle site of canine CCL (Paatsama 1952; Vasseur, Pool et al. 1985; Comerford, Tarlton et al. 2006b). This result is consistent to what has been previously reported for keratocan, as it has been previously found to increase at the compressed/ fibrocartilaginous region in tendon (Rees, Wagget et al. 2009).

Chondroitin-6 sulphate stub antibody produced bands ranging from 80-260 kDa by Western blot analysis in the canine CCL. Chondroitin -0 sulphate stub antibody also identified a band at 260 kDa and above. Chondroitin-6 sulphate stub and Chondroitin-0 sulphate stub antibodies have been shown to be expressed previously in adult bovine tendon, where heterogeneous bands were shown from

150-260 kDa (Rees, Flannery et al. 2000), and this was similar to what we found in this study.

In our CCLs chondroitin-4 sulphate stub antibody detected two molecular weight species; the first was a high molecular weight band from 80-260 kDa, and the second species was a band at 40 kDa. In tendon, the low molecular weight of chondroitin-4 sulphate stub has been previously detected at approximately 50 kDa (Rees, Flannery et al. 2000).

The small molecular weight (50 kDa) recognised by chondroitin-4 sulphate stub antibody may represent small molecular weight species such as decorin or biglycan (Rees, Flannery et al. 2000). The high molecular weight found on chondroitin-6 sulphate stub (150-260 kDa), chondroitin-0 sulphate stub (150-260 kDa), and chondroitin-4 sulphate (80-260) may indicate that stubs present on high molecular weight proteoglycan species such as aggrecan or versican. Our assumption is that chondroitin -4, -6, and -0 sulphate stubs are mostly associated with large aggregating proteoglycans, whilst only chondroitin -4 sulphate stubs is mostly associated with small proteoglycans, as It has been previously shown with disaccharide analysis in tendon that large proteoglycans were mostly associated with chondroitin -4, -6, and -0 sulphate, and that small proteoglycans mostly had chondroitin-4 sulphate (Evanko and Vogel 1993). The molecular weight proteoglycan species found for keratan sulphate high molecular weight stubs (80-260 kDa) are likely to be solely associated with aggrecan, as versican does not carry any keratan sulphate chains (Krusius, Gehlsen et al. 1987).

Densitometry analysis between different anatomical regions of Staffordhsire bull terrier CCLs by Western blot showed that the high molecular weight bands detected by the anti-chondroitin-4 sulphate stub antibody showed to be significantly higher in middle and insertion regions compared to the origin. These findings might be explained by the fact that they are identifying a large aggregating proteoglycan, such as aggrecan or versican. The CCL insertion site onto the proximal tibia is another compressive site containing a fibrocartilaginous matrix (Arnoczky 1983). As mentioned earlier, aggrecan and versican are known to be located in fibrocartilaginous regions of tendon that encounters compression (Vogel and Koob 1989; Benjamin and Ralphs 1998; Evako and Vogel 1993).

Real time RT-PCR analysis in our study found the gene expression of aggrecan to be significantly increased in the Staffordshire bull terrier in relation to greyhound

CCLs, whilst Western blot analysis detected an aggrecan fragment at 55 kDa that appeared to be enriched in the Staffordshire bull terriers compared to greyhounds (Figue 3-6 A). The levels of this fragment were not statistically different upon densiometric analysis (p= 0.21). It is possible that increasing sample numbers could have demonstrated a significant difference in the 55 kDa fragment between breeds. These results may indicate that the Staffordshire bull terrier is more susceptible to compressive loads on its CCL, as increased aggrecan in regions susceptible to compressive loads in tendon has been previously determined (Vogel and Koob 1989; Evanko and Vogel 1993; Huisman, Andersson et al. 2014), especially where type II collagen is increased (Vogel 2004; Smith, Shu et al. 2010). In addition, the increase of aggrecan gene expression and higher amount of the aggrecan fragment in the Staffordshire bull terrier CCL could lead to the progression of CCLD/ R, as several studies have found increased aggrecan gene expression levels in pathological tendons (Corps, Robinson et al. 2006; Samiric, Parkinson et al. 2009) and ligament (Clements, Carter et al. 2008).

Gene expression data revealed that decorin was significantly higher in the greyhound CCL compared to Staffordshire bull terriers, while Western blot analysis did not show any significant differences between the two dog breed CCLs in regards to decorin core protein. However, when decorin dimer band at 80 kDa was measured, it was shown to be significantly higher in greyhounds when compared to Staffordshire bull terrier CCLs. Decorin dimer might have a role in regulating collagen fibrillogenesis (Weber, Harrison et al. 1996). It has been shown that decorin functions by inhibiting lateral collagen fibril fusion *in vitro*, thereby resulting in the formation of thinner collagen fibrils (Birk, Nurminskaya et al. 1995). It is interesting to know that decorin is increased 700 folds in the greyhound CCL, as this may show how decorin is essential for collagen fibrillogenesis and strength in the racing greyhound that rarely ruptures its CCL. The important role of decorin in collagen fibrillogenesis can be supported by the decorin knockout mice study in tendon, where collagen fibrils in cross sections have been known to contain irregular outlines and were variable in size compared to controls (Danielson, Baribault et al. 1997). In addition to this, electron microscopy was used to measure the cross sections of collagen fibril diameter in the greyhound (low risk to CCLD/ R) and the Labrador retriever CCLs (high risk to CCLD/ R), and found that the Labrador retriever contained a variation in collagen fibril size population ranging from small to large, and included a peak of distribution at 50 nm. Whereas greyhounds had a larger (100-150 nm) and more evenly shaped distribution of

collagen fibril sizes (Comerford, Tarlton et al. 2006b). The large fibrils in ex-racing greyhounds could be formed as a consequence of its racing activity, as it has been previously shown that the increase of fibril size is associated with physical activity (Tipton, Matthes et al. 1975). Dermatan sulphate, a GAG chain present on decorin and biglycan, has been previously shown to be associated with large sized fibrils (>150) (Parry, Flint et al. 1982). Previous reports also showed that decorin and hyaluronic acid content is increased with exercise in chicken gastrocnemius tendons (Hae Yoon, Brooks et al. 2003). These studies support why decorin expression may be greater in previously exercised greyhounds CCLs compared to the CCLs from the non-athletic Staffordshire bull terrier. In determining biglycan by Western blot analysis, we found a variation between the greyhound donors (Figure 3-7 B). Since greyhounds are known to be an exercising dog breed, it could be that these greyhounds have had different exercise regimes explaining their individual variability. However, we did not have any detailed information on the exercise history of the greyhound donors. Fibromodulin regulates collagen fibrillogenesis in normal tendon (Jepsen, Wu et al. 2002), and binds to growth factors such as TGF-β (Iozzo 1999). Both real time RT-PCR and Western blot analysis confirmed that fibromodulin was significantly upregulated in Staffordshire bull terrier compared to greyhound CCLs. It has been proposed that fibromodulin controls the mineralisation of the soft/ hard tissue border of human peridontal ligament (Cheng, Caterson et al. 1999; Matias, Li et al. 2003). Furthermore, fibromodulin has been shown to be localised at the compressive sites that were fibrocartilaginous in human flexor carpi ulnaris tendon, pisometacarpal and pisohamate ligaments (Adamczyk, Milz et al. 2008). Since the ACL does no not calcify (Arnoczky 1983), it could be the significant increase of fibromodulin in the Staffordshire bull terrier CCL indicate that It develops more sites of fibrocartilage secondary to compression, as it might be that fibromodulin functions to regulate fibrocartilaginous cells differentiation, as fibromodulin has been previously shown to regulate the differentiation of chondrocytes (Embree, Kilts et al. 2010). However, fibromodulin gene expression levels have been found to increase in human patellar tendinopathy (Samiric, Parkinson et al. 2009), and this could indicate that fibromodulin also contributes to CCLD/ R in the Staffordshire bull terrier. We have found that chondroitin-6 sulphate stubs were significantly higher in the Staffordshire bull terrier compared to greyhound CCLs. It is known that chondroitin-6 sulphate content increases compared to chondroitin-4 sulphate in areas associated with compressive loading in tendon (Evanko and Vogel et al. 1993). We have previously concluded that

Staffordshire bull terriers may exhibit more areas of compressive loading, and this could also be a similar reason for the increase of chondroitin-6 sulphate. ADAMTS4 gene expression was shown to be significantly upregulated in greyhound compared to Staffordshire bull terrier CCLs. Evidence of increased catabolism in greyhounds CCLs associated with high expression of ADAMTS4 could be linked to increased expression and content of certain proteoglycans, such as decorin. The significant increase of decorin gene expression could be related to increased ADAMTS4 activity since we have detected a catabolic fragment below the decorin core protein at 30 kDa (Figure 3-7 B). The significant increase of ADAMTS4 in greyhound CCLs could be required to degrade high anabolic rate of decorin that maintains the normal CCL metabolism, as the greyhound is an athletic and exercising dog breed that rarely ruptures its CCL.

3.6 **Conclusions**

Western blot analysis showed significant differences in certain proteoglycans of the Staffordshire bull terrier CCL anatomical regions. Versican and keratocan were significantly highest in the middle region, and the high molecular weight bands detected by the anti-chondroitin-4 sulphate stub antibody were found to be significantly higher in middle and insertion anatomical region compared to its origin. These results may indicate that versican, keratocan, and chondroitin-4 sulphate high molecular stubs serve the CCL at specific anatomical regions that are subjected to compressive loads. The gene expression of aggrecan content and Western blot analysis of chondroitin-6 sulphate was shown to be increased in Staffordshire bull terrier CCLs compared to those of the greyhounds, and could be due to increased areas of fibrocartilage as a result of compression in the CCLs of the Staffordshire bull terrier. The significant increase of fibromodulin by RT-PCR and Western blot analysis in the Staffordshire bull terrier CCLs could further confirm that the CCLs from this dog breed develop more fibrocartilaginous areas as a result of compressive loads, as it may have a role in controlling the differentiation process of fibrocartilaginous cells. We suggest that the increase of aggrecan and fibromodulin in the Staffordhsire bull terrier CCL may compromise the normal CCL mechanical and structural properties, and therefore leading to CCLD/ R. The significant increase of decorin shown by Western blot and RT-PCR in the greyhound CCL could be vital for its collagen fibril maintenance, orientation, and strength. Furthermore, the significant increase in ADAMTS-4 gene expression in the exercising, low risk greyhound CCLs indicates that these ligaments may have a higher rate of catabolism in order to maintain their normal function.

Chapter 4: Evaluating regional and breed differences in the glycosaminoglycan content of the canine cranial cruciate ligament.

4.1 Introduction

Glycosaminoglycans (GAGs) are complex carbohydrate structures (Hardingham and Fosang 1992). There are seven major GAGs present in connective tissues; hyaluronic acid, chondroitin-6 sulphate, chondroitin-4 sulphate, dermatan sulphate, keratan sulphate, heparin, and heparan sulphate (Hardingham 1981).

GAGs are repeating disaccharide units that contain sulphated hexosamine and hexuronic acid, with the exception of keratan sulphate, as it does not contain uronic acid (Hardingham and Fosang 1992). Hyaluronic acid is the only GAG that does not have a sulphate group on its disaccharide and, unlike other GAGs, it does not attach covalently to a proteoglycan core protein (Ajit Varki 2009). In addition, hyaluronic acid is not further epimerised from glucuronic acid to iduronic acid (Ajit Varki 2009). Sulphated glycosaminoglycans (sGAGs) have been reported to comprise of 0.081 % (Smith, Clegg et al. 2014) and 2% (Kharaz 2015) of the canine cranial cruciate ligament (CCL) dry weight.

Tendons and ligaments that pass through or wrap around bony structures are subjected to compression and tensile forces depending on their mechanical demands (See Chapter 1 - Section 1.1.4). Increase in alcian blue staining, which is a stain specific to sGAGs, has been demonstrated in compressed regions of where tendon and ligament become fibrocartilaginous (Feitosa, Reis et al. 2006). Chondroitin -6 sulphate content was found to increase compared to chondroitin -4 sulphate in tendon under cyclic compressive loading in vitro (Evanko and Vogel 1993).

In the dog, narrowing of the distal femoral intercondylar notch is thought to cause compression and impingement of the CCL, thus creating a CCL impingement region, and narrowing of the intercondylar notch has been found to occur in the Labrador retriever (a high risk dog breed to CCLD/ R) (Comerford, Tarlton et al. 2006a) (See Chapter 1 – Section 1.4.6.3). sGAGs levels were found to increase significantly in the CCL impingement region of the high risk Labrador retriever compared to those of the greyhounds (low risk to CCLD/ R), suggesting that sGAGs may have increased in the high risk Labrador retriever as a result of the CCL compressing against the intercondylar notch (Comerford, Tarlton et al. 2006a).

It has been demonstrated in tendon (Feitosa, Reis et al. 2006) and in Chapter 3 of this thesis that GAGs may differ between the anatomical regions of tendon and ligament. In addition, previous studies on these tissues have shown that the GAG

content is increased in pathological tendons and ligaments (Riley, Harral et al. 1994a; Comerford, Innes et al. 2004; Halper, Kim et al. 2006; Fu, Chan et al. 2007; Samiric, Parkinson et al. 2009). Therefore, we hypothesis that GAGs may differ between the anatomical regions of the CCL and between two dog breeds with a differing predisposition to CCLD/ R.

The aim of this work is to determine the GAG and water content in different regions of the CCL in two differentially predisposed dog breeds to CCLD/ R, and to further observe whether if there are any significant differences of GAGs and water content between these differentially predisposed dog breeds. The GAGs to be characterised for this chapter include sGAGs, uronic acid, hyaluronic acid, keratan sulphate, and sGAGs after chondroitinase ABC (eliminates chondroitin and dermatan sulphate) digestion.

For this study, we have selected the Staffordshire bull terriers (moderate-high risk) and greyhounds (low risk) to CCLD/ R, in order to compare the individual GAGs and water content between them and within their anatomical regions.

4.2 Materials and methods

4.2.1 Canine sample collection

Staffordshire bull terrier CCLs (n=5) were divided into origin, middle, and insertion anatomical regions. Archived CCLs from ex-racing greyhounds (n=5) had been previously sectioned from the origin and insertion anatomical regions. These samples were obtained with ethical permission and full owner consent where appropriate (See Chapter 2 – Section 2.1.1 and 2.1.2). Inclusion/ exclusion criteria for samples are described in Chapter 2; Tables 2-1 and 2-2. Samples were stored at -20°C until required.

4.2.2 Biochemical analysis

Water content

CCL samples were thawed at room temperature and the wet weight was then measured. This was followed by freeze drying the CCL samples over night in order to measure the dry weight and to calculate the CCL water content. The water content % of the CCL was calculated using the following equation;

$$\text{Water content \%} = ([\text{wet weight} - \text{dry weight}] / \text{wet weight}) \times 100$$

sGAGs

The content of sGAGs was measured using the DMMB assay (Farndale, Buttle et al. 1986), either with or without enzymatic digestion using Chondroitinase ABC enzyme, as ChABC is used to remove chondroitin and dermatan sulphate GAG chains (Yamagata, Saito et al. 1968). Shark chondroitin sulphate (Sigma, UK) was used as the standard (See Chapter 2 - Section 2.3.2).

Uronic acid assay

Uronic acid concentration or content was determined using the carbazole assay (Bitter and Muir 1962). Glucuronic acid lactone was used as the standard (See Chapter 2 - Section 2.3.3).

Hyaluronic acid

The concentration of hyaluronic acid (HA) in the tissue was indirectly estimated by assuming that UA comprised 36 % of the dry weight of GAGs and 45 % of the dry weight of HA, as presented in the following equation (Riley, Harrall et al. 1994);

$$[\text{HA}] = [\text{UA}] - ([\text{Total sGAG}] \times 0.36)$$

0.45

Keratan sulphate

Keratan sulphate content was measured using the competitive enzyme linked immunosorbent assay (ELISA) methodology obtained from Caterson and others (Caterson, Cristner et al. 1983). Bovine articular cartilage aggrecan was used as the standard (See Chapter 2 - Section 2.3.4).

4.3 **Statistical analysis**

Data were tested for normality by using the Kolmogorov-Smirnov test. If distributed normally, a student t-test was performed to detect differences between two groups, and a One-Way ANOVA to compare three groups followed by a Bonferroni *post hoc* test. If data did not have a normal distribution, a Mann Whitney U test was selected for detecting differences between two groups, or a Kruskal-Wallis test for three groups followed by a Dunn's *post hoc* test. Results are presented as mean values ± SEM and a significance level of $p < 0.05$ was used. The three groups selected for analysis were anatomical regions (origin, middle, and insertion) for the Staffordshire bull terrier CCL, whilst the two groups selected for analysis were either the anatomical regions (origin and insertion) of the greyhoud CCL or the two dog breeds (Staffordshire bull terrier and greyhound). There were two unpaired goups chosen for analysis, as the first group was Staffordshire bull terrier CCL vs. greyhound CCL after the mean value of the origin and insertion anatomical regions of the two dog breeds were averaged, and the second group was greyhound CCL origin anatomical region vs. greyhound CCL insertion anatomical region. Graphpad Prism (Version 6, GraphPad Software, La Jolla California, USA) software was used for statistical analysis of all data.

4.4 Results

4.4.1 Canine CCL data summary

The history of canine cadavers was recorded which consisted of the dog breed, age, bodyweight and gender where applicable.

Table 4-1: Summary of the age, bodyweight and gender of canine cadaveric cranial cruciate ligament (CCLs) samples selected for biochemical analysis.

(SBT= Staffordshire bull terrier; GH= greyhound; N/ A= not available)

Breed	Ligament	Age	Weight (Mean ± SEM)	Male	Female
SBT	N=10	2-5 years	20 ± 1.7 kg	4	1
GH	N=10	3-5 years	N/ A	N/ A	N/ A

4.4.2 Water and GAGs content

4.4.2.1 Water content

Staffordshire bull terrier (SBT): Water content % ranged from 67 to 73 %, (average 70 ± 1.0 %). There were no statistically significant differences between regions (origin, middle, insertion) of the SBT CCLs (p=0.39) (Figure 4-1)**.**

Greyhound (GH): Water content % ranged from 61 to 68 %, (average 64 ± 1.2 %). There were no statistically significant differences between regions (origin vs. insertion) of the GH CCLs (p=0.2) (Figure 4-1)**.**

Staffordshire bull terrier vs. greyhound: Staffordshire bull terrier CCLs had a significantly higher water content % than greyhound CCLs after the values from the origin and insertion regions were averaged between the two dog breeds (p=0.002) (Figure 4-2)**.**

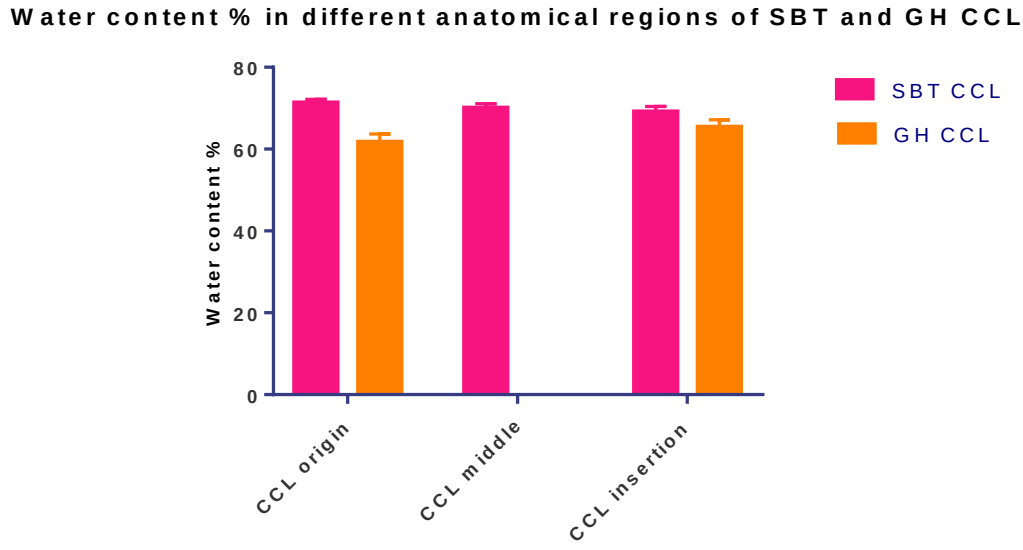

Figure 4-1: Water content % in the different anatomical regions of the moderate-high risk Staffordshire bull terrier and low risk greyhound CCLs.

CCL= cranial cruciate ligament, n= 5.

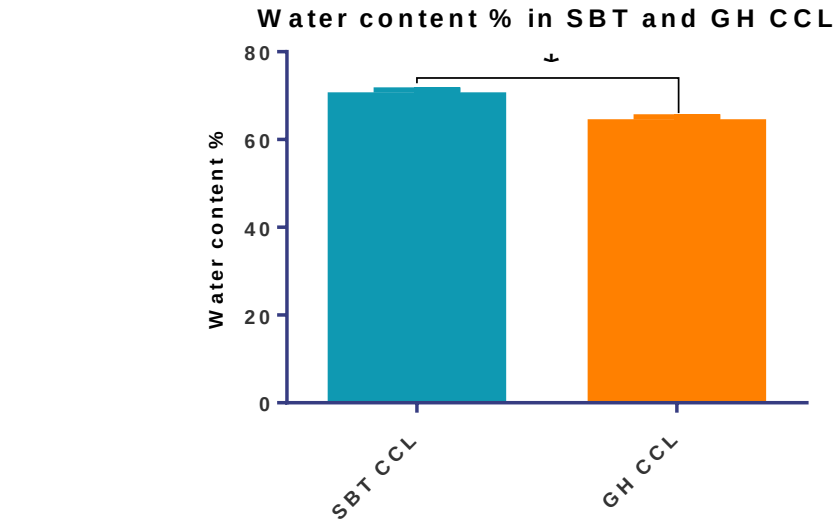

Figure 4-2: Water content % in the moderate-high risk Staffordshire bull terrier and low risk greyhound CCLs.

Staffordshire bull terrier CCLs contained significantly higher WC % when compared to greyhound CCL (p=0.002). CCL= cranial cruciate ligament; SBT= Staffordshire bull terrier; GH = greyhound, n= 5.

4.4.2.2 **Uronic acid**

Staffordshire bull terrier: Uronic acid content as a percentage of dry weight ranged from 1.3 to 4 %, (average 2.3 ± 0.5 %). There were no statistically significant differences between regions (origin, middle, and insertion) of the SBT CCLs (p=0.63) (Figure 4-3).

Greyhound: Uronic acid as a percentage of dry weight ranged from 1.1 to 1.7 %, (average 1.4 ± 0.1 %). There were no statistically significant differences between regions (origin vs. insertion) of the GH CCLs (p=0.42) (Figure 4-4).

Staffordshire bull terrier vs. greyhound: There were no statistically significant differences in uronic acid % between Staffordshire bull terrier and greyhound CCLs after the values from the origin and insertion regions were averaged between the two dog breeds (p=0.13).

4.4.2.3 **Hyaluronic acid**

Staffordshire bull terrier: Hyaluronic acid content as a percentage of dry weight ranged from 1.1 to 7.7 %, (average 3.8 ± 1.4 %). There were no statistically significant differences in hyaluronic acid content between regions (origin, middle, and insertion) of the SBT CCLs (p=0.6) (Figure 4-3).

Greyhound: Hyaluronic acid as a percentage of dry weight ranged from 0.9 to 2.6 %, (average 1.7 ± 0.3 %). There were no statistically significant differences between regions (origin vs. insertion) of the GH CCL (p=0.31) (Figure 4-4).

Staffordshire bull terrier vs. greyhound: There were no statistically significant differences in hyaluronic acid % between Staffordshire bull terrier and greyhound CCLs after the values from the origin and insertion regions were averaged between the two dog breeds (p=0.23).

4.4.2.4 **sGAGs**

Staffordshire bull terrier: sGAG content as a percentage of dry weight ranged from 1.3 to 2.2 %, (average 1.9 ± 0.2 %). There were no statistically significant differences between regions (origin, middle, and insertion) of the SBT CCLs (p=0.27) (Figure 4-3).

Greyhound: sGAG content as a percentage of dry weight ranged from 1.3 to 2.1 %, (average 1.7 ± 0.2 %). There were no statistically significant differences between regions (origin vs. insertion) of the GH CCL (p=0.016) (Figure 4-4).

Staffordshire bull terrier vs. greyhound: There were no statistically significant differences in sGAG % between Staffordshire bull terrier and greyhound CCLs after the values from the origin and insertion regions were averaged between the two dog breeds (p=0.19).

4.4.2.5 **sGAGs after Chondroitinase ABC (ChABC)**

Staffordshire bull terrier: sGAGs after ChABC content as a percentage of dry weight ranged from 1.4 to 1.5 %, (average 1.4 ± 0.03 %). There were no statistically significant differences between regions (origin, middle, and insertion) of the SBT CCL (p=0.78) (Figure 4-3).

Greyhound: sGAGs after ChABC content as a percentage of dry weight ranged from 0.5 to 1 %, (average 0.7 ± 0.1 %) there were no statistically significant differences between regions (origin vs. insertion) of the GH CCL (p=0.57) (Figure 4-4).

Staffordshire bull terrier vs. greyhound: Staffordshire bull terrier CCLs had a significantly higher sGAGs % after ChABC digestion than greyhound CCLs after the values from the origin and insertion regions were averaged between the two dog breeds (p= 0.0003) (Figure 4-5).

4.4.2.6 **Keratan sulphate**

Staffordshire bull terrier: Keratan sulphate content as a percentage of dry weight ranged from 0.5 to 0.9 %, (average 0.7 ± 0.06 %). There were no statistically significant differences between regions (origin, middle, and insertion) of the SBT CCLs (p=0.3) (Figure 4-3).

Greyhound: Keratan sulphate content as a percentage of dry weight ranged from 1.2 to 0.3 %, (average 0.6 ± 0.1 %). There were no statistically significant differences between regions (origin vs. insertion) of the GH CCLs (p=0.3) (Figure 4-4).

Staffordshire bull terrier vs. greyhound: There were no statistically significant differences in keratan sulphate % between Staffordshire bull terriers and greyhounds CCLs after the values from the origin and insertion regions were averaged between the two dog breeds (p=0.34).

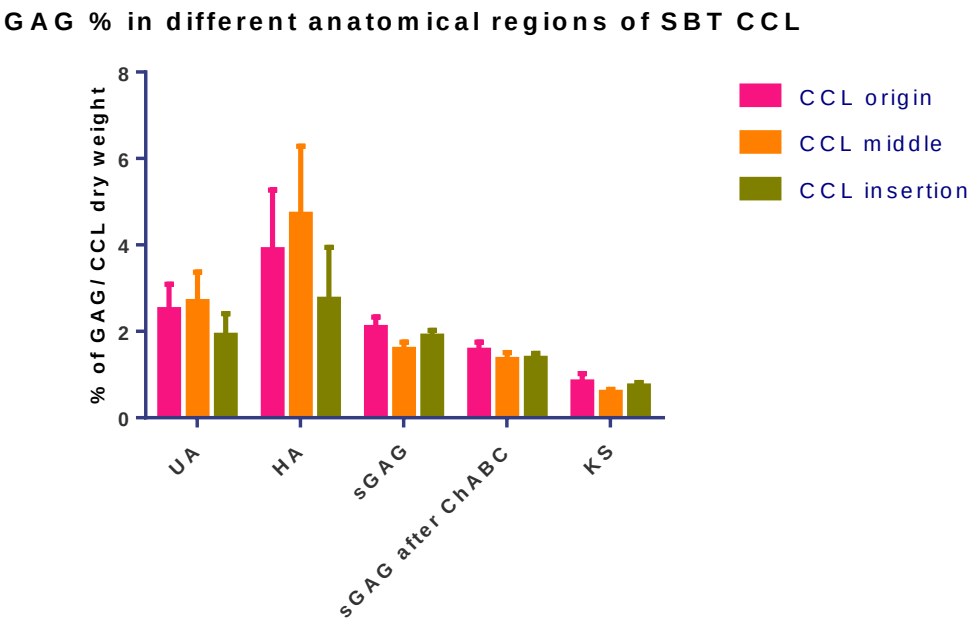

Figure 4-3: GAG content in the origin, middle, and insertion anatomical regions of the moderate-high risk Staffordshire bull terrier CCLs (% dry weight).

UA= uronic acid; HA= hyaluronic acid; sGAG= sulphated glycosaminoglycans; ChABC= Chondroitinase ABC; KS= keratan sulphate, n= 5.

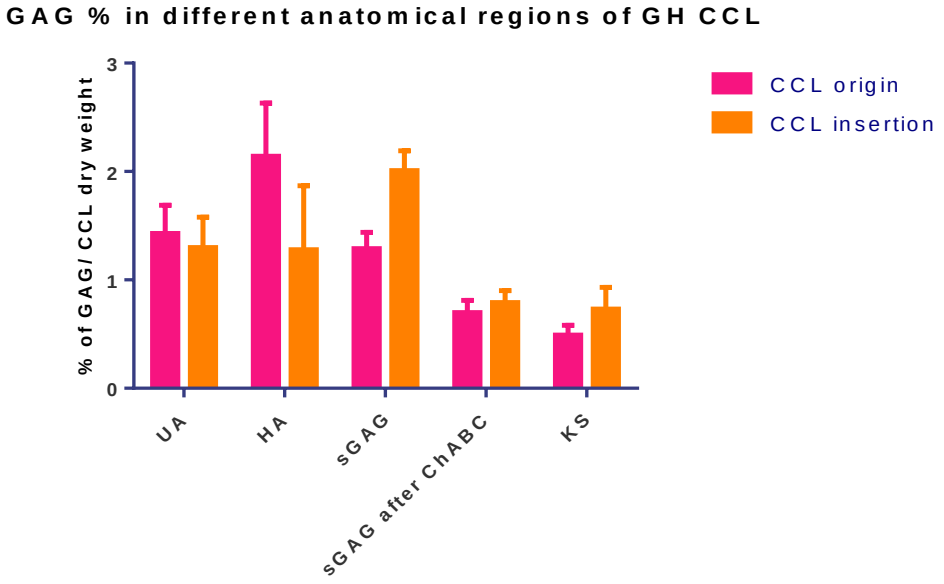

Figure 4-4: GAG content in the origin and insertion anatomical regions of the low risk greyhound CCLs (% dry weight).

UA= uronic acid; HA= hyaluronic acid; sGAG= sulphated glycosaminoglycans; ChABC= Chondroitinase ABC; KS = keratan sulphate, n= 5.

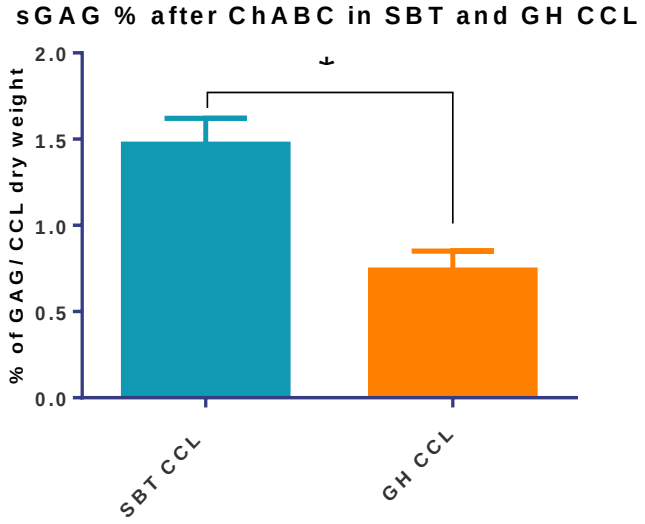

Figure 4-5: sGAGs % of dry weight after ChABC digestion between the moderate-high Staffordshire bull terrier and low risk greyhound CCLs.

Staffordshire bull terrier CCL contained significantly higher sGAGs after ChABC when compared to greyhound CCL (p= 0.0003). CCL= cranial cruciate ligament; SBT= Staffordshire bull terrier; GH= greyhound; sGAG= sulphated glycosaminoglycans; ChABC= chondroitinase ABC, n=5.

Table 4-2: Water and GAG content % within different anatomical regions of the Staffordshire bull terrier CCLs.

All GAG values in the CCLs were calculated as μg/ mg dry weight of tissue and then converted to a percentage. Values are displayed as mean ± SEM, n= 5.

Water content & GAGs	CCL origin	CCL middle	CCL insertion
Water content	71.3 ± 0.9	70.1 ± 1.0	69.1 ± 1.3
Uronic acid	2.5 ± 0.6	2.7 ± 0.7	1.9 ± 0.5
Hyaluronic acid	3.9 ± 1.4	4.7 ± 1.6	2.7 ± 1.2
sGAGs	2.1 ± 0.2	1.6 ± 0.2	1.9 ± 0.1
sGAG after ChABC	1.6 ± 0.2	1.4 ± 0.2	1.4 ± 0.1
Keratan sulphate	0.9 ± 0.2	0.6 ± 0.1	0.7 ± 0.1

Table 4-3: Water and GAG content % in different anatomical regions of the greyhound CCLs.

All GAG values in the CCLs were calculated as µg/ mg dry weight of tissue and then converted to a percentage. Values are displayed as mean ± SEM, n= 5.

Water content & GAGs	CCL origin	CCl insertion
Water content	61.7 ± 1.95	65.4 ± 1.8
Uronic acid	1.4 ± 0.3	1.3 ± 0.3
Hyaluronic acid	2.1 ± 0.5	1.3 ± 0.6
sGAGs	1.3 ± 0.2	2.0 ± 0.2
sGAG after ChABC	0.7 ± 0.1	0.8 ± 0.1
Keratan sulphate	0.5 ± 0.1	0.7 ± 0.2

4.5 **Discussion**

Determination of the levels of individual GAGs and water content in different anatomical regions of the canine CCL and between differentially predisposed dog breeds to CCLD/ R may help in understanding on how these GAGs may contribute to ligament structure and function. We have found differences in GAGs in the CCLs between the two dog breeds, but no significant differences in GAGs were found between the different anatomical regions of the Staffordshire bull terrier and greyhound CCLs. Significantly greater water content was found in the Staffordshire bull terrier compared to greyhound CCLs. Furthermore, sGAGs content after ChABC enzymatic digestion was significantly decreased in greyhound CCLs compared to those of the Staffordshire bull terrier.

The ligament is known to be composed of two thirds water and one thirds solids (Frank 2004; Rumian, Wallace et al. 2007). We have determined the water content of the CCLs of the Staffordshire bull terrier and greyhound to be 70% and 64 % respectively. Our water content values are in agreement with previous studies (Smith 2010; Kharaz 2015). In addition, the water content has shown to be significantly increased in Staffordshire bull terrier CCLs in comparison to greyhound CCLs ($p=0.002$).

The increased water content in Staffordshire bull terrier CCLs could indicate a high deposition of GAGs and proteoglycans that function to retain water in ligament. It has been previously indicated that sGAG removal with ChABC increased water permeability and decreased compressive stress in porcine medial collateral ligament (Henninger, Underwood et al. 2010). Aggrecan is a large aggregating proteoglycan that is known to retain water in order to provide resilience, space filling capacities, and hydration for the tissue (Hardingham and Bayliss 1990). An aggrecan monomer consists of approximately 100 chondroitin sulphate and 50 keratan sulphate chains, with the addition of O- and N- linked oligosaccharides (Hardingham and Bayliss 1990). The Staffordshire bull terrier CCL has been previously shown to have significantly higher aggrecan gene expression in comparison to greyhounds (See Chapter 3), and we speculate that Staffordshire bull terrier CCL withstands higher compressive forces or forces that are changing the CCL structure to become more compressive than the greyhound CCLs. It could be that the higher water content in Staffordshire bull terrier CCL is linked with higher compressive forces. However, increased water content in Staffordshire bull terrier CCLs could also contribute to increase compressive loading of the CCL, thus

leading to CCLD/ R. This indicates that a pathological outcome may exist in the Staffordshire bull terrier, as no evident of pathology in the Staffordshire bull terrier has been previously reported. Comerford and others have shown that the water content significantly increased in ruptured CCLs compared to intact CCLs (Comerford, Innes 2004). In addition, increased water content and large aggregating proteoglycans in pathological tendons has been previously reported (Riley, Harrall et al. 1994b; Samiric, Parkinson et al. 2009).

The hyaluronic acid disaccharide consists of glucuronic acid and N-acetyl glucosamine, and is known to be the only GAG that does not contain sulphate groups (Hardingham and Fosang 1992). It is known to attach non-covalently to the large aggregating proteoglycans (Ajit Varki 2009).

In this part of study, hyaluronic acid averaged 3.4 % of the CCL dry weight in Staffordshire bull terriers and 1.7 % of the CCL dry weight in greyhounds. Although Staffordshire bull terriers CCLs had a higher mean content of hyaluronic acid than greyhound CCLs, statistical analysis did not show any significant differences between the breeds. The reason could be the high variability of hyaluronic acid observed in Staffordshire bull terrier donors (1.1-7.7 %). Hyaluronic acid has been previously determined in human supraspinatus tendon (0.9 % of tendon dry weight) and common biceps tendon (1.1 % of tendon dry weight) (Riley, Harrall et al. 1994a). Hyaluronan could have a role in maintaining the viscosity and viscoelastic properties of the CCL, as it has been previously reported to function similarly in the eye and skeletal joints (Ajit Varki 2009). The high content of hyaluronic acid in ex-racing greyhounds could be essential in order to strengthen their CCL, as increased levels of hyaluronic acid have been found in exercised chicken gastrocnemius tendon (Hae Yoon, Brooks et al. 2003). However, the high content of this non-sulphated GAG could also contribute to CCLD/ R in the Staffordshire bull terrier, as hyaluronic acid content was found to increase in human pathological supraspinatus tendon (Riley, Harrall et al. 1994a).

Uronic acid is known to be present in all GAGs with the exception of keratan sulphate, whereas sGAGs are present in all GAGs with the exception of hyluronic acid (Hardingham and Fosang 1992). The uronic acid and sGAG contents in the CCL were 2.3 and 1.9 % for Staffordshire bull terriers, as well as 1.4 and 1.7 % for greyhounds. There were no statistically significant differences of uronic acid levels between the Staffordshire bull terrier and greyhound CCL. Comerford and others also reported that there were no statistical significant differences of uronic acid

levels between the Labrador retriever (high risk dog breed to CCLD/ R) and greyhound (low risk dog breeds to CCLD/ R) CCLs (Comerford, Tarlton et al. 2005).

The sGAG content was previously determined in the Staffordshire bull terrier CCL and was found to be 1.5% of the CCL dry weight (Kharaz 2015), which was close to our reported value of 1.9 % of the CCL dry weight. However, the sGAG value for greyhound CCLs in our study was slightly higher (1.4 % of the CCL dry weight) than what has been previously reported (0.081 % of the CCL dry weight) in greyhound CCLs (Smith, Clegg et al. 2014), and this could be due to the different exercise regime history between the two groups of greyhound donors.

There were no statistically significant differences between different anatomical regions of Staffordshire bull terrier and greyhound in regards to sGAG content, and this agrees with other unpublished studies that attempted to detect regional differences in sGAG content between the canine CCL anatomical regions (Kharaz 2015). Since sGAG content has been previously found to be significantly elevated in the fibrocartilaginous anatomical regions of the porcine superficial and deep digital flexor tendon (Fietosa, Ries et al. 2006), we anticipated to detect an increase of sGAG in the middle anatomical region, which has been found to mainly consist of fibrocartilaginous areas (Paatsama 1952; Vasseur, Pool et al. 1985; Comerford, Tarlton et al. 2006b). In addition, fibrocartilaginous areas are also present at the site where the CCL inserts into bone (Arnoczky 1983; Zhu, Zhang et al. 2012). This could suggest that sGAGs are distributed abundantly across the CCL anatomical regions which might have caused the sGAGs to be statistically insignificant across the regions.

The chondroitin sulphate disaccharide consists of N-acetylgalactosamine and glucuronic acid (Hardingham and fosang 1992; Ajit Varki 2009). Dermatan sulphate arises from the same precursor of chondroitin sulphate as it is generated via epimerization of glucuronic acid into iduronic acid (Hardingham and Muir 1974; Hascall and Heinegard 1974). Chondroitinase ABC is a degrading enzyme which acts to remove chondroitin sulphate (-4, and -6) and dermatan sulphate (Yamagata, Saito et al. 1968). This may indicate that other GAG chains remain after chondroitinase ABC such as keratan sulphate, heparin, and heparan sulphate.

In this part of study, greyhound CCLs had significantly reduced sGAGs content in comparison to Staffordshire bull terrier CCLs following digestion with ChABC. This finding could indicate that there is a higher dermatan/ chondrotin sulphate content in

the greyhound in comparison to Staffordshire bull terrier CCLs. This results also supports findings in Chapter 3, where gene expression of the chondrotin/ dermatan sulphate proteoglycan decorin was significantly upregulated in greyhounds in comparison to Staffordshire bull terrier CCLs. In addition, greyhound CCLs have been known to be associated with large (>150) and intermediate (150-100) collagen fibril diameters (Comerford, Tarlton et al. 2006b). A previous study has concluded that dermatan sulphate is associated with larger collagen fibril diameter (>150 nm), while tissues with intermediate sized collagen fibrils have been found to be rich with chondroitin sulphate (60-150 nm) (Parry, Flint et al. 1982). However, it could be that greyhounds CCLs only contain higher amounts of dermatan sulphate than Staffordshire bull terrier CCLs and not chondroitin sulphate. Since we have found in Chapter 3 that chondroitin-6 sulphate and the large chondroitin/ keratan sulphate proteoglycan, aggrecan, were both significantly increased in the Staffordshire bull terrier in relation to greyhound CCLs.

Keratan sulphate is composed of disaccharide repeats of N-acetyl glucosamine and galactose (Hardingham and Muir 1974; Hascall and Heinegard 1974). Keratan sulphate content was low in the CCL, at 0.7 % of the CCL dry weight in the Staffordshire bull terriers and 0.6 % of the CCL dry weight in greyhounds CCLs indicating that keratan sulphate may be the GAG at lowest concentration in the CCLs. The keratan sulphate content has also been previously determined to be low in human supraspinatus (0.04 % of the tendon dry weight) and common biceps tendon (0.004 % of the tendon dry weight) (Riley, Harrall et al. 1994a).

A limitation of this study is that we were unable to determine the individual content of chondroitin sulphate and dermatan sulphate. However, these two individual GAGs have been previously determined (Reily, Harrall et al. 1994a). The procedure involves digesting samples with chondroitinase ABC and chondroitinase AC (removes only dermatan sulphate) in order to calculate chondroitin sulphate and dermatan sulphate content (Reily, Harrall et al. 1994a). We have made an attempt to detect chondroitin and dermatan sulphate content individually by following this method, however, the results of most of our data appeared as negative values. Individual contents of chondrotitn sulphate and dermatan sulphate therefore still needs to be investigated in the canine CCL.

4.6 **Conclusion**

- The significant increase of water content in Staffordshire bull terrier CCL could be linked to increase areas of compressive loads in the CCLs, and may further contribute to CCLD/ R in this moderate-high risk dog breeds.
- sGAG content after ChABC enzymatic digestion was found to be significantly reduced in greyhound CCLs compared to those of the Staffordshire bull terriers, which might indicate higher levels of chondroitin/ dermatan sulphate proteoglycans such as decorin in the greyhound.
- Hyaluronic acid content may be essential in order to maintain the viscoelastic properties and strength of the racing greyhound CCLs. However, it may also be a contributing factor to CCLD/ R in the Staffordshire bull terrier.

Chapter 5: The structural morphology and proteoglycan distribution in different regions of the canine cranial cruciate ligament and between dog breeds at a differing risk to CCL disease and rupture.

5.1 **Introduction**

The microscopic hierarchical structure of ligament has been reported to be similar to that described in tendons consisting of collagen fibre bundles, fibres, subfibrils, microfibrils, and tropocollagen (See Chapter 1 – Figure 1-1) (Kastelic, Galeski et al. 1978).

In ligament, collagen fibre bundles are divided by cells (Amiel, Frank et al. 1984; Clark and Sidles 1990), and bundles are grouped into interdigitating membranes named fascicles (Clark and Sidles 1990). Fascicles are separated by septa (Clark and Sidles 1990). The septa separating the fascicles are referred as endoligament (Chowdhury, Matyas et al. 1991).

Decorin, lumican and fibromodulin are members of the small leucine rich proteoglycan (SLRPs) that bind to collagen fibrils and organise collagen fibrillogenesis (Scott 1996). Aggrecan and versican are known as the large aggregating proteoglycans (Iozzo and Murdoch 1996; Iozzo and Schaefer 2015). Aggrecan allows tendon the capacity to withstand compressive forces associated with loading (Vogel and Koob 1989; Evanko and Vogel 1993; Huisman, Andersson et al. 2014), whereas versican regulates cell migration and adhesion as well as contributing to the ECM structural properties (Dours-Zimmermann and Zimmermann 1994; Isogai, Aspberg et al. 2002).

The cranial cruciate ligament (CCL) and the caudal cruciate ligament (CaCL) form the cruciate ligament (CL) complex in the canine stifle joint (Arnoczky and Marshall 1977). Macroscopically, the CCL consists of two bands; the craniomedial band (CMB) and the caudolateral band (CLB), and the CaCL consists of the large cranial band and the smaller caudal band (Arnoczky and Marshall 1977).

Tendons and ligaments that pass through or wrap around bony structures are subjected to compression and tensile forces depending on their mechanical demands, and at these points tendon and ligament become fibrocartilage as a result of compression (See Chapter 1 - Section 1.1.5). Fibrocartilage can be histologically distinguished from non-fibrocartilaginous sites, as the collagen fibre bundles

orientation change from parallel into different angles running into one another, and the cell shape alters from spindle to rounded, exhibiting a similar phenotype to cartilage (Vogel 2004).

A fibrocartilaginous appearance in disease free CCLs has been observed in Labrador retriever (high in risk to CCLD/ R) and greyhound (low in risk to CCLD/ R) CCLs that was associated with increased Alcian blue staining, a dye which stains glycosaminoglycans (GAGs) (Comerford, Tarlton et al. 2006b). It was suggested that the fibrocartilage appearance in racing greyhounds is an adaptation to altered loads but was considered as a degenerative sign in Labrador retrievers. Since this study was only descriptive, it could be that semi-objective histology scoring analysis may have shown differences in tissue morphology and GAG deposition between different anatomical regions of the CCL and between two differentially predisposed dog breeds to CCLD/ R. Similar degenerative changes have been observed in CCLs of young beagles bred for laboratory use, and have been suggested to be a result of lacking exercise (Narama, Masuoka-Nishiyama et al. 1996).

It has been reported that dogs over 5 years of age with an increased bodyweight 15> kg exhibited a reduction in the CCL mechanical properties, and were found to have histological signs of fibrocartilage considered to be degenerative changes that occurred prior CCLD/ R (Vasseur, Pool et al. 1985). In ruptured canine CCLs, areas of cell loss accompanied with alterations in cellular phenotype (fibrocartilage progression) have been observed mostly in the middle anatomical region of the CCL (Hayashi, Frank et al. 2003). Loss of cells as a result of apoptosis or necrosis has also been observed in ruptured and partially ruptured CCLs (Hayashi, Frank et al. 2003; Gyger, Botteron et al. 2007; Krayer, Rytz et al. 2008). Loss of cells and altered cell phenotype was found to be associated with a reduction of crimp pattern (the periodic wave of collagen fibrils) in ruptured CCLs (Hayashi, Frank et al. 2003). Such degenerative changes might be primarily associated with high risk dog breeds predisposed to CCLD/ R.

Differences in proteoglycans localisation have been detected between different anatomical regions in tendons using Western blot analysis (See Chapter 3 - Section 3.1). In addition, immunohistochemical studies have previously found that certain proteoglycans are specifically localised within particular anatomical regions (tendon vs. compression) (Waggett, Ralphs et al. 1998; Vogel and Peters 2005). Aggrecan and biglycan have been mainly found in fibrocartilaginous areas where tendon is subjected to compression, and versican was found to mainly localise in the central

region where tendon is subjected to tension (Waggett, Ralphs et al. 1998). Decorin, on the other hand, was found to have a similar distribution in both compressed/ fibrocartilage and tensional regions of tendon (Vogel and Peters 2005). These studies demonstrate that proteoglycans have a functional role in different anatomical sites of tendon, and therefore may differ between various anatomical regions of the canine CCL and between dog breeds with a different predisposition to CCLD/ R.

Therefore, we aim to use semi-objective histology measurements in order to identify the CCL structure, morphological characteristics and sulphated glycosaminoglycan (sGAG) deposition between three dog breeds with a different predisposition to CCLD/ R, and to assess whether there are differences between their anatomical regions. We hypothesise that the structural morphology and sGAG deposition may be altered between these differentially predisposed dog breeds to CCLD/ R.

Furthermore, we aim to perform immunohistochemistry to characterise the localisation and distribution of large aggregating proteoglycans and SLRPs between different anatomical regions of the CCL, and between different dog breeds with a different predisposition to CCLD/ R. We hypothesise that each proteoglycan may have a unique localisation and distribution throughout the CCL that may alter between dog breeds at different risks to CCLD/ R. We further hypothesis that proteoglycans may differ between different anatomical regions of the CCL.

For histological assessment, we have examined CCLs between three dog breeds with a different predisposition to CCLD/ R, these are the racing greyhound (low risk), the Staffordshire bull terrier (moderate-high risk), and the Labrador retriever (high risk) (Whitehair, Vasseur et al. 1993; Duval, Budsberg et al. 1999; Baird, Carter et al. 2014b). For immunohistochemistry staining, we have examined CCLs from the racing greyhound and the Staffordshire bull terrier.

5.2 Materials and methods

5.2.1 Canine sample collection

For histological analysis, Staffordshire bull terrier CCLs (n=6) were divided into origin, middle, and insertion regions. Archived CCLs from ex-racing greyhounds (n=8) and Labrador retrievers (n=7) that had been previously sectioned from the craniomedial band (CMB) or the caudolateral band (CLB) were used. Sections available for CMB were n=7 for greyhounds, and n= 6 for Labrador retrievers, whilst for CLB were n=6 for greyhounds, and n=2 for Labrador retrievers. For immunohistochemistry, Staffordshire bull terrier CCLs (n=6) were divided into origin, middle, and insertion regions. Archived CCLs from ex-racing greyhounds (n=5) were previously sectioned from the craniomedial band (CMB). These samples were obtained with ethical permission and full owner consent where appropriate. Inclusion/exclusion criteria for samples are described in Chapter 2; Tables 2-1 and 2-2. See Chapter 2 - Section 2.1.1 and 2.1.2 for detailed sample collection.

5.2.2 Histology and immunohistochemistry

Samples obtained from Staffordshire bull terriers were fixed in 4% paraformaldyhyde overnight at 4°C, then were processed and embedded in paraffin wax. Tissue blocks embedded in paraffin obtained from Labrador retrievers and greyhounds were previously archived materials. All tissue blocks were sectioned at 4 µm and mounted onto poly lysine coated slides. Images were captured using a Nikon Eclipse 80i microscope. For histological assessment, haematoxylin and eosin stain (H&E) was used to detect CCL structural morphology, and sGAGs were assessed by using Alcian blue and Toluidine blue dyes. An objective scoring system was developed and assessed by two independent observers blinded to tissue sections. The scoring sheet can be seen in Chapter 2, Tables 2-7, and 2-8.

For immunohistochemistry, staining was performed with the following antibodies; aggrecan, versican, decorin, biglycan, lumican, fibromodulin, and keratocan. For more details about the immunohistochemistry protocol, see Chapter 2 – Section 2.5.2.

5.3 **Statistical analysis**

For histological analysis, data were checked for the normality with using Kolmogorov-Smirnov test. If they were normally distributed, a student-t test was performed to detect differences between two groups, and a one-way ANOVA was used to compare three groups followed by a Bonferroni *post hoc* test. If data were not normally distributed, a Mann Whitney U test was selected for detecting differences between two groups, or a Kruskal-Wallis test for three groups followed by a Dunn's *post hoc* test. We have compared the histology scoring between the different regions of the CCL for each in dog breed, and further compared anatomical regions between greyhound (low in risk to CCLD/ R) and Labrador retriever (high in risk to CCLD/ R) CCLs. We were not able to analyse the CLB region for Labrador retriever as we had only two donors. Results are presented as mean values ± standard error of the mean (SEM). Exact p-values are presented and a significance level of $p < 0.05$ was used. Immunohistological observations were asessed subjectively based on the intesity of staining (heavy vs. faint), distribution within the CCL structure (interfascicular region, collagen bundles, and ligament substance), and if they were localised around (pericellular) or within (intracellular) the cells. Graphpad Prism (Version 6, GraphPad Software, La Jolla California, USA) software was used for statistical analysis of all data.

5.4 Results

5.4.1 Canine data summary

The history of canine cadavers was recorded which consisted of the dog breed, age, bodyweight and gender where applicable.

Table 5-1: Summary of the age, bodyweight and gender of canine cadaveric cranial cruciate ligament (CCL) samples selected for histology/ immunohistochemistry analysis.

(SBT= Stafford shire bull terrier; GH= greyhound; LR= Labrador retriever; N/ A= not available).

Breed	Ligament	Age	Weight (Mean ± SEM)	Male	Female
SBT	N=12	2-5 years	18.2 ± 2.3 kg	4	1
GH	N=8	3-5 years	N/ A	N/ A	N/ A
LR	N=7	3-5 years	N/ A	N/ A	N/ A

5.4.2 Histology

5.4.2.1 Inter- and intra- observer agreement of the histology scoring system

Kendal's coefficient of concordance analysis was used to assess the strength of agreement between inter- and intra- observer for each histology scoring criteria. Kendal coefficient agreement values lie between a scale from 0 to 1, where 0.6 to 0.9 indicates a good agreement, whilst > 0.9 indicates an excellent agreement. Kendall's coefficient concordance resulted in an average of 0.77 and 0.69 for ob1 and ob2 intra-observer variation, whereas the value between the two observers was 0.77. Details for Inter- and intra- observer agreement calculations are provided in appendix IV.

5.4.2.2 **Haematoxylin and Eosin (H&E) staining**

5.4.2.2.1 **Collagen architecture**

Results showed that CCLs from each dog breed exhibited a mixture of normal, reduced and abnormal collagen architecture. Normal collagen architecture was found to have a regular crimp pattern. In addition, collagen bundles seemed to have a parallel (Figure 5-1 A) or a helical distribution. Reduced collagen architecture was accompanied with a homogenous appearance of collagen bundles with a slightly disorganised collagen matrix (Figure 5-1 B), whilst abnormal collagen architecture had a disruptive appearance of collagen bundles with areas of cell loss (Figure 5-1 A). The scoring data chart for the three dog breeds can be observed in Figure 5-2 (A, B). There were no statistically significant differences between anatomical regions of the CCL or between different dogs with a differing predisposition to CCLD/ R.

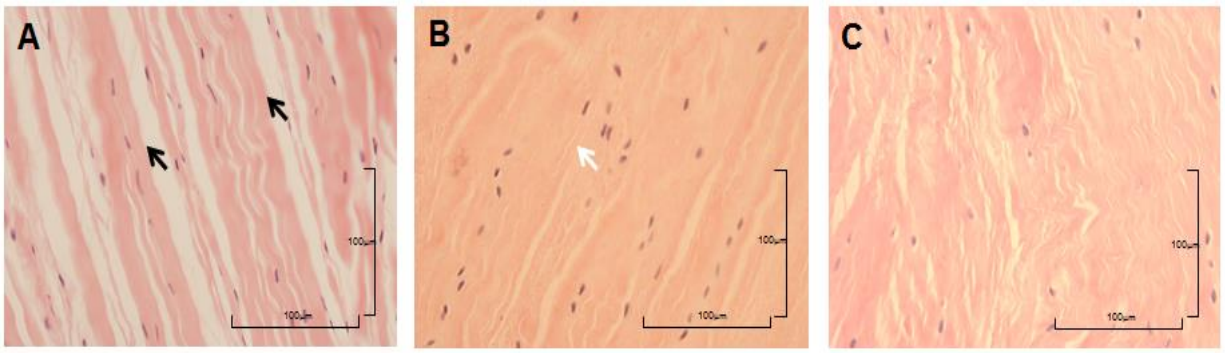

Figure 5-1: Histology image of collagen architecture in the canine CCL.

A) Normal structure of collagen from greyhound CCLs where primary collagen bundles are present (black arrow). B) Reduced structure of collagen bundles from Staffordshire bull terrier CCLs (white arrow). C) Abnormal structure of collagen from Labrador retriever CCLs where collagen bundles are disrupted in association with cell loss (Bar 100µm, H & E)**.**

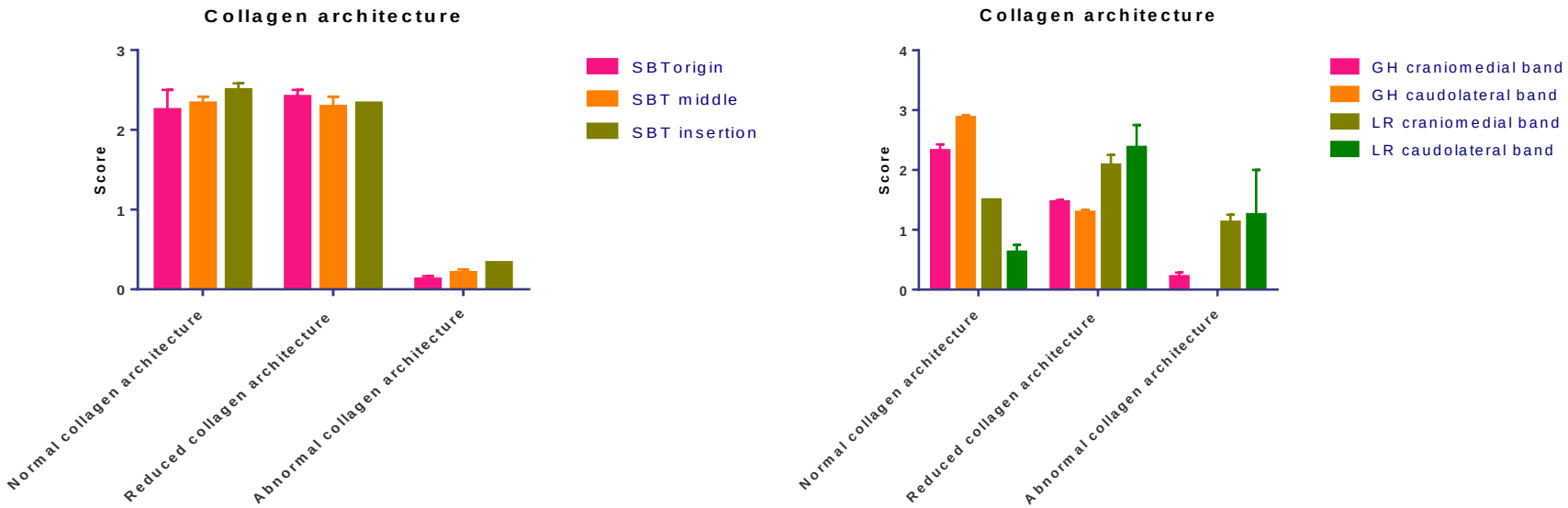

Figure 5-2: The collagen architecture scores in differentially predisposed dog breeds.

Histology results for collagen architecture with H&E staining in different anatomical regions for Staffordshire bull terrier (A), greyhound (B), and Labrador retriever (B) CCLs. (SBT= Staffordshire bull terrier; GH= greyhound; LR= Labrador retriever). A) The Staffordshire bull terrier had the highest scoring for normal and reduced collagen architecture. B) The greyhound had most scoring for normal collagen architecture, whilst the Labrador retriever had most scoring for reduced collagen architecture.

5.4.2.2.2 **Cell shape**

In general, the CCLs from all dog breeds exhibited a mixture of cell nuclei shapes, ranging from spindle (Figure 5-3, A), mixed (spindle and rounded) (Figure 5-3, B), and rounded with halo formation (manifestation of cell border with cytoplasmic enlargement) (Figure 5-3, C). The scoring data chart for the three dog breeds can be observed in Figure 5-4 (A, B). There were no statistically significant differences found between anatomical regions of the CCL or between different dogs with a differing predisposition to CCLD/ R.

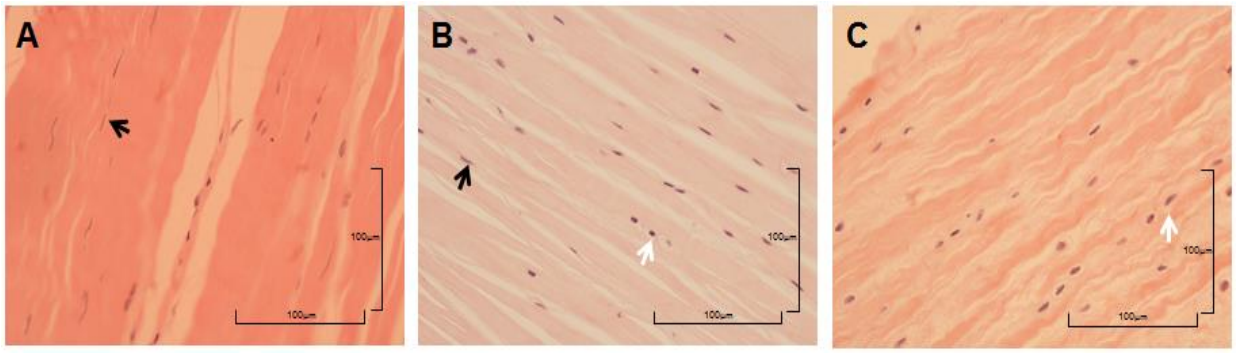

Figure 5-3: Histology image of cell nuclei shapes in the canine CCL.

A) Spindle shape (black arrow) from greyhound CCLs. B) Spindle (black arrow) and rounded (white arrow) shapes from Staffordshire bull terrier CCLs. C) Rounded shape (white arrow) from greyhound CCLs (Bar 100µm, H & E).

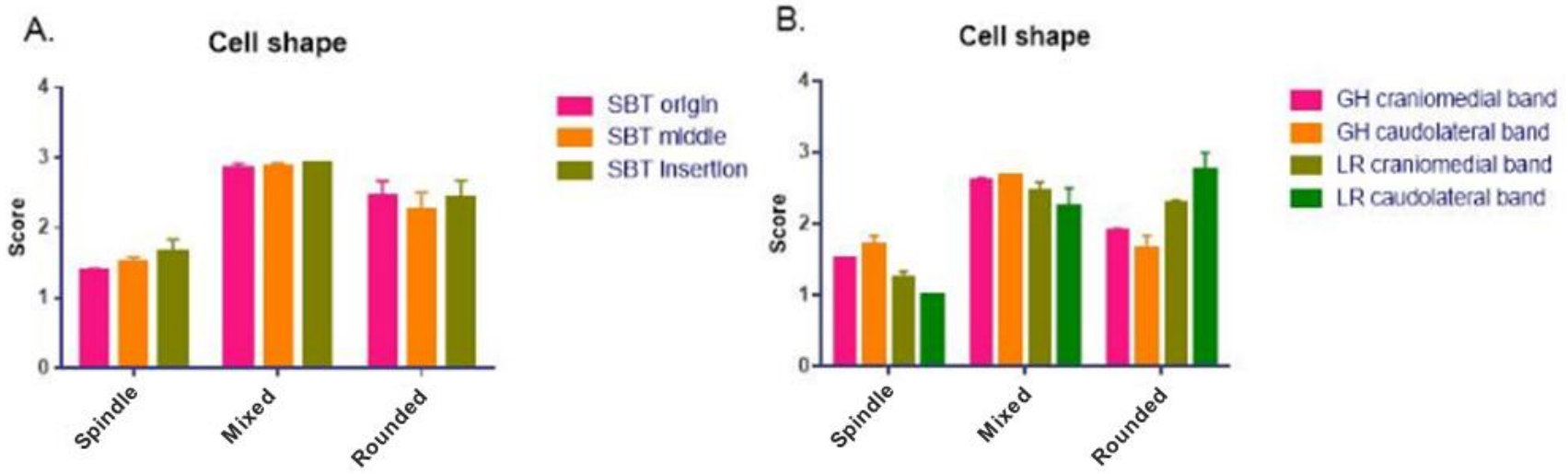

Figure 5-4: The cell shape scores in differentially predisposed dog breeds.

Histology results for cell shape with H&E staining in different anatomical regions in Staffordshire bull terrier (A), greyhound (B), and Labrador retriever (B) CCLs. (SBT= Staffordshire bull terrier; GH= greyhound; LR= Labrador retriever).

5.4.2.2.3 **Cellular distribution**

The CCL exhibited different cellular distributions. Cells that were located at the surface of collagen bundles had a normal distribution (Figure 5-5, A), whereas cells associated with a homogenous collagen structure (loss of collagen bundles) had an orientation similar to rows of chains (Figure 5-5, B). The scoring data chart for the three dog breeds can be observed in Figure 5-6 (A, B). There were no statistically significant differences between anatomical regions of the CCL or between different dogs with a differing predisposition to CCLD/ R.

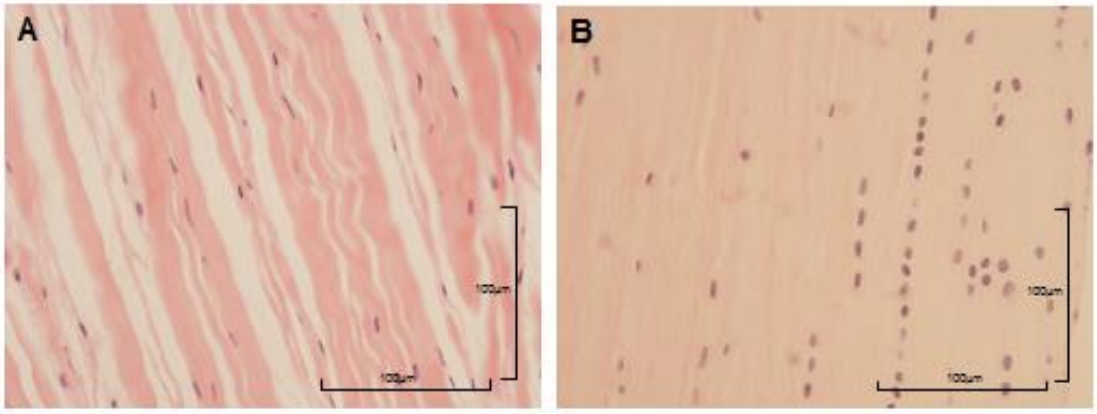

Figure 5-5: Histology image of cell distribution in the canine CCL.

A) Normally distributed cells located on the surface of collagen bundles. Image obtained from greyhound CCLs. B) Cell chain formation associated with a homogenous collagen structure. Image obtained from Staffordshire bull terrier CCLs (Bar 100µm, H & E).

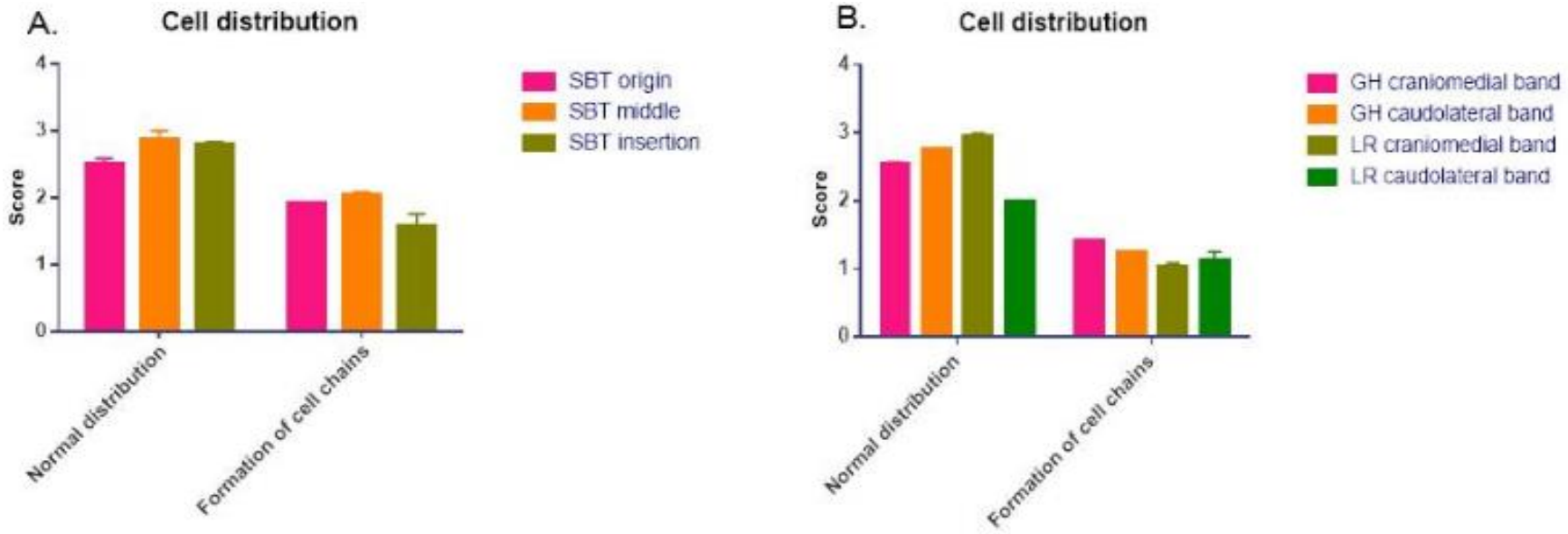

Figure 5-6: The cell distribution scores in differentially predisposed dog breeds.

Histology results for cell distribution with H&E staining in different anatomical regions in Staffordshire bull terrier (A), greyhound (B) and Labrador retriever (B) CCLs. (SBT= Staffordshire bull terrier; GH= greyhound; LR= Labrador retriever). All dog breeds exhibit both normal distribution of cells and cell chains.

5.4.2.2.4 **Vascularisation and inflammation**

The blood vessels in the CCL were monitered by size and quantity. The CCLs from all dog breeds exhibited mostly a low number and small sized blood vessels, and had a normal appearance (not dilated). Blood vessels were mostly observed in the interfascicular region of the CCL (Figure 5-7 A, B). The presence of inflammation in the tissues was scored based on the location of inflammatory cells such as neutrophils (granules in the cytoplasm and nucleus has 2-5 lobes), lymphocytes (rounded cytoplasm and nucleus that are slightly larger than ligementocytes) and macrophages (large cytoplasm and nucleus). Overall, there were little or no inflammatory cells in the CCLs from all dog breeds. The scoring data chart for the three dog breeds can be observed in Figure 5-8 (A, B). There were no statistically significant differences between anatomical regions of the CCL or between different dogs with a differing predisposition to CCLD/ R.

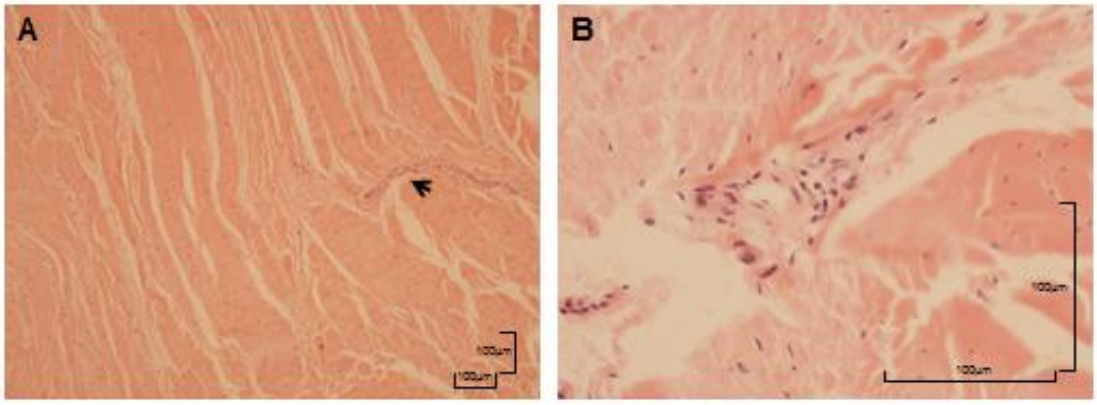

Figure 5-7: Histology image of the blood vessel in the canine CCL.

A) Blood vessels in the interfascicular region (black arrow) (Bar 100µm, H & E). B) A higher magnification of blood vessels in the interfascicular region (Bar 100µm, H & E). Image obtained from greyhound CCLs.

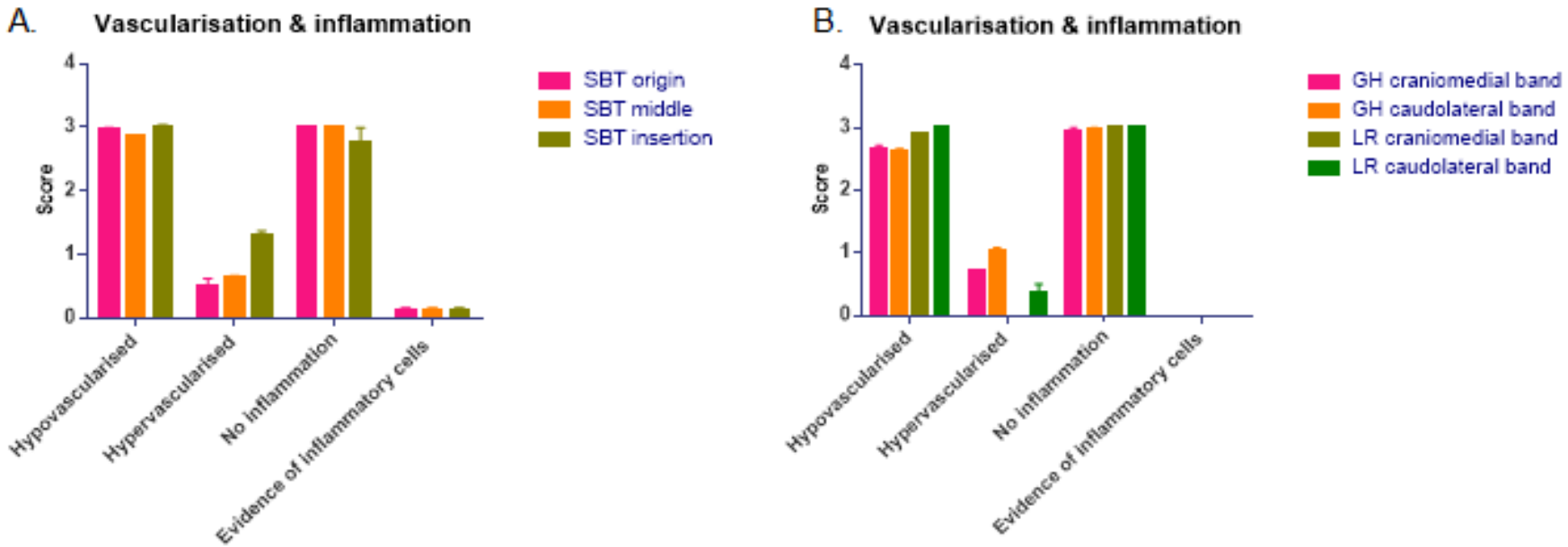

Figure 5-8: The vascularisation and inflammation scores in differentially predisposed dog breeds.

Histology results for vascularisation and inflammation with H&E staining in different anatomical regions in Staffordshire bull terrier (A), greyhound (B), and Labrador retriever (B) CCLs. (SBT= Staffordshire bull terrier; GH= greyhound; LR= Labrador retriever).

5.4.2.3 **Toluidine blue staining**

Toluidine blue is a thiazine metachromatic dye that stains sGAGs (Ball and Jackson 1953; Sridharan and Shanker 2012). Metachromasia indicates a change in the color of staining in the tissue, as Toluidine blue stain changes from blue to purple or red depending on the glycosaminoglycan content (Ball and Jackson 1953).

5.4.2.3.1 **Overall staining**

Toluidine blue staining was observed in all CCL tissues. Toluidine blue had a faint or marked staining on the CCLs (Figure 5-9 A, B). The scoring data chart for the three dog breeds can be observed in Figure 5-10 (A, B). There were no statistically significant differences found between the CCL anatomical regions or between differentially predisposed dog breeds to CCLD/ R.

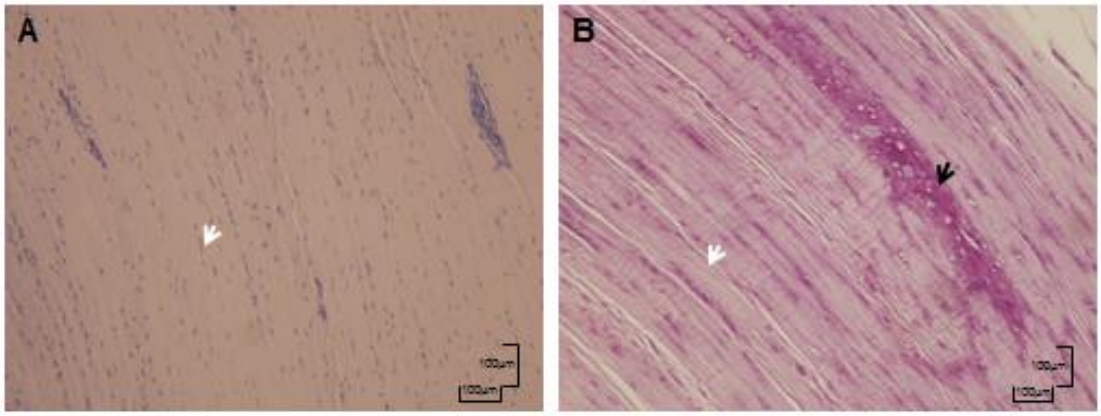

Figure 5-9: The intensity of Toluidine blue staining in the canine CCL.

A) Faint staining of collagen bundles (white arrow). Image obtained from greyhound CCLs. B) Marked staining of collagen bundles (white arrow) and interfascicular regions (black arrow). Image obtained from Staffordshire bull terrier CCLs (Bar 100µm).

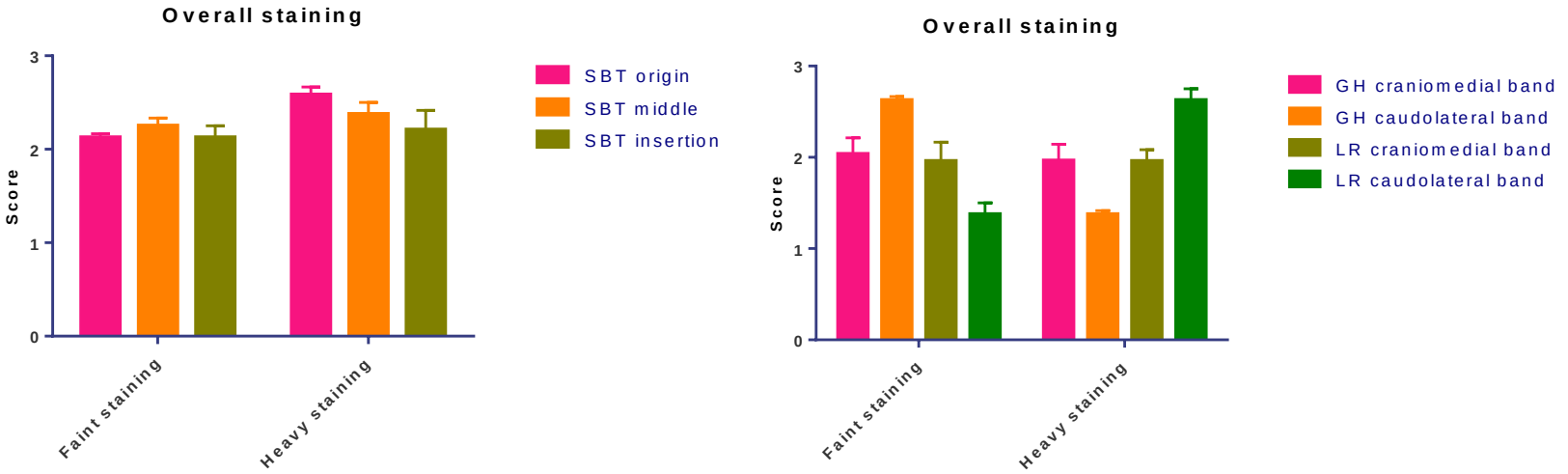

Figure 5-10: Overall staining scores with Touidine blue in differentially predisposed dog breeds.

Histology results for the overall staining with Toluidine blue in different anatomical regions in Staffordshire bull terrier (A), greyhound (B), and Labrador retriever (B) CCLs. (SBT= Staffordshire bull terrier; GH= greyhound; LR= Labrador retriever). All dog breeds had regions of both faint and heavy staining with Toluidine blue.

5.4.2.3.2 **CCL structure**

Our observations showed that Toluidine blue staining in the CCLs of all dog breeds was deposited in collagen bundles, interfascicular region, and ligament substance (covering collagen bundle) in the CCL. Faint staining was associated with normal collagen structure and spindle shaped cells (Figure 5-11 A), whilst more intense staining was associated with regions of reduced collagen density with rounded shaped cells (Figure 5-11 B). The Staffordshire bull terrier CCLs had a significantly greater deposition of Toluidine blue in their ligament substance in the origin anatomical regional compared to the insertion anatomical region (p= 0.02). The scoring data chart for the three dog breeds can be observed in Figure 5-12 (A, B).

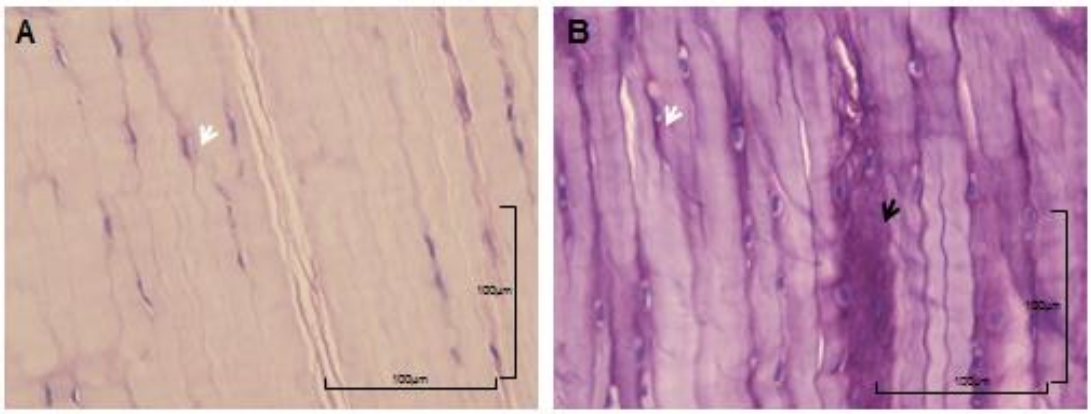

Figure 5-11: Toluidine blue staining in the CCL structure.

A) Faint staining of collagen bundles (white arrow), image obtained from greyhound CCLs. B) Marked staining of collagen bundles (white arrow) and interfascicular regions (black arrow). Image obtained from Staffordshire bull terrier CCLs (Bar 100µm).

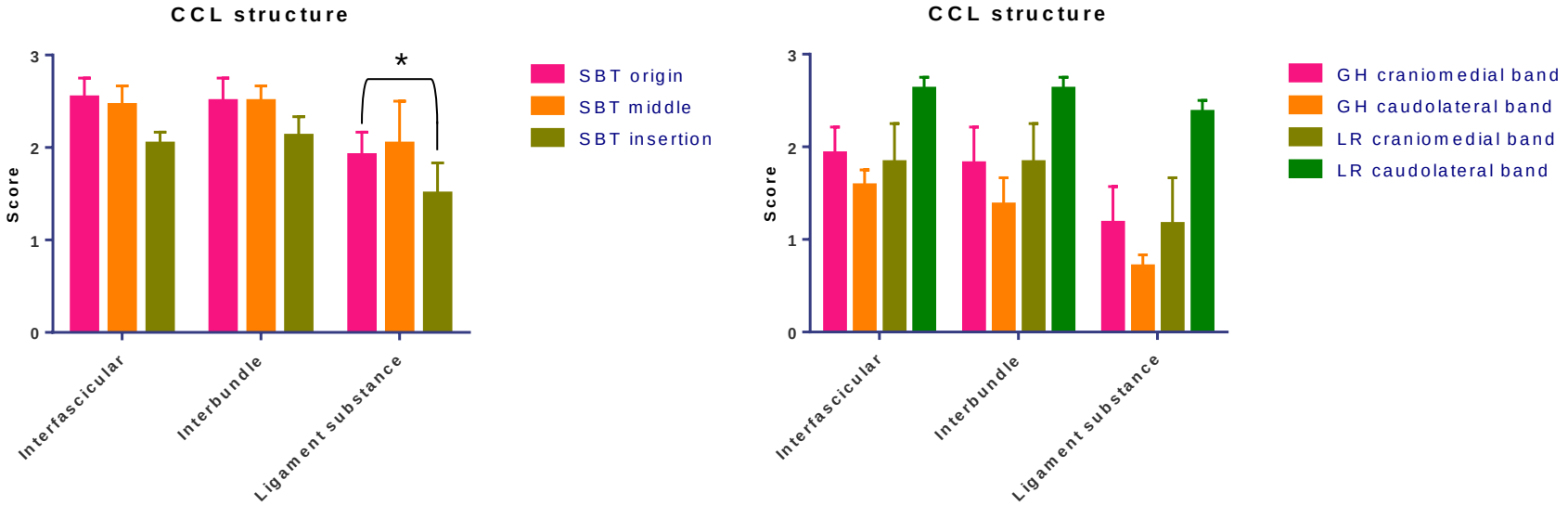

Figure 5-12: The CCL structure scores for Toluidine blue staining in differentially predisposed dog breeds.

Histology results for the CCL structure with Toluidine blue staining in different anatomical regions in Staffordshire bull terrier (A), greyhound (B), and Labrador retriever (B) CCLs. (SBT= Staffordshire bull terrier; GH= greyhound; LR= Labrador retriever). Staffordshire bull terrier CCLs had a significantly higher deposition of Toluidine blue in its ligament substance in the origin anatomical regional compared to the insertion anatomical region (p= 0.02). All dog breeds had Toluidine blue staining in the interfascicular, interbundle, and ligament substance sites.

5.4.2.3.3 **CCL cells**

Our observations showed that the CCLs from all dog breed demonstrated Toluidine blue staining around the cells (pericellular) and within the cell (intracellular). CCLs with rounded cells had the most pericellular and intracellular staining (Figure 5-13). Staffordshire bull terrier had significantly increased Toluidine blue staining within the cells of its origin region compared to its insertion region (p= 0.002). Althought Toluidine blue staining within the cells of the Labrador retriever craniomedial band appeared to be significantly higher than the greyhound craniomedial band, statistical analysis was not applicable due to the low number of the Labrador retriever biological replicates (n= 2). The scoring data chart for the three dog breeds can be observed in Figure 5-14 (A, B).

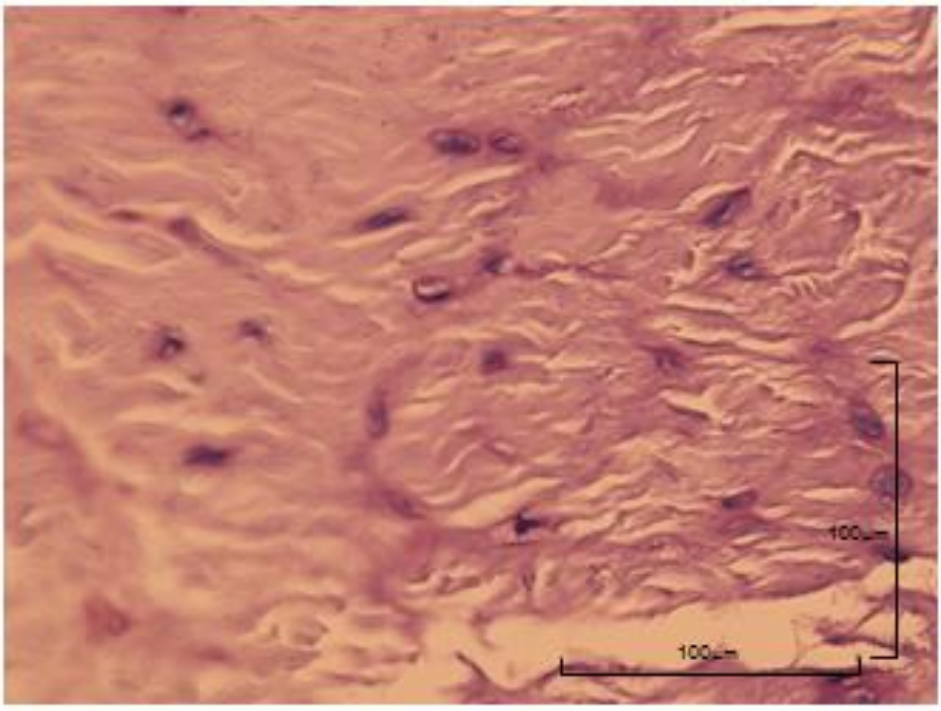

Figure 5-13: Toluidine blue staining in the canine CCL cells.

Toluidine blue staining is shown to be deposited around and within cells. Image obtained from greyhound CCLs (Bar 100µm).

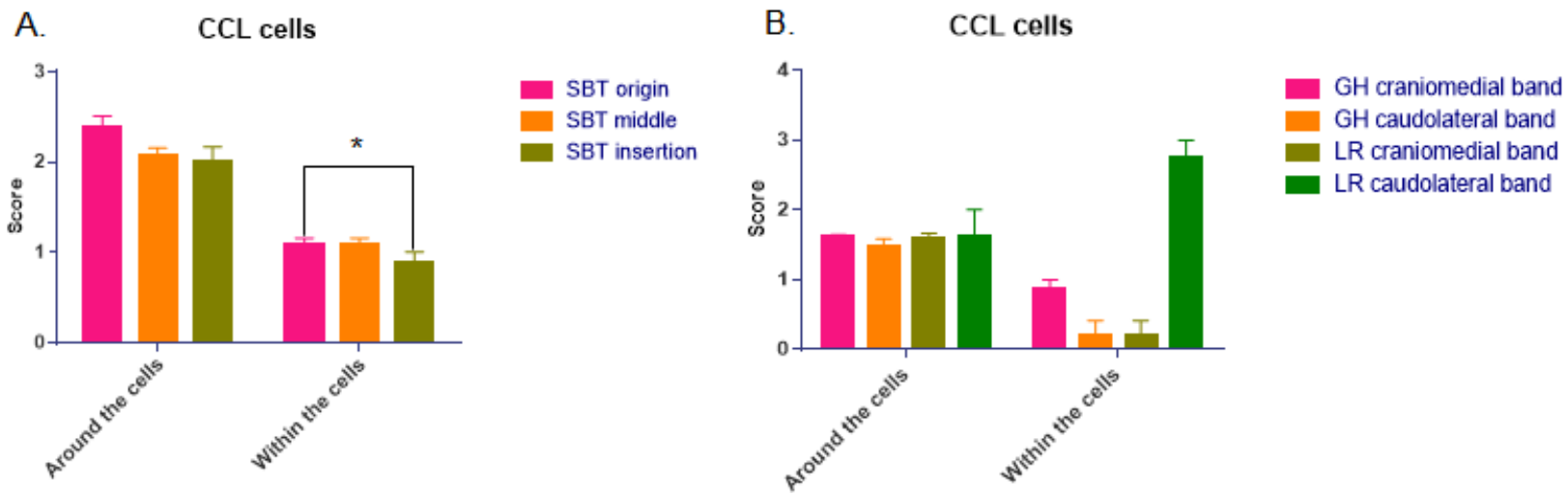

Figure 5-14: Scores for Toluidine blue staining in the CCL cells of differentially predisposed dog breeds.

Histology results for the CCL cells with Toluidine blue staining in different anatomical regions in Staffordshire bull terrier (A), greyhound (B), and Labrador retriever (B) CCLs. (SBT= Staffordshire bull terrier; GH= greyhound; LR= Labrador retriever). Staffordshire bull terrier CCLs had significantly greater Toluidine blue staining within the cell of its origin anatomical region compared to its insertion region (p= 0.002). All dog breeds had Toluidine blue staining within and around the cells.

5.4.2.4 **Alcian blue staining**

Alcian blue is a dye that has been reported to stain sGAGs at pH 2.5, and the blue colour is due to the existence of copper (Lin, Shuster et al. 1997). The significance of Alcian blue/ Eosin Y staining over Toluidine blue is that Eosin Y acts as a counterstain, which allows a clearer distinction of the sGAGs stained by Alcian blue.

5.4.2.4.1 **Overall staining**

Alcian blue staining was observed in all CCL tissues. Alcian blue had a faint or marked staining on the CCLs (Figure 5-15 A, B). Greyhounds had significantly higher marked staining for its craniomedial band compared to its caudolateral band ($p=0.0006$). The scoring data chart for the three dog breeds can be observed in Figure 5-16 (A, B).

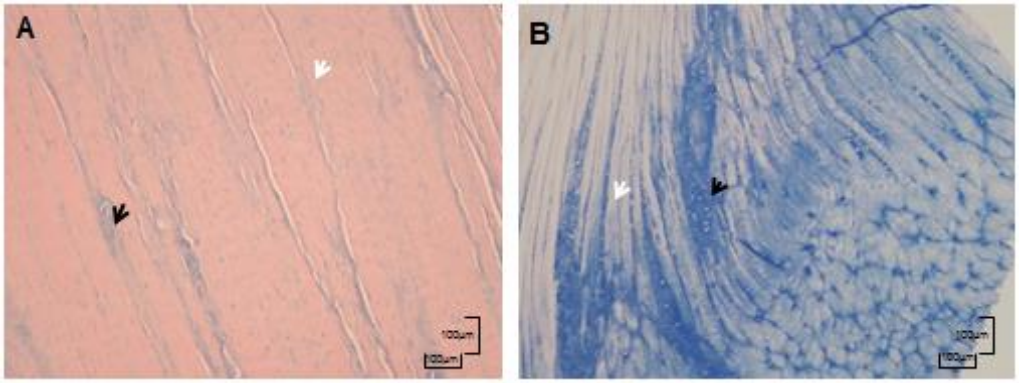

Figure 5-15: The intensity of Alcian blue staining in the canine CCL.

A) Faint staining of collagen bundles (white arrow) and fascicular structure (black arrow). Image obtained from greyhound CCLs. B) Marked staining of collagen bundles (white arrow) and interfascicular regions (black arrow). Image obtained from Staffordshire bull terrier CCLs (Bar 100µm).

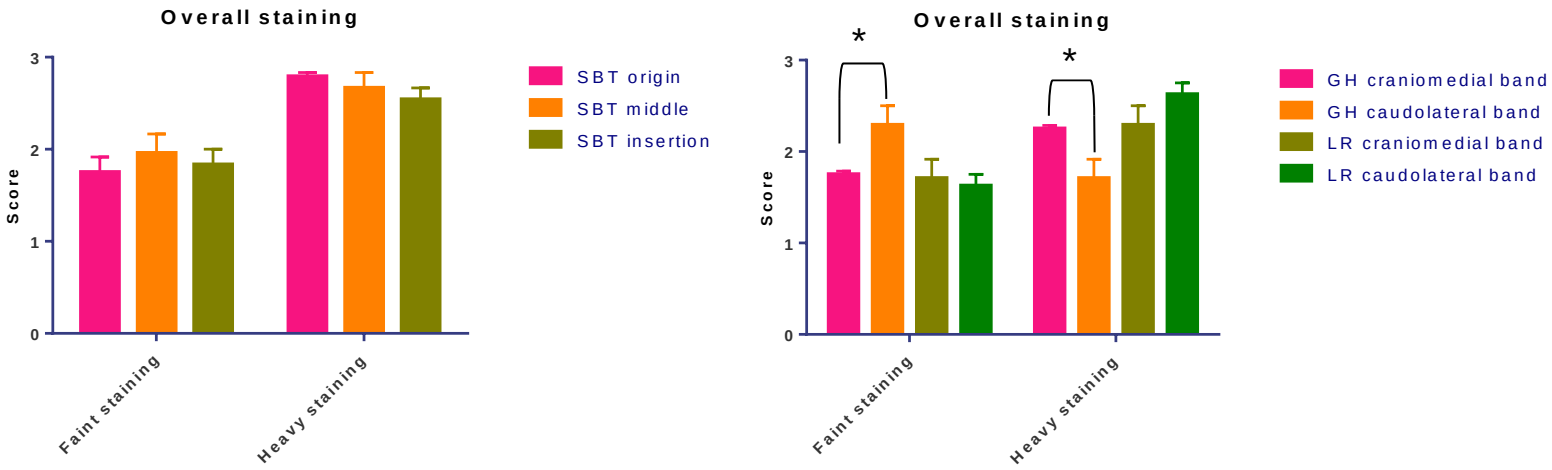

Figure 5-16: The overall staining of Alcian blue scores in differentially predisposed dog breeds.

Histology results for overall staining with Alcian blue in different anatomical regions in Staffordshire bull terrier (A), greyhound (B), and Labrador retriever (B) CCLs. (SBT= Staffordshire bull terrier; GH= greyhound; LR= Labrador retriever). All dog breeds had both faint and heavy staining of Alcian blue. Greyhounds CCLs had a significantly higher marked staining for their craniomedial band compared to their caudolateral band (p=0.0006).

5.4.2.4.2 **CCL structure**

Our observations showed that Alcian blue staining in the CCLs of all dog breeds was deposited in collagen bundles, interfascicular region, and ligament substance (covering collagen bundles) in the CCL. Faint staining was associated with normal collagen structure and spindle shaped cells (Figure 5-17 A), Whilst more intense staining was associated with regions of reduced collagen density with rounded shaped cells (Figure 5-17 B), The greyhounds had a significant increase in ligament substance staining in its craniomedial band anatomical region compared to its caudolateral band (p=0.0389). The scoring data chart for the three dog breeds can be observed in Figure 5-18 (A, B).

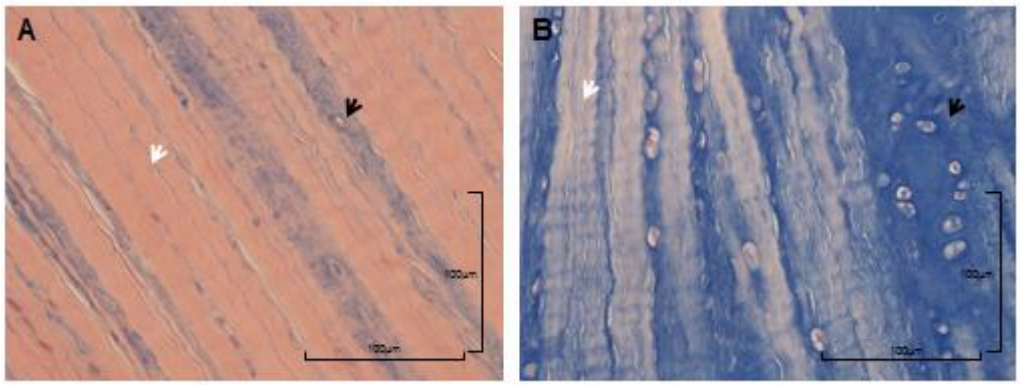

Figure 5-17: Alcian blue staining in the canine CCL structure.

A) Faint staining of collagen bundles (white arrow) and fascicular region (black arrow). Image obtained from Staffordshire bull terrier CCLs. B) Marked staining of collagen fibril bundles (white arrow) and interfascicular regions (black arrow). Image obtained from Staffordshire bull terrier CCLs (Bar 100µm).

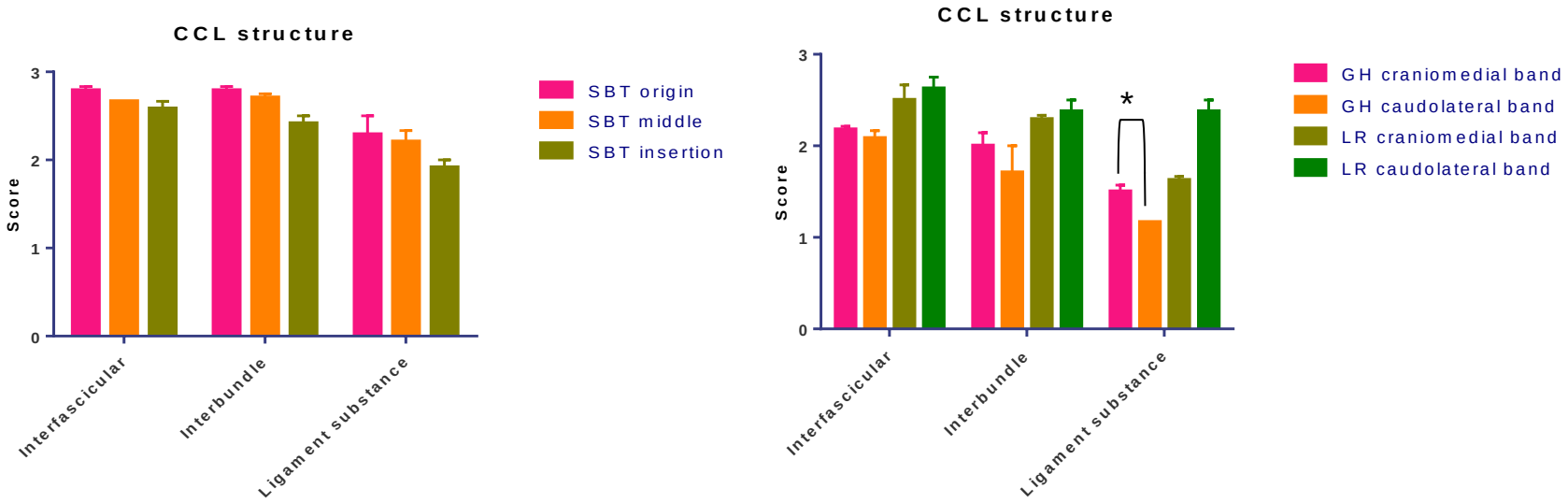

Figure 5-18: The CCL structure scores for Alcian blue staining in differentially predisposed dog breeds.

Histology results for the CCL structure with Alcian blue staining in different anatomical regions in Staffordshire bull terrier (A), greyhound (B), and Labrador retriever (B) CCLs. (SBT= Staffordshire bull terrier; GH= greyhound; LR= Labrador retriever). Greyhounds CCLs had a significant increase in ligament substance staining in their craniomedial band anatomical regions compared to their caudolateral band (p=0.0389).

5.4.2.4.3 **CCL cells**

Our observations showed that the CCLs from all dog breed had Alcian blue staining around the cells (pericellular) and within the cell (intracellular). CCLs with rounded cells had the most pericellular and intracellular staining (Figure 5-19). The scoring data chart for the three dog breeds can be observed in Figure 5-20 (A, B). There were no statistically significant differences between anatomical regions of the CCL or between different dogs with a differing predisposition to CCLD/ R.

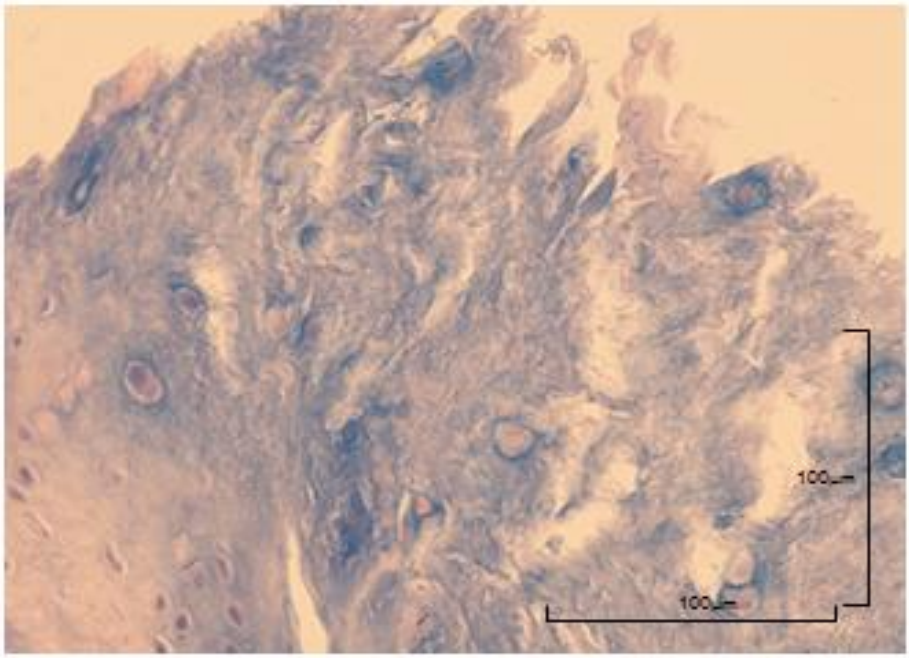

Figure 5-19: Alcian blue staining in the canine CCL cells.

Alcian blue staining is shown to be deposited around and within cells. Image obtained from greyhound CCLs (Bar 100µm).

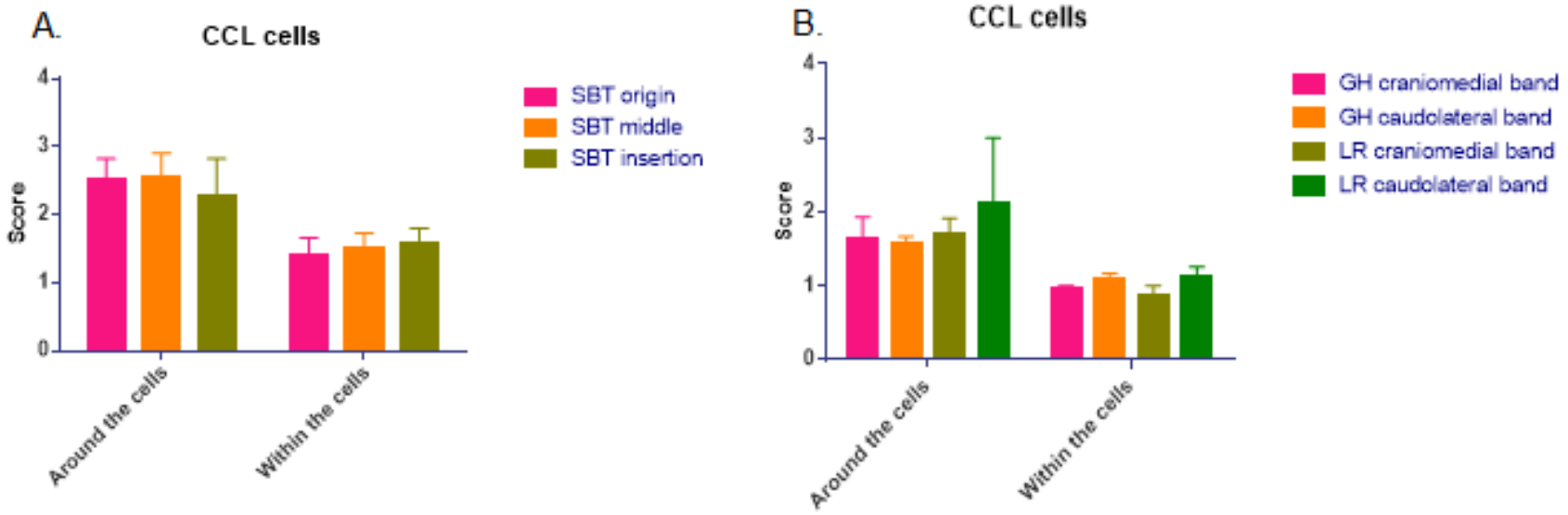

Figure 5-20: Alcian blue staining in the CCL cells in differentially predisposed dog breeds.

Histology results for CCL cells with Alcian blue staining in different anatomical regions in Staffordshire bull terrier (A), greyhound (B), and Labrador retriever (B) CCLs. (SBT= Staffordshire bull terrier; GH= greyhound; LR= Labrador retriever). All dog breeds had Alcian blue staining within and around the cells.

Table 5-2: Histology scoring results for Staffordshire bull terrier.

Results are displayed for H & E, Alcian blue, and Toluidine blue staining (mean ± SEM), n= 6 for all anatomical regions. (H&E= Haematoxylin and Eosin; TB= Toluidine blue; AB= Alcian blue; SBT= Staffordshire bull terrier). * indicates a significant difference at $p < 0.05$.

Stain		SBT origin	SBT middle	SBT insertion
H & E	Normal collagen architecture	2.25±0.25	2.33±0.08	2.50±0.08
	Reduced collagen architecture	2.42±0.08	2.29±0.13	2.33±0.00
	Abnormal collagen architecture	0.13±0.04	0.21±0.04	0.33±0.00
	Spindle cells	1.38±0.04	1.50±0.08	1.67±0.17
	Mixed cells	2.83±0.08	2.88±0.04	2.92±0.00
	Rounded cells	2.46±0.21	2.25±0.25	2.42±0.25
	Normal distribution of cells	2.50±0.08	2.88±0.13	2.79±0.04
	Formation of cell chains	1.92±0.00	2.04±0.04	1.58±0.17
	Hypovascularised	0.50±0.13	2.88±0.00	3.00±0.04
	Hypervascularised	2.96±0.04	0.63±0.04	1.29±0.08
	No inflammation	3.00±0.00	3.00±0.00	2.75±0.25
	Evidence of inflammatory cells	0.13±0.04	0.13±0.04	0.13±0.04
TB	Faint staining	2.13±0.04	2.25±0.08	2.13±0.13
	Heavy staining	2.58±0.08	2.38±0.13	2.21±0.21
	Interfascicular	2.54±0.21	2.46±0.21	2.04±0.13
	Interbundle	2.50±0.25	2.50±0.17	2.13±0.21
	Ligament substance*	1.92±0.25	2.04±0.46	1.50±0.33
	Around the cells	2.38±0.13	2.08±0.08	2.00±0.17
	Within the cells*	1.08±0.08	1.08±0.08	0.88±0.13
AB	Faint staining	1.75±0.17	1.96±0.21	1.83±0.17
	Heavy staining	2.79±0.04	2.67±0.17	2.54±0.13
	Interfascicular	2.79±0.04	2.67±0.00	2.58±0.08
	Interbundle	2.79±0.04	2.71±0.04	2.42±0.08
	Ligament substance	2.29±0.21	2.21±0.13	1.92±0.08
	Around the cells	2.50±0.33	2.54±0.37	2.29±0.54
	Within the cells	1.42±0.25	1.50±0.23	1.58±0.22

Table 5-3: Histology scoring results for greyhound and Labrador retriever.

Results are displayed for H & E, Alcian blue, and Toluidine blue staining (mean ± SEM). The number of donors for each breed and anatomical region are; GH CMB (n= 7); GH CLB (n= 6); LR CMB (n= 6); and LR CLB (n= 2). (H&E= Haematoxylin and Eosin; TB= Toluidine blue; AB= Alcian blue; GH= greyhound; LR= Labrador retriever; CMB= craniomedial band; CLB= caudolateral band). * indicates a significant difference at $p < 0.05$.

Stain		GH CMB	GH CLB	LR CMB	LR CLB
H & E	Normal collagen architecture	2.32±0.11	2.88 ±0.04	1.50±0.00	0.63±0.13
	Reduced collagen architecture	1.46±0.04	1.29±0.04	2.08±0.17	2.08±0.38
	Abnormal collagen architecture	0.21±0.07	0.00±0.00	1.13±0.13	1.25±0.13
	Spindle cells	1.50±0.00	1.71±0.13	1.25±0.08	1.00±0.00
	Mixed cells	2.61±0.04	2.67±0.00	2.46±0.13	2.25±0.25
	Rounded cells	1.89±0.04	1.67±0.17	2.29±0.04	2.75±0.25
	Normal distribution of cells	2.54±0.04	2.75±0.00	2.96±0.04	2.00±0.00
	Formation of cell chains	1.43±0.00	1.25±0.00	1.04±0.04	1.13±0.13
	Hypovascularised	2.64±0.07	2.63±0.04	2.92±0.00	3.00±0.00
	Hypervascularised	0.71±0.00	1.04±0.04	0.00±0.00	0.38±0.13
	No inflammation	2.93±0.07	2.96±0.04	3.00±0.00	3.00±0.00
	Evidence of inflammatory cells	0.00±0.00	0.00±0.00	0.00±0.00	0.00±0.00
TB	Faint staining	2.04±0.18*	2.63±0.04*	1.96±0.21	1.38±0.13
	Heavy staining	1.96±0.18*	1.38±0.04*	1.96±0.13	2.63±0.13
	Interfascicular	1.93±0.29	1.58±0.17	1.83±0.42	2.63±0.13
	Interbundle	1.82±0.39	1.38±0.29	1.83±0.42	2.63±0.13
	Ligament substance	1.18±0.39*	0.71±0.13*	1.17±0.50	2.38±0.13
	Around the cells	1.61±0.04	1.46±0.13	1.58±0.08	1.63±0.38
	Within the cells	0.86±0.14	0.21±0.21	0.21±0.21	2.75±0.25
AB	Faint staining	1.75±0.04	2.29±0.21	1.71±0.21	1.63±0.13
	Heavy staining	2.25±0.04	1.71±0.21	2.29±0.21	2.63±0.13
	Interfascicular	2.18±0.04	2.08±0.08	2.50±0.17	2.63±0.13
	Interbundle	2.00±0.14	1.71±0.29	2.29±0.04	2.38±0.13
	Ligament substance	1.50±0.07	2.32±0.00	1.63±0.04	2.38±0.13
	Around the cells	1.64±0.29	1.58±0.08	1.71±0.21	2.13±0.88
	Within the cells	0.96±0.04	1.08±0.08	0.88±0.13	1.13±0.13

5.4.3 Immunolocalisation of proteoglycans and their distribution in the CCL tissue

5.4.3.1 Negative controls

Negative controls were included for every antibody immunostaining. Primary antibodies used were raised either in rabbit or mouse. No immunostaining was detected with negative controls using non-specific rabbit IgG or mouse IgG and IgM immunoglubulins or in the absence of primary antibodies (Figures 5-21, 5-22, and 5-23).

5.4.3.2 Large aggregating proteoglycans (aggrecan and versican)

In different anatomical regions of the Staffordshire CCLs

Aggrecan immunostaining was found in the interfascicular regions and collagen bundles in all anatomical regions. In addition, aggrecan was increased in fibrocartilaginous regions and was shown to localise within the fibrocartilaginous cells (rounded nuclei with halo formation) cells (intracellular), (Figure 5-24, A-C). Aggrecan mainly stained the fibrocartilaginous cells (rounded nuclei with halo formation) intracellularly compared to spindled shaped nuclei (Figure 5-25, A, B). Versican was mainly located in the interfascicular regions rather than the collagen bundles (Figure 5-26, A-C).

In CMB of greyhound CCLs

Aggrecan had a faint staining for the interfascicular regions and collagen bundles. In addition, aggrecan in greyhounds were rarely seen localised in the fibrocartilaginous cells intracellularly (Figure 5-34, A). Versican in all donors was mainly located in the interfascicluar regions and to a lesser extent in collagen bundles (Figure 5-34, B).

5.4.3.3 **Chondroitin sulphate proteoglycans (decorin and biglycan)**

In different anatomical regions of the Staffordshire CCLs

Decorin stained fascicular regions and collagen bundles which covered the ligament substance (Figure 5-27, A-C), whilst biglycan had less staining for collagen bundles (Figure 5-28, D-F). However, biglycan showed increased staining in the fibrocartilaginous regions and showed positive staining for fibrocartilaginous cells intracellularly compared to spindle shaped nuclei (Figure 5-29, A, B).

In CMB of greyhound CCLs

Decorin mainly stained the interfascicular region and collagen bundles covering the ligament substance (Figure 5-35, A). Biglycan faintly stained the collagen bundles, and also rarely stained the fibrocartilaginous cells intracellularly (Figure 5-35, B).

5.4.3.4 **Keratan sulphate proteoglycans (lumican, fibromodulin, keratocan)**

In different anatomical regions of the Staffordshire CCLs

Lumican (Figure 5-30, A-C) and fibromodulin (Figure 5-31, A-C) mainly stained the collagen bundles rather than the interfascicular regions. In addition, fibromodulin additionally was found to surround the fibrocartilaginous cells, and stained some cells pericellularly and intracellularly (Figure 5-32, A, B). Keratocan also stained the collagen bundles rather than the fascicular regions. (Figure 5-33, A-C).

In CMB of greyhound CCLs

Lumican, fibromodulin, and keratocan mainly stained the collagen bundles, and to a lesser degree stained the interfascicular regions. (Figure 5-36 A, B, and C).

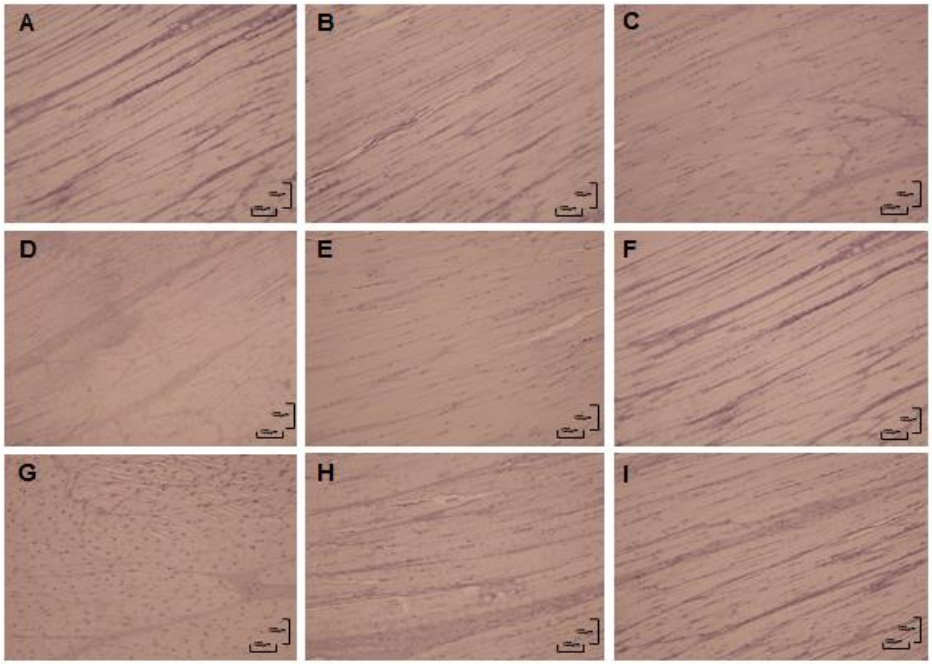

Figure 5-21: Representative immunostaining pictures of negative controls In Staffordshire bull terrier CCLs obtained by omitting the addition of the primary antibody.

(A) Origin part stained with secondary goat-anti mouse IgG. (B) Middle part stained with secondary goat-anti mouse IgG. (C) Insertion part stained with secondary goat-anti mouse IgG. (D) Origin part stained with secondary goat-anti mouse IgM. (E) Middle part stained with secondary goat-anti mouse IgM. (F) Insertion part stained with secondary goat-anti mouse IgM. (G) Origin part stained with secondary goat-anti rabbit IgG. (H) Middle part stained with secondary goat-anti rabbit IgG. (I) Insertion part stained with secondary goat-anti rabbit IgG (Bar 100μm).

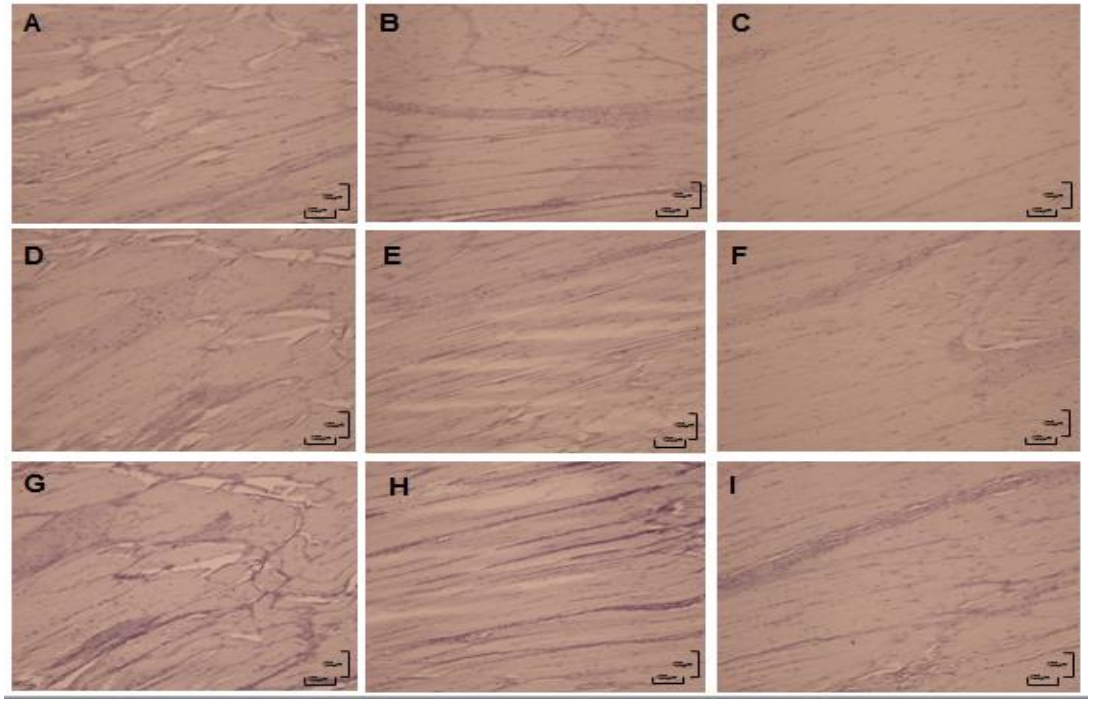

Figure 5-22: Representative immunostaining pictures of negative controls In Staffordshire bull terrier CCLs by substituting the primary antibody with immunoglobulins.

(A) Origin part stained with mouse IgG. (B) Middle part stained with mouse IgG. (C) Insertion part stained with mouse IgG. (D) Origin part stained with mouse IgM. (E) Middle part stained with mouse IgM. (F) Insertion part stained with mouse IgM. (G) Origin part stained with rabbit IgG. (H) Middle part stained with rabbit IgG. (I) Insertion part stained with rabbit IgG (Bar 100μm).

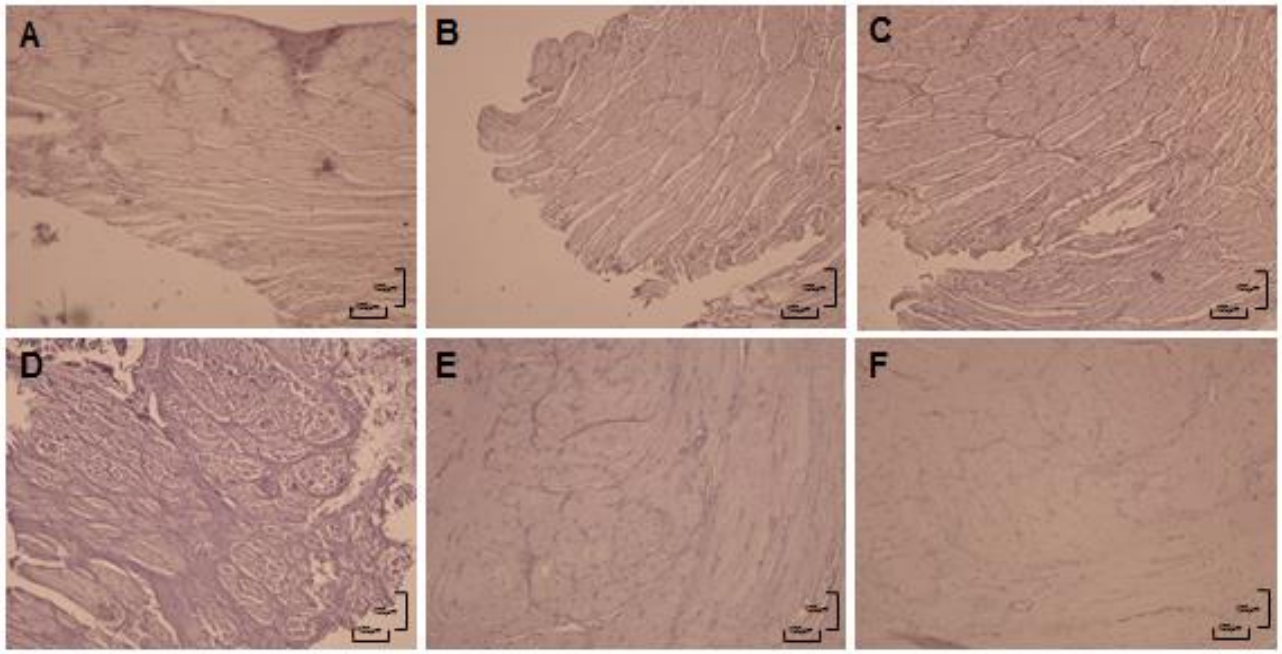

Figure 5-23: Representative immunostaining pictures of negative controls in greyhound CCLs by substituting the primary antibody with immunoglobulins or by omitting the addition of primary antibody.

(A) Craniomedial band stained with secondary goat-anti mouse IgG. (B) Craniomedial stained band with secondary goat-anti mouse IgM. (C). craniomedial band stained with secondary goat-anti rabbit IgG. (D) Craniomedial band stained with mouse IgG. (E) Craniomedial band stained with mouse IgM. (F) Craniomedial band stained with rabbit IgG (Bar 100μm).

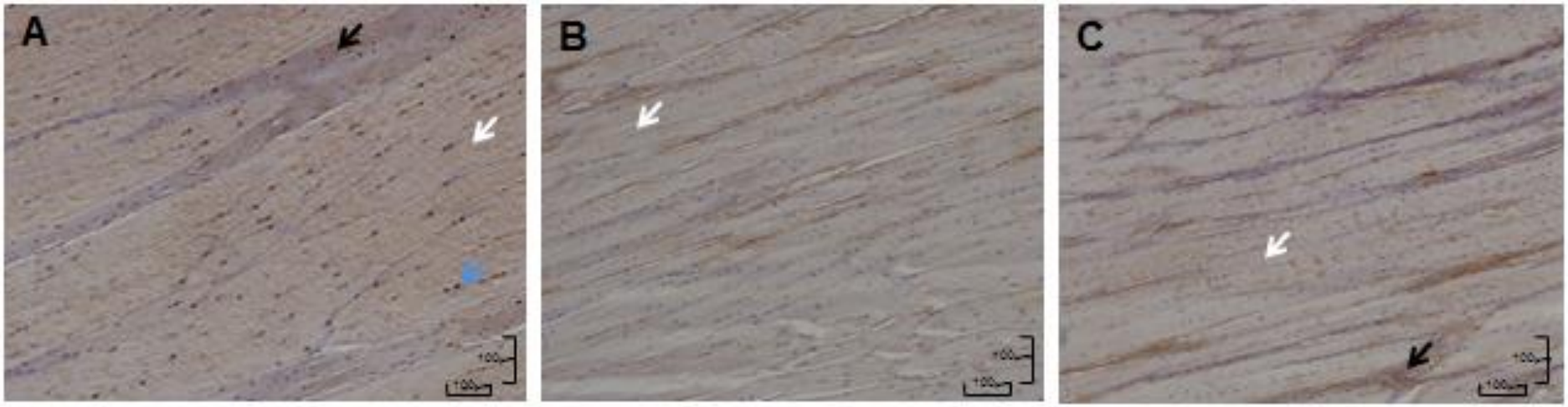

Figure 5-24: Representative immunostaining of aggrecan in different anatomical regions of the Staffordshire bull terrier CCL.

(A) Aggrecan at origin site. (B) Aggrecan at middle site. (C) Aggrecan at insertion site. Aggrecan was shown to stain the fibrocartilaginous cells intracellularly (blue arrow), interfascicular region (black arrow), and collagen bundles (white arrow) (Bar 100μm).

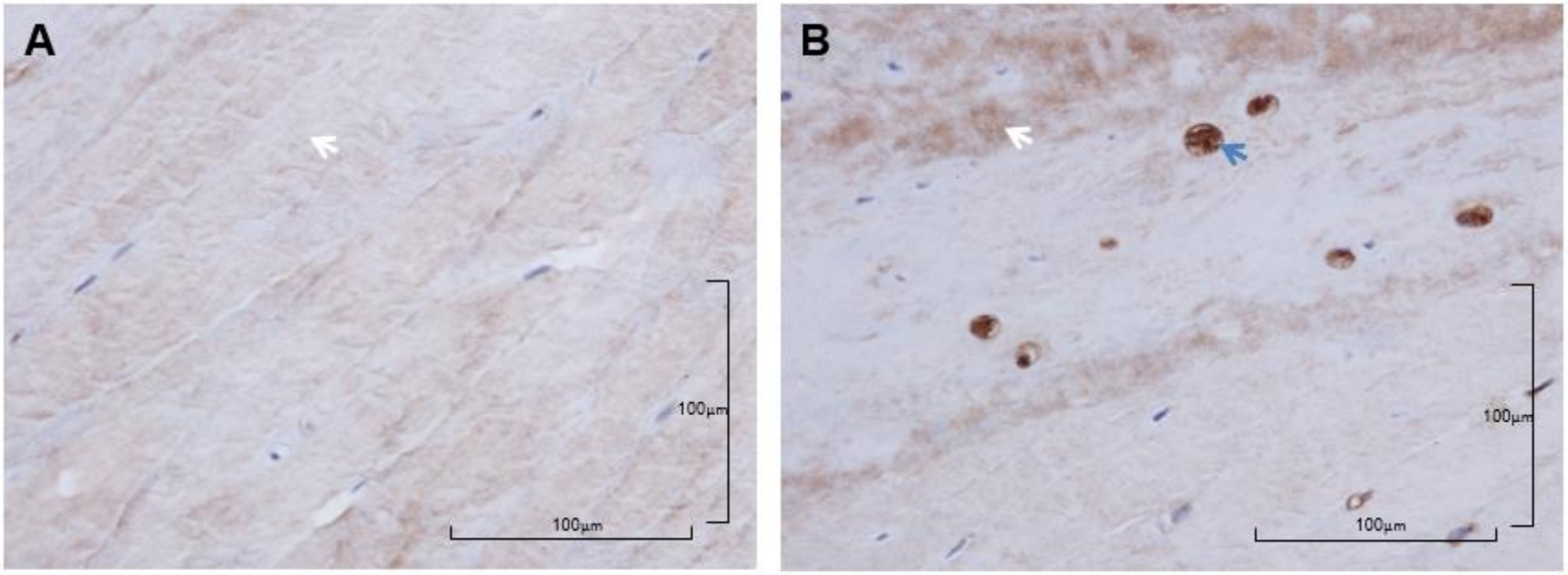

Figure 5-25: Representative immunostaining of aggrecan in the Staffordshire bull terrier CCL.

(A) Aggrecan shows little or no staining for spindle shaped nuclei as it mainly stained the collagen bundles (white arrow). (B) Aggrecan shows staining for the collagen bundles (white arrow) and intracellular staining for the fibrocartilaginous cells (blue arrow) (Bar 100µm).

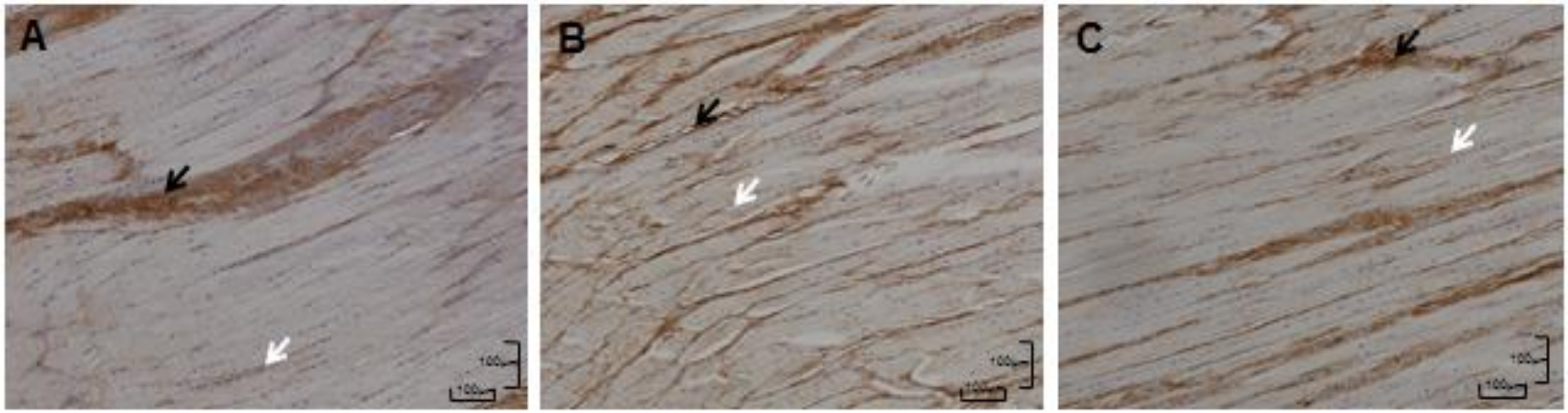

Figure 5-26: Representative immunostaining of versican in different anatomical regions of the Staffordshire bull terrier CCL.

(A) Versican at origin site. (B) Versican at middle site. (C) Versican at insertion site. Versican was mainly present in the interfascicular region (black arrow) and to a lesser extent in collagen bundles (white arrow) (Bar 100μm).

Figure 5-27: Representative immunostaining of decorin in different anatomical regions of the Staffordshire bull terrier CCL.

(A) Decorin at origin site. (B) Decorin at middle site. (C) Decorin at insertion site. Decorin staining was found over collagen bundles (white arrow) covering the ligament substance, and in the interfascicular region (black arrow) (Bar 100μm).

Figure 5-28: Representative immunostaining of biglycan in different anatomical regions of the Staffordshire bull terrier CCL.

(A) Biglycan at origin site. (B) Biglycan at middle site. (C) Biglycan at insertion site. Biglycan shows faint staining over collagen bundles (white arrow) and in the interfascicular region (black arrow) (Bar 100µm).

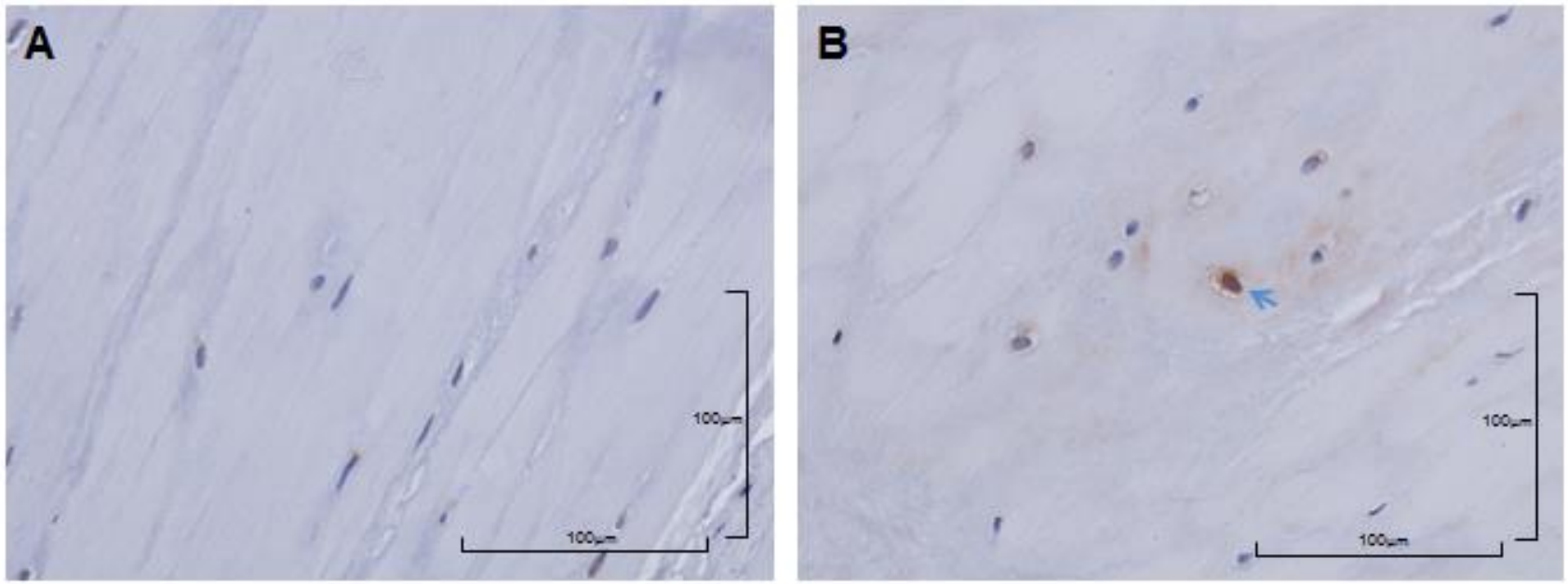

Figure 5-29: Representative immunostaining of biglycan in the Staffordshire bull terrier CCL.

(A) Biglycan shows no staining of spindle shaped nuclei. (B) Biglycan shows intracellular staining for the fibrocartilaginous cells (blue arrow) (Bar 100µm).

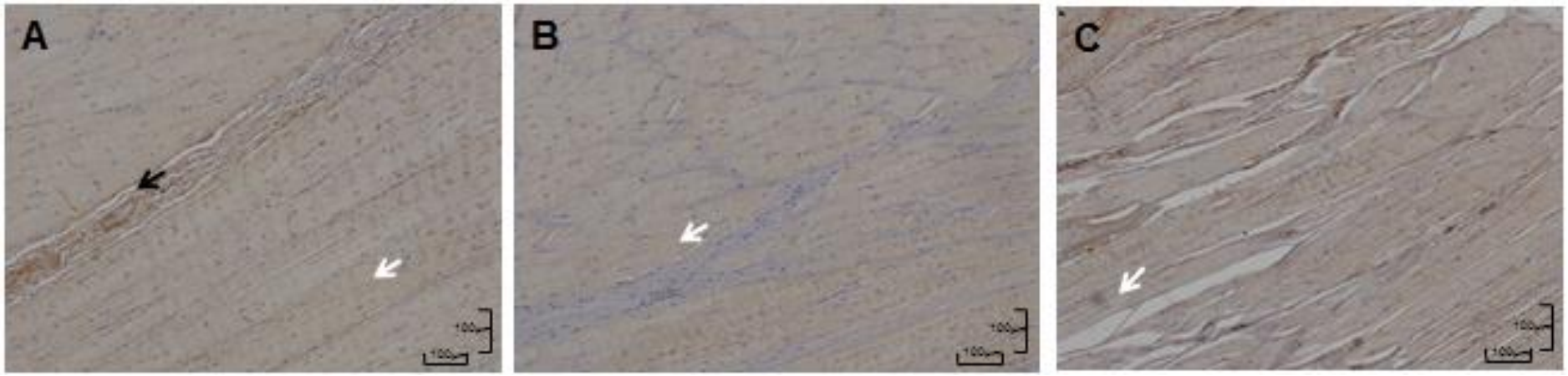

Figure 5-30: Representative immunostaining of lumican in different anatomical regions of the Staffordshire bull terrier CCL.

(A) Lumican at origin site. (B) Lumican at middle site. (C) Lumican at insertion site. Lumican staining was mostly observed over the collagen bundles (white arrow), and showed some staining for the interfascicular region (black arrow) (Bar 100μm).

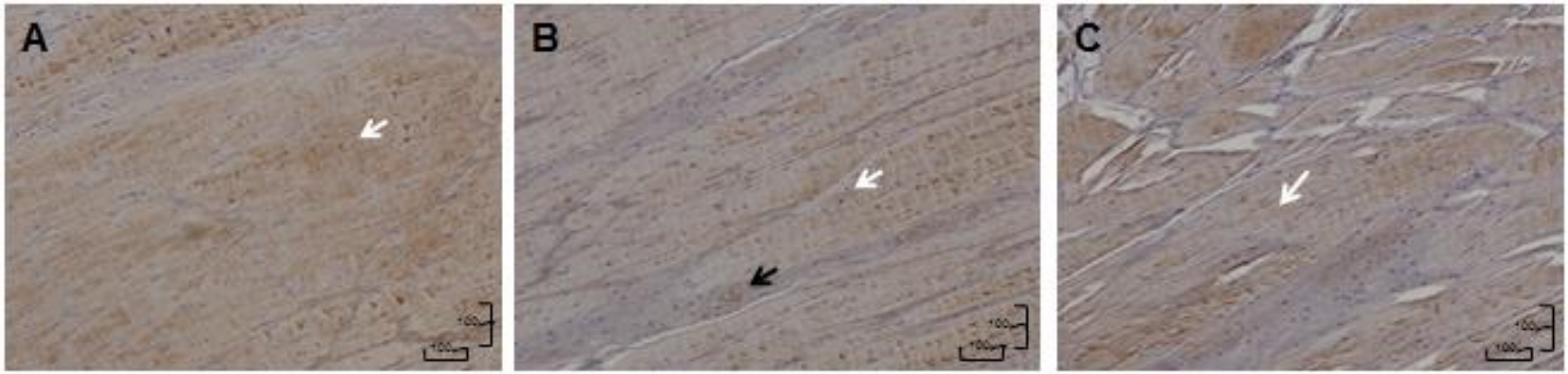

Figure 5-31: Representative immunostaining of fibromodulin in different anatomical regions of the Staffordshire bull terrier CCL.

(A) Fibromodulin at origin site. (B) Fibromodulin at middle site. (C) Fibromodulin at insertion site. Fibromodulin staining was mostly present over the collagen bundles (white arrow), and showed minor staining in the interfascicular region (black arrow) (Bar 100μm).

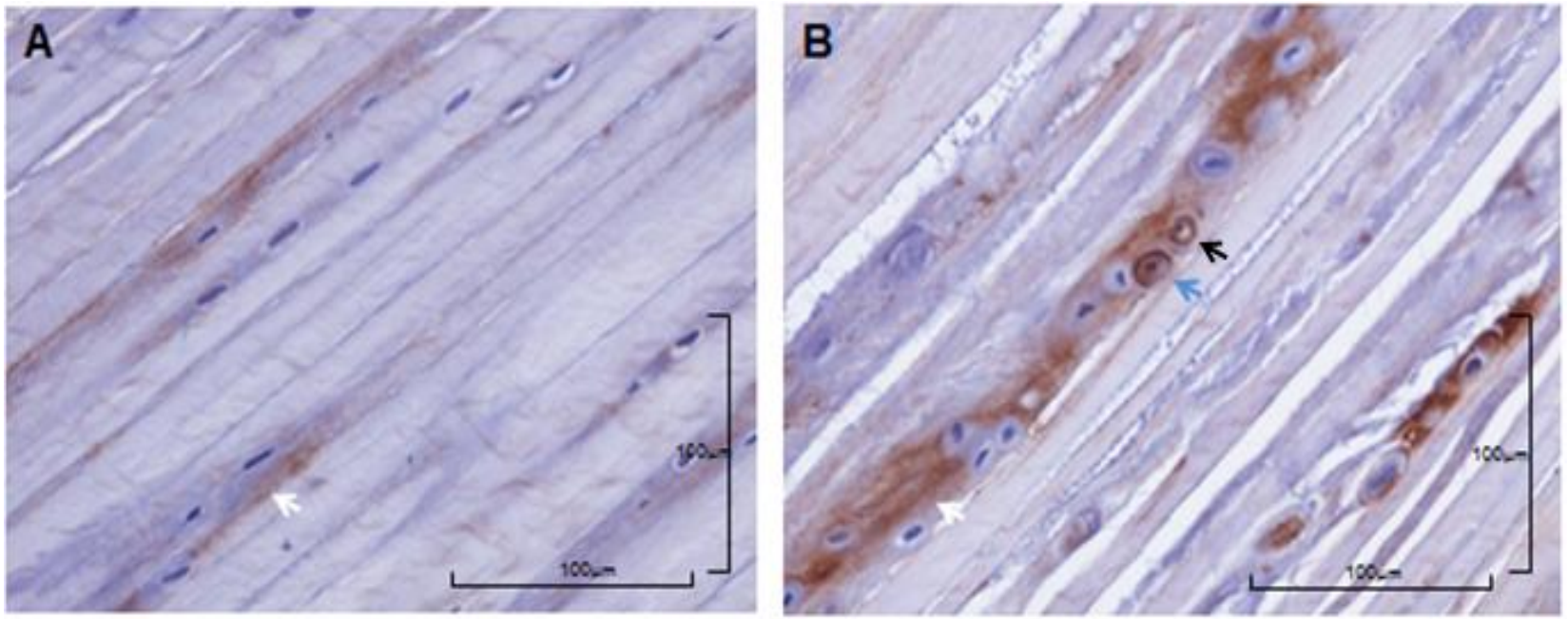

Figure 5-32: Representative immunostaining of fibromodulin in the Staffordshire bull terrier CCL.

(A) Fibromodulin staining is present over the collagen bundles (white arrow) shows no positive staining for the spindle shaped nucleus. (B) Fibromodulin stained the collagen bundles and surrounded a group of fibrocartilaginous cells (white arrow), and stained some of the fibrocartilaginous cells pericellularly (black arrow) and intracellularly (blue arrow) (Bar 100µm).

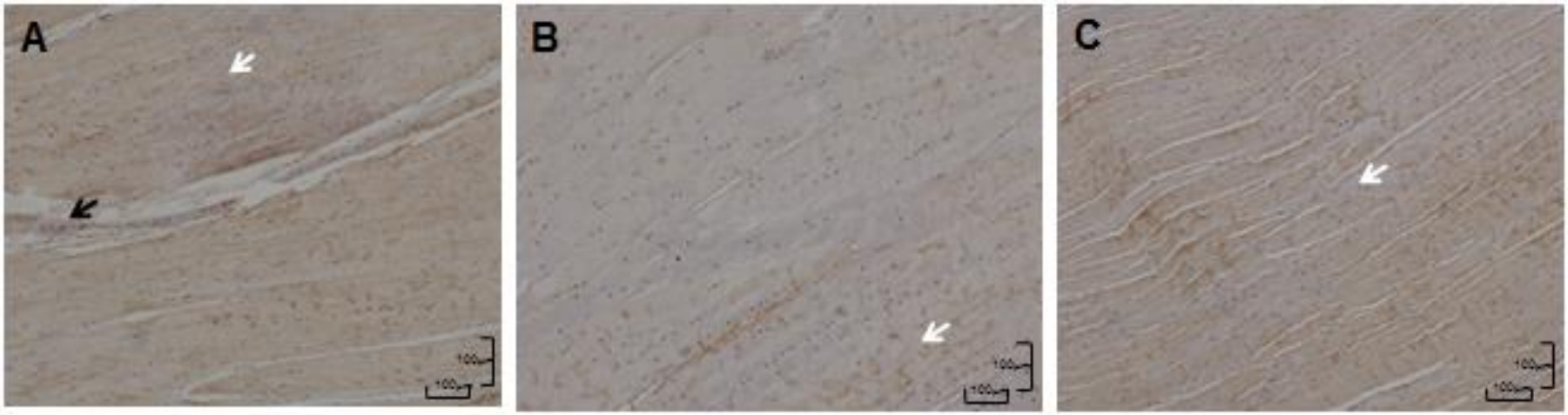

Figure 5-33: Representative immunostaining of keratocan in different anatomical regions of the Staffordshire bull terrier CCL.

(A) Keratocan at origin site. (B) Keratocan at middle site. (C) Keratocan at insertion site. Keratocan staining was mostly present over the collagen bundles (white arrow), and showed minor staining for the interfascicular region (black arrow) (Bar 100μm).

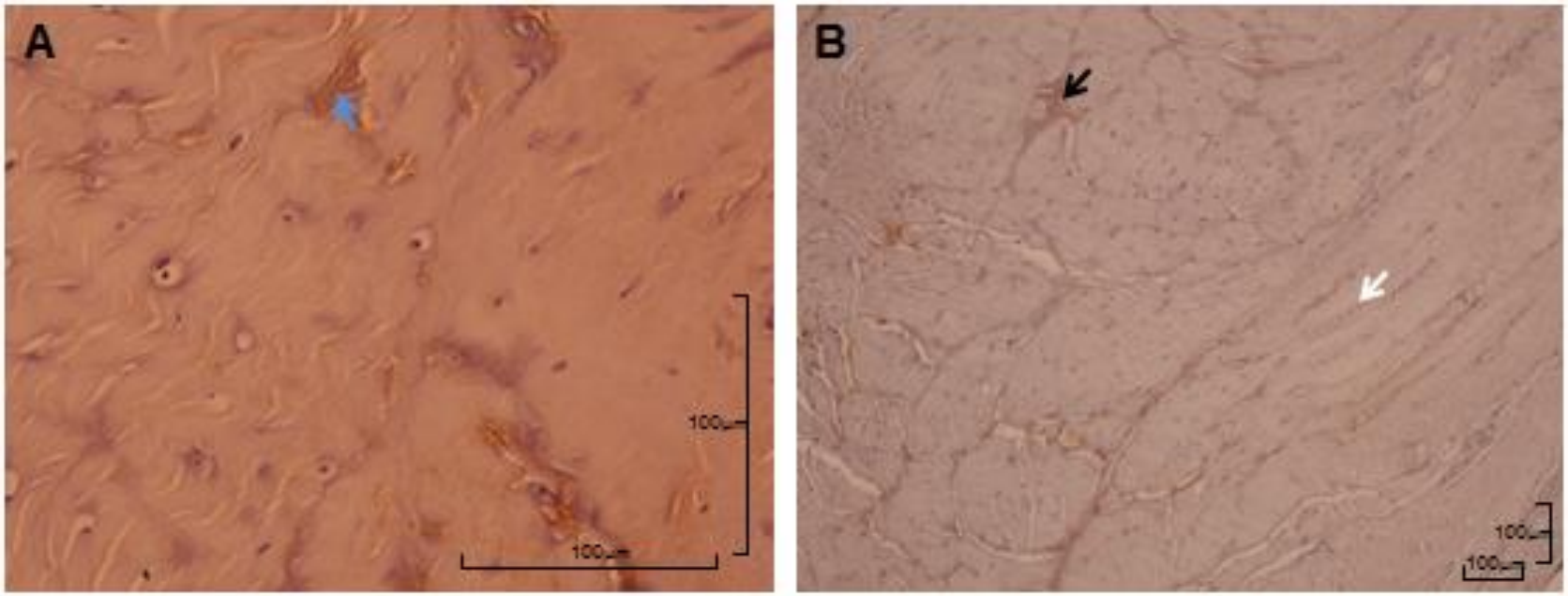

Figure 5-34: Representative immunostaining of large aggregating proteoglycans (aggrecan and versican) in the craniomedial band anatomical region of the greyhound CCL.

(A) Aggrecan. (B) Versican. Aggrecan staining was present over some rounded (fibrocartilaginous) cells intracellularly (blue arrow), and versican staining was present over the interfascicular region (black arrow) and to a lesser extent the collagen bundles (white arrow) (Bar 100µm).

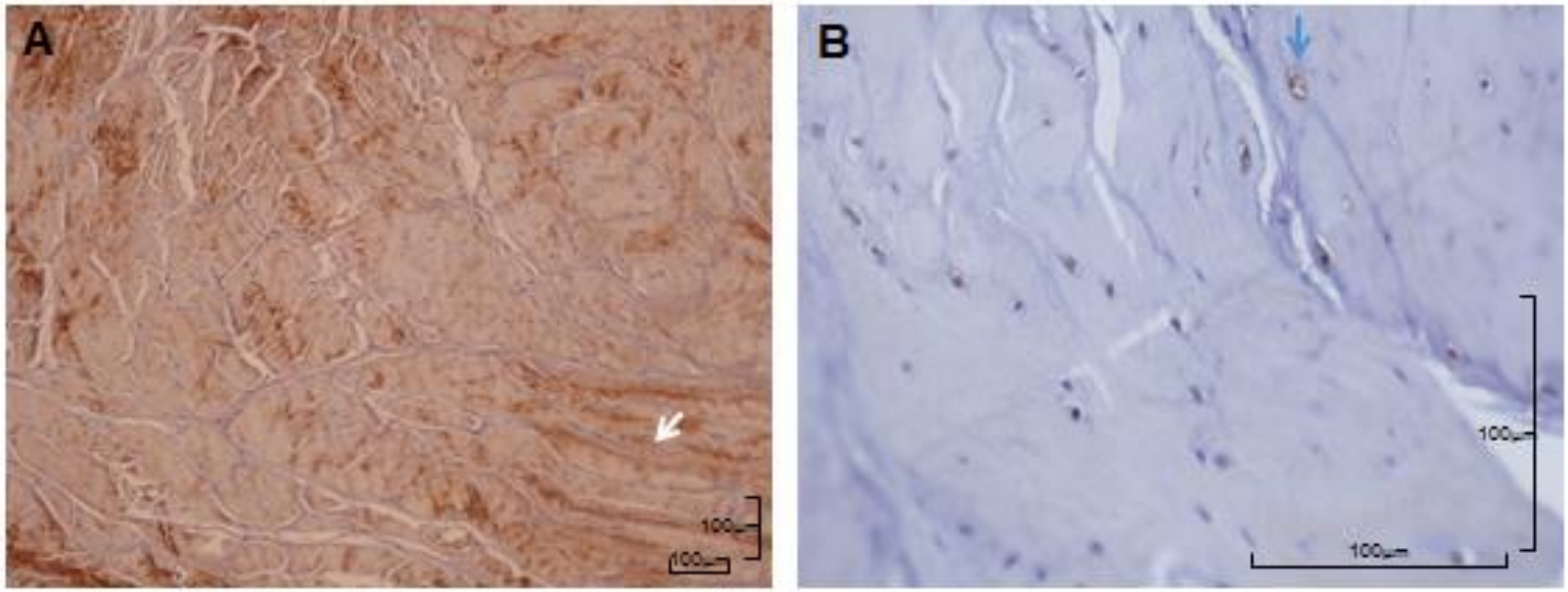

Figure 5-35: Representative immunostaining of chondroitin/ dermatan sulphate proteoglycans (decorin and biglycan) in the craniomedial band anatomical region of the greyhound CCL.

(A) Decorin. (B) Biglycan. Decorin staining was present over collagen bundles (white arrow) covering the ligament substance, and biglycan stained some of the fibrocartilaginous cells intracellularly (blue arrow) (Bar 100µm).

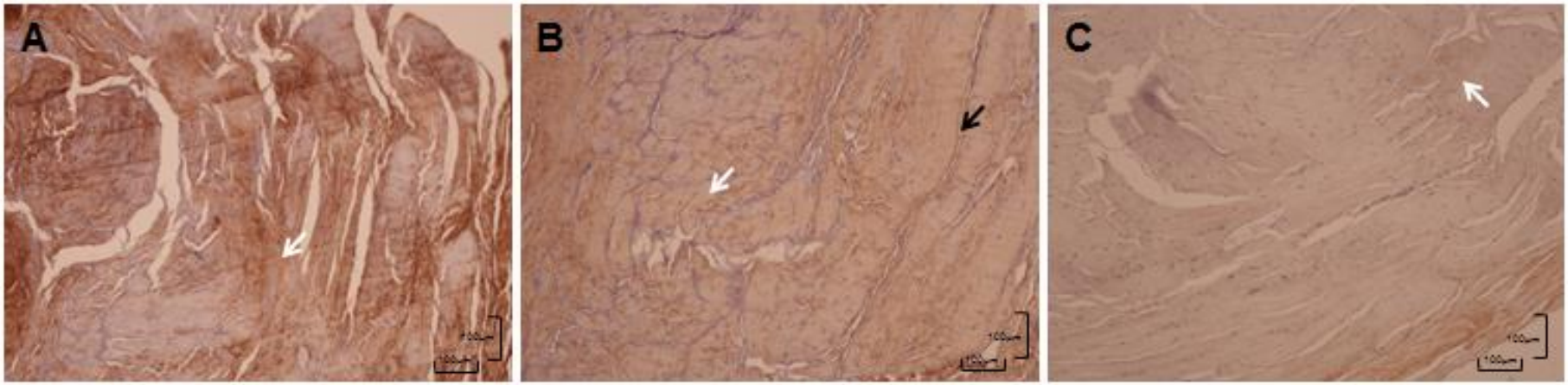

Figure 5-36: Representative immunostaining of keratan sulphate proteoglycans (lumican, fibromodulin, and keratocan) in the craniomedial band anatomical region of the greyhound CCL.

(A) Lumican. (B) Fibromodulin. (C) Keratocan. Fibromodulin, lumican, and keratocan showed staining was mainly present over the collagen bundles (white arrow), and to a lesser extent the interfascicular region (black arrow shown for fibromodulin only) (Bar 100μm).

5.5 **Discussion**

In this Chapter, we have characterised the morphological structure of the CCL and sGAG content histologically by performing semi-objective histology scoring in different anatomical regions of three dog breeds with a differing predisposition to CCLD/ R. We have found increased sGAGs in areas with reduced collagen architecture and rounding of cells, thus displaying areas of fibrocartilage in the CCL.

Immunohistochemistry was performed to characterise proteoglycans and their distribution in the greyhound CCL (low risk to CCLD/ R) and in different anatomical regions of the Staffordshire bull terrier CCL (moderate-high risk to CCLD/ R). Interestingly, each proteoglycan had a unique distribution across the CCL.

5.5.1 **Histology of canine CCLs**

Staining with H&E showed that all dog breed CCLs mainly had a normal and reduced architecture of collagen fibrils. The normal collagen architecture had a parallel and helical arrangement of collagen fibrils (Yahia and Drouin 1989; Zhu, Zhang et al. 2009), whilst the reduced collagen architecture had a homogenous structure of collagen fibrils with loss of some collagen bundles (Narama, Masuoka-Nishiyama et al. 1996; Zhu, Zhang et al. 2009). Abnormal collagen architecture had a disorganised collagen matrix with areas of cell loss (Vasseur, Pool et al.1985). Furthermore, normal collagen fibrils were associated with spindle shaped nuclei, whereas regions with reduced collagen architecture had a mixture of spindle and rounded nuclei, and this agrees with previous studies performed in beagle (Narama, Masuoka-Nishiyama et al. 1996), greyhound, and Labrador retriever CCLs (Comerford, Tarlton et al. 2006b). Overall, all dog breed has a low number of blood vessles, which agrees with a previous that showed that the normal intact canine CCL is hypovascular in nature (Hayashi, Bhandal et al. 2011) Immunohistochemical techniques with antibodies such as factor VIII (for endothelial cell) and laminin (for basement membrane) may be used to detect blood vessels.

We also observed increased degrees of Toluidine blue and Alcian blue staining (two dyes that stain sGAGs) in areas of fibrocartilage in the CCL (Figure 5-11, B and 5-17, B). Areas of fibrocartilage have been shown in the CCL of dogs over 5 years with a body weight of >15 kg, suggesting it to be a degenerative outcome for older dogs prior CCLD/ R (Vasseur, Pool et al. 1985). In addition, fibrocartilage and increased Alcian blue staining has been observed in the CCL of young beagles bred

for laboratory use speculated by the authors to be a degenerative sign due to lack of exercise (Narama, Masuoka-Nishiyama et al. 1996).

However, other aurthors have suggested that the formation of fibrocartilage in the CCL is an adaptive response to compressive loads, and not a sign of degeneration (Comerford, Tarlton et al. 2006b; Zhu, Zhang et al. 2012). This suggestion was also supported studies in tendon (Vogel, Ordog et al. 1993; Benjamin and Ralphs 1998; Vogel 2004).

Comerford and others found fibrocartilage with increased Alcian blue staining to occur in the ex-racing greyhound CCL (low risk to CCLD/ R) and in the Labrador retriever (high risk to CCLD/ R) CCL (Comerford, Tarlton et al. 2006b). Increased evidence of fibrocartilage was demonstrated not to be a degenerative sign in CCLs of the greyhound, but might be an adaptation to their physiological demands requiring greater CCL strength (Tipton, Matthes et al. 1975), whereas it was suggested to be a mild degenerative change in CCLs of the non-athletic Labrador retriever (Comerford, Tarlton et al. 2006b).

We have observed in our study that fibrocartilage occurred mostly in the Staffordshire bull terrier and Labrador retriever CCL (predisposed breeds to CCLD/ R) compared to the greyhound CCL (not predisposed to CCLD/ R). However, no significant differences were observed in CCL structural morphology between the low risk dog breed (greyhound) and high risk dog breed (Labrador retriever). It is possible that this study requires a greater power and increasing the number of donors to 10 biological replicates could result in significant differences between breeds being achieved.

Statistical analysis of Toluidine blue scoring data showed that the Staffordshire bull terrier CCL origin anatomical region had more Toluidine blue staining in the ligament substance (covering collagen bundles) and within cells in comparison to its insertion site of the CCL. However, Alcian blue staining showed different statistically significant results, where the craniomedial band of the greyhound CCL had significantly higher Alcian blue staining in the ligament substance and a higher marked overall staining of Alcian blue compared to the caudolateral band.

One possible reason for the differences between the Toluidine blue and Alcian blue data could be that Eosin Y was used as a counter staining for Alcian blue, and thus sGAG were more easily distinguished than in the Toluidine blue sections. Therefore, the lack of counter stain for Toluidine blue might have created some confusion when

Toluidine blue staining was assessed. Therefore, we suggested that assessing sGAGs with Alcian blue might have been more accurate. It had been previously shown that the CCL of the porcine craniomedial and caudolateral band had structural differences in terms of their collagen fibre bundle orientation (Zhou, Grimshaw et al. 2009), and might be that they also exhibit structural differences in terms of cell shape and sGAGs. Our statistical data could indicate that there are morphological structural differences between the functional craniomedial band and the caudolateral band of the greyhound. However, further studies are required to evaluate the structural differences of these two CCL bands.

5.5.2 **Immunohistochemistry of canine CCLs**

Our first aim of the immunohistochemical study was observe whether there were differences in the proteoglycan distribution between the anatomical regions of the Staffordshire bull terrier. However, our subjective observations made it difficult for us to detect whether the proteoglycan distribution differed between the origin, middle and insertion sites of Staffordshire bull terrier.

Our second aim of the immunohistochemical study was to characterise the distribution and localisation of proteoglycans throughout the CCL in two dog breeds differentially predisposed to CCLD/ R.

Our study has shown that aggrecan, versican, decorin, biglycan, lumican, fibromodulin, and keratocan were expressed in the Staffordshire bull terrier (moderate-high risk) and greyhound (low risk) CCL, with each proteoglycan having a unique distribution within the CCL tissue. Such proteoglycans have been previously immunolocalised in the canine CCL (Yang, Culshaw et. al. 2011; Kharaz 2015).

In the Staffordshire bull terrier CCL, aggrecan was found to stain the interfascicular region and collagen bundles. In addition, it showed increased staining for the fibrocartilage matrices and stained fibrocartilaginous cells intracellularly (Figure 5-25 B). Greyhounds CCLs had a faint staining for aggrecan at the interfascicular region and collagen bundles. In addition, there was less intracellular staining for the fibrocartilaginous cells. The increase of aggrecan staining in Staffordshire bull terrier compared to greyhound CCLs could be that they encounter more areas of fibrocartilaginous matrices that are secondary to compression, as aggrecan has been previously shown to withstanding compressive forces in tendon (Vogel and

Koob 1989; Evanko and Vogel 1993; Robbins, Evanko et al. 1997). The deposition of aggrecan between collagen bundles may indicate that it facilitates sliding of collagen bundles relative to one another thus preventing damage of fibrils during extreme loading, and this role for aggrecan has been similarly reported in tendon (Vogel and Peters 2005). The intracellular staining for aggrecan in fibrocartilaginous cells could indicate its important role in withstanding compressive forces applied to the CCL. Aggrecan has been similar shown to stain intracellularly in cartilage (Melrose, Smith et al. 2005; Smith, Shu et al. 2010).

Versican is known to be the major large aggregating proteoglycan in ligament (Ilic, Carter et al. 2005). Versican mainly stained the interfascicular regions of the CCL more than collagen bundles, which agrees with a previous study (Kharaz 2015). In addition, versican was similarly distributed in the Staffordshire bull terrier and greyhound CCLs. The deposition of aggrecan and versican in the interfascicular region of the CCL could suggest that the may lubricate this structural region.

Decorin was shown to stain interfascicular regions and over collagen bundles thus covering the ligament substance. A similar distribution of decorin was also found in the rabbit anterior cruciate ligament (ACL) (Kavanagh and Ashhurst 2001). This broad distribution for decorin is not surprising since it is the most abundant proteoglycan found in ligament (Ilic, Carter et al. 2005), and its main role is to regulate collagen fibrillogenesis by interacting with collagen fibres (Vogel, Paulsson et al. 1984; Birk, Nurminskaya et al. 1995; Danielson, Baribault et al. 1997). Decorin distribution was found to be similar in the Staffordshire bull terrier and the greyhound CCL.

In the Staffordshire bull terrier and greyhound CCL, biglycan showed minor staining for collagen bundles. However, biglycan was increased in fibrocartilaginous regions of the CCL and was found to predominantly stain the fibrocartilaginous cells intracellularly (Figure 5-29 B), which is consistent with a previous study where biglycan was found to stain collagen bundles and fibrocartilaginous cells of the the rabbit ACL (Kavanagh and Ashhurst 2001). The positive staining for biglycan in collagen bundles could indicate that it interacts with collagen type I (Schonherr, Witschprehm et al. 1995), whilst the increase of biglycan in the fibrocartilaginous matrix could be secondary to compressive forces applied to the CCL, as biglycan has been shown to increase in compressed regions of tendon (Evanko, Vogel et al. 1993; Vogel, Ordog et al. 1993; Robbins, Evanko et al. 1997). Staffordshire bull terrier CCLs showed more biglycan staining in the fibrocartilaginous regions

compared to greyhound CCLs, and could be due to increased fibrocartilaginous matrices in the Staffordshire bull terrier CCL. The cellular staining of biglycan in fibrocartilage cells also agrees with other studies that stained biglycan in tendon (Vogel and Petres 2005). Biglycan could have a role in morphogenesis and differentiation of fibrocartilaginous cells (Bianco, Fisher et al. 1990; Embree, Kilts et al. 2010).

Fibromodulin, lumican, and keratocan were mainly located along the collagen fibre bundles of the CCL, and showed to be similarly distributed in Staffordshire bull terriers and greyhounds. Collagen type I is the predominant collagen in ligament (Frank 2004). Fibromodulin and lumican are known to attach to collagen type I (Svensson, Narlid et al. 2000), and keratocan has been shown to co-localised with type I collagen in tendon (Rees, Wagget et al. 2009). The specific immunolocalisation of fibromodulin, lumican, and keratocan in collagen bundles could indicate their importance in regulating collagen fibrillogenesis.

Fibromodulin stained around and within the rounded shaped cells in the fibrocartilage region (Figure 5-32 B), which were mainly detected in Staffordshire bull terriers compared to greyhound CCLs, which could also indicate that the Staffordshire bull terrier CCL consists of more fibrocartilaginous matrices. Similar deposition of fibromodulin was also found in the fibrocartilage zone of tendon and ligament (Adamczyk, Milz et al. 2008). This could suggest that fibromodulin may have a similar role to biglycan in that it may regulate cellular differentiation and morphogenesis, as fibromodulin and biglycan have been shown to regulate cellular differentiation and morphogenesis in chondrocytes (Embree, Kilts et al. 2010).

A limitation to this part of study was that the greyhound CCL tissue sections were much smaller compared to Staffordshire bull terriers, and therefore it was difficult for us to observe clearly if there were any differences in terms of proteoglycan distribution between the two differentially predisposed dog breeds. Furthermore, we were unable to quantify whether there were any significant differences in proteoglycans distribution between the three anatomical regions of the Staffordshire bull terriers. In general, our immunohistochemical observation was qualitative, allowing us to determine general distributions of proteoglycans in the ligament tissue. However, the distribution of proteoglycan quantity between anatomical regions of the canine CCL and within dog breeds with a differing risk to CCLD/ R needs yet to be determined. We further aim to undertake semi-quantitative

immunohistochemistry analysis by measuring the staining intensity of proteoglycans.

5.6 **Conclusion**

- Increase in sGAG staining is associated with increased fibrocartilaginous sites in the CCL, which may be a result of compression.
- The distribution of the large aggregating proteoglycans (aggrecan and versican) in the CCL could indicate that they may lubricate the interfascicular regions and aid in sliding between collagen bundles thus preventing damage of fibrils during increased compressive loading.
- The distribution of decorin, lumican, fibromodulin and keratocan in the collagenous matrix in both dog breeds may indicate their importance in regulating collagen fibrillogenesis in the CCL.

Chapter 6: General discussion and future work.

6.1 General discussion

The ligament extracellular matrix (ECM) is composed of two thirds of water, and one third of solids, such as collagen, elastin, proteoglycans, and glycoproteins (Frank 2004; Rumain, Wallace et al. 2007). Proteoglycans consist of a core protein attached to one or more glycosaminoglycan (GAG) chain (Hardingham and Fosang 1992; Iozzo and Schaefer 2015).

Cranial cruciate ligament (CCL) disease and rupture (CCLD/ R) is one of the most common orthopaedic conditions to affect dogs leading to stifle joint osteoarthritis (Bennett, Tennant et al. 1988). Previous studies have shown that different dog breeds have a different predisposition to CCLD/ R. Such breeds are the Labrador retriever (high risk), and the racing greyhound (low risk) (Whitehair, Vasseur et al. 1993; Duval, Budsberg et al. 1999). Other dog breeds are known to be moderate-high in risk such as the Staffordshire bull terrier (Baird, Carter et al. 2014b).

The aim of this work was to detect whether proteoglycans and GAGs varied between different anatomical regions of dog breeds with a different predisposition to CCLD/ R. In addition, we further aimed to identify whether certain proteoglycans and GAGs differed between dog breeds that have different risks to this disease. We hypothesised that certain proteoglycans and GAGs may differ significantly between anatomical regions of the CCL and between dog breeds with a different predisposition to CCLD/ R.

Therefore, our objectives were to use semi-quantitative Western blot analysis, biochemical analysis, semi-objective histology scoring analysis, and immunohistochemistry to determine if there were differences with proteoglycans and GAGs in different anatomical regions of the canine CCL and between dog breeds with a different predisposition to CCLD/ R.

Previous studies using Western blot analysis have identified proteoglycans and GAGs in different anatomical regions of tendon tissues (Robbins, Evanko et al. 1997; Waggett, Ralphs et al. 1998; Rees, Flannery et al. 2000; Samiric, Ilic et al. 2004; Ilic, Carter et al. 2005; Rees, Wagget et al. 2009). The Western blot results of

this study showed that the core protein of versican fragments and keratocan were significantly higher in the middle anatomical region in comparison to other anatomical regions of the Staffordshire bull terrier CCL, and that chondroitin -4 sulphate high molecular weight stubs were found to increase significantly at the insertion and middle region of the Staffordshire bull terrier CCL compared to its origin region. The middle (Paatsama 1952; Vasseur, Pool et al. 1985; Comerford, Tarlton et al. 2006b) and insertion (Arnoczky 1983; Zhu, Zhang et al. 2012) anatomical regions of the CCL have been shown to be fibrocartilaginous. This fibrocartilaginous site is likely to be secondary to physical compression. Therefore, it is likely that these proteoglycans (versican and keratocan) and GAGs (chondroitin-4 sulphate) are specific for fibrocartilaginous regions as a result of compression (Vogel and Koob 1989; Evanko and Vogel 1993; Rees, Wagget et al. 2009; Huisman, Andersson et al. 2014). Our limitations of this part of study is that we were unable to obtain enough CCLs from greyhounds in order to study the anatomical variation of proteoglycans and GAGs, as it would have been interesting to detect whether the anatomical regions of the greyhound CCLs differed in their proteoglycan and GAG composition compared to Staffordshire bull terrier CCLs. However, Western blot analysis is only semi-quantitative for proteins, we further aim to use other techniques such as matrix assisted laser desorption ionisation mass spectrometry imaging (MALDI-MSI), which is a special proteomic method in order to detect proteoglycans in different anatomical region of the Staffordshire bull terrier and greyhound CCL, as proteomic analysis has shown to be a sensitive and quantitative technique to detect specific proteins (Beine, Diehl et al. 2016).

Certain GAGs and proteoglycans have been shown to increase in tendon/ ligament pathology (Riley, Harral et al. 1994a; Lo, Marchuk et al. 1998; Corps, Robinson et al. 2006; Halper, Kim et al. 2006; Fu, Chan et al. 2007; Samiric, Parkinson et al. 2009), and sulphated glycosaminoglycans (sGAGs) have been shown to increase in the CCLs from high risk dog breeds to CCLD/ R (Comerford, Tarlton et al. 2006a). In Chapter 3, Western blot and gene expression analysis of fibromodulin, gene expression of aggrecan, and Western blot analysis of chondroitin-6 sulphate stubs were significantly higher in Staffordshire bull terrier CCLs compared to those of the greyhounds. Aggrecan and chondroitin-6 sulphate have been shown to increase in regions of tendon subjected to compression (Vogel and Koob 1989; Evanko and Vogel 1993; Huisman, Andersson et al. 2014). The significant increase of aggrecan and chondroitin-6 sulphate stubs in Staffordshire bull terriers CCLs compared to greyhound CCLs could be that it develops more sites of fibrocartilage secondary to

compression, and may both function to withstand compressive loading in the Staffordshire bull terrier CCLs.

Fibromodulin has been previously shown to localise at the fibrocartilaginous sites of human flexor carpi ulnaris tendon, pisometacarpal and pisohamate ligaments (Adamczyk, Milz et al. 2008). In addition, we found in Chapter 5 that fibromodulin surrounded the fibrocartilaginous cells with some pericellular/ intracellular staining. Therefore, the significant increase of fibromodulin in the Staffordshire bull terrier CCL could be that this moderate-high risk dog breed develops more sites of fibrocartilage, which may be a result of compression. Fibromodulin may have a role in promoting cellular differentiation in the CCL fibrocartilaginous region, as a similar role for fibromodulin has been shown in cartilage tissue (Embree, Kilts et al. 2010).

The increase of compressive regions in the Staffordshire bull terrier CCL is likely to be due to a narrowed intercondylar notch, and it could be that the Staffordshire bull terrier has a narrowed intercondylar notch that compresses against the CCL. The intercondylar notch index and femoral condyle height and width have been shown to be significantly lower in Labrador retriever and Golden retriever CCLs (high risk to CCLD/ R) compared to those of the greyhounds (low risk to CCLD/ R) (Comerford and Tarlton et al. 2006a). In addition, narrowing of the intercondylar notch has been associated with CCLD/ R and osteoarthritis in the dog (Aiken, Kass et al. 1995; Wada, Tatsuo et al. 1999), and the normal ACL function in humans has been shown to be impeded when it passes through a narrowed intercondylar notch, resulting in damage to the ACL (Muneta, Takakuda et al. 1997). The intercondylar notch index in the Staffordshire bull terrier has not been determined yet, as we only made an assumption that it may have a narrowed intercondylar notch compared to what has been reported for the narrowed intercondylar notches of high risk dog breeds (Comerford, Tarlton et al. 2006a). Therefore, it would be worth measuring the intercondylar notch height and width index in the moderate-high risk Staffordshire bull terrier.

However, the significant increase in aggrecan and fibromodulin could also be associated CCLD/ R in the moderate-high risk Staffordshire bull terrier, as fibromodulin (Samiric, Parkinson et al. 2009), and aggrecan (Corps, Robinson et al. 2006; Samiric, Parkinson et al. 2009) gene expression have been found to increase in tendon pathology. In addition, aggrecan gene expression has been found to increase in ruptured CCLs of the Labrador retrievers (high risk to CCLD/ R) (Clements, Carter et al. 2008). The increase of aggrecan in the Staffordshire bull

terrier could also be related to the significant increase of water content compared to those of the greyhound CCLs (See Chapter 4), as one of the functions for aggrecan is to retain water in the tissue matrix (Hardingham and Bayliss 1990). Conversely, the significant increase of the water content in the Staffordshire bull terrier CCL may be a pathological sign for the contribution to CCLD/ R, as Comerford and others have shown that the increase of water content was statistically significant in ruptured CCLs compared to intact CCLs of the high-risk Labrador retriever (Comerford, Innes 2004). Studies have shown that pathological tendons are also accompanied with increased water content (Riley, Harral et al. 1994b; Samiric, Parkinson et al 2009).

Gene expression and Western blot analysis showed that the low-risk greyhound had a significant increase of decorin compared to those of the Staffordshire bull terrier CCLs. In a decorin knockout mice study, tendon collagen fibrils in cross-section had uneven outlines with variability in fibril size (Danielson, Baribault et al. 1997). In addition, transmission electron microscopy (TEM) has shown that the Labrador retriever (high risk dog breed to CCLD/ R) had non-uniform and small collagen fibril sizes (approximately 50 nm), whereas the collagen fibril diameter measured in greyhound (from 100-150 nm) (low risk dog breed to CCLD/ R) were more uniform and larger in size (Comerford, Tarlton et al. 2006). Decorin might have a role in regulating collagen fibrillogenesis in the greyhound CCL, by maintaining its size and strength, thus preventing it from CCLD/ R, and we predict that decorin content is less in the Staffordshire bull terrier (moderate-high risk to CCLD/ R) as it may have irregular and small fibril diameters similar to the Labrador retriever (high risk to CCLD/ R). However, our further work is to perform TEM to identify the collagen fibril morphology with cross sections and to measure the fibril diameter in Staffordshire bull terriers.

It is interesting to highlight that several studies which determined the gene expression levels of proteoglycans in pathological tendons and ligaments, have observed an increase in proteoglycans such as aggrecan, biglycan, fibromodulin, but not decorin (Lo, Marchuk et al. 1998; Corps, Robinson et al. 2006; Clements, Carter et al. 2008; Samiric, Parkinson et al. 2009) This could indicate that decorin is a proteoglycan that is not associated with pathology, and may solely function to maintain collagen fibrils in tendons (Vogel, Paulsson et al. 1984; Birk, Nurminskaya et al. 1995; Danielson, Baribault et al. 1997) and ligament.

ADAMTS4 is secreted as an active enzyme and is known to cleave proteoglycans within specific sites of their core protein (Kashiwagi, Enhild et al. 2004). The gene expression of ADAMTS-4 was shown to be significantly upregulated in greyhounds CCLs compared to Staffordshire bull terriers. Evidence of increased catabolism in greyhounds CCLs associated with high expression of ADAMTS-4 could be linked to increased expression and anabolism of its proteoglycan substrates, such as decorin (Kashiwagi, Enhild et al. 2004; Porter, Clark et al. 2005). The significant increase of decorin gene expression could be related to increased ADAMTS-4 activity since we have detected a catabolic fragment below the decorin core protein at 30 kDa (Figure 3-7 B), and we predict that this fragment could be generated from ADAMTS-4 activity. To confirm whether the decorin fragment is generated by ADAMTS4 acitivity, we further aim to incubate the CCLs with an ADAMTS4 inhibitor such as tissue inhibitor of metalloproteinase-3 (Hashimoto, Aoki et al. 2001), and then perform Western blot analysis on the CCLs with decorin antibody in order to observe whether the 30 kDa fragment of decorin is absent due to the degradation of ADAMTS4 by tissue inhibitor of metalloproteinase-3 (Porter, Clark et al. 2005), versican (Sandy, Westling et al. 2001), biglycan (Melching, Fisher et al. 2006), and fibromodulin (Porter, Clark et al. 2005). However, it could be that ADAMTS-4 is more efficient in cleaving decorin due to its gene levels being highly expressed in normal greyhound CCL. The significant increase of ADAMTS-4 in greyhound CCLs thus could be required to maintain normal CCL metabolism, as it is an exercising dog breed that rarely ruptures its CCL. Further work includes performing Western blotting with ADAMTS-4 antibody to identify whether there are significant differences in ADAMTS-4 catabolic fragments in the Staffordshire bull terrier and greyhound CCL. This will give us a better understanding on how ADAMTS-4 is affecting the metabolism of its substrates in the CCL of the different predisposed dog breeds.

Glycosaminoglycans (GAGs) are covalently attached to a proteoglycan core protein with the exception of hyaluronic acid (Hardingham 1981; Ajit Varki 2009). GAGs are known to be comprised of a hexosamine (i.e. glucosamine or galactosamine), and an uronic acid (glucoronic acid and or iduronic acid) or galactose (Hardingham and Fosang 1992). The results of this study showed that hyaluronic acid was one of the major GAGs of the CCL in both dog breeds, whereas keratan sulphate was one of the lowest GAGs (See Chapter 4). We conclude that the high content of hyaluronic acid could have a role in maintaining the viscosity and viscoelastic properties of the CCL, as has been reported for other tissues (eye and skeletal joints) (Ajit Varki 2009). It would have been useful to determine the rest of the individual GAG

contents in the CCL, such as chondroitin sulphate-6, chondroitin sulphate-4, dermatan sulphate, and heparin sulphate, as we might have observed statistical significant differences with these individual GAGs between the regions of the CCL and between the CCL of dog breeds with a different predisposition to CCLD/ R. Therefore, we further aim to use other techniques such as disaccharide analysis with high liquid performance chromatography to determine the individual contents of chondroitin sulphate-6, chondroitin sulphate-4, dermatan sulphate, and heparan sulphate in the CCLs of the Staffordshire bull terrier and greyhound (Hae Yoon, Brooks et al. 2003).

In Chapter 5, we have performed semi objective histology scoring analysis in order to determine the CCL structural morphology and sGAG deposition between anatomical regions of three dog breeds with a different predisposition to CCLD/ R namely the greyhound (low in risk), the Staffordshire bull terrier (moderate – high in risk), and the Labrador retriever (high in risk).

H & E staining showed that each dog breed had differences in the collagen architecture of their CCL, where most displayed normal (Yahia and Drouin 1989; Zhu, Zhang et al. 2009) and reduced (Narama, Masuoka-Nishiyama et al. 1996; Zhu, Zhang et al. 2009) collagen architectures. Furthermore, a heterogeneous population of cell nuclei (spindle and rounded) was observed in the CCL of all dogs, where spindle shaped cells were mostly seen with normal collagen bundles, and rounded cells were mainly seen in areas with reduced/ homogenous collagen bundles (Narama, Masuoka-Nishiyama et al. 1996; Comerford, Tarlton et al. 2006b), thus demonstrating areas of fibrocartilage.

An increase in Toluidine blue and Alcian blue staining were present in fibrocartilaginous regions of the CCL (Figure 5-11, B and 5-17, B), which is in agreement with other studies (Comerford, Tarlton et al. 2006b; Feitosa, Reis et al. 2006). H&E staining showed that fibrocartilage regions occurred mainly in the Staffordshire bull terrier and Labrador retriever CCLs (breeds predisposed to CCLD/ R) compared to those of the greyhounds (not predisposed to CCLD/ R) (Figure 5-1), the increase in fibrocartilaginous matrices in the Staffordshire bull terrier and Labrador retriever could be secondary to compressive forces applied to the CCL. However, no significant differences were observed in CCL structural morphology between non-predisposed dog breeds (greyhound), and predisposed dog breeds (Staffordshire bull terrier and Labrador retriever), and it could be possible that with

performing a power calculation and increasing the number of donors accordingly could have showed significance between the differentially predisposed dog breeds.

Further in Chapter 5, we have performed immunohistochemistry staining with proteoglycan antibodies in the Staffordshire bull terrier and greyhound CCL. We found that aggrecan was distributed in the CCL interfascicular and collagen bundles. In addition, aggrecan was increase in the fibrocartilage regions and stained the fibrocartilaginous cells intracellularly which was more evident in Staffordshire bull terrier CCLs. Immunolocalisation of aggrecan in cells has been similarly shown in cartilage tissue (Melrose, Smith et al. 2005; Smith, Shu et al. 2010). The increase of aggrecan in the fibrocartilaginous matrix of the Staffordshire bull terrier CCLs may indicate that it has a role in withstanding compressive forces in tendon (Vogel and Koob 1989; Evanko and Vogel 1993; Huisman, Andersson et al. 2014) and ligament.

Versican, on the other hand, mainly stained the interfascicular regions of the CCL, and showed less staining over collagen bundles (Kharaz 2015). The location of aggrecan and versican at the interfascicular region of the CCL could indicate that they both have a role in lubricating the interfascicular matrix.

Decorin was found to stain the interfascicular region and collagen bundles, which covered the ligament substance, whilst biglycan showed minor staining for collagen bundles. However, biglycan was increased in fibrocartilaginous regions and stained the fibrocartilaginous cells. Overall, biglycan staining in fibrocartilaginous regions was more apparent in Staffordshire bull terrier CCLs compared to those of the greyhounds

The broad distribution of decorin in the collagen bundles could indicate its key essential role in regulating collagen fibrillogenesis in the canine CCL, as several studies have indicated of the important role of decorin in regulating collagen fibrillogenesis in tendon (Vogel, Paulsson et al. 1984; Birk, Nurminskaya et al. 1995; Danielson, Baribault et al. 1997). The positive staining for biglycan in collagen bundles could indicate that it may interact with collagen type I (Schonherr, Witschprehm et al. 1995) in the CCL, whilst the increase of biglycan in the fibrocartilaginous matrix of the Staffordshire bull terrier could be secondary to compressive forces in the CCL, as biglycan has been shown to increase in compressed regions of tendon (Evanko, Vogel et al. 1993; Vogel, Ordog et al. 1993; Robbins, Evanko et al. 1997). The cellular staining of biglycan in fibrocartilage cells

agrees with other studies that stained tendon with biglycan antibody (Vogel and Petres 2005). Biglycan could have a role in morphogenesis and differentiation of fibrocartilaginous cells, as biglycan has been shown to regulate cells of cartilage and other tissues (cornea and skin) (Bianco, Fisher et al. 1990; Embree, Kilts et al. 2010).

Fibromodulin, lumican, and keratocan mainly stained in the collagen bundles of the CCL. The staining over collagen bundles for lumican and fibromodulin could indicate that they have a similar role to decorin in the CCL, in which they regulate collagen fibrillogenesis in tendon (Svensson, Aszodi et al. 1999; Ezura, Chakravarti et al. 2000). In addition, keratocan has been found to co-localise with type I collagen in bovine deep digital flexor tendon (Rees, Wagget et al. 2009). Therefore, keratocan may also play a role in regulating collagen fibrollogenesis in the CCL tissue.

Overall Staffordshire bull terriers had more aggrecan and biglycan staining in their CCLs in comparison to greyhounds. However, the limitations of this study is that we were unable to obtain similar tissue sections from the Staffordshire bull terrier and greyhound, as the tissue sections of the greyhound were much smaller, and therefore made it difficult to compare the differences between the two dog breeds. However, further work includes obtaining similar CCL sections from the greyhound and Staffordshire bull terrier and performing semi quantitative measurements of immunohistochemistry staining in order to detect statistical significant differences of proteoglycans between the two dog breeds and between their anatomical regions.

6.2 **Conclusion**

The significant elevated levels of decorin in greyhounds could be compulsory for maintaining its collagen fibril strength, whilst the significant increase of ADAMTS4 levels in the ex-racing greyhound could be essential to maintain its regular CCL homeostasis. The significant Increase of aggrecan, fibromodulin, and chondroitin-6 sulphate in Staffordshire bull terriers CCLs could be that this dog breed has an increase in fibrocartilage regions as a result of compressive loads. High compressive loading in the Staffordshire bull terrier might encounter the CCL to develop higher stress levels and therefore compromising the CCL to disease and rupture.

6.3 **Future Work**

- Recommendations for further work to determine proteoglycans and GAGs of the CCL in different anatomical regions and between dog breeds at different risks to CCLD/ R include;

  - Accurate determination of proteoglycans between anatomical regions by performing MALDI-MSI.
  - To measure the intercondylar notch width and height of the moderate-high risk Staffordshire bull terrier.
  - To measure and determine the collagen fibril diameter in the moderate-high risk Staffordshire bull terrier.
  - To detect other individual contents of GAGs (chondroitin sulphate -6. chondroitin sulphate -4, dermatan sulphate, and heparin sulphate) by performing disaccharide analysis with high liquid performance chromatography.
  - Semi quantitative measurements of immunohistochemical staining.

REFERENCES

Adamczyk, C., S. Milz, et al. (2008). "An immunohistochemical study of the extracellular matrix of entheses associated with the human pisiform bone." J Anat 212(5): 645-653.

Aiken, S. W., P. H. Kass, et al. (1995). "Intercondylar notch width in dogs with and without cranial cruciate ligament injuries." VCOT Archive 8(3): 6-10.

Ajit Varki, R. D. C., Jeffrey D Esko, Hudson H Freeze, Pamela Stanley, Carolyn R Bertozzi, Gerald W Hart, and Marilynn E Etzler. (2009). Chapter 15: "Hyaluronan", Essentials of Glycobiology, 2nd edition. 219-229.

Ajit Varki, R. D. C., Jeffrey D Esko, Hudson H Freeze, Pamela Stanley, Carolyn R Bertozzi, Gerald W Hart, and Marilynn E Etzler. (2009). Chapter 16: "proteoglycans and sulphated glycosaminoglycans", Essentials of Glycobiology, 2nd edition. 229-249.

Almeida, R., S. B. Levery, et al. (1999). "Cloning and expression of a proteoglycan UDP-galactose:beta-xylose beta1,4-galactosyltransferase I. A seventh member of the human beta4-galactosyltransferase gene family." J Biol Chem 274(37): 26165-26171.

Ameye, L., D. Aria, et al. (2002). "Abnormal collagen fibrils in tendons of biglycan/fibromodulin-deficient mice lead to gait impairment, ectopic ossification, and osteoarthritis." The FASEB Journal 16(7): 673-680.

Amiel, D., C. Frank, et al. (1984). "Tendons and ligaments: a morphological and biochemical comparison." Journal of Orthopaedic Research 1(3): 257-265.

Antonsson, P., D. Heinegard, et al. (1991). "Posttranslational Modifications of Fibromodulin." Journal of Biological Chemistry 266(25): 16859-16861.

Apte, S. S. (2009). "A disintegrin-like and metalloprotease (reprolysin-type) with thrombospondin type 1 motif (ADAMTS) superfamily: functions and mechanisms." J Biol Chem 284(46): 31493-31497.

Arcand, M. A., S. Rhalmi, et al. (2000). "Quantification of mechanoreceptors in the canine anterior cruciate ligament." Int Orthop 24(5): 272-275.

Arnoczky, S. P. (1983). "Anatomy of the anterior cruciate ligament." Clin Orthop Relat Res(172): 19-25.

Arnoczky, S. P. and J. L. Marshall (1977). "The cruciate ligaments of the canine stifle: an anatomical and functional analysis." American journal of veterinary research 38(11): 1807-1814.

Arnoczky, S. P., R. M. Rubin, et al. (1979). "Microvasculature of the Cruciate Ligaments and Its Response to Injury - Experimental-Study in Dogs." Journal of Bone and Joint Surgery-American Volume 61(8): 1221-1229.

Aspberg, A., R. Miura, et al. (1997). "The C-type lectin domains of lecticans, a family of aggregating chondroitin sulfate proteoglycans, bind tenascin-R by protein-protein interactions independent of carbohydrate moiety." Proc Natl Acad Sci U S A 94(19): 10116-10121.

Aydog, S. T., P. Korkusuz, et al. (2006). "Decrease in the numbers of mechanoreceptors in rabbit ACL: the effects of ageing." Knee Surg Sports Traumatol Arthrosc 14(4): 325-329.

Bai, X. M., D. P. Zhou, et al. (2001). "Biosynthesis of the linkage region of glycosaminoglycans - Cloning and activity of galactosyltransferase II, the sixth member of the beta 1,3-galactosyltransferase family (beta 3GalT6)." Journal of Biological Chemistry 276(51): 48189-48195.

Baird, A. E., S. D. Carter, et al. (2014a). "Genome-wide association study identifies genomic regions of association for cruciate ligament rupture in Newfoundland dogs." Anim Genet 45(4): 542-549.

Baird, A. E., S. D. Carter, et al. (2014b). "Genetic basis of cranial cruciate ligament rupture (CCLR) in dogs." Connect Tissue Res 55(4): 275-281.

Ball, J. and D. S. Jackson (1953). "Histological, chromatographic and spectrophotometric studies of toluidine blue." Stain Technology 28(1): 33-40.

Barnes, A. J. (1977). "Rupture of the anterior cruciate ligament of the dog: a survey from practices in the Kent region BSAVA." Journal of Small Animal Practice 18(1): 55-59.

Bayliss, M. T., D. Osborne, et al. (1999). "Sulfation of chondroitin sulfate in human articular cartilage - The effect of age, topographical position, and zone of cartilage on tissue composition." Journal of Biological Chemistry 274(22): 15892-15900.

Beine, B., H. C. Diehl, et al. (2016). "Tissue MALDI Mass Spectrometry Imaging (MALDI MSI) of Peptides." Proteomics in Systems Biology: Methods and Protocols 1394: 129-150.

Benjamin, M., E. J. Evans, et al. (1986). "The Histology of Tendon Attachments to Bone in Man." Journal of Anatomy 149: 89-100.

Benjamin, M., S. Qin, et al. (1995). "Fibrocartilage associated with human tendons and their pulleys." Journal of Anatomy 187: 625-633.

Benjamin, M. and J. R. Ralphs (1998). "Fibrocartilage in tendons and ligaments—an adaptation to compressive load." Journal of Anatomy 193(04): 481-494.

Bennett, D., B. Tennant, et al. (1988). "A reappraisal of anterior cruciate ligament disease in the dog." Journal of Small Animal Practice 29(5): 275-297.

Beye, J. A., D. A. Hart, et al. (2006). "Denervation alters mRNA levels of repair-associated genes in a rabbit medial collateral ligament injury model." Journal of orthopaedic research 24(9): 1842-1853.

Bianco, P., L. W. Fisher, et al. (1990). "Expression and localization of the two small proteoglycans biglycan and decorin in developing human skeletal and non-skeletal tissues." Journal of Histochemistry & Cytochemistry **38**(11): 1549-1563.

Bidanset, D. J., C. Guidry, et al. (1992). "Binding of the proteoglycan decorin to collagen type VI." J Biol Chem 267(8): 5250-5256.

Birch, H. L., J. V. Bailey, et al. (1999). "Age-related changes to the molecular and cellular components of equine flexor tendons." Equine Vet J 31(5): 391-396.

Birch, H. L., C. T. Thorpe, et al. (2013). "Specialisation of extracellular matrix for function in tendons and ligaments." Muscles Ligaments Tendons J 3(1): 12-22.

Birk, D. E., M. V. Nurminskaya, et al. (1995). "Collagen fibrillogenesis in situ: fibril segments undergo post-depositional modifications resulting in linear and lateral growth during matrix development." Dev Dyn 202(3): 229-243.

Bitter, T. and H. M. Muir (1962). "A modified uronic acid carbazole reaction." Analytical biochemistry 4(4): 330-334.

Bredrup, C., P. M. Knappskog, et al. (2005). "Congenital stromal dystrophy of the cornea caused by a mutation in the decorin gene." Investigative Ophthalmology & Visual Science 46(2): 420-426.

Buckley, M. R., G. R. Huffman, et al. (2013). "The location-specific role of proteoglycans in the flexor carpi ulnaris tendon." Connective tissue research 54(6): 367-373.

Buote, N., J. Fusco, et al. (2009). "Age, Tibial Plateau Angle, Sex, and Weight as Risk Factors for Contralateral Rupture of the Cranial Cruciate Ligament in Labradors." Veterinary Surgery 38(4): 481-489.

Butler, D. L. and D. C. Stouffer (1983). "Tension-torsion characteristics of the canine anterior cruciate ligament--Part II: Experimental observations." J Biomech Eng 105(2): 160-165.

Cabaud, H. E., A. Chatty, et al. (1980). "Exercise Effects on the Strength of the Rat Anterior Cruciate Ligament." American Journal of Sports Medicine 8(2): 79-86.

Cabrera, S. Y., T. J. Owen, et al. (2008). "Comparison of tibial plateau angles in dogs with unilateral versus bilateral cranial cruciate ligament rupture: 150 cases (2000-2006)." J Am Vet Med Assoc 232(6): 889-892.

Calabro, A., V. C. Hascall, et al. (1992). "Monoclonal antibodies directed against epitopes within the core protein structure of the large aggregating proteoglycan (aggrecan) from the swarm rat chondrosarcoma." Arch Biochem Biophys 298(2): 349-60.

Canty, E. G. and K. E. Kadler (2005). "Procollagen trafficking, processing and fibrillogenesis." Journal of Cell Science 118(7): 1341-1353.

Cao, M., M. Stefanovic-Racic, et al. (2000). "Does nitric oxide help explain the differential healing capacity of the anterior cruciate, posterior cruciate, and medial collateral ligaments?" Am J Sports Med 28(2): 176-182.

Carlsson, P., J. Presto, et al. (2008). "Heparin/heparan sulfate biosynthesis - Processive formation of N-sulfated domains." Journal of Biological Chemistry 283(29): 20008-20014.

Carpenter, D. H., Jr. and R. C. Cooper (2000). "Mini review of canine stifle joint anatomy." Anatomia Histologia Embryologia 29(6): 321-329.

Caterson, B., J. E. Christner, et al. (1983). "Identification of a Monoclonal-Antibody That Specifically Recognizes Corneal and Skeletal Keratan Sulfate - Monoclonal-Antibodies to Cartilage Proteoglycan." Journal of Biological Chemistry 258(14): 8848-8854.

Chai, W. G., C. T. Yuen, et al. (1999). "High prevalence of 2-mono- and 2,6-di-substituted Manol-terminating sequences among O-glycans released from brain glycopeptides by reductive alkaline hydrolysis." European Journal of Biochemistry 263(3): 879-888.

Chakravarti, S., J. Paul, et al. (2003). "Ocular and scleral alterations in gene-targeted lumican-fibromodulin double-null mice." Investigative Ophthalmology & Visual Science 44(6): 2422-2432.

Chakravarti, S., W. M. Petroll, et al. (2000). "Corneal opacity in lumican-null mice: defects in collagen fibril structure and packing in the posterior stroma." Invest Ophthalmol Vis Sci 41(11): 3365-3373.

Cheng, H., B. Caterson, et al. (1999). "Identification and immunolocalization of chondroitin sulfate proteoglycans in tooth cementum." Connect Tissue Res 40(1): 37-47.

Chi, S. S., J. B. Rattner, et al. (2005). "Gap junctions of the medial collateral ligament: structure, distribution, associations and function." J Anat 207(2): 145-154.

Chowdhury, P., J. R. Matyas, et al. (1991). "The "epiligament" of the rabbit medial collateral ligament: a quantitative morphological study." Connect Tissue Res 27(1): 33-50.

Chuang, C., M. A. Ramaker, et al. (2014). "Radiographic Risk Factors for Contralateral Rupture in Dogs with Unilateral Cranial Cruciate Ligament Rupture." Plos One 9(9).

Clark, J. M. and J. A. Sidles (1990). "The Interrelation of Fiber-Bundles in the Anterior Cruciate Ligament." Journal of orthopaedic research 8(2): 180-188.

Clements, D. N., S. D. Carter, et al. (2006). "Analysis of normal and osteoarthritic canine cartilage mRNA expression by quantitative polymerase chain reaction." Arthritis Res Ther 8(6): R150.

Clements, D. N., S. D. Carter, et al. (2008). "Gene expression profiling of normal and ruptured canine anterior cruciate ligaments." Osteoarthritis Cartilage 16(2): 195-203.

Colborne, G. R., J. F. Innes, et al. (2005). "Distribution of power across the hind limb joints in Labrador Retrievers and Greyhounds." American journal of veterinary research 66(9): 1563-1571.

Colige, A., S. W. Li, et al. (1997). "cDNA cloning and expression of bovine procollagen I N-proteinase: a new member of the superfamily of zinc-metalloproteinases with binding sites for cells and other matrix components." Proc Natl Acad Sci U S A 94(6): 2374-2379.

Colige, A., I. Vandenberghe, et al. (2002). "Cloning and characterization of ADAMTS-14, a novel ADAMTS displaying high homology with ADAMTS-2 and ADAMTS-3." J Biol Chem 277(8): 5756-5766.

Comerford, E. J., J. F. Innes, et al. (2004). "Investigation of the composition, turnover, and thermal properties of ruptured cranial cruciate ligaments of dogs." American journal of veterinary research 65(8): 1136-1141.

Comerford, E. J., J. F. Tarlton, et al. (2006a). "Distal femoral intercondylar notch dimensions and their relationship to composition and metabolism of the canine anterior cruciate ligament." Osteoarthritis and cartilage 14(3): 273-278.

Comerford, E. J., J. F. Tarlton, et al. (2005). "Metabolism and composition of the canine anterior cruciate ligament relate to differences in knee joint mechanics and predisposition to ligament rupture." Journal of orthopaedic research 23(1): 61-66.

Comerford, E. J., J. F. Tarlton, et al. (2006b). "Ultrastructural differences in cranial cruciate ligaments from dogs of two breeds with a differing predisposition to ligament degeneration and rupture." Journal of comparative pathology 134(1): 8-16.

Corps, A. N., G. C. Jones, et al. (2008). "The regulation of aggrecanase ADAMTS-4 expression in human Achilles tendon and tendon-derived cells." Matrix biology 27(5): 393-401.

Corps, A. N., A. H. Robinson, et al. (2004). "Versican splice variant messenger RNA expression in normal human Achilles tendon and tendinopathies." Rheumatology (Oxford) 43(8): 969-972.

Corps, A. N., A. H. N. Robinson, et al. (2006). "Increased expression of aggrecan and biglycan mRNA in Achilles tendinopathy." Rheumatology 45(3): 291-294.

Corsi, A., T. Xu, et al. (2002). "Phenotypic effects of biglycan deficiency are linked to collagen fibril abnormalities, are synergized by decorin deficiency, and mimic Ehlers-Danlos-like changes in bone and other connective tissues." Journal of Bone and Mineral Research 17(7): 1180-1189.

Cribb, A. M. and J. E. Scott (1995). "Tendon Response to Tensile-Stress - an Ultrastructural Investigation of Collagen - Proteoglycan Interactions in Stressed Tendon." Journal of Anatomy 187: 423-428.

Danielson, K. G., H. Baribault, et al. (1997). "Targeted disruption of decorin leads to abnormal collagen fibril morphology and skin fragility." Journal of Cell Biology 136(3): 729-743.

De Bruin, T., H. De Rooster, et al. (2007). "Radiographic assessment of the progression of osteoarthrosis in the contralateral stifle joint of dogs with a ruptured cranial cruciate ligament." Veterinary Record 161(22): 745-750.

De Rooster, H., T. De Bruin, et al. (2006). "Invited review—morphologic and functional features of the canine cruciate ligaments." Veterinary Surgery 35(8): 769-780.

Dhillon, M. S., K. Bali, et al. (2012). "Differences among mechanoreceptors in healthy and injured anterior cruciate ligaments and their clinical importance." Muscles Ligaments Tendons J 2(1): 38.

Doege, K. J., K. Garrison, et al. (1994). "The structure of the rat aggrecan gene and preliminary characterization of its promoter." J Biol Chem 269(46): 29232-29240.

Douglas, T., S. Heinemann, et al. (2006). "Fibrillogenesis of collagen types I, II, and III with small leucine-rich proteoglycans decorin and biglycan." Biomacromolecules 7(8): 2388-2393.

Dours-Zimmermann, M. T. and D. R. Zimmermann (1994). "A Novel Glycosaminoglycan Attachment Domain Identifieind Two Alternative Splice Variants of Human Versican." Jounal of bological chemistry 269(52): 32992-32998.

Dourte, L. M., L. Pathmanathan, et al. (2013). "Mechanical, compositional, and structural properties of the mouse patellar tendon with changes in biglycan gene expression." Journal of orthopaedic research 31(9): 1430-1437.

Doverspike, M., P. B. Vasseur, et al. (1993). "Contralateral Cranial Cruciate Ligament Rupture - Incidence in 114 Dogs." Journal of the American Animal Hospital Association 29(2): 167-170.

Duerr, F. M., C. G. Duncan, et al. (2007). "Risk factors for excessive tibial plateau angle in large-breed dogs with cranial cruciate ligament disease." J Am Vet Med Assoc 231(11): 1688-1691.

Dunlevy, J. R., P. J. Neame, et al. (1998). "Identification of the N-linked oligosaccharide sites in chick corneal lumican and keratocan that receive keratan sulfate." Journal of Biological Chemistry 273(16): 9615-9621.

Dunlevy, J. R. and J. A. Rada (2004). "Interaction of lumican with aggrecan in the aging human sclera." Invest Ophthalmol Vis Sci 45(11): 3849-3856.

Duval, J. M., S. C. Budsberg, et al. (1999). "Breed, sex, and body weight as risk factors for rupture of the cranial cruciate ligament in young dogs." Journal of the American Veterinary Medical Association 215(6): 811-814.

Edney, A. T. and P. M. Smith (1986). "Study of obesity in dogs visiting veterinary practices in the United Kingdom." Vet Rec 118(14): 391-396.

Ehnis, T., W. Dieterich, et al. (1997). "Localization of a binding site for the proteoglycan decorin on collagen XIV (undulin)." J Biol Chem 272(33): 20414-20419.

Embree, M. C., T. M. Kilts, et al. (2010). "Biglycan and Fibromodulin Have Essential Roles in Regulating Chondrogenesis and Extracellular Matrix Turnover in Temporomandibular Joint Osteoarthritis." American Journal of Pathology 176(2): 812-826.

Evanko, S. P. and K. G. Vogel (1993). "Proteoglycan Synthesis in Fetal Tendon Is Differentially Regulated by Cyclic Compression in-Vitro." Archives of biochemistry and biophysics 307(1): 153-164.

Ezura, Y., S. Chakravarti, et al. (2000). "Differential expression of lumican and fibromodulin regulate collagen fibrillogenesis in developing mouse tendons." J Cell Biol 151(4): 779-788.

Farndale, R. W., D. J. Buttle, et al. (1986). "Improved quantitation and discrimination of sulphated glycosaminoglycans by use of dimethylmethylene blue." Biochimica et Biophysica Acta (BBA)-General Subjects 883(2): 173-177.

Feitosa, V. L. C., F. P. Reis, et al. (2006). "Comparative ultrastructural analysis of different regions of two digital flexor tendons of pigs." Micron 37(6): 518-525.

Fernandes, R. J., S. Hirohata, et al. (2001). "Procollagen II amino propeptide processing by ADAMTS-3. Insights on dermatosparaxis." J Biol Chem 276(34): 31502-31509.

Fessel, G. and J. G. Snedeker (2009). "Evidence against proteoglycan mediated collagen fibril load transmission and dynamic viscoelasticity in tendon." Matrix biology 28(8): 503-510.

Fisher, L. W., J. D. Termine, et al. (1989). "Deduced Protein-Sequence of Bone Small Proteoglycan-I (Biglycan) Shows Homology with Proteoglycan-Ii (Decorin) and Several Nonconnective Tissue Proteins in a Variety of Species." Journal of Biological Chemistry 264(8): 4571-4576.

Font, B., E. Aubert-Foucher, et al. (1993). "Binding of collagen XIV with the dermatan sulfate side chain of decorin." J Biol Chem 268(33): 25015-25018.

Font, B., D. Eichenberger, et al. (1996). "Characterization of the interactions of type XII collagen with two small proteoglycans from fetal bovine tendon, decorin and fibromodulin." Matrix Biol 15(5): 341-348.

Frank, C., D. Amiel, et al. (1985). "Normal Ligament Properties and Ligament Healing." Clinical Orthopaedics and Related Research(196): 15-25.

Frank, C. B. (2004). "Ligament structure, physiology and function." J Musculoskelet Neuronal Interact 4(2): 199-201.

Frieden, E. (1975). "Non-covalent interactions: key to biological flexibility and specificity." Journal of chemical education 52(12): 754.

Fu, S.-C., K.-M. Chan, et al. (2007). "Increased deposition of sulfated glycosaminoglycans in human patellar tendinopathy." Clinical Journal of Sport Medicine 17(2): 129-134.

Fukuda, M. and S. T. Tsuboi (1999). "Mucin-type O-glycans and leukosialin." Biochimica Et Biophysica Acta-Molecular Basis of Disease 1455(2-3): 205-217.

Fukuda, M. N. (2001). "Endo-beta-galactosidases and keratanase." Curr Protoc Mol Biol Chapter 17: Unit17 17B.

Fuller, M. C., K. Hayashi, et al. (2014). "Evaluation of the radiographic infrapatellar fat pad sign of the contralateral stifle joint as a risk factor for subsequent contralateral cranial cruciate ligament rupture in dogs with unilateral rupture: 96 cases (2006-2007)." Javma-Journal of the American Veterinary Medical Association 244(3): 328-338.

Funderburgh, J. L. (2000). "Keratan sulfate: structure, biosynthesis, and function." Glycobiology 10(10): 951-958.

Geiger, M. H., M. H. Green, et al. (1994). "An in-Vitro Assay of Anterior Cruciate Ligament (Acl) and Medial Collateral Ligament (Mcl) Cell-Migration." Connective Tissue Research 30(3): 215-224.

Geng, Y. Q., D. McQuillan, et al. (2006). "SLRP interaction can protect collagen fibrils from cleavage by collagenases." Matrix biology 25(8): 484-491.

Goldberg, V. M., A. Burstein, et al. (1982). "The influence of an experimental immune synovitis on the failure mode and strength of the rabbit anterior cruciate ligament." J Bone Joint Surg Am 64(6): 900-906.

Gopalakrishnan, B., W. M. Wang, et al. (2004). "Biosynthetic processing of the Pro-alpha1(V)Pro-alpha2(V)Pro-alpha3(V) procollagen heterotrimer." J Biol Chem 279(29): 30904-30912.

Gotting, C., J. Kuhn, et al. (2000). "Molecular cloning and expression of human UDP-D-xylose : proteoglycan core protein beta-D-xylosyltransferase and its first isoform XT-II." Journal of Molecular Biology 304(4): 517-528.

Grabski, A. C. and R. R. B. Novagen (2010). "Preparation of protein samples for SDS-polyacrylamide gel electrophoresis: procedures and tips."

Grierson, J., L. Asher, et al. (2011). "An investigation into risk factors for bilateral canine cruciate ligament rupture." Veterinary and Comparative Orthopaedics and Traumatology 24(3): 192-196.

Grumet, M., A. Flaccus, et al. (1993). "Functional characterization of chondroitin sulfate proteoglycans of brain: interactions with neurons and neural cell adhesion molecules." J Cell Biol 120(3): 815-824.

Grumet, M., P. Milev, et al. (1994). "Interactions with tenascin and differential effects on cell adhesion of neurocan and phosphacan, two major chondroitin sulfate proteoglycans of nervous tissue." J Biol Chem 269(16): 12142-12146.

Gyger, O., C. Botteron, et al. (2007). "Detection and distribution of apoptotic cell death in normal and diseased canine cranial cruciate ligaments." The Veterinary Journal 174(2): 371-377.

Hae Yoon, J., R. Brooks, et al. (2003). "Proteoglycans in chicken gastrocnemius tendons change with exercise." Arch Biochem Biophys 412(2): 279-286.

Halper, J., B. Kim, et al. (2006). "Degenerative suspensory ligament desmitis as a systemic disorder characterized by proteoglycan accumulation." BMC veterinary research 2(1): 12.

Halpert, I., U. I. Sires, et al. (1996). "Matrilysin is expressed by lipid-laden macrophages at sites of potential rupture in atherosclerotic lesions and localizes to areas of versican deposition, a proteoglycan substrate for the enzyme." Proceedings of the National Academy of Sciences of the United States of America 93(18): 9748-9753.

Harasen, G. (2008). "Canine cranial cruciate ligament rupture in profile: 2002–2007." The Canadian Veterinary Journal 49(2): 193.

Hardingham, T. (1981). "Proteoglycans: Their structure, interactions and molecular organization in cartilage." Biochemical Society Transactions 9: 489-497.

Hardingham, T. and M. Bayliss (1990). "Proteoglycans of articular cartilage: changes in aging and in joint disease." Semin Arthritis Rheum 20(3 Suppl 1): 12-33.

Hardingham, T. E. and A. J. Fosang (1992). "Proteoglycans: many forms and many functions." FASEB J 6(3): 861-870.

Hardingham, T. E. and H. Muir (1974). "Hyaluronic acid in cartilage and proteoglycan aggregation." Biochemical Journal 139(3): 565-581.

Hart, D. A., P. Sciore, et al. (1998). "Pregnancy induces complex changes in the the pattern of mRNA expression in knee ligaments of the adolescent rabbit." Matrix Biol 17(1): 21-34.

Hasegawa, A., H. Nakahara, et al. (2013). "Cellular and extracellular matrix changes in anterior cruciate ligaments during human knee aging and osteoarthritis." Arthritis Res Ther 15(1): R29.

Hasegawa, A., S. Otsuki, et al. (2012). "Anterior cruciate ligament changes in the human knee joint in aging and osteoarthritis." Arthritis Rheum 64(3): 696-704.

Hashimoto, G. Aoki, T, et al. (2001). "Inhibition of ADAMTS4 (aggrecanase-1) by tissue inhibitors of metalloproteinases (TIMP-1, 2, 3 and 4)." FEBS Lett 494(3): 192-5.

Hassell, J. R., J. H. Kimura, et al. (1986). "Proteoglycan Core Protein Families." Annual Review of Biochemistry 55: 539-567.

Hayashi, K., J. D. Frank, et al. (2003). "Evaluation of ligament fibroblast viability in ruptured cranial cruciate ligament of dogs." American Journal of Veterinary Research 64(8): 1010-1016.

Hayashi, K. Bhandal, et al. (2011). " Immunohistochemical and histomorphometric evaluation of vascular distribution in intact canine cranial cruciate ligament." Veterinary Surgery 40(2): 192-7.

Hedbom, E. and D. Heinegard (1993). "Binding of fibromodulin and decorin to separate sites on fibrillar collagens." J Biol Chem 268(36): 27307-27312.

Heffron, L. E. and J. R. Campbell (1978). "Morphology, histology and functional anatomy of the canine cranial cruciate ligament." The Veterinary Record 102(13): 280-283.

Henninger, H. B., C. J. Underwood, et al. (2010). "Effect of sulfated glycosaminoglycan digestion on the transverse permeability of medial collateral ligament." Journal of Biomechanics 43(13): 2567-2573.

Huisman, E. S., G. Andersson, et al. (2014). "Regional molecular and cellular differences in the female rabbit Achilles tendon complex: potential implications for understanding responses to loading." J Anat 224(5): 538-547.

Igwe, J. C., Q. Gao, et al. (2011). "Keratocan is Expressed by Osteoblasts and Can Modulate Osteogenic Differentiation." Connective tissue research 52(5): 401-407.

Ilic, M. Z., P. Carter, et al. (2005). "Proteoglycans and catabolic products of proteoglycans present in ligament." Biochemical Journal 385(Pt 2): 381-388.

Imai, K., A. Hiramatsu, et al. (1997). "Degradation of decorin by matrix metalloproteinases: identification of the cleavage sites, kinetic analyses and

transforming growth factor-beta1 release." Biochemical Journal 322 (Pt 3): 809-814.

Iozzo, R. V. (1998). "Matrix proteoglycans: from molecular design to cellular function." Annu Rev Biochem 67: 609-652.

Iozzo, R. V. (1999). "The biology of the small leucine-rich proteoglycans - Functional network of interactive proteins." Journal of Biological Chemistry 274(27): 18843-18846.

Iozzo, R. V. and A. D. Murdoch (1996). "Proteoglycans of the extracellular environment: clues from the gene and protein side offer novel perspectives in molecular diversity and function." FASEB J 10(5): 598-614.

Iozzo, R. V. and L. Schaefer (2015). "Proteoglycan form and function: A comprehensive nomenclature of proteoglycans." Matrix biology 42: 11-55.

Isogai, Z., A. Aspberg, et al. (2002). "Versican interacts with fibrillin-1 and links extracellular microfibrils to other connective tissue networks." J Biol Chem 277(6): 4565-4572.

Ito, K., T. Shinomura, et al. (1995). "Multiple forms of mouse PG-M, a large chondroitin sulfate proteoglycan generated by alternative splicing." J Biol Chem 270(2): 958-965.

Ivie, T. J., R. C. Bray, et al. (2002). "Denervation impairs healing of the rabbit medial collateral ligament." Journal of orthopaedic research 20(5): 990-995.

Jacobsen, E., A. J. Dart, et al. (2015). "Focal experimental injury leads to widespread gene expression and histologic changes in equine flexor tendons." Plos One 10(4): e0122220.

Jauernig, S., A. Schweighauser, et al. (2001). "The effects of doxycycline on nitric oxide and stromelysin production in dogs with cranial cruciate ligament rupture." Veterinary Surgery 30(2): 132-139.

Jepsen, K. J., F. Wu, et al. (2002). "A syndrome of joint laxity and impaired tendon integrity in lumican- and fibromodulin-deficient mice." Journal of Biological Chemistry 277(38): 35532-35540.

Johansson, H., P. Sjolander, et al. (1991). "A sensory role for the cruciate ligaments." Clin Orthop Relat Res(268): 161-178.

Jones, G. C. and G. P. Riley (2005). "ADAMTS proteinases: a multi-domain, multi-functional family with roles in extracellular matrix turnover and arthritis." Arthritis Res Ther 7(4): 160-169.

Kadler, K. E., C. Baldock, et al. (2007). "Collagens at a glance." Journal of Cell Science 120(12): 1955-1958.

Kalamajski, S., A. Aspberg, et al. (2009). "Asporin competes with decorin for collagen binding, binds calcium and promotes osteoblast collagen mineralization." Biochemical Journal 423: 53-59.

Kalamajski, S. and A. Oldberg (2007). "Fibromodulin binds collagen type I via Glu-353 and Lys-355 in leucine-rich repeat 11." J Biol Chem 282(37): 26740-26745.

Kalamajski, S. and A. Oldberg (2009). "Homologous Sequence in Lumican and Fibromodulin Leucine-rich Repeat 5-7 Competes for Collagen Binding." Journal of Biological Chemistry 284(1): 534-539.

Kashiwagi, M., J. J. Enghild, et al. (2004). "Altered proteolytic activities of ADAMTS-4 expressed by C-terminal processing." J Biol Chem 279(11): 10109-10119.

Kastelic, J., A. Galeski, et al. (1978). "The multicomposite structure of tendon." Connect Tissue Res 6(1): 11-23.

Kavanagh, E. and D. E. Ashhurst (2001). "Distribution of biglycan and decorin in collateral and cruciate ligaments and menisci of the rabbit knee joint." Journal of Histochemistry & Cytochemistry 49(7): 877-885.

Kelwick, R., I. Desanlis, et al. (2015). "The ADAMTS (A Disintegrin and Metalloproteinase with Thrombospondin motifs) family." Genome Biology 16.

Kharaz, Y. A. (2015). "THE MOLECULAR AND CELLULAR DIFFERENCES BETWEEN TENDONS AND LIGAMENTS." PhD thesis, University of Liverpool.

Kiani, C., L. Chen, et al. (2002). "Structure and function of aggrecan." Cell Res 12(1): 19-32.

Kielty, C. M., M. J. Sherratt, et al. (2002). "Elastic fibres." Journal of Cell Science 115(14): 2817-2828.

Kilts, T., L. Ameye, et al. (2009). "Potential roles for the small leucine-rich proteoglycans biglycan and fibromodulin in ectopic ossification of tendon induced by exercise and in modulating rotarod performance." Scandinavian journal of medicine & science in sports 19(4): 536-546.

Kitagawa, H., Y. Tone, et al. (1998). "Molecular cloning and expression of glucuronyltransferase I involved in the biosynthesis of the glycosaminoglycan-protein linkage region of proteoglycans." Journal of Biological Chemistry 273(12): 6615-6618.

Kiviranta, I., M. Tammi, et al. (1988). "Moderate Running Exercise Augments Glycosaminoglycans and Thickness of Articular-Cartilage in the Knee-Joint of Young Beagle Dogs." Journal of orthopaedic research 6(2): 188-195.

Klein, L., J. S. Player, et al. (1982). "Isotopic evidence for resorption of soft tissues and bone in immobilized dogs." J Bone Joint Surg Am 64(2): 225-230.

Kobayashi, S., H. Baba, et al. (2006). "Microvascular system of anterior cruciate ligament in dogs." Journal of Orthopaedic Research 24(7): 1509-1520.

Krayer, M., U. Rytz, et al. (2008). "Apoptosis of ligamentous cells of the cranial cruciate ligament from stable stifle joints of dogs with partial cranial cruciate ligament rupture." American Journal of Veterinary Research 69(5): 625-630.

Krusius, T., K. R. Gehlsen, et al. (1987). "A Fibroblast Chondroitin Sulfate Proteoglycan Core Protein Contains Lectin-Like and Growth Factor-Like Sequences." Journal of Biological Chemistry 262(27): 13120-13125.

Laprade, R. F. and Q. M. Burnett (1994). "Femoral Intercondylar Notch Stenosis and Correlation to Anterior Cruciate Ligament Injuries - a Prospective-Study." American Journal of Sports Medicine 22(2): 198-203.

Legerlotz, K., G. P. Riley, et al. (2013). "GAG depletion increases the stress-relaxation response of tendon fascicles, but does not influence recovery." Acta Biomaterialia 9(6): 6860-6866.

Lehmann, O. J., M. F. El-ashry, et al. (2001). "A novel keratocan mutation causing autosomal recessive cornea plana." Invest Ophthalmol Vis Sci 42(13): 3118-3122.

Lin, W. Q., S. Shuster, et al. (1997). "Patterns of hyaluronan staining are modified by fixation techniques." Journal of Histochemistry & Cytochemistry 45(8): 1157-1163.

Liu, C. Y., D. E. Birk, et al. (2003). "Keratocan-deficient mice display alterations in corneal structure." Journal of Biological Chemistry 278(24): 21672-21677.

Lo, I. K. Y., L. Marchuk, et al. (2001). "Ligament cell are organized in a 3-D network that is disrupted during healing." Trans. Orthop. Res. Soc 26: 701.

Lo, I. K. Y., L. L. Marchuk, et al. (1998). "Comparison of mRNA levels for matrix molecules in normal and disrupted human anterior cruciate ligaments using reverse transcription polymerase chain reaction." Journal of Orthopaedic Research 16(4): 421-428.

Lo, I. K. Y., Y. Ou, et al. (2002). "The cellular networks of normal ovine medial collateral and anterior cruciate ligaments are not accurately recapitulated in scar tissue." Journal of Anatomy 200(3): 283-296.

Longpre, J. M., D. R. McCulloch, et al. (2009). "Characterization of proADAMTS5 processing by proprotein convertases." International Journal of Biochemistry & Cell Biology 41(5): 1116-1126.

Louis, E., K. A. Remer, et al. (2006). "Nitric oxide and metalloproteinases in canine articular ligaments: a comparison between the cranial cruciate, the medial genual collateral and the femoral head ligament." The Veterinary Journal 172(3): 466-472.

Lujan, T. J., C. J. Underwood, et al. (2007). "Effect of dermatan sulfate glycosaminoglycans on the quasi-static material properties of the human medial collateral ligament." Journal of orthopaedic research 25(7): 894-903.

Lujan, T. J., C. J. Underwood, et al. (2009). "Contribution of glycosaminoglycans to viscoelastic tensile behavior of human ligament." Journal of Applied Physiology 106(2): 423-431.

Maccarana, M., S. Kalamajski, et al. (2009). "Dermatan Sulfate Epimerase 1-Deficient Mice Have Reduced Content and Changed Distribution of Iduronic Acids in Dermatan Sulfate and an Altered Collagen Structure in Skin." Molecular and Cellular Biology 29(20): 5517-5528.

Macias, C., W. M. McKee, et al. (2002). "Caudal proximal tibial deformity and cranial cruciate ligament rupture in small-breed dogs." Journal of Small Animal Practice 43(10): 433-438.

Majava, M., P. N. Bishop, et al. (2007). "Novel mutations in the small leucine-rich repeat protein/proteoglycan (SLRP) genes in high myopia." Hum Mutat 28(4): 336-344.

Malfait, F., A. Kariminejad, et al. (2013). "Defective Initiation of Glycosaminoglycan Synthesis due to B3GALT6 Mutations Causes a Pleiotropic Ehlers-Danlos-Syndrome-like Connective Tissue Disorder." American Journal of Human Genetics 92(6): 935-945.

Margolis, R. U. and R. K. Margolis (1994). "Aggrecan-versican-neurocan family proteoglycans." Methods Enzymol 245: 105-126.

Marianayagam, N. J., M. Sunde, et al. (2004). "The power of two: protein dimerization in biology." Trends Biochem Sci 29(11): 618-25.

Matias, M. A., H. Li, et al. (2003). "Immunohistochemical localization of fibromodulin in the periodontium during cementogenesis and root formation in the rat molar." Journal of Periodontal Research 38(5): 502-507.

Matuszewski, P. E., Y. L. Chen, et al. (2012). "Regional variation in human supraspinatus tendon proteoglycans: decorin, biglycan, and aggrecan." Connect Tissue Res 53(5): 343-348.

McEwan, P. A., P. G. Scott, et al. (2006). "Structural correlations in the family of small leucine-rich repeat proteins and proteoglycans." Journal of Structural Biology 155(2): 294-305.

McNeilly, C. M. (1997). "Tendon cells in vivo form a three dimensional network of cell processes linked by gap junctions (vol 189, pg 593, 1996)." Journal of Anatomy 190: 477-478.

Melching, L. I., W. D. Fisher, et al. (2006). "The cleavage of biglycan by aggrecanases." Osteoarthritis and cartilage 14(11): 1147-1154.

Melrose, J., E. S. Fuller, et al. (2008). "Fragmentation of decorin, biglycan, lumican and keratocan is elevated in degenerate human meniscus, knee and hip articular cartilages compared with age-matched macroscopically normal and control tissues." Arthritis Research & Therapy 10(4).

Melrose, J., S. Smith, et al. (2005). "Perlecan displays variable spatial and temporal immunolocalisation patterns in the articular and growth plate cartilages of the ovine stifle joint." Histochemistry and Cell Biology 123(6): 561-571.

Millesi, H., R. Reihsner, et al. (1995). "Biomechanical properties of normal tendons, normal palmar aponeuroses and palmar aponeuroses from patients with Dupuytren's disease subjected to elastase and chondroitinase treatment." Connect Tissue Res 31(2): 109-115.

Milligan, D. L. and D. E. Koshland, Jr. (1988). "Site-directed cross-linking. Establishing the dimeric structure of the aspartate receptor of bacterial chemotaxis." J Biol Chem 263(13): 6268-6275.

Miyagawa, A., M. Kobayashi, et al. (2001). "Surface ultrastructure of collagen fibrils and their association with proteoglycans in human cornea and sclera by atomic force microscopy and energy-filtering transmission electron microscopy." Cornea 20(6): 651-656.

Monfort, J., G. Tardif, et al. (2006). "Degradation of small leucine-rich repeat proteoglycans by matrix metalloprotease-13: identification of a new biglycan cleavage site." Arthritis Research & Therapy 8(1).

Moore, K. W. and R. A. Read (1995). "Cranial Cruciate Ligament Rupture in the Dog - a Retrospective Study Comparing Surgical Techniques." Australian Veterinary Journal 72(8): 281-285.

Mostafa, A. A., D. J. Griffon, et al. (2009). "Morphometric characteristics of the pelvic limbs of Labrador Retrievers with and without cranial cruciate ligament deficiency." American journal of veterinary research 70(4): 498-507.

Muir, P., Z. Schwartz, et al. (2011). "Contralateral Cruciate Survival in Dogs with Unilateral Non-Contact Cranial Cruciate Ligament Rupture." Plos One 6(10).

Muneta, T., K. Takakuda, et al. (1997). "Intercondylar notch width and its relation to the configuration and cross-sectional area of the anterior cruciate ligament. A cadaveric knee study." Am J Sports Med 25(1): 69-72.

Murray, M. M. and M. Spector (1999). "Fibroblast distribution in the anteromedial bundle of the human anterior cruciate ligament: the presence of alpha-smooth muscle actin-positive cells." J Orthop Res 17(1): 18-27.

Murray, M. M., K. P. Spindler, et al. (2007). "Enhanced histologic repair in a central wound in the anterior cruciate ligament with a collagen-platelet-rich plasma scaffold." Journal of Orthopaedic Research 25(8): 1007-1017.

Myllyharju, J. and K. I. Kivirikko (2004). "Collagens, modifying enzymes and their mutations in humans, flies and worms." Trends in Genetics 20(1): 33-43.

Nagineni, C. N., D. Amiel, et al. (1992). "Characterization of the intrinsic properties of the anterior cruciate and medial collateral ligament cells: an in vitro cell culture study." Journal of Orthopaedic Research 10(4): 465-475.

Nakagawa, H., Y. Mikawa, et al. (1994). "Elastin in the Human Posterior Longitudinal Ligament and Spinal Dura - a Histologic and Biochemical-Study." Spine 19(19): 2164-2169.

Narama, I., M. Masuoka-Nishiyama, et al. (1996). "Morphogenesis of degenerative changes predisposing dogs to rupture of the cranial cruciate ligament." J Vet Med Sci 58(11): 1091-1097.

Naso, M. F., J. L. Morgan, et al. (1995). "Expression pattern and mapping of the murine versican gene (Cspg2) to chromosome 13." Genomics 29(1): 297-300.

Nathan, C. (1992). "Nitric-Oxide as a Secretory Product of Mammalian-Cells." Faseb Journal 6(12): 3051-3064.

Newton, P. M., V. C. Mow, et al. (1997). "Winner of the 1996 Cabaud Award. The effect of lifelong exercise on canine articular cartilage." Am J Sports Med 25(3): 282-287.

Nielen, A. L., B. W. Knol, et al. (2003). "[Genetic and epidemiological investigation of a birth cohort of boxers]." Tijdschr Diergeneeskd 128(19): 586-590.

O'Connor, B. L. and P. Woodbury (1982). "The primary articular nerves to the dog knee." J Anat 134(Pt 3): 563-572.

Okajima, T., K. Yoshida, et al. (1999). "Human homolog of Caenorhabditis elegans sqv-3 gene is galactosyltransferase I involved in the biosynthesis of the glycosaminoglycan-protein linkage region of proteoglycans." Journal of Biological Chemistry 274(33): 22915-22918.

Oohira, A., F. Matsui, et al. (1994). "Developmentally regulated expression of a brain specific species of chondroitin sulfate proteoglycan, neurocan, identified with a monoclonal antibody IG2 in the rat cerebrum." Neuroscience 60(1): 145-157.

Orgel, J. P. R. O., A. Eid, et al. (2009). "Decorin Core Protein (Decoron) Shape Complements Collagen Fibril Surface Structure and Mediates Its Binding." Plos One 4(9).

Paatsama, S. (1952). "Ligament injuries in the canine stifle joint."

Parkinson, J., T. Samiric, et al. (2010). "Change in Proteoglycan Metabolism Is a Characteristic of Human Patellar Tendinopathy." Arthritis Rheum 62(10): 3028-3035.

Parry, D. A. D., M. H. Flint, et al. (1982). "A Role for Glycosaminoglycans in the Development of Collagen Fibrils." FEBS Lett 149(1): 1-7.

Pietraszek, K., A. Chatron-Colliet, et al. (2014). "Lumican: a new inhibitor of matrix metalloproteinase-14 activity." FEBS Lett 588(23): 4319-4324.

Plaas, A., J. D. Sandy, et al. (2011). "Biochemical Identification and Immunolocalizaton of Aggrecan, ADAMTS5 and Inter-Alpha-Trypsin-Inhibitor in Equine Degenerative Suspensory Ligament Desmitis." Journal of orthopaedic research 29(6): 900-906.

Plaas, A. H. K., P. J. Neame, et al. (1990). "Identification of the Keratan Sulfate Attachment Sites on Bovine Fibromodulin." Journal of Biological Chemistry 265(33): 20634-20640.

Porter, S., I. M. Clark, et al. (2005). "The ADAMTS metalloproteinases." Biochemical Journal 386(Pt 1): 15-27.

Pringle, G. A. and C. M. Dodd (1990). "Immunoelectron microscopic localization of the core protein of decorin near the d and e bands of tendon collagen fibrils by use of monoclonal antibodies." Journal of Histochemistry & Cytochemistry 38(10): 1405-1411.

Quasnichka, H. L., J. M. Anderson-MacKenzie, et al. (2005). "Cruciate ligament laxity and femoral intercondylar notch narrowing in early-stage knee osteoarthritis." Arthritis Rheum 52(10): 3100-3109.

Ragetly, C. A., D. J. Griffon, et al. (2010). "Inverse Dynamics Analysis of the Pelvic Limbs in Labrador Retrievers With and Without Cranial Cruciate Ligament Disease." Veterinary Surgery 39(4): 513-522.

Ragetly, C. A., D. J. Griffon, et al. (2008). "Noninvasive determination of body segment parameters of the hind limb in Labrador Retrievers with and without cranial cruciate ligament disease." American journal of veterinary research 69(9): 1188-1196.

Rauch, U., L. Karthikeyan, et al. (1992). "Cloning and primary structure of neurocan, a developmentally regulated, aggregating chondroitin sulfate proteoglycan of brain." J Biol Chem 267(27): 19536-19547.

Read, R. A. and G. M. Robins (1982). "Deformity of the proximal tibia in dogs." Veterinary Record 111(13): 295-298.

Redaelli, A., S. Vesentini, et al. (2003). "Possible role of decorin glycosaminoglycans in fibril to fibril force transfer in relative mature tendons - a computational study from molecular to microstructural level." Journal of Biomechanics 36(10): 1555-1569.

Rees, S., C. Flannery, et al. (2000). "Catabolism of aggrecan, decorin and biglycan in tendon." Biochem. J 350: 181-188.

Rees, S. G., A. D. Waggett, et al. (2009). "Immunolocalisation and expression of keratocan in tendon." Osteoarthritis Cartilage 17(2): 276-279.

Reif, U. and C. W. Probst (2003). "Comparison of tibial plateau angles in normal and cranial cruciate deficient stifles of Labrador retrievers." Veterinary Surgery 32(4): 385-389.

Reinboth, B., E. Hanssen, et al. (2002). "Molecular interactions of biglycan and decorin with elastic fiber components: biglycan forms a ternary complex with tropoelastin and microfibril-associated glycoprotein 1." J Biol Chem 277(6): 3950-3957.

Renstrom, P., A. Ljungqvist, et al. (2008). "Non-contact ACL injuries in female athletes: an International Olympic Committee current concepts statement." British journal of sports medicine 42(6): 394-412.

Rigozzi, S., R. Muller, et al. (2009). "Local strain measurement reveals a varied regional dependence of tensile tendon mechanics on glycosaminoglycan content." Journal of Biomechanics 42(10): 1547-1552.

Rigozzi, S., R. Muller, et al. (2013). "Tendon glycosaminoglycan proteoglycan sidechains promote collagen fibril sliding-AFM observations at the nanoscale." Journal of Biomechanics 46(4): 813-818.

Riley, G. (2004). "Tendon and ligament biochemistry and pathology." Soft tissue rheumatology: 20-53.

Riley, G. (2005). "Chronic tendon pathology: molecular basis and therapeutic implications." Expert Reviews in Molecular Medicine 7(5): 1-25.

Riley, G. P., R. L. Harrall, et al. (1994a). "Glycosaminoglycans of human rotator cuff tendons: changes with age and in chronic rotator cuff tendinitis." Annals of the rheumatic diseases 53(6): 367-376.

Riley, G. P., R. L. Harrall, et al. (1994b). "Tendon degeneration and chronic shoulder pain: changes in the collagen composition of the human rotator cuff tendons in rotator cuff tendinitis." Ann Rheum Dis 53(6): 359-366.

Ritty, T. M., R. Roth, et al. (2003). "Tendon cell array isolation reveals a previously unknown fibrillin-2-containing macromolecular assembly." Structure 11(9): 1179-1188.

Robbins, J. R., S. P. Evanko, et al. (1997). "Mechanical loading and TGF-beta regulate proteoglycan synthesis in tendon." Arch Biochem Biophys 342(2): 203-211.

Robinson, P. S., T.-F. Huang, et al. (2005). "Influence of decorin and biglycan on mechanical properties of multiple tendons in knockout mice." Journal of biomechanical engineering 127(1): 181-185.

Rosc, D., W. Powierza, et al. (2002). "Post-traumatic plasminogenesis in intraarticular exudate in the knee joint." Med Sci Monit 8(5): CR371-378.

Rosenberg, L. C., H. U. Choi, et al. (1986). "Biological Roles of Dermatan Sulfate Proteoglycans." Ciba Foundation Symposia 124: 47-68.

Ruehland, C., E. Schonherr, et al. (2007). "The glycosaminoglycan chain of decorin plays an important role in collagen fibril formation at the early stages of fibrillogenesis." Febs Journal 274(16): 4246-4255.

Rumian, A. P., A. L. Wallace, et al. (2007). "Tendons and ligaments are anatomically distinct but overlap in molecular and morphological features - A comparative study in an ovine model." Journal of orthopaedic research 25(4): 458-464.

Salo, P. (1999). "The role of joint innervation in the pathogenesis of arthritis." Canadian Journal of Surgery 42(2): 91-100.

Samiric, T., M. Z. Ilic, et al. (2004). "Characterisation of proteoglycans and their catabolic products in tendon and explant cultures of tendon." Matrix biology 23(2): 127-140.

Samiric, T., J. Parkinson, et al. (2009). "Changes in the composition of the extracellular matrix in patellar tendinopathy." Matrix Biol 28(4): 230-236.

Sandy, J. D., J. Westling, et al. (2001). "Versican V1 proteolysis in human aorta in vivo occurs at the Glu441-Ala442 bond, a site that is cleaved by recombinant ADAMTS-1 and ADAMTS-4." Journal of Biological Chemistry 276(16): 13372-13378.

Sato, S., F. Rahemtulla, et al. (1985). "Proteoglycans of Adult Bovine Compact-Bone." Connective tissue research 14(1): 65-75.

Schaefer, L. (2011). "Small leucine-rich proteoglycans in kidney disease." J Am Soc Nephrol 22(7): 1200-1207.

Schaefer, L. and R. V. Iozzo (2008). "Biological functions of the small leucine-rich proteoglycans: from genetics to signal transduction." J Biol Chem 283(31): 21305-21309.

Schaefer, L. and R. M. Schaefer (2010). "Proteoglycans: from structural compounds to signaling molecules." Cell and Tissue Research 339(1): 237-246.

Schmalfeldt, M., M. a. T. Dours-Zimmermann, et al. (1998). "Versican V2 is a major extracellular matrix component of the mature bovine brain." Journal of Biological Chemistry 273(25): 15758-15764.

Schmittgen, T. D. and B. A. Zakrajsek (2000). "Effect of experimental treatment on housekeeping gene expression: validation by real-time, quantitative RT-PCR." Journal of Biochemical and Biophysical Methods 46(1-2): 69-81.

Schmitz, N., S. Laverty, et al. (2010). "Basic methods in histopathology of joint tissues." Osteoarthritis Cartilage 18 Suppl 3: S113-116.

Schonherr, E., H. T. Jarvelainen, et al. (1991). "Effects of platelet-derived growth factor and transforming growth factor-beta 1 on the synthesis of a large versican-like chondroitin sulfate proteoglycan by arterial smooth muscle cells." J Biol Chem 266(26): 17640-17647.

Schonherr, E., P. Witschprehm, et al. (1995). "Interaction of Biglycan with Type-I Collagen." Journal of Biological Chemistry 270(6): 2776-2783.

Scott, I. C., I. L. Blitz, et al. (1999). "Mammalian BMP-1/tolloid-related metalloproteinases, including novel family member mammalian tolloid-like 2, have differential enzymatic activities and distributions of expression relevant to patterning and skeletogenesis." Dev Biol 213(2): 283-300.

Scott, J. E. (1996). "Proteodermatan and proteokeratan sulfate (decorin, lumican/fibromodulin) proteins are horseshoe shaped. Implications for their interactions with collagen." Biochemistry 35(27): 8795-8799.

Scott, J. E. and M. Haigh (1988). "Identification of Specific Binding-Sites for Keratan Sulfate Proteoglycans and Chondroitin Dermatan Sulfate Proteoglycans on Collagen Fibrils in Cornea by the Use of Cupromeronic Blue in Critical-Electrolyte-Concentration Techniques." Biochemical Journal 253(2): 607-610.

Scott, J. E., C. R. Orford, et al. (1981). "Proteoglycan-collagen arrangements in developing rat tail tendon. An electron microscopical and biochemical investigation." Biochem J 195(3): 573-581.

Scott, P. G., P. A. McEwan, et al. (2004). "Crystal structure of the dimeric protein core of decorin, the archetypal small leucine-rich repeat proteoglycan." Proc Natl Acad Sci U S A 101(44): 15633-15638.

Selmi, A. L. and J. G. Padilha Filho (2001). "Rupture of the cranial cruciate ligament associated with deformity of the proximal tibia in five dogs." J Small Anim Pract 42(8): 390-393.

Sharon, N. (1986). "IUPAC-IUB Joint Commission on Biochemical Nomenclature (JCBN). Nomenclature of glycoproteins, glycopeptides and peptidoglycans. Recommendations 1985." European Journal of Biochemistry 159(1): 1-6.

Shelbourne, K. D., T. J. Davis, et al. (1998). "The relationship between intercondylar notch width of the femur and the incidence of anterior cruciate ligament tears - A prospective study." American Journal of Sports Medicine 26(3): 402-408.

Simons, B. L., M. C. King, et al. (2002). "Covalent cross-linking of proteins without chemical reagents." Protein Science 11(6): 1558-1564.

Slauterbeck, J. R., K. Pankratz, et al. (2004). "Canine ovariohysterectomy and orchiectomy increases the prevalence of ACL injury." Clinical Orthopaedics and Related Research 429: 301-305.

Smith, K. D., P. D. Clegg, et al. (2014). "Elastin content is high in the canine cruciate ligament and is associated with degeneration." Vet J 199(1): 169-174.

Smith, K. D., A. Vaughan-Thomas, et al. (2012). "Variations in cell morphology in the canine cruciate ligament complex." Vet J 193(2): 561-566.

Smith, S. M., C. Shu, et al. (2010). "Comparative immunolocalisation of perlecan with collagen II and aggrecan in human foetal, newborn and adult ovine joint tissues demonstrates perlecan as an early developmental chondrogenic marker." Histochemistry and Cell Biology 134(3): 251-263.

Spindler, K. P., J. T. Andrish, et al. (1996). "Distribution of cellular repopulation and collagen synthesis in a canine anterior cruciate ligament autograft." Journal of Orthopaedic Research 14(3): 384-389.

Spindler, K. P., C. Devin, et al. (2006). "The central ACL defect as a model for failure of intra-articular healing." Journal of Orthopaedic Research 24(3): 401-406.

Spreng, D., N. Sigrist, et al. (2000). "Nitric oxide metabolite production in the cranial cruciate ligament, synovial membrane, and articular cartilage of dogs with cranial cruciate ligament rupture." American Journal of Veterinary Research 61(5): 530-536.

Sridharan, G. and A. A. Shankar (2012). "Toluidine blue: A review of its chemistry and clinical utility." J Oral Maxillofac Pathol 16(2): 251-255.

Stein, V., L. Li, et al. (2010). "The relation of femoral notch stenosis to ACL tears in persons with knee osteoarthritis." Osteoarthritis and cartilage 18(2): 192-199.

Stouffer, D. C., D. L. Butler, et al. (1983). "Tension-torsion characteristics of the canine anterior cruciate ligament—Part I: Theoretical framework." Journal of biomechanical engineering 105(2): 154-159.

Svensson, L., A. Aszodi, et al. (1999). "Fibromodulin-null mice have abnormal collagen fibrils, tissue organization, and altered lumican deposition in tendon." Journal of Biological Chemistry 274(14): 9636-9647.

Svensson, L., D. Heinegard, et al. (1995). "Decorin-Binding Sites for Collagen Type-I Are Mainly Located in Leucine-Rich Repeats 4-5." Journal of Biological Chemistry 270(35): 20712-20716.

Svensson, L., I. Narlid, et al. (2000). "Fibromodulin and lumican bind to the same region on collagen type I fibrils." FEBS Lett 470(2): 178-182.

Sztrolovics, R., R. J. White, et al. (1999). "Resistance of small leucine-rich repeat proteoglycans to proteolytic degradation during interleukin-1-stimulated cartilage catabolism." Biochemical Journal 339 (Pt 3): 571-577.

Talwar, G. P. (2016). Chapter 3: "Proteins: Chemistry-Structure-Conformation". Textbook of Biochemistry, Biotechnology, Allied and Molecular Medicine, 4th edition. 27-35.

Tang, Z. Y., L. Yang, et al. (2009). "Contributions of Different Intraarticular Tissues to the Acute Phase Elevation of Synovial Fluid MMP-2 following Rat ACL Rupture." Journal of Orthopaedic Research 27(2): 243-248.

Tipton, C. M., R. D. Matthes, et al. (1975). "The influence of physical activity on ligaments and tendons." Med Sci Sports 7(3): 165-175.

Tirgari, M. (1978). "The surgical significance of the blood supply of the canine stifle joint." J Small Anim Pract 19(8): 451-462.

Tirgari, M. and L. C. Vaughan (1975). "Arthritis of the canine stifle joint." Vet Rec 96(18): 394-399.

Tortorella, M. D., E. C. Arner, et al. (2005). "ADAMTS-4 (aggrecanase-1): N-Terminal activation mechanisms." Archives of biochemistry and biophysics 444(1): 34-44.

Trowbridge, J. M. and R. L. Gallo (2002). "Dermatan sulfate: new functions from an old glycosaminoglycan." Glycobiology 12(9): 117r-125r.

Unsold, C., W. N. Pappano, et al. (2002). "Biosynthetic processing of the pro-alpha 1(V)2pro-alpha 2(V) collagen heterotrimer by bone morphogenetic protein-1 and furin-like proprotein convertases." J Biol Chem 277(7): 5596-5602.

Varelas, J. B., N. R. Zenarosa, et al. (1991). "Agarose Polyacrylamide Minislab Gel-Electrophoresis of Intact Cartilage Proteoglycans and Their Proteolytic Degradation Products." Analytical biochemistry 197(2): 396-400.

Vasseur, P. B., R. R. Pool, et al. (1985). "Correlative Biomechanical and Histologic-Study of the Cranial Cruciate Ligament in Dogs." American Journal of Veterinary Research 46(9): 1842-1854.

Vesentini, S., A. Redaelli, et al. (2005). "Estimation of the binding force of the collagen molecule-decorin core protein complex in collagen fibril." Journal of Biomechanics 38(3): 433-443.

Vogel, K. (2004). "What happens when tendons bend and twist? Proteoglycans." J Musculoskelet Neuronal Interact 4(2): 202-203.

Vogel, K. G. and D. Heinegård (1985). "Characterization of proteoglycans from adult bovine tendon." Journal of Biological Chemistry 260(16): 9298-9306.

Vogel, K. G. and T. J. Koob (1989). "Structural specialization in tendons under compression." Int Rev Cytol 115: 267-293.

Vogel, K. G., A. Ordog, et al. (1993). "Proteoglycans in the compressed region of human tibialis posterior tendon and in ligaments." J Orthop Res 11(1): 68-77.

Vogel, K. G., M. Paulsson, et al. (1984). "Specific-Inhibition of Type-I and Type-Ii Collagen Fibrillogenesis by the Small Proteoglycan of Tendon." Biochemical Journal 223(3): 587-597.

Vogel, K. G. and J. A. Peters (2005). "Histochemistry defines a proteoglycan-rich layer in bovine flexor tendon subjected to bending." J Musculoskelet Neuronal Interact 5(1): 64-69.

Vogel, K. G., J. D. Sandy, et al. (1994). "Aggrecan in bovine tendon." Matrix Biol 14(2): 171-179.

Wada, M., H. Tatsuo, et al. (1999). "Femoral intercondylar notch measurements in osteoarthritic knees." Rheumatology (Oxford) 38(6): 554-558.

Waggett, A. D., J. R. Ralphs, et al. (1998). "Characterization of collagens and proteoglycans at the insertion of the human Achilles tendon." Matrix biology 16(8): 457-470.

Wang, V. M., R. M. Bell, et al. (2012). "Murine tendon function is adversely affected by aggrecan accumulation due to the knockout of ADAMTS5." Journal of orthopaedic research 30(4): 620-626.

Weber, I. T., R. W. Harrison, et al. (1996). "Model structure of decorin and implications for collagen fibrillogenesis." J Biol Chem 271(50): 31767-31770.

Whitehair, J. G., P. B. Vasseur, et al. (1993). "Epidemiology of Cranial Cruciate Ligament Rupture in Dogs." Journal of the American Veterinary Medical Association 203(7): 1016-1019.

Wiberg, C., E. Hedbom, et al. (2001). "Biglycan and decorin bind close to the n-terminal region of the collagen VI triple helix." J Biol Chem 276(22): 18947-18952.

Wiberg, C., A. R. Klatt, et al. (2003). "Complexes of matrilin-1 and biglycan or decorin connect collagen VI microfibrils to both collagen II and aggrecan." Journal of Biological Chemistry 278(39): 37698-37704.

Widmer, W. R., K. A. Buckwalter, et al. (1994). "Radiographic and Magnetic-Resonance-Imaging of the Stifle Joint in Experimental Osteoarthritis of Dogs." Veterinary Radiology & Ultrasound 35(5): 371-383.

Wilke, V. L., M. G. Conzemius, et al. (2006). "Inheritance of rupture of the cranial cruciate ligament in Newfoundlands." J Am Vet Med Assoc 228(1): 61-64.

Williamson, K. (2012). "Loss of Vascular Homeostasis with Age: Correlation of Structural Changes in Endothelial Glycosaminoglycans with Endothelial Progenitor Cell Function." PhD thesis, University of Manchester.

Wingfield, C., A. A. Amis, et al. (2000a). "Comparison of the biomechanical properties of rottweiler and racing greyhound cranial cruciate ligaments." J Small Anim Pract 41(7): 303-307.

Wingfield, C., A. A. Amis, et al. (2000b). "Cranial cruciate stability in the rottweiler and racing greyhound: an in vitro study." J Small Anim Pract 41(5): 193-197.

Witsberger, T. H., J. A. Villamil, et al. (2008). "Prevalence of and risk factors for hip dysplasia and cranial cruciate ligament deficiency in dogs." Javma-Journal of the American Veterinary Medical Association 232(12): 1818-1824.

Woo, S., J. Maynard, et al. (1988). "Ligament, tendon, and joint capsule insertions to bone. In: Woo S L-Y, Buckwalter JA (eds) Injury and repair of the musculoskeletal soft tissues." American Academy of Orthopaedic Surgeons: 133-166.

Wustefeld-Janssens, B. G., R. A. Pettitt, et al. (2015). "Peak Vertical Force and Vertical Impulse in Dogs With Cranial Cruciate Ligament Rupture and Meniscal Injury." Vet Surg.

Xu, T., P. Bianco, et al. (1998). "Targeted disruption of the biglycan gene leads to an osteoporosis-like phenotype in mice." Nat Genet 20(1): 78-82.

Yahia, L. H. and G. Drouin (1989). "Microscopical investigation of canine anterior cruciate ligament and patellar tendon: collagen fascicle morphology and architecture." J Orthop Res 7(2): 243-251.

Yamada, H., K. Watanabe, et al. (1994). "Molecular cloning of brevican, a novel brain proteoglycan of the aggrecan/versican family." J Biol Chem 269(13): 10119-10126.

Yamagata, T., H. Saito, et al. (1968). "Purification and properties of bacterial chondroitinases and chondrosulfatases." J Biol Chem 243(7): 1523-1535.

Yamagishi, K., K. Suzuki, et al. (2003). "Purification, characterization, and molecular cloning of a novel keratan sulfate hydrolase, endo-β-N-acetylglucosaminidase, from Bacillus circulans." Journal of Biological Chemistry 278(28): 25766-25772.

Yang, C. H., G. J. Culshaw, et al. (2012). "Canine tissue-specific expression of multiple small leucine rich proteoglycans." Vet J.

Zhang, G., S. Chen, et al. (2009). "Genetic evidence for the coordinated regulation of collagen fibrillogenesis in the cornea by decorin and biglycan." J Biol Chem 284(13): 8888-8897.

Zhang, G., Y. Ezura, et al. (2006). "Decorin regulates assembly of collagen fibrils and acquisition of biomechanical properties during tendon development." Journal of cellular biochemistry 98(6): 1436-1449.

Zheng, J., W. Luo, et al. (1998). "Aggrecan synthesis and secretion. A paradigm for molecular and cellular coordination of multiglobular protein folding and intracellular trafficking." J Biol Chem 273(21): 12999-13006.

Zhou, T., P. N. Grimshaw, et al. (2009). "A biomechanical investigation of the anteromedial and posterolateral bands of the porcine anterior cruciate ligament." Proc Inst Mech Eng H 223(6): 767-775.

Zhu, J., X. Zhang, et al. (2012). "Ultrastructural and morphological characteristics of human anterior cruciate ligament and hamstring tendons." Anat Rec (Hoboken) 295(9): 1430-1436.

APPENDIX I – MATERIALS

1-bromo-3-chloropropane	B9673	Sigma-Aldrich, UK
2-mercaptoethanol	M-6250	Sigma-Aldrich, UK
2-propanol	19030	Sigma-Aldrich, UK
3, 3′-Diaminobenzidine tablets	D4293	Sigma, UK
6-aminohexanoic acid	07260	Sigma-Aldrich, UK
Acid-Phenol: Chloroform, pH 4.5	AM9720	Ambion, USA
Alcian Blue solution, pH 2.5	B8438	Sigma, UK
Ammonium Acetate 5 M	AM9070G	Ambion, USA
Anti-Mouse IgG AP Conjugate	S372B	Promega, UK
Benzamidine	12072	Sigma-Aldrich, UK
Bovine Serum Albumin	B4287	Sigma, UK
Carbazole	C5132	Sigma, UK
Cellulose Dialysis Membrane	133336	Spectrum labs, NL
Chondroitinase ABC	C2905	Sigma, UK
Chondroitinase AC	C2780	Sigma, UK
Cover slip 24x40 mm	12362118	Fisher scientific, UK
Cyanogen bromide	C91492	Sigma, UK
D-(+)-Glucuronic acid γ-lactone	05566	Sigma, UK
Diethanolamine buffer 10X	D8885	Sigma, UK
DNase I	AM2222	Ambion, USA
DNase I Buffer 10X	AM8170G	Ambion, USA
dNTP mix 100mM	BIO-39029	Bioline, UK
DPX Mountant for histology	06522	Sigma, UK

Eosin Y solution	318906-500ML	Sigma, UK
Formic acid	F0507	Sigma, UK
GlycoBlue™ Coprecipitant	AM9515	Ambion, USA
Goat serum	G9023	Sigma, UK
GoTaq(R) qPCR Master Mix	A6002	Promega, UK
Hematoxylin solution	03971	Sigma, UK
Hydrochloric acid	435570	Sigma, UK
Hydrogen peroxide solution	31642	Sigma, UK
Isopentane	270342	Sigma, UK
Keratanase I	100-810-1	AMS, UK
Keratanase II	100-812-1	AMS, UK
M-MLV-RT	M1701	Promega, UK
M-MLV-RT 5X	M531A	Promega, UK
Mouse monoclonal IgG	ab37355	Abcam, UK
Mouse monoclonal IgM	ab18401	Abcam, UK
N-Ethylmaleimide	E3876	Sigma-Aldrich, UK
Normal goat serum	S-1000	Vector laboratories, UK
Novex® Sharp Pre-stained Protein Standard	LC5800	Life technologies, UK
NUPAGE MES SDS Running Buffer (20x)	NP0002	Life technologies, UK
NUPAGE transfer buffer (20x)	NP0006-1	Life technologies, UK
NuPAGE® Novex 4-12% Bis-Tris Gel-10 well	NP0321BOX	Life technologies, UK
NuPAGE® Novex 4-12% Bis-Tris Gel-12 well	NP0322BOX	Life technologies, UK
Papain	P4762	Sigma-Aldrich, UK
Paraformaldehyde	28794.295	Prolabo, UK
Peroxidase conjugate-goat anti-mouse IgG	A8924	Sigma-Aldrich, UK
Peroxidase conjugate-goat anti-mouse IgM	A8786	Sigma-Aldrich, UK
Peroxidase conjugate-goat Anti-Rabbit IgG	A0545	Sigma-Aldrich, UK
PNPP tablets	37620	Fischer scientific, UK
POLY FROST	MSS61012S	Solmedia, UK
Rabbit polyclonal IgG abcam	ab27472	Abcam, UK
Random primers	C1181	Promega, UK
RNasin® Plus RNase Inhibitor	N2611	Promega, UK
Sodium azide	S2002	Sigma, UK
Sodium chloride	32038	Sigma, UK
Sodium hydroxide	S5881	Sigma, UK
Sodium tetraborate	221732	Sigma, UK
Sulphuric acid	450061Q	VWR, UK
TE, pH 8.0	AM9858	Ambion, USA
Trizol	15596-026	Life technologies, UK
Versican	12C5	DSHB, USA
Western Lightning Plus_ECL	NEL105001EA	Perkin Elmer, NL
Xylenes	534056	Sigma, UK

APPENDIX II – PRIMERS STANDARD CURVE PLOT

Plate I

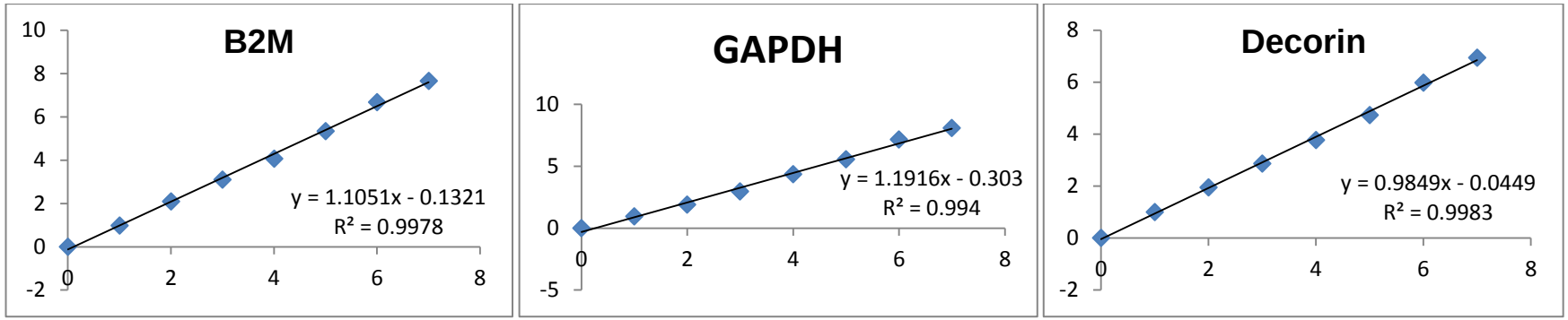

Plate II

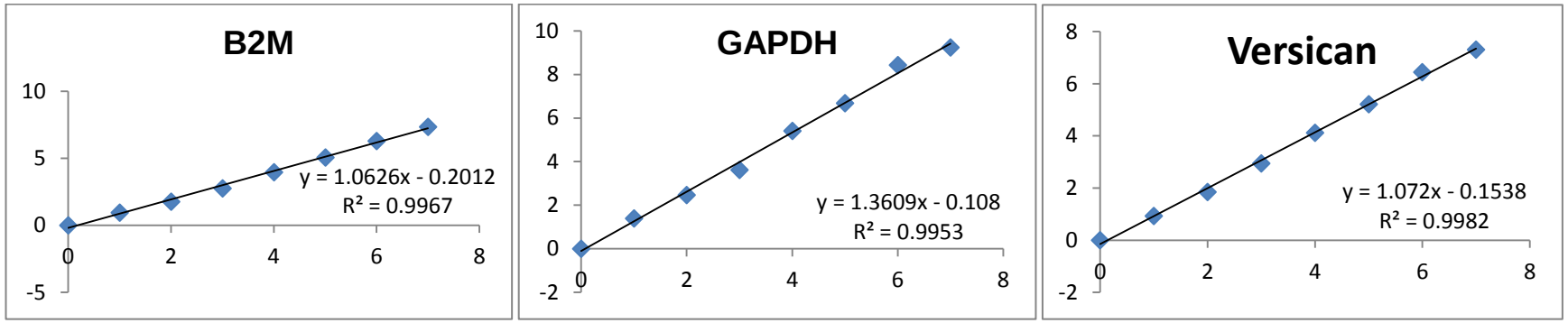
B2M
y = 1.0626x - 0.2012
R² = 0.9967
GAPDH
y = 1.3609x - 0.108
R² = 0.9953
Versican
y = 1.072x - 0.1538
R² = 0.9982

Plate III

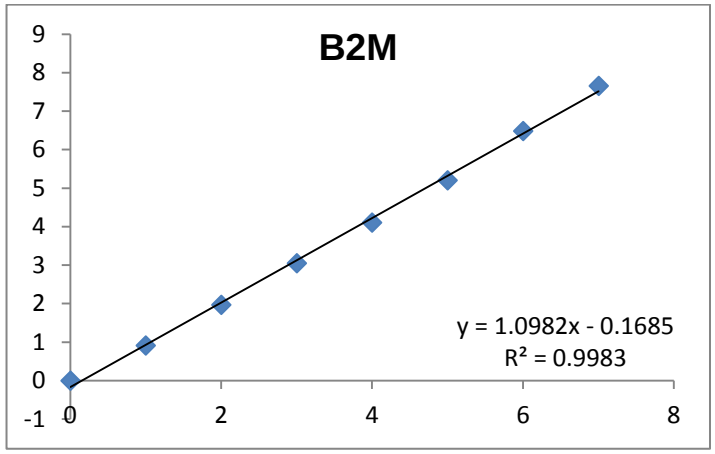
B2M
y = 1.0982x - 0.1685
R² = 0.9983

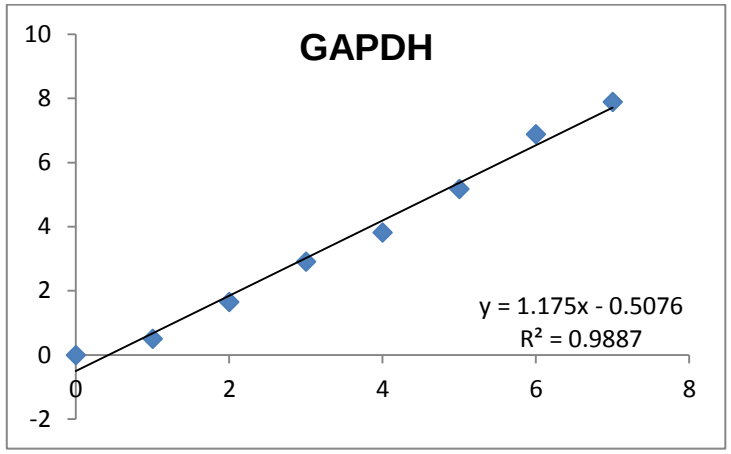
GAPDH
y = 1.175x - 0.5076
R² = 0.9887

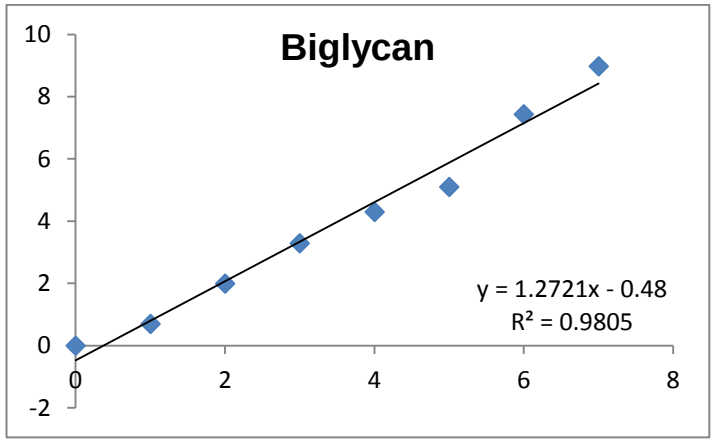
Biglycan
y = 1.2721x - 0.48
R² = 0.9805

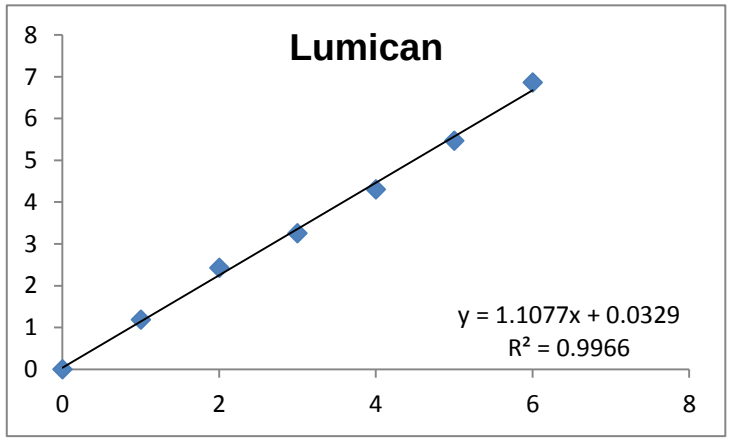
Lumican
y = 1.1077x + 0.0329
R² = 0.9966

Plate IV

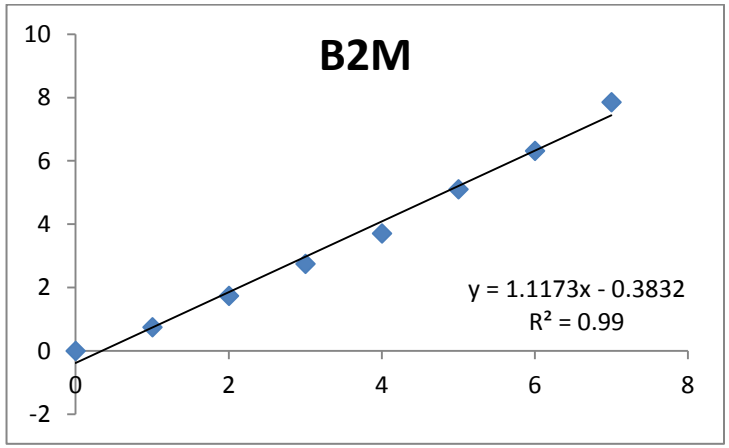
B2M
y = 1.1173x - 0.3832
R² = 0.99

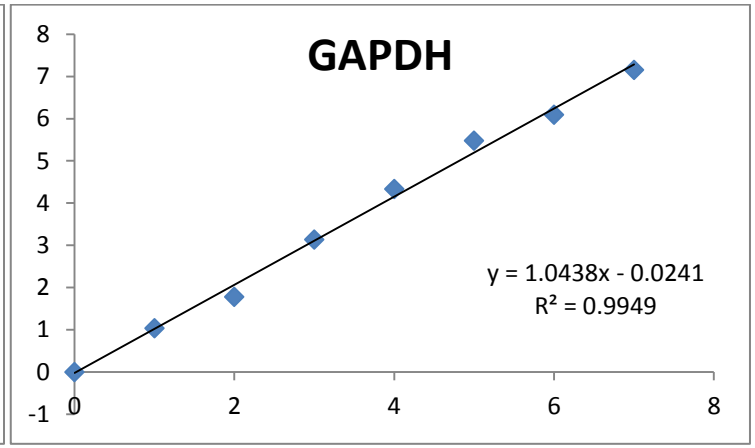
GAPDH
y = 1.0438x - 0.0241
R² = 0.9949

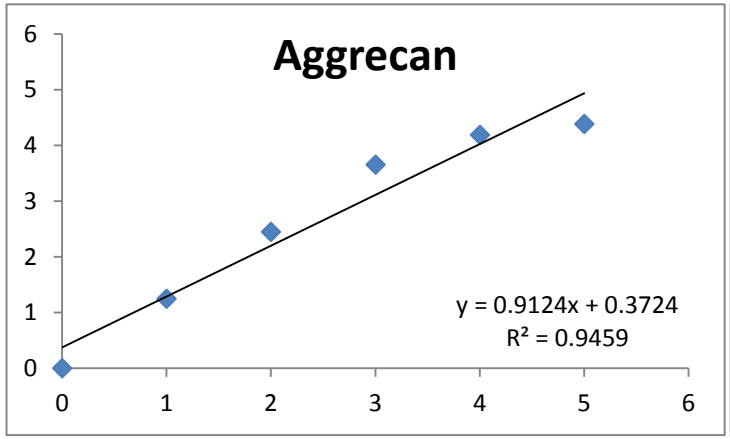
Aggrecan
y = 0.9124x + 0.3724
R² = 0.9459

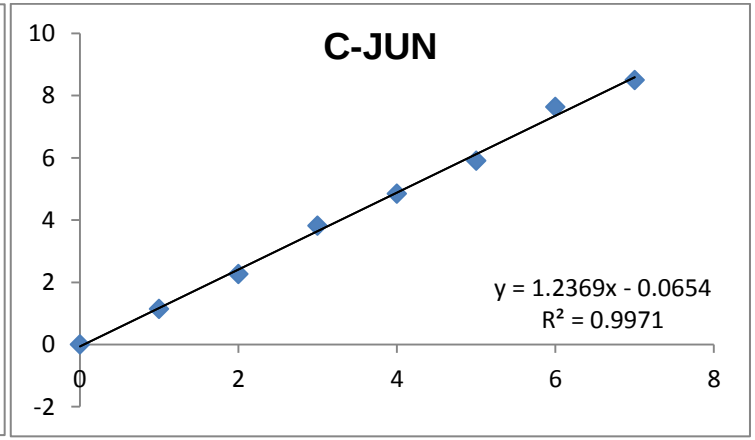
C-JUN
y = 1.2369x - 0.0654
R² = 0.9971

Plate V

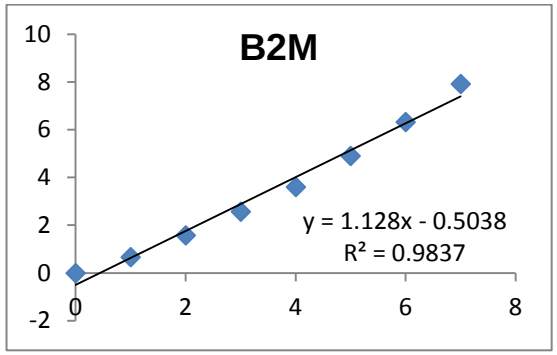
B2M
y = 1.128x - 0.5038
R² = 0.9837

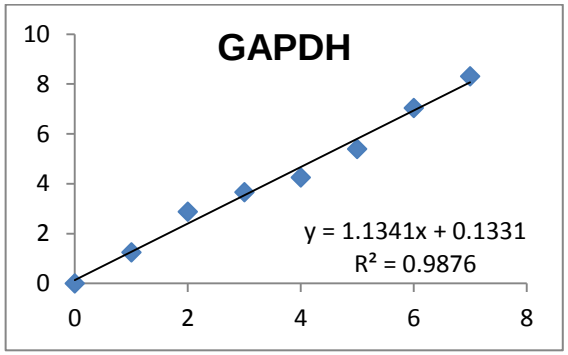
GAPDH
y = 1.1341x + 0.1331
R² = 0.9876

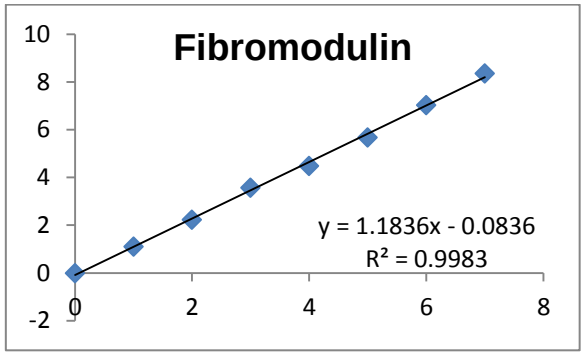
Fibromodulin
y = 1.1836x - 0.0836
R² = 0.9983

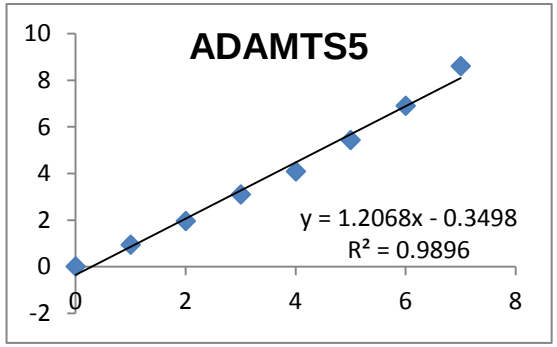
ADAMTS5
y = 1.2068x - 0.3498
R² = 0.9896

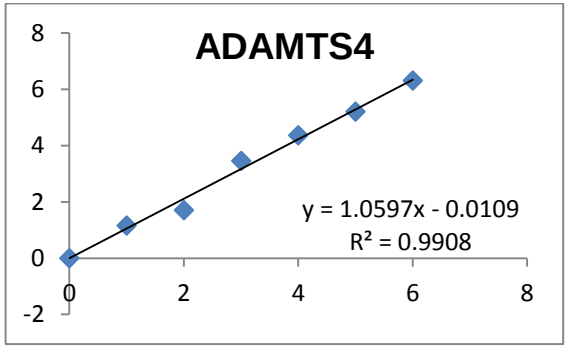
ADAMTS4
y = 1.0597x - 0.0109
R² = 0.9908

APPENDIX II – MELT CURVE ANALYSIS

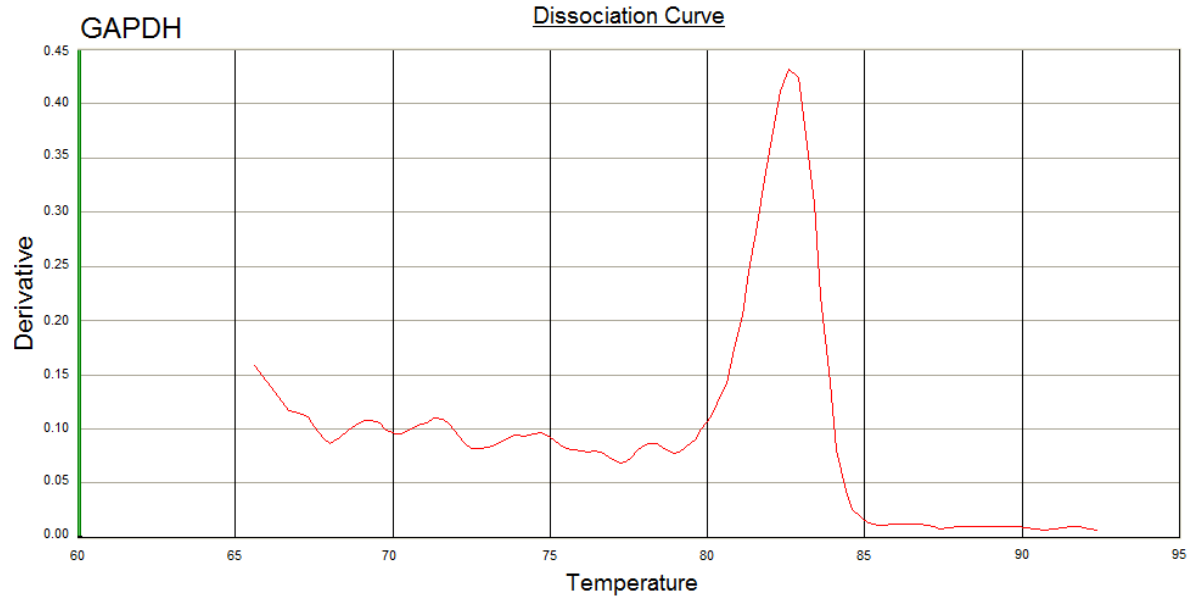

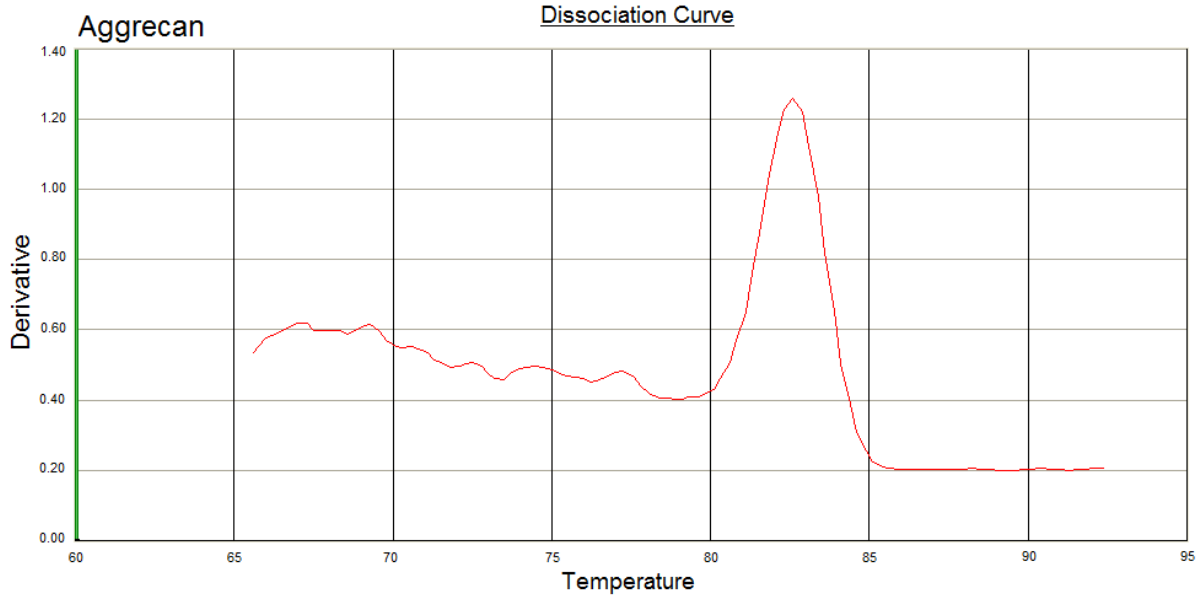

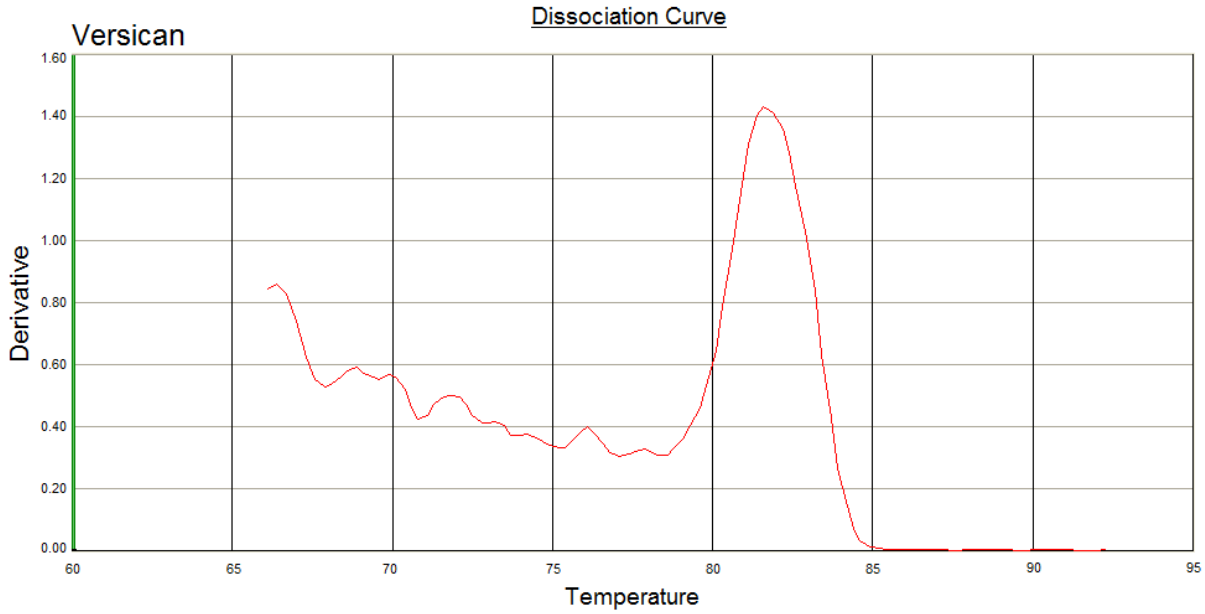
Dissociation Curve
Versican
Derivative
1.60
1.40
1.20
1.00
0.80
0.60
0.40
0.20
0.00
60
65
70
75
80
85
90
95
Temperature

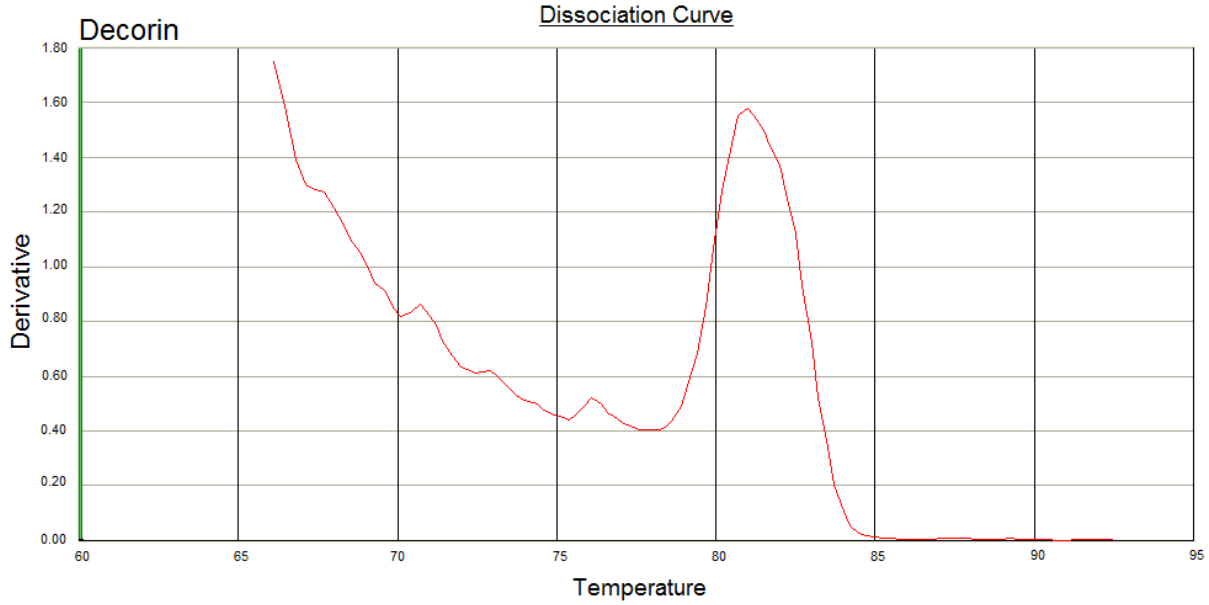
Dissociation Curve
Decorin
Derivative
1.80
1.60
1.40
1.20
1.00
0.80
0.60
0.40
0.20
0.00
60
65
70
75
80
85
90
95
Temperature

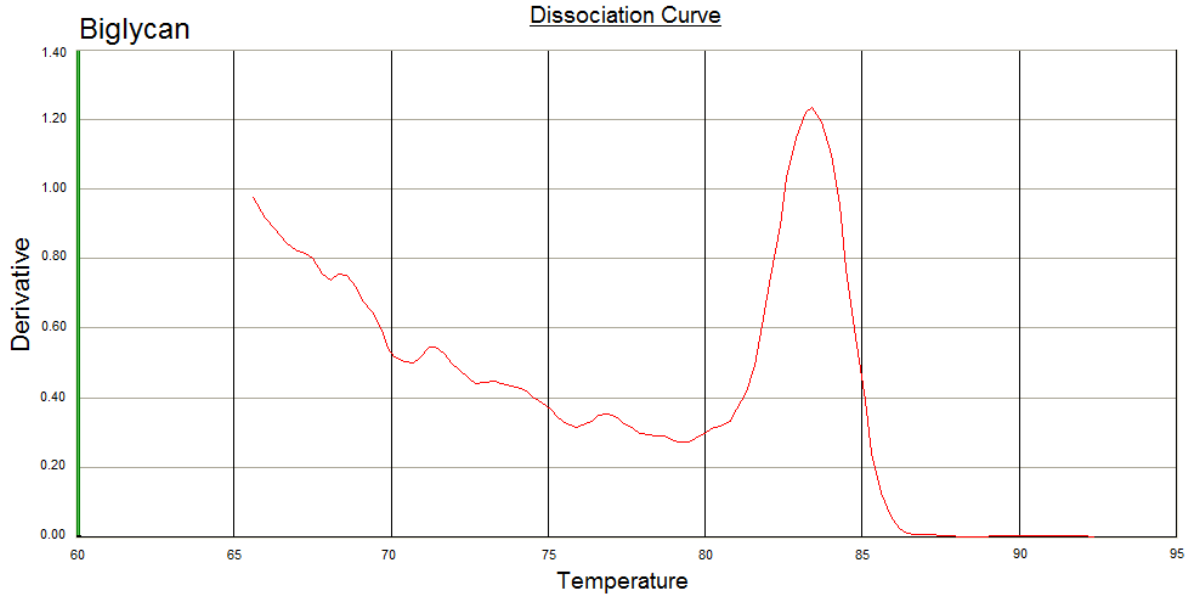
Biglycan
Dissociation Curve
Derivative
1.40
1.20
1.00
0.80
0.60
0.40
0.20
0.00
60
65
70
75
80
85
90
95
Temperature

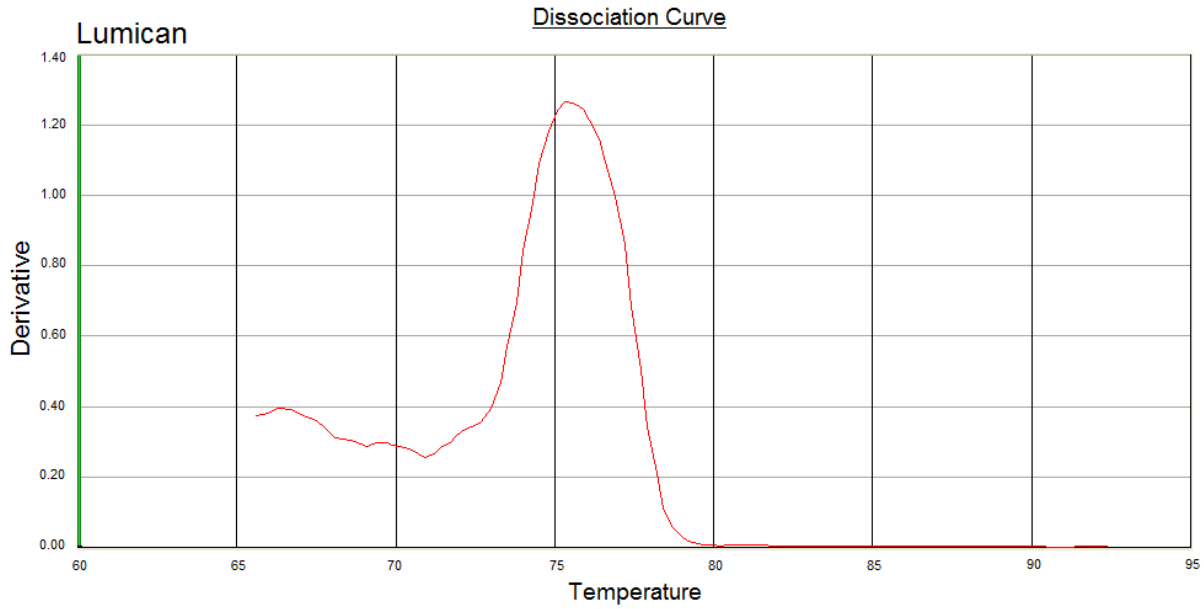
Lumican
Dissociation Curve
Derivative
1.40
1.20
1.00
0.80
0.60
0.40
0.20
0.00
60
65
70
75
80
85
90
95
Temperature

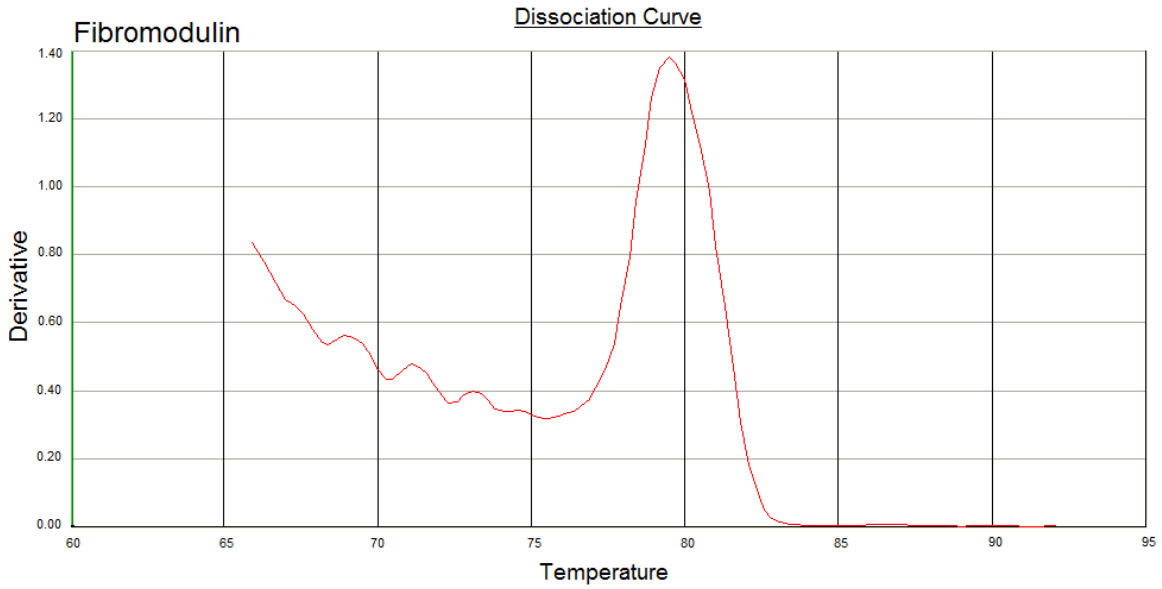
Dissociation Curve
Fibromodulin
Derivative
1.40
1.20
1.00
0.80
0.60
0.40
0.20
0.00
60
65
70
75
80
85
90
95
Temperature

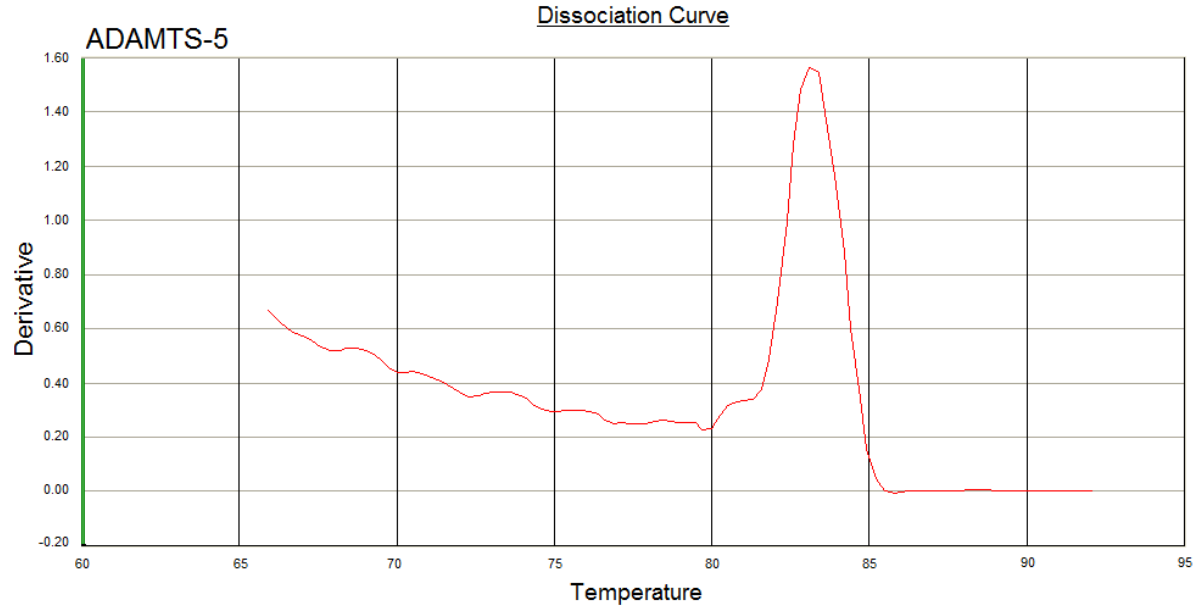
Dissociation Curve
ADAMTS-5
Derivative
1.60
1.40
1.20
1.00
0.80
0.60
0.40
0.20
0.00
-0.20
60
65
70
75
80
85
90
95
Temperature

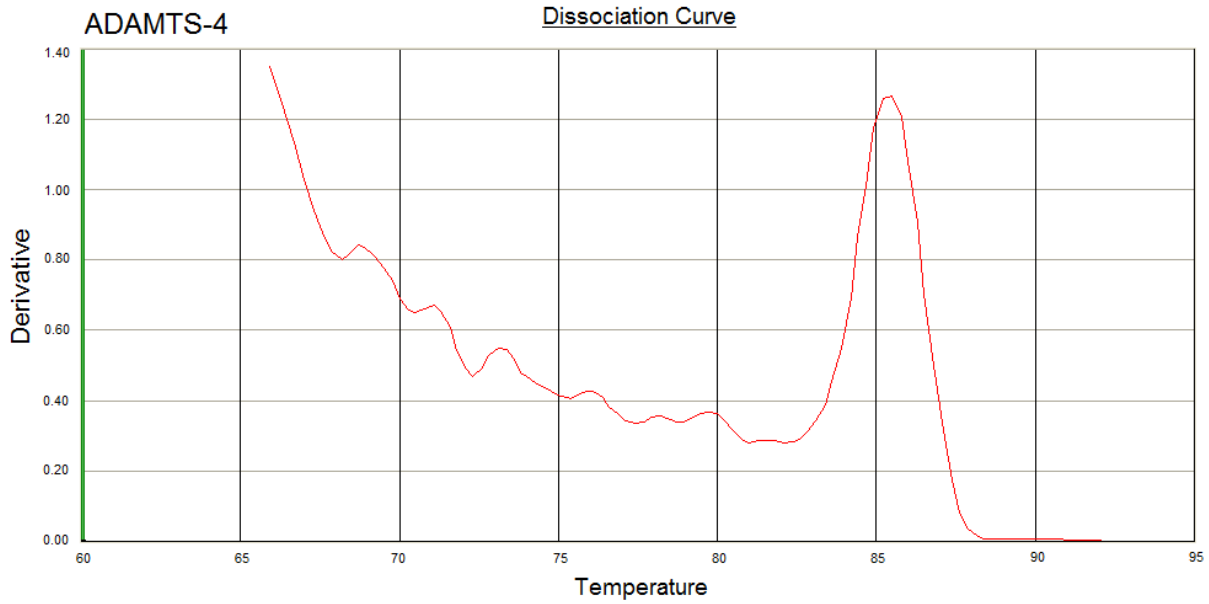
ADAMTS-4
Dissociation Curve
Derivative
1.40
1.20
1.00
0.80
0.60
0.40
0.20
0.00
60
65
70
75
80
85
90
95
Temperature

APPENDIX IV – NEGATIVE CONTROLS FOR WESTERN BLOT ANALYSIS

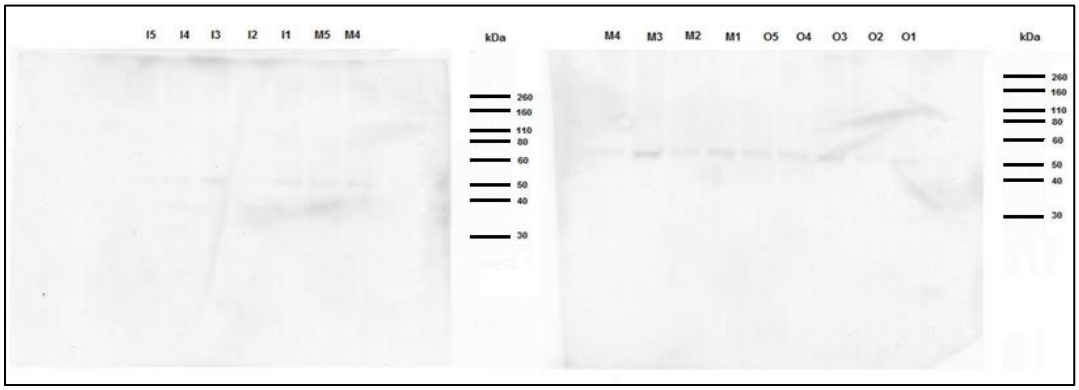

Figure 1. Anatomical regions of Staffordshire bull terrier CCL. Membrane probed with goat anti-mouse IgG secondary antibody (O=origin; M= middle; I= insertion).

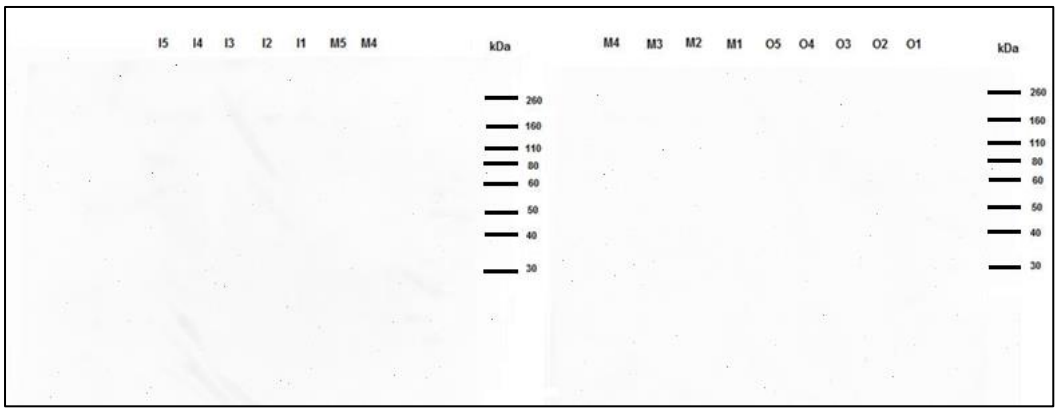

Figure 2. Anatomical regions of Staffordshire bull terrier CCL. Membrane probed with goat anti-mouse IgM secondary antibody (O=origin; M= middle; I= insertion).

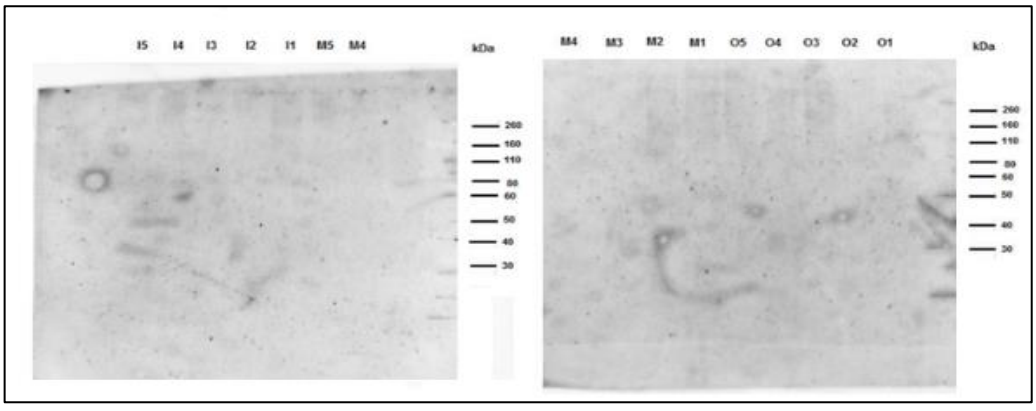

Figure 3. Anatomical regions of Staffordshire bull terrier CCL. Membrane probed with goat ant-rabbit IgG secondary antibody (O=origin; M= middle; I= insertion).

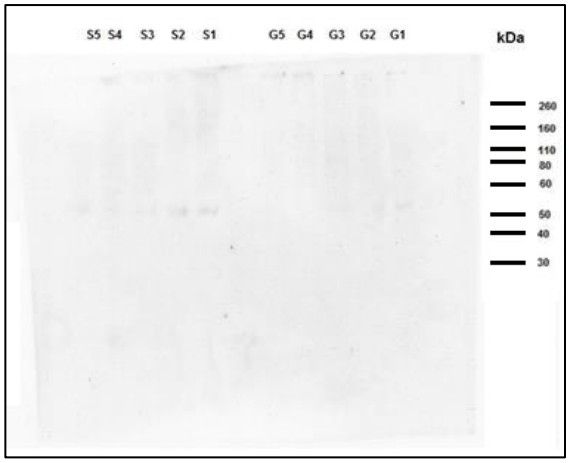

Figure 4. CCLs of two differentially predisposed dog breeds. Membrane probed with goat anti-mouse IgG secondary antibody (S= Staffordshire bull terrier; G= greyhound).

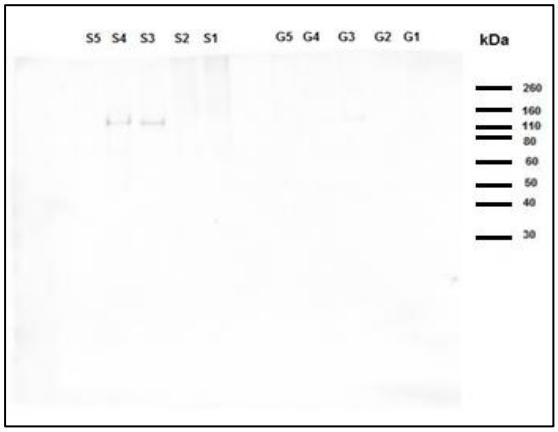

Figure 5. CCLs of two differentially predisposed dog breeds. Membrane probed with goat anti-mouse IgM secondary antibody (S= Staffordshire bull terrier; G= greyhound).

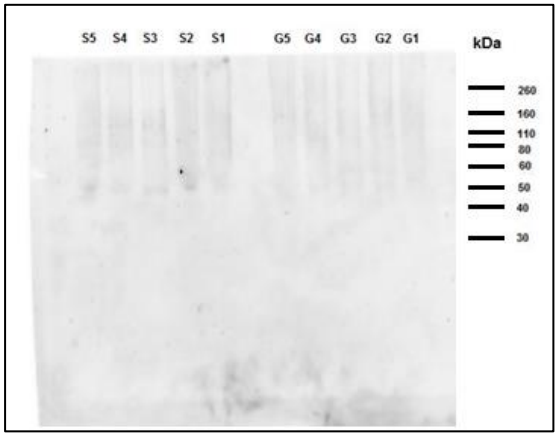

Figure 6. CCLs of two differentially predisposed dog breeds. Membrane probed with goat anti-rabbit IgG secondary antibody (S= Staffordshire bull terrier; G= greyhound).

APPENDIX V – KENDALL'S COEFFICIENT OF CONCORDANCE RESULTS FOR HISTOLOGY SCORING

Stain	Intra observer 1	Intra observer 2	Inter observer
H & E	0.8	0.8	0.8
Toluidine blue	0.3	0.4	0.2
Alcian blue	0.3	0.5	0.3